

Investigating the Biochemical Basis of Muscle Cell Dysfunction in Chronic Fatigue Syndrome

Gina Rutherford

MSc. (hons), BSc. (hons)



April 2016

Thesis submitted for the degree of Doctor of Philosophy in the Institute of Cellular Medicine,
Newcastle University

i. Abstract

Chronic fatigue syndrome/ Myalgic Encephalomyelitis (CFS/ME) is a debilitating disorder of unknown aetiology and is characterised by severe disabling fatigue in the absence of an alternative diagnosis. Historically, there has been a tendency to draw psychological explanations for the origin of fatigue. However, this model is at odds with patient descriptions of their fatigue, with many citing difficulty in maintaining muscle activity due to perceived lack of energy and discomfort.

In vivo studies have revealed profound and sustained intracellular acidosis following a standardised exercise protocol, suggestive of underlying bio-energetic abnormality and pointing towards an over-utilisation of the lactate dehydrogenase pathway. Similarly, a recent *in vitro* pilot investigation reported aberrantly low intracellular pH in CFS/ME patient myoblast samples when compared to healthy controls. Remarkably, intracellular pH in CFS/ME myoblasts was normalised to control level following treatment with pyruvate dehydrogenase kinase (PDK) inhibitor dichloroacetate (DCA), suggesting bio-energetic dysfunction in CFS/ME may be modifiable and therefore treatable.

In this thesis, *in vitro* approaches were used to investigate possible mechanisms leading to muscle dysfunction and the fatigue phenotype exhibited in CFS/ME. Validation work was performed to assess the capacity of a novel pH responsive nanosensor system to measure intracellular pH in CFS/ME patient myoblast cells. The work was unable to reliably detect any acidosis in CFS/ME cells, or any difference between CFS/ME and control cells. In addition, DCA did not modify intracellular pH in either CFS/ME or control cells.

The fluorescent pH responsive dye 2'7'-bis (2-carboxyethyl)-5 (6) carboxyfluorescein (BCECF) was used to measure intracellular pH at rest, following electrical pulse stimulation (EPS) and after treatment with DCA in myoblast and differentiated myotube cells.

Intracellular pH did not differ between CFS/ME patient and control cells at rest or post-EPS. In addition, treatment with DCA did not modify pH in either CFS/ME patient or control cells.

Glycolytic function was assessed via a combination of extracellular flux analysis (XF) and through the measurement of cellular L-lactate concentration. XF analysis revealed extracellular acidification rate (ECAR) measurements for all glycolytic

parameters to be comparable in CFS/ME patient muscle samples when compared to controls. Additionally, DCA did not alter ECAR in either group. L-lactate concentration was elevated at rest of post-EPS in CFS/ME cells compared to controls. DCA did not modify L-lactate concentration in either sample group.

Mitochondrial function was assessed via extracellular flux analysis. Bio-energetic function was investigated by manipulating glucose substrate availability in the assay medium. Basal oxygen consumption rate (OCR) was reduced in CFS/ME myoblasts under hypoglycaemic conditions compared to control cells, however this was not observed in CFS/ME myotubes. ATP-linked OCR was reduced in CFS/ME myoblasts under hyperglycaemic conditions compared to control cells but was not observed in CFS/ME myotube cells. There was no difference between CFS/ME and control cells for any of the other mitochondrial parameters tested.

A direct real-time electrochemical approach was used to monitor superoxide ($O_2^{\cdot-}$) generation in CFS/ME cells following ethanol stimulation and lactic acidification of the assay medium. $O_2^{\cdot-}$ generation was not elevated in CFS/ME cells compared to controls following ethanol stimulation or lactic acidification.

The *in vitro* muscle culture approaches reported in this thesis have enabled the investigation of the biochemical basis of muscle cell dysfunction in patients with CFS/ME. It is possible to conclude there to be no evidence of impaired muscle function in CFS/ME patients. Additionally, there was no impairment found in PDK enzyme function. Therefore, it can be determined that bioenergetic function is normal in CFS/ME patients and cannot be attributed to the excessive peripheral muscle fatigue phenotype frequently exhibited

ii. Declaration

The work presented in this thesis was conducted within the Diagnostic and Therapeutic Technologies Department within the Institute of Cellular Medicine, Newcastle University between April 2013 and April 2016. All work reported is original unless acknowledged via reference.

No part of this work has been submitted for a degree, diploma or any other qualification at this University or any other institution

iii. Acknowledgements

Firstly, I would like to thank my supervisors Professor Julia L Newton and Dr Philip Manning for their continuous support and guidance throughout the PhD process. I also offer my sincere thanks to the charity Action for ME who made this research journey possible.

I am incredibly thankful to Dr Aurora Gomez-Duran who provided technical training and outstanding support which was central to the successful completion of this thesis.

Additionally, I would like to thank Dr Audrey Brown, a true expert in muscle cell culture who was always there to share her knowledge and experience.

To my friends Cara, Emily and Hannah thanks for keeping me sane with a cup of coffee and a chat when cells would not grow and experiments did not work, which was far too often. I am grateful to each of you.

To Mum and Dad and my brother Greg thank you for never doubting my capabilities, helping to put things in perspective and always being there with a positive outlook, you deserve a medal. Finally, thank you Lewis for your unwavering support and encouragement, even though at times you probably wanted to strangle me.

iv. Table of Contents

Contents

ii. Declaration	iii
iii. Acknowledgements	iv
iv. Table of Contents	v
v. List of Figures and Tables	xxiv
Chapter 1 General Introduction.....	1
1.1 Definition and History	1
1.1.1 Clinical features and diagnosis.....	3
1.1.2 Treatment and prognosis	4
1.1.4 Charity involvement	5
1.1.5 Cellular bio-energetic function overview	5
1.1.6 Bio-energetic muscle dysfunction.....	7
1.1.7 Myoblasts and differentiated myotubes	8
1.1.8 Electrical pulse stimulation.....	9
1.2 Literature Review	11
1.2.1 Autonomic dysfunction	11
1.2.2 Central sensitisation.....	14
1.2.3 Immune dysfunction	15
1.2.4 Oxidative stress.....	18
1.2.5 Mitochondrial dysfunction	22
1.2.6 Post-exertional malaise and immune function.....	25
1.2.7 Muscle bio-energetic dysfunction.....	26
1.2.7.1 Intracellular acidosis.....	26
1.2.7.2 Acidosis as a consequence of impaired PDC function.....	30
1.2.8 Abnormal AMPK activation and glucose uptake	31
1.3 Conclusion	33
1.4 Aims.....	33
References.....	35
Chapter 2.....	53
2.1 Introduction.....	53
2.1.1 Intracellular pH and Cell Function.....	54

2.1.2 Acidosis and fatigue development.....	54
2.1.2 Intracellular sensing techniques	55
2.1.3 PEBBLE Nanosensors.....	57
2.1.4 Nanosensor delivery.....	59
2.1.5 pH sensitive nanosensor application.....	60
2.1.6 Hypotheses.....	62
2.2 Materials and Methods.....	63
2.2.1 Study participants	63
2.2.2 Cell culture and preparation.....	63
2.2.3. Intracellular optical sensing.....	65
2.2.3.1 pH responsive nanosensor production	65
2.2.3.2 pH sensitive nanosensor calibration	65
2.2.4 Resazurin cytotoxicity assay	67
2.2.4.6 pH Measurement of DCA in a cell-free system.....	69
2.2.5 pH Sensitive nanosensor internalisation with varying lipofectamine concentration.....	69
2.2.6 pH Sensitive nanosensor internalisation and DCA treatment	69
2.2.7 Data analysis	70
2.3 Results.....	71
2.3.1 pH Sensitive nanosensor calibration curve in a cell-free system.....	71
2.3.2 pH responsive nanosensor optimisation.....	72
2.3.2.1 Myoblast viability following exposure to dye-free (blank) nanosensors.....	72
2.3.2.2 Myoblast viability following exposure to Oregon green and FAM.....	73
2.3.2.3 Myoblast viability following treatment with Lipofectamine 2000.....	74
2.3.2.4 Myoblast viability following incubation with DCA.....	75
2.3.2.4 pH measurement of DCA in a cell-free nanosensor system	77_Toc448404063
2.3.3 Nanosensor application.....	77
2.3.3.1 Myoblast pH with varied lipofectamine 2000 concentration	77
2.3.3.2 Myoblast pH with varied DCA treatment	78
2.4 Discussion.....	80
2.4.1 pH nanosensor optimisation.....	80
2.4.2 pH Nanosensor application	83
2.4.3 Limitations	86
2.4.4 Conclusion	87
2.5 References.....	88

Chapter 3 Direct, Real-time Electrochemical Detection of Superoxide Generation in CFS/ME Patient Myoblasts.....	94
3. 1 Introduction.....	94
3.1.1 Free-radical overview.....	95
3.1.2 O ₂ ⁻ detection techniques	96
3.1.2.1 spectroscopic O ₂ ⁻ measurement	96
3.1.2.2 Electron spin resonance spectroscopy.....	97
3.1.2.3 Amperometric extracellular O ₂ ⁻ monitoring.....	98
3.1.3 Hypotheses.....	100
3.2 Materials and Methods.....	101
3.2.1 Cell culture and preparation.....	101
3.2.1.1 Direct real-time electrochemistry.....	101
3.2.1.2 Preparation of superoxide specific electrode.....	101
3.2.1.3 Electrode calibration	102
3.2.1.4 Cellular superoxide measurement following acidification of myoblasts.....	103
3.2.2 Cell viability in response to lactic acidification	104
3.2.3 Data analysis	104
3.3 Results.....	105
3.3.1 Direct real-time electrochemistry.....	105
3.3.1.1 Xanthine/XOD calibration curve.....	105
3.3.1.2 Cellular superoxide response to ethanol in myoblasts	105
3.3.1.3 Superoxide generation following acidification in myoblasts	107
3.3.2 Cytotoxicity with lactic acidification.....	108
3.4 Discussion.....	109
3.4.1 Ethanol stimulation.....	110
3.4.2 Extracellular acidification	111
3.4.3 Limitations	112
3.4.4 Conclusion	113
3.5 References.....	114
Chapter 4.....	120
Application of 2'7'-bis (2-carboxyethyl)-5 (6) Carboxyfluorescein to Measure Intracellular pH in CFS/ME Myoblasts and Myotubes.....	120
4.1 Introduction.....	120
4.1.1 Intracellular sensing.....	121

4.1.2 Electrical pulse stimulation.....	123
4.1.3 Hypotheses.....	124
4.2 Materials and Methods.....	125
4.2.1 Cell culture and preparation.....	125
4.2.2 Intracellular pH calibration.....	126
4.2.3 Myoblast viability following treatment with BCECF-AM.....	126
4.2.4 BCECF-AM intracellular pH measurement.....	127
4.2.5 Electrical pulse stimulation.....	127
4.2.6 Data analysis.....	127
4.3 Results.....	129
4.3.1 BCECF-AM pH <i>In Situ</i> Calibration.....	129
4.3.2 Myoblast viability following exposure to BCECF-AM.....	130
4.3.3 Myoblast intracellular pH determination with DCA treatment.....	132
4.3.4 Myotube intracellular pH measurement at rest and post-EPS.....	133
4.4 Discussion.....	136
4.4.1 Optimisation.....	137
4.4.2 Intracellular pH determination.....	137
4.4.3 Limitations.....	141
4.4.4 Conclusion.....	141
4.5 References.....	143
Chapter 5 An Exploration of Glycolytic Function in CFS/ME Primary Myoblasts and Myotubes via Extracellular Flux Analysis and L-lactate Quantification.....	147
5.1 Introduction.....	147
5.1.1 Overview of cellular glycolysis.....	147
5.1.2 Techniques to measure cellular glycolytic flux.....	148
5.1.3 Hypotheses.....	151
5.2 Materials and Methods.....	152
5.2.1 Study participants.....	152
5.2.2 Cell culture and preparation.....	153
5.2.3 Electrical pulse stimulation.....	153
5.2.4.1 L-lactate assay.....	154
5.2.4.2 Standard curve and sample preparation.....	154
5.2.4.3 Assay procedure.....	154
5.2.4.4 L-lactate flurometric measurement setup.....	155

5.2.5 Extracellular flux analysis.....	155
5.2.5.1 Assay preparation	155
5.2.5.2 Compound injection.....	155
5.2.5.3 Glycolytic stress test.....	156
5.2.5.4 Normalisation	156
5.2.6 Data analysis	156
5.3 Results	157
5.3.1.1 L-Lactate standard curve	157
5.3.1.2 Myoblast L-lactate measurement	157
5.3.1.3 Myotube L-lactate measurement at rest and post-EPS	158
5.3.2 Extracellular Flux Analysis.....	159
5.3.2.1 Myoblast glycolytic stress testing with DCA treatment.....	159
5.3.2.2 Myotube glycolytic stress testing with DCA treatment.....	162
5.4 Discussion	164
5.4.1 L-lactate concentration	165
5.4.2 Glycolytic parameters	165
5.4.3 Conclusion	167
5.5 References.....	168
Chapter 6 An Investigation of Mitochondrial Function in CFS/ME Patient Myoblast and Myotube samples via Extracellular Flux Analysis.....	172
6.1 Introduction.....	172
6.1.1 Oxidative phosphorylation overview	172
6.1.2 Evidence of mitochondrial dysfunction in CFS/ME.....	173
6.1.3 Mitochondrial respiration measurement techniques	174
6.1.4 Assessment of mitochondrial function.....	178
6.1.5 Hypotheses	178
6.2 Materials and Methods	180
6.2.1 Study participants	180
6.2.2 Cell culture and preparation.....	181
6.2.3 Extracellular flux analysis.....	181
6.2.3.1 Assay preparation	181
6.2.3.2 Compound preparation.....	182
6.2.3.3 Optimisation	182
6.2.3.4 Mitochondrial stress test.....	182

6.2.3.5 Normalisation	183
6.2.4 Data analysis	183
6.3 Results	184
6.3.1 Mitochondrial stress testing with varied glucose	184
6.3.2 Basal respiration	184
6.3.3 ATP-linked respiration	185
6.3.4 Maximal respiration	187
6.3.5 Spare respiratory capacity	188
6.4 Discussion	190
6.4.1 Mitochondrial parameters	191
6.4.2 Limitations	194
6.4.3 Conclusion	195
6.5 References	196
Chapter 7	General
Conclusions and Future Directions	201
7.1 Conclusions	201
7.2 Future Work	203
7.3 References	204

v. List of Figures and Tables

Figures

- 1.1:** (a) Human primary myoblasts in culture and (b) following differentiation into myotubes.....9
- 1.2:** Complex I and II have both been accepted as major sites of electron leakage and O_2^- production. If O_2^- enters the cytosol, it may further react with NO. and redox ions to form additional reactive oxygen species e.g. H_2O_2 and $OONO^-$19
- 1.3:** Diagram outlining PDC function when down-regulated, leading to an over utilisation of the lactate dehydrogenase pathway.....31
- 2.1:** Graphic representation of an ‘optode’ used for intracellular analysis.....56
- 2.2:** Schematic representing a PEBBLE nanosensor.....57
- 2.3:** Graphical representation of the different endocytic pathways that provide entry into the mammalian cell. The possible routes through the endosomal network following internalization are depicted.....59
- 2.4:** Preliminary data generated by Boulton [2012], depicting confocal imaging of discrete-z-slice in a control myoblast. A first distribution of nanosensors through the cell are observed. FITC fluorescence A, Alexafluor568 B, bright field C and Merged.....60

2.5: Preliminary data generated by Boulton [2012]. Myoblasts were treated with 16µM DCA. No change in pH between treated and untreated control myoblasts. DCA boosted pH beyond the baseline level of normal myoblasts. Untreated CFS/ME myoblasts exhibited a significantly lower pH. Data presented as mean ±SD, N=4 *** denotes P<0.005.....	62
2.6: Schematic of lower limb anatomy as depicted by Dixit et al. [2007].....	64
2.7: Calibration of pH responsive nanosensors containing FAM-D & OG-D Fluorescent ratio was shown to be linearly dependent upon pH (y= 6.0624). The data is presented as mean ±SD, n=5, R ² =0.9885.....	71
2.8: CFS/ME & control myoblast viability (% of untreated control) following 3 hours incubation with 1µM- 1mM DCA. Viability (% untreated control) was assessed following the addition of 0.03% resazurin. Myoblast viability remained high across concentrations (>79%) in both CFS/ME and control sample groups. Data presented as mean ±SD.....	72
2.9: Control myoblast viability (%) after incubation with varying concentrations (5-20µg/mL) of pH sensitive OG & FAM. Data presented as mean ±SD, n=3. Significant difference in viability between 1 & 2 hours at 20µg/mL and similarly between 2 & 3 hours as denoted by **** (P<0.0005).....	73
3.0: CFS/ME myoblast viability (%) after incubation with varying concentrations	

(5-20µg/mL) of pH sensitive OG & FAM. Data presented as mean ±SD
significant difference in viability between 1 & 2 hours at 20µg/mL and
similarly between 2 & 3 as denoted by *** (P<0.005).....82

3.1: CFS/ME & control myoblast viability (%) following 3 hours
incubation with varying concentrations (0.003-3%) of lipofectamine
data presented as mean of triplicate measures for n=2, ±SD.
Significant reduction in viability at 3% verses 0.003% concentration
For both CFS/ME & control myoblasts, denoted by *** (P<0.005).....74

3.2: CFS/ME (n=2) & control (n=2) myoblast viability (%) following 3
hours incubation with 1µM-1mM DCA. Viability (% untreated control)
was assessed following the addition of 0.03% resazurin. Myoblast
viability remained high across concentrations (>79%) in both
CFS/ME and control sample groups. Data presented as mean ±SD.....76

3.2: CFS/ME (n=2) and control (n=2) myoblast viability (%) following
6 hours incubation with 1µM-1mM DCA. Viability (% untreated control)
(% untreated control) was assessed following the addition of 0.03%
Resazurin. Viability remained high across concentrations (>87%)
in both CFS/ME and control sample groups. Data presented as mean
±SD.....76

3.3: CFS/ME (n=2) and control (n=2) myoblast viability (%) following
3 hours incubation with varying concentrations (0.003-3%) of
lipofectamine data presented as mean ±SD. Significant

reduction in viability at 3% verses 0.003% concentration for both CFS/ME and control sample groups. Data presented as mean \pm SD.....	76
3.4: Calculated pH for varying concentrations of DCA (0 μ M- 40 μ M). pH measured by nanosensors at 10mg/mL concentration. Data presented as mean of triplicated measures, \pm SD.....	77
3.5: CFS/ME and control myoblast intracellular pH with varied lipofectamine concentration (0.003-3%). Data presented as mean of triplicate measures \pm SD. Significantly lower intracellular pH for control myoblasts across all lipofectamine concentrations. Denoted by *** (P<0.005), n=2 donors.....	78
3.6: CFS/ME and control myoblast intracellular pH at baseline (0 μ M) and following treatment with DCA (10-20 μ M). pH measured with nanosensors at 10mg/mL concentration. Significantly lower intracellular pH for control compared to CFS/ME myoblasts at baseline and following treatment with all concentrations of DCA. P<0.0005 denoted by ****. Data presented as mean of triplicate measures \pm SD, n=2 donors.....	79
3.7: Free radicals are atoms that contain an unpaired electron in their outermost shell, resulting in a highly unstable configuration and radicals rapidly reacting with other molecules and radicals to achieve a stable configuration.....	96

3.8: Schematic representation of the electrochemical superoxide Sensor described by Manning et al [1998].....	99
3.9: Superoxide production by the action of xanthine oxidase (XOD) on Xanthine.....	102
4.0: Superoxide calibration curve with varying concentrations of xanthine Oxidase (0.25-1.0µM) in the presence of constant xanthine (1.5mM) Produced a linear increase in current ($R^2=0.9582$, $n=4$, $\pm SD$).....	105
4.1: (a) Superoxide generation in CFS/ME myoblasts cells following Stimulation with varying concentration (2-5%) of ethanol. There was a small linear relationship between ethanol concentration and recorded current ($R^2=0.7007$). The response was inhibited with 500U/mL of SOD. Data presented as mean $\pm SD$ of 3 replicate measures, $n=2$	107
4.1: (b) Superoxide generation in CFS/ME myoblasts cells following stimulation with varying concentration (2-5%) of ethanol. There was a small linear relationship between ethanol concentration and recorded current ($R^2=0.6814$). The response was inhibited with 500U/mL of SOD. Data presented as mean $\pm SD$ of 3 replicate measures, $n=2$	107
4.2: Lactic acidification (2mM, pH 5.36) over time (30 minutes- 24 hours) did not induce any meaningful change in superoxide	

Generation over-time in CFS/ME or control myoblast samples.
 Data presented as mean \pm SD of 3 replicate measures, n=2.....102

4.3: Lactic acidification of CFS/ME and control myoblasts over
 24-hours resulted in significantly lower viability in control
 compared CFS/ME cells following treatment with 1mM, 1.5mM,
 2mM lactic acid (pH 6.61, 6.11 and 5.36 respectively). There
 was no significant difference between CFS/ME and control cells
 following 0.5mM acidification (pH 7.09). Data presented as
 mean \pm SD of 3 replicate measures **** denotes $P < 0.0005$108

4.4: The synthesis and hydrolysis of Am and acetate ester as
 illustrated by Han and Burgess [2010].....121

4.5: EPS was performed using the C-pace EP cell pace (Ion optic, Dublin).....123

4.6: *In situ* calibration curve conducted in myoblast samples following
 incubation with BCECF-AM. A polynomial second-order
 fitting enabled the successful determination of pH within
 the physiological range from the FI ratio measures provided
 ($y = 0.3758x^2 - 3.4706x + 9.4155$, $R^2 = 0.999$). The data is
 presented as mean \pm SD.....129

4.7: *In situ* calibration curve conducted in myotube samples following
 incubation with BCECF-AM. A polynomial second-order

fitting enabled the successful determination of pH within the physiological range from the FI ratio measures provided ($y=0.4119x^2 - 3.8228X + 10.002$, $R^2=0.995$). The data is presented as mean \pm SD.....129

4.8: (a) CFS/ME and control myoblast viability after 3-hours
 Incubation with BCECF-AM at 0.5-2 μ M concentrations
 no significant difference in viability was observed between samples or with varying concentrations of BCECF-AM.
 Data presented as mean \pm SD, n=3.....130

4.8: (b) CFS/ME and control myoblast viability after 6-hours
 incubation with BCECF-AM at 0.5-2 μ M concentrations
 no significant difference in viability was observed between samples or with varying concentrations of BCECF-AM.
 Data presented as mean \pm SD, n=3.....131

4.8: (c) CFS/ME and control myoblast viability after 24-hours
 incubation with BCECF-AM at 0.5-2 μ M concentrations
 no significant difference in viability was observed between samples or with varying concentrations of BCECF-AM.
 Data presented as mean \pm SD, n=3.....132

5.0: (a) myoblasts in culture, (b) myotubes 7-days differentiation.....132

5.1 (a) CFS/ME (n=4) and control (n=4) resting myotube
pH at baseline following treatment with DCA (40µM).
no significant difference in pH between groups at baseline
or following DCA treatment. DCA did not exhibit any
within group differences in pH when compared to baseline
for both samples. Data presented as mean ±SD.....134

5.1: (b) CFS/ME myotube intracellular pH measurements
post-EPS at baseline and following treatment with DCA (40µM).
DCA did not induce any significant alteration in pH at any point
during the recovery period. Data presented as mean ±SD, n=4.....134

5.1: (c) Control myotube intracellular pH measurements post-EPS
at baseline and following treatment with DCA (40µM). DCA did
not induce any significant alteration in pH at any point during the
recovery period. Data presented as mean ±SD, n=4.....135

5.2: Schematic illustration of cellular glycolysis, adapted from
Winer et al. [2011].....147

5.3: An illustration of an XF microplate and sensor cartridge as depicted
by Ferrick et al. [2008].....149

5.4: Schematic illustration of glycolytic flux following the addition of
stress test reagents to provide the parameters glycolysis, glycolytic
capacity and non-glycolytic acidification.....151

5.5: Standard curve conducted with varying L-lactate standard concentrations.
mean FI was linearly dependent upon the L-lactate concentration
($y=99.613x$, $R^2=0.973$, $n=5$). The data is presented as mean \pm SD, N=5.....157

5.6: L-lactate concentration in CFS/ME verses control myoblasts at baseline
(0 μ M) and following treatment with 40 μ M DCA. No significant
difference in L-lactate concentration was observed when the
groups were compared. Additionally, no significant within group
effects were observed as a consequence of DCA treatment. Data is
presented as mean \pm SD, n=9.....158

5.7: L-lactate concentration in CFS/ME and control myotubes at rest and
following 24-hours EPS. L-lactate concentration did not significantly
differ at rest or following 24-hours EPS at both 0 μ M and 40 μ M DCA
concentrations. The data is presented as mean \pm SD, n=7.....159

5.8: Glycolysis ECAR in CFS/ME and control myoblasts following
treatment with DCA (40 μ M). No significant difference in
ECAR at baseline (0 μ M) between samples, however
ECAR significantly reduced in control compared to CFS/ME
samples following DCA treatment. No within group effects
as a consequence of DCA treatment were observed.
Data presented as mean \pm SD, n=8, *** denoted $P<0.05$159

5.9: Glycolytic capacity ECAR is CFS/ME and control myoblast

samples. No significant difference was exhibited at baseline and following DCA treatment for CFS/ME verses control myoblasts samples. No within group effects were observed for either group following DCA treatment. Data presented as mean \pm SD, n=8.....160

6.0: Glycolytic reserve capacity ECAR in CFS/ME and control myoblast samples. No significant difference was exhibited at baseline and following DCA treatment for CFS/ME verses control myoblast samples. No within group effects were observed for either group following DCA treatment. Data presented as mean \pm SD, n=8.....161

6.1: Glycolysis ECAR in myotube samples. No significant difference was exhibited at baseline following DCA treatment for the CFS/ME verses control myotube samples. No within group effects were observed for either group following DCA treatment. Data presented as mean \pm SD, n=8.....162

6.2: Glycolytic capacity ECAR in myotube samples. No significant difference in ECAR at 0 μ M and 40 μ M in CFS/ME samples. However, following treatment with 40 μ M DCA this significant relationship was lost. No other significant effects were observed.....162

6.3: Created by Yong-ling et al [2008]. The electron transport chain with 4 membrane bound complexes (I-IV). Electrons pass through the complexes with assistance

from electron carrier ubiquinone (Q) and cytochromes. The movement of electrons is associated with proton (H⁺) pumping from the mitochondrial matrix to the intermembrane space. This creates a proton motive force, which drives ATP synthesis.....172

6.4: Mitochondrial respiration OCR during XF stress test. Mitochondrial parameters depicted in relation to substrate injection. Image provided by Seahorse Bioscience.....177

6.5: Basal OCR in myoblasts with varied glucose media concentration. CFS/ME samples Exhibited significantly lower OCR compared to controls at 2.5mM glucose. Data presented as mean ± SD, n=8, *** denoted P<0.05.....184

6.6: Basal OCR in myotubes with varied glucose media concentration. no significant difference in OCR for CFS/ME verses control myotubes was observed across the glucose concentrations. No significant within-group differences were found as a consequence of varied glucose concentration. data presented as mean ±SD, n=6.....185

6.7: ATP-linked OCR in myoblast samples following incubation with varied concentrations of glucose media. At 10mM glucose media concentration OCR was significantly lower in the CFS/ME sample group compared to controls. No significant within-group differences were found as a consequence of varied glucose concentration. Data presented as mean

±SD, n=6, ** denoted P<0.05.....	186
6.8: ATP-linked OCR in myotube samples following incubation with varied concentrations of glucose media. No significant within-group differences were found as a consequence of varied glucose concentration. Data presented as mean ± SD, n=6.....	186
6.9: Myoblast maximal respiration with varied concentrations of glucose media. No significant difference in OCR for CFS/ME verses control across glucose media concentrations. No significant within-group differences were found as a consequence of varied glucose media concentration. Data presented as mean ±SD, n=6.....	186
7.0: Myotube maximal respiration with varied concentrations of glucose media. No significant difference in OCR for CFS/ME verses controls across glucose media concentrations. No significant within-group differences were found as a consequence of varied glucose concentration. Data presented as mean ±SD, n=6.....	187
7.1: Myoblast spare respiratory capacity OCR was not significantly different in CFS/ME compared to control myoblasts at any of the glucose media concentrations investigated. No within-group differences between any of the glucose concentrations was observed.....	188

7.2: Myotube spare respiratory capacity OCR was not significantly different

In CFS/ME compared to control myoblasts at any of the glucose media
Concentrations investigated. No within-group differences between any of
the glucose concentrations were observed.....188

Tables

1.1 The volumes required of the stock concentrations of sodium phosphate dibasic
(0.2M) and citric acid monohydrate (0.1M) required to make buffer solutions
pH 4-8.....66

vi. List of Abbreviations

ADP	Adenosine diphosphate
AMPK	5' AMP-activated protein kinase
ANS	Autonomic nervous system
ATP	Adenosine triphosphate
BCA	Bicinchoninic acid
BCECF-AM	(2',7'-Bis-(2-Carboxyethyl)-5-(and-6)-Carboxyfluorescein, Acetoxymethyl Ester
BMPO	5-tert- butoxycarbonyl-5 methyl-pyrroline-N-oxide
CBT	Cognitive behavioural therapy
CNS	Central nervous system
CFS	Chronic Fatigue Syndrome
CYP2E1	Cytochrome P450 2E1
DCA	Dichloroacetate
2-DG	2-deoxy-D-glucose
DMEM	Dulbecco's modified eagles medium
DNA	Deoxyribonucleic acid
DMPO	O ₂ ⁻ 5, 5 dimethylol-pyrroline-N-oxides
DTSSP	3-3'-dithiobis (sulfosuccinimidyl-propionate
ECAR	Extracellular acidification rate
EPS	Electrical pulse stimulation
ESR	Electron spin resonance spectroscopy
FADH	Flavin adenine dinucleotide phosphate
FCCP	carbonylcyanide p-trifluoromethoxyphenylhydrazone

FI	Fluorescent intensity
fMRI	functional magnetic resonance spectroscopy
GET	Graded exercise therapy
H ₂ O ₂	Hydrogen peroxide
HF	High frequency
HR	Heart rate
IL	Interleukin
IOM	Institute of medicine
LDH	Lactate dehydrogenase
LF	Low frequency
MCT	Monocarboxylate transporters
ME	Myalgic Encephalomyelitis
MRF	Myogenic regulatory factor
MRS	Magnetic resonance spectroscopy
MYOG	Myogenin
NADH	Nicotineamide adenine dinucleotide phosphate
NICE	National institute for health and care excellence
NK	Natural killer cell
O ₂ ⁻	Superoxide
O ₂ K	oxygraph 2K
OCR	Oxygen consumption rate
·OH	hydroxyl radical
PEBBLE	Probes encapsulated by biologically localised embedding
PDC	Pyruvate dehydrogenase complex
PDK	Pyruvate dehydrogenase kinase

PEM	Post exertional malaise
PMA	Phorbol-12 myristate-13 acetate
PMRS	Phosphorus magnetic resonance spectroscopy
RNS	Reactive nitrogen species
ROS	Reactive oxygen species
SBP	Systolic blood pressure
SEID	Systemic Exertional Intolerance Disease
SOD	Superoxide dismutase
TCA	Tricarboxylic acid
XF	Extracellular flux
XOD	Xanthine oxidase

Chapter 1

General Introduction

Rutherford, G. Manning, P. Newton, J,L. (2016) Understanding Muscle Dysfunction in Chronic Fatigue Syndrome. *Journal of Aging Research*. 2016, 13

1.1 Definition and History

Chronic Fatigue Syndrome (CFS/ME) also known as Myalgic Encephalomyelitis (ME), is a heterogeneous disorder of unknown aetiology [Bradley et al. 2013]. The condition is characterised by severe disabling fatigue in the absence of alternative diagnosis and is associated with a myriad of other symptoms including but not limited to post exertional malaise, sleep disturbance and cognitive dysfunction [Bradley et al. 2013; Jones et al. 2012; Perrin et al. 2007; Prins et al. 2007; Wessley et al. 1997]. One of the primary symptoms of CFS/ME is generalised abnormal muscle fatigue that occurs after relatively mild activity [Fukuda et al. 1994; Jones et al. 2010; Macintyre et al. 1992]. Fatigue can be defined as a progressive impairment in maximal force generating capacity that develops during muscular activity [Lancet (editorial) 1998].

The prevalence of CFS/ME in the adult population is estimated at around 0.2%-2.6% worldwide [Nacul et al. 2011; NICE. 2007; Prins. 2006; Wessley et al. 1997]. However, the Centre for Disease Control 1994 criteria (CDC4) [Fukuda et al. 1994] and the Canadian criteria [Carruthers et al. 2003] provide a strict definition and estimate prevalence to be 0.2%, lower than previously reported in a primary care setting whereby a less stringent criteria was applied [Wessley et al. 1997]. In the UK, the condition affects approximately 600,000 individuals, with a peak incidence in the 20-40 age group and a preponderance in females, at a ratio of 6:1 [NICE, 2007; Action for ME. 2012]. Moreover, CFS/ME has been reported in children as young as two years of age and would seem to affect all socioeconomic groups to a similar extent [Shepherd. 2006]. Therefore, CFS/ME is a major clinical problem, imposing substantial burden on the health of the UK population in addition to economic costs on society, mainly in the form of informal care and loss of employment. Thus, the development of treatments that recognise these impacts are vital [Perrin et al. 2011].

CFS/ME is historically a complex and poorly understood disorder [Lorusso et al. 2009] and has been the subject of a number of debates. One important challenge has been to define and delineate the illness, which has proven difficult [Hossenbaccus & White. 2013]. Furthermore, controversies surrounding the disorder largely date back to an editorial in the Lancet (1956) that introduced ME into medical language as a severe post-infectious illness involving symptoms that affected peripheral muscle and the brain. However, medical opinion remained sceptical and it was only during the 1980s that interest was renewed, one result being the redefinition and renaming of ME as CFS. In 1998, in an attempt to produce a degree of consensus as regards the diagnosis and management of the disorder, the chief medical officer appointed a working group to produce a report [Department of Health. 2002]. Consequently, CFS/ME was recognised as a genuine and disabling condition in the UK [Shepherd.2006].

Another subject of debate has been in the naming of the condition. For example, the condition was originally referred to as ME, which describes an unproven inflammatory process in the brain and spinal cord, a term that many health practitioners are reluctant to use. Alternatively, CFS is a term that makes no definitive assumptions regarding cause. Two major criticisms regarding the use of this term have been firstly that it fails to reflect symptomology and the severity of the illness. Secondly, it may be a convenient label that could be applied to anyone experiencing unexplained chronic fatigue [Hossenbaccus & White. 2013; Shepherd. 2006]. More recently, early in 2015 the Institute of Medicine (IOM) [IOM, 2015] issued a report that proposed a new case definition for CFS/ME, recommending renaming the illness Systemic Exertion Intolerance Disease (SEID). This new case definition requires a substantial reduction in ability to complete pre-illness activities, unrefreshing sleep, post-exertional malaise and either cognitive or orthostatic intolerance. In a recent study conducted by Jason et al. [2015] the new SEID criteria was reported to identify a group of patients comparable in size to the Fukuda criteria but a larger group than the Canadian criteria. Additionally, the name was reported to select more patients who had less impairment and fewer symptoms than a four item empiric criteria. Presently, there is considerable debate among scientist as regards which case definition to use for clinical and research purposes. As indicated in the IOM report [IOM, 2015] funding was limited so an inadequate number of studies have focused on the validity and reliability of the case definition [Jason et al. 2015]. Thus, further research utilising empirical methods is required to fully evaluate the criteria and develop a consensus among researchers, clinicians and the patient community [Jason et al. 2015].

Additionally, confusion also exists as to whether the nature of the condition is psychological or physiological which is exemplified by the way it is classified, for example the World Health Organisation have classified CFS under the international classification for diseases (ICD-10) as a neurological disease, with the classification suggesting a 'fatigue syndrome' should be classified as a neurasthenia in the mental and behavioural disorders chapter [Hossenbaccus & White. 2012; WHO.1992]. While the UK National Institute for Health and Clinical Excellence emphasise the condition to be a genuine illness with physical symptoms which can be as disabling as multiple sclerosis, systemic lupus erythematosus, rheumatoid arthritis and other chronic conditions [Action for ME. 2012; NICE. 2007].

1.1.1 Clinical features and diagnosis

NICE recommend in their 2007 guidelines that health practitioners should consider the possibility of CFS/ME if the patient has fatigue with all of the following features; New or a specific onset (that is, it is not lifelong), persistent and/or recurrent, unexplained by other conditions, has resulted in a substantial reduction in activity levels, characterised by post-exertional malaise and/or fatigue (typically delayed, for example by at least 24-hours, with slow recovery over several days). In addition to one or more of the following symptoms; difficulty with sleeping (hypersomnia, unrefreshing sleep, a disturbed sleep-wake cycle), headaches, painful lymph nodes without pathological enlargement, sore throat, cognitive dysfunction (inability to concentrate, impaired short-term memory, difficulties with word finding), general malaise or 'flu-like' symptoms, nausea and/or dizziness and palpitations in the absence of identified cardiac pathology.

In this PhD thesis muscle samples were obtained from CFS/ME patient donors who met the Fukuda (1994) diagnostic criteria. The Fukuda criteria requires a medical professional to perform a full medical history, physical examination, mental status examination and laboratory tests to rule out other conditions that may require treatment. A patient is then classified as exhibiting CFS/ME by meeting the following criteria. Firstly, unexplained persistent or relapsing chronic fatigue is new or has a definite onset and is not caused by ongoing exertion and is not alleviated by rest, resulting in a substantial decrease in pre-illness activities e.g. occupational, educational, social and personal. Secondly, the individual must also exhibit 4 concurrent symptoms which include the following; A substantial impairment in

short term memory, sore throat, tender lymph nodes, muscle pain, joint pain without redness or swelling, headache that is new in type, severity or pattern, unrefreshing sleep and post-exertional malaise lasting more than 24 hours. To obtain a diagnosis the symptoms must have persisted or recurred during at least 6 months of illness and must not have occurred prior to the onset of chronic fatigue.

Interestingly, CFS/ME exhibits a number of similarities with fibromyalgia which is another condition characterised by severe fatigue and of unknown aetiology. However, to achieve a fibromyalgia diagnosis patients must have experienced widespread pain for up to 3 months to achieve a diagnosis. Although only 18% of fibromyalgia patients have also been diagnosed with CFS/ME it has been reported that around 80% of CFS/ME patients have a diagnosis of fibromyalgia. Demonstrating a clear link between the conditions [Courtois et al. 2015].

1.1.2 Treatment and prognosis

Currently, there is no recognised cure for CFS/ME, however, there are treatments recommended to reduce and manage symptoms [White et al. 2011]. For example, NICE recommend Cognitive Behavioural Therapy (CBT) and Graded Exercise Therapy (GET).

Cognitive Behavioural Therapy (CBT) is a psychological therapy model that is commonly used to treat a range of psychological and chronic pain conditions. CBT facilitates the identification of unhelpful, anxiety provoking thoughts and challenges these negative automatic thoughts and dysfunctional underlying assumptions [Price et al. 2008]. In relation to the treatment of CFS/ME, CBT combines a rehabilitative approach of a graded increase in activity with a psychological approach addressing thoughts and beliefs about CFS/ME that may hinder recovery [Price et al. 2008; White et al. 2011]. Effectively, a gradual increase in activity with a psychological approach addressing thoughts and beliefs, such as the link between increased physical activity and worsened physical symptoms can be tested.

Alternatively, GET is an approach that focuses on the basis of deconditioning and exercise tolerance theories of CFS/ME. Such theories assume that CFS/ME is perpetuated by reversible physiological changes of deconditioning and avoidance of activity. Consequently, these changes lead to deconditioning being maintained, which causes an increased perception of effort and leading to further inactivity. Thus, the aim of GET treatment is to gradually

return the patient to appropriate levels of physical activity, in a manner similar to sports training to reverse deconditioning and reduce associated fatigue and disability [White et al. 2011].

A number of systematic reviews support the use of CBT and GET in the management and improvement of symptoms in patients with mild to moderate CFS/ME. Nevertheless, a lot of this evidence is restricted to small trials [Edmonds et al. 2004; Malouff et al. 2008].

However, in the recent PACE study which is the largest CBT and GET study to date White et al. [2011] reported both CBT and GET to moderately improve CFS/ME outcomes when combined with specialist medical care.

Another systematic review conducted by Cairns et al. [2005] investigated patient prognosis in response to both interventions and no treatment. The authors concluded full recovery from untreated CFS/ME was rare, however symptoms may be improved through CBT and/or GET.

1.1.4 Charity involvement

Action for ME is the UK's leading charity for individuals with CFS/ME and their carers. The charity provides information and support, in addition to being at forefront of research promoting more effective treatment and better services since 1989. Action for ME works in partnership with other organisations in order to transform the lives of people with CFS/ME in the longer term [Action for ME. 2012]. This work was partially funded by Action for ME.

1.1.5 Cellular bio-energetic function overview

The cellular bio-energetic function of CFS/ME patient muscle samples will be discussed at length in this thesis, therefore the following section will provide an overview of the key bio-energetic processes occurring at the cellular level.

Mammalian cells require energy in the form of adenosine-5-triphosphate (ATP) to perform a wide variety of cellular processes. Cells rely upon oxidative phosphorylation and glycolysis to produce ATP [Calderon-Montano et al. 2011]. In terms of the overall contribution of each,

under normal conditions oxidative phosphorylation accounts for around 70% of total ATP yield [Zheng. 2012].

During aerobic glycolysis, pyruvate is able to enter the mitochondria to be oxidised to acetyl-coenzyme-A (Acetyl-CoA), which then combines with oxaloacetate to initiate the tricarboxylic acid cycle (TCA) cycle [Zheng. 2012]. This process enables the production of energy in the form of ATP, as well as the generation of nicotinamide adenine dinucleotide phosphate (NADH) and flavin adenine dinucleotide phosphate (FADH) [Harris et al. 2002]. In terms of oxidative phosphorylation, this oxygen-dependent process couples the oxidation of NADH and FADH generated during the TCA cycle with the phosphorylation of adenosine diphosphate (ADP) to form ATP [Cooper. 2000]. This is achieved through the movement of electrons originating from NADH and FADH₂ oxidation through the electron transport chain, which is located in the inner mitochondrial membrane. Effectively, movement of electrons through the chain causes H⁺ to travel from the mitochondrial matrix into the intermembrane space and in the process producing an electrochemical gradient across the inner membrane mitochondrial space [Cooper. 2000]. The resultant electrochemical gradient, promotes H⁺ movement into the mitochondrial matrix through ATP-synthase, enabling the regeneration of ATP from ADP and inorganic phosphate [Calderon-Montano et al. 2011]. In contrast during anaerobic glycolysis pyruvate is reduced to lactate by the cytoplasmic enzyme lactate dehydrogenase before lactate is excreted into the extracellular space through the monocarboxylate transporters (MCTs), the process producing only 2 ATP molecules [Zheng . 2012].

Pyruvate dehydrogenase complex (PDC) is 3-enzyme complex located in the mitochondrial matrix. It controls the conversion of pyruvate to Acetyl-CoA, functioning as the link step between glycolysis and oxidative metabolism. In terms of structure, PDC is completely nuclear encoded and consists of a variety of copies of 2 structures which are distinct but remain functionally interdependent enzymes (E₁- E₃) [Smolle et al. 2006]. PDC is a large complex which combines; pyruvate dehydrogenase (E1), dihydrolipoyl transacetylase (E2), E3 binding domain [E3BP] and dihydrolipoyl dehydrogenase (E3). Pyruvate dehydrogenase (E1) is the first enzyme component of PDC [Jha et al. 2012; Harris et al. 1997; Sanderson et al. 1996; Reed et al. 1990].

PDC is tightly regulated by the enzyme pyruvate dehydrogenase kinase (PDK), PDK is a kinase enzyme which operates by inhibiting PDC through phosphorylation with ATP. It is

regulated by the concentration of ATP and acetyl-coA. Four tissue specific isoforms of PDK have been described (1-4), in human skeletal muscle tissue isoforms 1 and 4 have been reported [Nellemann et al. 2013].

Elevated PDK4 expression has been reported in patients in a number of disease states including but not limited to diabetes [Nellemann et al. 2013; Kulkarni et al. 2012], pulmonary hypertension [Piao et al. 2013] and cancer [Sameen et al. 2011]. Interestingly, glycolytic inhibitors are the subject of intense research to explore the therapeutic potential of specific PDK inhibitors to treat diseases characterised by bio-energetic dysfunction [Jha et al. 2012]. Dichloroacetate (DCA) is a small molecule (150 Da) [Michelakis et al. 2008] which functions to activate PDH enzyme function through inhibition of PDK [Stacpoole, 1989], inducing a greater delivery of pyruvate to the mitochondria [Jha et al. 2012]. The molecule occupies the pyruvate-binding site in the N-terminal regulatory (R) domain of the PDK enzyme [Knoechel et al. 2006]. In terms of sensitivity, the isoform PDK2 has been reported as the most sensitive, PDK3 most resistant and PDK1 and PDK4 relatively sensitive [Baker et al. 2000; Bowker-Kinley, 1998]. Furthermore, the inhibitor has been reported to downregulate glycolysis in both *in vitro* and *in vivo* studies and has been reported to exhibit a substantial therapeutic benefit in many cancer types [Bonnet et al. 2007; Pan and Mak. 2007].

1.1.6 Bio-energetic muscle dysfunction

Although currently the aetiology of CFS/ME remains elusive, previous research has demonstrated inter-linked changes in muscle bio-energetic function in CFS/ME and has identified key therapeutic targets for the reversal of acidosis. For example, *in vivo* studies have demonstrated lowering of anaerobic threshold compared to age, sex and BMI matched controls. Phosphorus magnetic resonance (P MRS) approaches have demonstrated CFS/ME patients to exhibit profound and sustained acidosis when undertaken a standard level of activity (35% maximal voluntary contraction) [Jones et al. 2012]. Effectively, P MRS functions by measuring the chemical content of MR visible nuclei, which includes metabolically relevant phosphorus (^{31}P). P MRS is particularly advantageous for assessing metabolism because chemical properties and environment of each nucleus determine the frequency at which it appears on the MR spectrum, giving rise to peaks corresponding not

only to specific metabolites but also the constituent nuclei of each metabolite [Befroy & Shulman. 2011].

Furthermore, pilot work performed by Boulton [2012] revealed aberrantly low intracellular pH in CFS/ME patient derived muscle following the utilisation of a novel pH nanosensor transfection approach, which enabled the fluorescent-based intracellular assessment of muscle cell pH in real time. The findings demonstrated significantly lower pH in CFS/ME derived muscle cells when compared to non-diseased control cells. Furthermore, dichloroacetate (DCA) a drug which up-regulates the function of PDH through inhibition of its inhibitory kinase PDK was reported to normalise pH. This observation suggested that muscle cell acidosis was in part a consequence of down-regulated PDC function and a concomitant increase in the metabolism of pyruvate to lactic acid. Importantly, this also suggested that intracellular acidosis was fully reversible and therefore peripheral muscle fatigue associated with CFS/ME may be treatable.

1.1.7 Myoblasts and differentiated myotubes

In this thesis, primary human muscle cells were used to investigate muscle bio-energetic function in CFS/ME. Muscle cultures were derived from satellite cells, which were isolated via muscle needle biopsy from the vastus lateralis of CFS/ME patients and control participants. The isolated cells first formed mononucleated myoblasts, which were then differentiated into multi-nucleated myotubes, which have been demonstrated to possess all the key characteristics associated with mature native skeletal muscle [Brown et al. 2015].

The fusion of myoblasts is pivotal to enable the formation of relatively mature multinucleated skeletal muscle myotubes. The myogenesis of skeletal muscle is a highly co-ordinated and complex process, which involves a wide range of intracellular signalling molecules [Brand-Saberi, 2005]. In cell culture, myoblast fusion can be induced by reducing the serum concentration of the media, which suggests differentiation is in part controlled by the signalling pathways of growth factors [Kitzman et al. 2001]. Human primary myoblasts and differentiated myotubes are displayed in culture in Figure 1.1.

In order for differentiation to occur cells must first leave the cell cycle and halt proliferation, to enable this requires the down-regulation of cell cycle activators such as cyclin and Cdk

and the upregulation of key cell cycle inhibitors such as Rb and P2, which are negatively regulated by growth factors [Kitzmann et al. 2001]. Furthermore, myoblast differentiation is also regulated by the expression of muscle-specific helix-loop-helix transcription factors (myogenic regulators, MRFS) such as MYF-5 and MYOG. These transcription factors function as promoters of muscle specific genes that influence upon the fusion of mononucleated myoblasts into mature myotubes [Ridgeway et al. 2000]. For example, MYOG produces heterodimers with proteins of the E family and binds to the Ebox DNA sequence CANNTG [Tapscott and Weintraub, 1991] and is expressed during the later stages of the differentiation process, with evidence suggesting it is upregulated from day 4 differentiation and peaks at day 16. Alternatively, MYF5 is upregulated during the early differentiation stages and has been reported to be highest at day 1 in mammalian cell culture following treatment with differentiation medium. Additionally, expression has been shown to decrease in a time-dependent manner until day 16 differentiation [Kitzman et al. 2001].

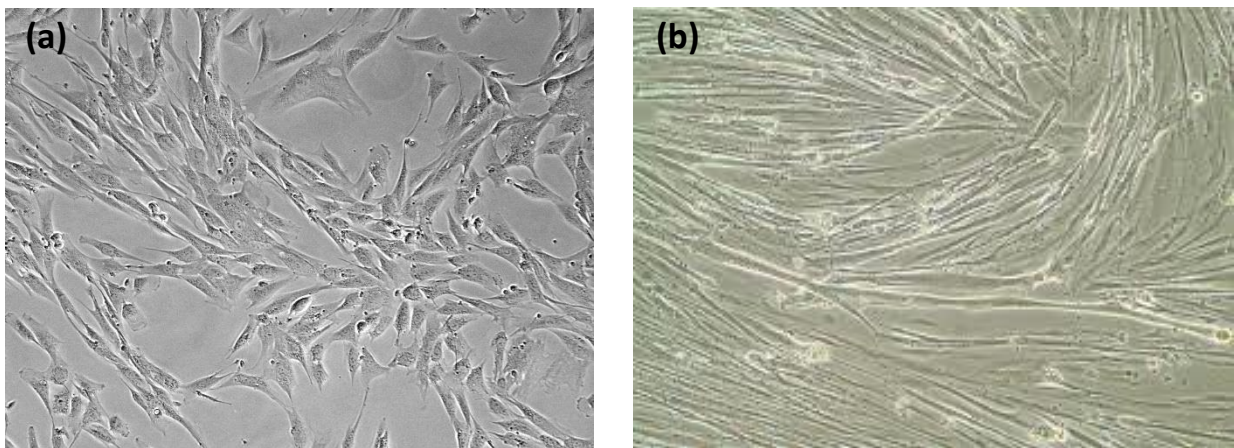


Figure 1.1: (a) Human primary myoblasts in culture and (b) following differentiation into myotubes

1.1.8 Electrical pulse stimulation

Electrical pulse stimulation (EPS) was reported as an *in vitro* exercise model throughout this thesis, enabling the contraction of skeletal muscle cells as a strategy to examine muscle bio-energetic function in CFS/ME muscle samples. A number of studies have reported the use of EPS to induce muscle contraction in skeletal muscle cells. For example, Fujita et al. [2007]

reported EPS to accelerate *de novo* sarcomere assembly, in addition to the induction of Ca²⁺ transients in C2C12 mouse skeletal muscle myotubes. Additionally, Nedachi et al [2008] utilising the same experimental model reported EPS to induce activation of 5' AMP-activated protein kinase (AMPK), increase glucose transport and enhance the release of chemokines such as IL-6. Interestingly, other papers have detailed the use of EPS to investigate human skeletal muscle myotube function [Lambernd et al. 2012; Nikolic et al. 2012], with these studies reporting the model to enhance sarcomere assembly, increase AMPK activation, glycolysis, glucose uptake as well as chemokine expression. More recently, Brown et al. [2015] reported EPS to provide an *in vitro* system to enable the pre-clinical testing of compounds that may influence upon muscle contraction and the metabolic changes associated with exercise. The authors utilised EPS to investigate muscle function in skeletal muscle myotube samples from patients with CFS/ME and controls. The authors reported alternating frequency (low/high) EPS to be successful in enabling muscle contraction and inducing metabolic changes associated with exercise. In healthy cells, EPS induced myotube contraction and increased AMPK activation whereas in the CFS/ME patient group AMPK activation and glucose uptake were impaired. The authors therefore concluded the exercise model to be an effective strategy to investigate metabolic and bio-chemical exercise associated dysfunction in cultured cells.

1.2 Literature Review

Historically, there has been a tendency to draw psychological explanations for the origin of fatigue in CFS/ME, however this model is at odds with patient perceptions of the nature of their condition, with many suggesting a ‘peripheral’ as opposed to ‘central’ basis [Jones et al. 2010]. Interestingly, patients frequently cite difficulty maintaining muscle activity due to perceived ‘lack of energy’ and/or ‘muscle pain’, which can often be serious enough to lead to the avoidance of exercise [Van Oosterwijck et al. 2010]. Thus, it is important to understand peripheral muscle dysfunction in CFS/ME further to inform potential effective treatments for fatigue.

The following sections will explore existing evidence for the role of physiological and biochemical abnormality in the pathophysiology of CFS/ME. Initially, providing an overview of the literature regarding autonomic and immune dysfunction before moving on to more specifically examine the role of peripheral muscle dysfunction as a pivotal cause of fatigue in CFS/ME

1.2.1 Autonomic dysfunction

The compromise of the vascular system and its regulation of the autonomic nervous system (ANS), is a consistent theme that spans throughout existing CFS/ME literature [La mancha et al. 1999; Newton et al. 2009; Rowe et al. 1998]. Effectively, such findings suggest that the abnormal regulation of the ANS plays a pivotal role in the pathogenesis and/or clinical expression of CFS/ME in all or sub-groups of patients [Hagglund et al. 2012; Newton et al. 2009]. The ANS functions as a major regulator of the cardiovascular system, modulating heart rate and blood pressure in the short-term to cope with everyday situations.

Parasympathetic (vagal) modulation functions to decrease heart rate and cardiac contractility, whereas activity of the sympathetic branch opposes these effects and regulates peripheral vasoconstriction. Balanced ANS function is based on strong parasympathetic and efficient but not overactive sympathetic modulation of the heart. Variability of these finely regulated mechanisms may therefore contribute to the expression of fatigue [Newton et al. 2009].

A number of studies have demonstrated the response of the ANS when standing to be abnormal in CFS/ME patients [Hollingsworth et al. 2010; La Manca et al.1999; Rowe et

al.1998]. For example, Hollingsworth et al. [2010] examined haemodynamic responses to immediate and prolonged standing in a large cohort of CFS/ME patients and matched controls. Results demonstrated left ventricular work index on standing to be significantly higher in the CFS/ME group, confirming that the hearts of the CFS/ME group appeared to be working harder in response to the stress of standing in comparison to controls. Similarly, Frith et al. [2012] reported autonomic dysfunction in CFS/ME patients, with results demonstrating systolic blood (SBP) pressure on standing to be significantly decreased with reductions in both sympathetic and parasympathetic components of SBP variability ($P < 0.0001$). These findings were in agreement with previous studies that have demonstrated spectral indices of blood pressure variability (BPV) to be significantly lower in CFS/ME patients when compared to controls [Duprez et al.1998; Yoshiuchi et al. 2004].53

In relation to the physiological mechanisms that may account for blood pressure variability, Frith et al. [2012] suggested it to be possible that CFS/ME patients suffer from pathological sympathetic activity over a period of time leading to autonomic effectors (heart and blood vessels) becoming resilient to physiological sympathetic stimulation.

Additionally, previous studies have also reported ANS dysfunction indicated by abnormalities in blood pressure measurements when performed over 24-hours [Newton et al. 2009; Yoshiuchi et al. 2004]. For example, in a study by Newton et al. [2009], CFS/ME and matched controls performed 24-hour ambulatory blood pressure assessment. Results demonstrated significantly lower SBP ($P < 0.0001$), mean arterial blood pressure ($P = 0.0002$), exaggerated diurnal variation ($P = 0.009$) and a significant inverse relationship between increasing fatigue and diurnal variation of blood pressure ($P < 0.05$). Thus, demonstrating lower BP and diurnal variation to occur in patients with CFS/ME. Effectively, the authors proposed three potential mechanisms to account for BP Variation. Firstly, BP may be secondary to fatigue, i.e. reflecting a decrease in the amount of physical activity (PA) (reduction in exercise induced BP) performed by patients who view themselves as fatigued. However, an argument against this explanation is that, firstly the effect is principally expressed when physical activity is low and secondly, previous studies have demonstrated PA to only explain one part of BP and HR variability [Cavelaars et al. 2004 and 2002]. Another potential mechanism relates to dysfunction of the hypothalamic pituitary adrenal axis and finally BP deregulation may be causally linked to fatigue expression, for example

low BP may give rise to fatigue through either or both the central nervous system and peripheral hypo perfusion [Newton et al. 2009].

Alternatively, a number of studies have failed to confirm the presence of autonomic dysfunction during rest [Boneva et al. 2007; Wyller et al. 2008; Yamamoto et al. 2003], leading to the suggestion that CFS/ME may be a physiological condition of orthostasis. For example, Wyller et al. [2008] assessed autonomic function in an adolescent CFS/ME patient group during rest and a mild orthostatic challenge. Results demonstrated CFS/ME patients to exhibit greater variability in Heart Rate (HR) and HR variability during an orthostatic challenge in comparison to the control. However, these measures did not significantly differ between the CFS/ME and control group during rest.

Nevertheless, in contrast Wyller et al. [2011] reported abnormal autonomic dysfunction during rest and a mild orthostatic challenge in adolescent CFS/ME patients. HR and blood pressure were recorded continuously and non-invasively during supine rest and lower body negative pressure of -20mmHg to stimulate mild orthostatic stress, indices of BP variability and baroreflex (α -gain) were computed from microvariate and bivariate spectra in the low frequency (LF) and high frequency (HF) band. Results demonstrated SBP in the HF range was lower in CFS/ME patients compared to controls at rest and during low body negative pressure (LBNP). Additionally, during LBNP compared to controls α -gain LF/ α -gain HF increased more in CFS/ME patients. Thus, the authors concluded all results to be suggestive of a greater shift from parasympathetic to sympathetic baro-reflex control in CFS/ME. Furthermore, the authors postulated an increase in the sympathetic component of the baroreceptor feedback with even mild orthostatic stress in CFS/ME patients to indicate early sympathetic activation and potentially reflect diminished baro-reflex reserve for more severe stressors. These changes further suggest that the baro-reflex may have diminished ability to buffer a variety of internal and external influences on arterial pressure, but particularly those related to upright activity and ambulation. These findings agree with an earlier report regarding the combined effect of orthostatic stress and isometric exercise in CFS/ME patients [Wyller et al. 2008]. However, it is important to acknowledge that the Wyller [2011] study did exhibit crucial methodological limitations. Firstly, respiratory activity has been demonstrated to change during orthostatic challenge and therefore may have influenced cardiovascular variability [Cooke et al. 1999] as this factor was not controlled during the

investigation. Secondly, blood and/or plasma volume were not measured, therefore hypovolemia could not be ruled out.

1.2.2 Central sensitisation

Central sensitisation is defined as an increase in the responsiveness of central neurons to input from unimodal and polymodal receptors [Meyer et al. 1995]. Central sensitisation involves a number of top-down and bottom-up mechanisms, which contribute to the hyper-responsiveness of the central nervous system to a variety of stimuli [Nijs et al. 2012]. It is important to note that an alteration in central pathways may impact upon peripheral muscle fatigue.

In terms of central impairment, the perception of fatigue during exercise is not always abnormal and serves an important function during significant physical exertion [Jones et al. 2012]. For example, in a study conducted by Amann and Dempsey [2008] peripheral muscle fatigue was induced in patients and consequently fatiguing muscle was reported to play a pivotal role in the determination of central motor drive and force output. Therefore, suggesting the presence of a feedback signal from peripheral muscle to the central nervous system, to ensure fatigue is confined to a certain level, preventing damage to the individual. However, it is plausible that peripheral fatigue experienced in CFS/ME is the direct result of excessive signal feedback, leading to a disproportionate perception of fatigue early in the fatiguing process associated with physical activity [Jones et al. 2010].

Interestingly, evidence exists to suggest the role of central impairment in CFS/ME patients. For example, Whiteside et al. [2004] reported CFS/ME patients to exhibit a dysfunction in nociceptive inhibition during exercise. This was evidenced by a decrease in pain threshold following exercise, which is abnormal as pain threshold usually increases during exercise due to a greater release of endogenous opioids and additional inhibitory mechanisms (descending inhibition). This exercise-induced abnormality was also reported in two additional studies [Meeus et al. 2010; Van Oosterwijck et al. 2010]. For example, Meeus and colleagues [2010] compared CFS/ME patients with chronic pain (n=26), healthy control participants (n=31) and chronic back pain patients (n=21). Participants all completed a submaximal aerobic exercise protocol, which was followed by venous blood sampling (nitric oxide) and algometry (hand,

arm, calf, lower back). Results demonstrated patients with CFS/ME to exhibit lower pain threshold compared to both the healthy control participants and chronic lower-back pain participants. Taken together the results demonstrated CFS/ME patients to have a lack of descending inhibition during exercise. The implication of a lack of endogenous inhibition has been suggested to account in part for the post-exertional malaise (PEM) experienced by CFS/ME patients.

Evidence also exists to suggest a role of generalised hyperalgesia in CFS/ME as outlined by Nijs et al. [2012]. It has been postulated that lower pain thresholds in symptomatic locations represents primary hyperalgesia due to sensitised nociceptors within injured peripheral muscle tissue. However, the authors also commented that when pain thresholds are detected in asymptomatic areas central sensitisation is at play. Two studies conducted by Vecchiet et al. [2003] investigated the effect of electrical stimulation of muscle tissue, skin and sub cutis in relation to pain threshold in CFS/ME patients and healthy control participants.

Interestingly, in both studies CFS/ME participants reported there to be no significant difference between groups for electrical pain threshold of skin and sub cutis. Nevertheless, a much lower electrical pain threshold was observed in all sites of muscle tissue (trapezius, quadriceps and deltoid) for the CFS/ME group only, illustrative of hyperalgesia in CFS/ME.

1.2.3 Immune dysfunction

Increasing evidence suggests that CFS/ME is characterised by a profound complex imbalance in immune function [Broderick et al. 2010; Harvey. 2008]. In relation to immunological dysfunction, there is largely no universal agreement as regards the mechanisms due to the varying methodological approaches and study quality. However, evidence suggests natural killer cell function, oxidative stress, altered cytokine profiles/increased pro-inflammatory cytokines and movement towards a Th2 dominant profile to be possible aetiological mechanisms underlying CFS/ME.

In relation to NKC function Maher et al. [2005] observed a significant reduction in NKC associated perforin levels in CFS/ME plasma samples compared to healthy controls moreover the authors also reported reduced perforin content in cytotoxic T cells in CFS/ME subjects. Perforin is a cytolytic protein capable of non-specifically lysing a number of target cells, thus the authors suggested such a deficiency to demonstrate altered immune function in

patients with CFS/ME. Fletcher [2010] also reported diminished NKC function in CFS/ME subjects due to a markedly reduced CD26 density on lymphocyte surfaces and a reduced concentration of the enzyme in the plasma. Collectively, these findings demonstrate a loss of innate immune function and chronic immune stimulation with CFS/ME.

In relation to cytokine abnormalities existing research suggests the pro-inflammatory cytokines it play a pivotal role in CFS/ME [Fletcher.2009; Patarca. 2001; Gupta. 1998]. For example, Robson-Ansley et al [2004] reported recombinant IL-6 (rIL-6) administration to reduce exercise performance in trained endurance athletes. Moreover, the authors speculated these findings to be transferable to patients suffering from CFS/ME, as the condition is associated with reduced exercise tolerance and exaggerated symptoms of fatigue. They suggested an increase in IL-6 to result in impaired neural function; essentially IL-6 may activate the hypothalamic pituitary-adrenal axis by enhancing a natural rise in serum prolactin a marker of neuroendocrine 5-hydroxytryptamine (5-HT) activity. Thus, this rise may stimulate the 5-HT receptors that control prolactin release. Interestingly, the central fatigue hypothesis suggests that 5HT concentrations to relate to impaired CNS function during exercise [Blomstrand. 1995].

In contrast, Robinson et al. [2010] suggested F2 isoprostanes, a marker of oxidative stress to be a key molecular mediator in CFS/ME as no difference in plasma IL-6 or its receptors (sgp-130/SIL-6R) were observed at rest or during exercise in CFS/ME patients. However, F2 isoprostanes were consistently higher at rest, during exercise and 24 hours post exercise. Thus demonstrating a possible role of reactive O₂ species in the pathology of CFS/ME, which has been reported by Jammes et al. [2005] and Kennedy [2005] who observed associations between levels of O₂ stress and CFS/ME symptoms.

However, in a recent report Broderick et al. [2010] criticised previous studies that had examined the expression and function of individual cytokines in CFS/ME as individual cytokine levels often do not differ between CFS/ME patients and healthy controls. Therefore, the authors examined the co-expression of 16 cytokines in 40 female CFS/ME patients. Results illustrated a diminution of Th1 and Th17 function and a movement towards Th2 type immunity in addition to evidence of increased NK cell function. Similarly, several groups have reported a shift from a Th1 to Th2 cytokine profile in CFS patients. Skowera [2004] for example examined the frequency of type 1 and 2 regulatory CD4 and CD8T cells in 35 patients with CFS/ME. Results illustrated a bias towards a Th2 immune response.

Furthermore, Breu et al. [2011] reported the presence of a possible imbalance in Th1/Th2 response in CFS/ME characterised by significant increase in IL-10, IFN γ - and TNF α in a CFS patient cohort when compared to healthy controls. Such increases in IL-10 are suggestive of a persistent chronic infectious state and may be associated with a dampening of NK cell and CD8+ immune response.

Regarding the relevance of this shift in immune response in relation to CFS/ME, Torres-Harding [2008] reported an increased Th2 response to be associated with a higher reported sleep disruption in patients. Interestingly Th2 cytokines IL-4 and IL-10 have been associated with decreased sleep and an increased Th2 response has been associated with increased cortisol levels, which were reported to increase slow wave sleep and inhibit REM [Buckley & Schatzberg. 2005]

In a study conducted by Bradley et al. [2013] the authors suggested alterations in B-cell maturation to lead to an increased tendency towards autoimmunity and subtle humoral immune dysfunction in a CFS/ME patient cohort. A detailed characterisation of the proportions of different B-cell subsets in 33 patients who met the Fukuda criteria for CFS/ME and 24 age and gender matched controls. Results demonstrated CFS/ME patients to exhibit a greater number of naïve B-cells as a percentage of lymphocytes when compared to controls (6.3% verses 3.9% respectively, $P=0.034$), a greater number of transitional B-cells, 65% verses 47% in controls ($P=0.003$), increased numbers of transitional B-cells 1.8% verses 0.8% in controls ($P=0.025$) and reduced numbers of plasmoblasts (0.5% verses 0.9% respectively ($P=0.013$)).

Remarkably, the finding that CFS/ME patients exhibited increased numbers of transitional B cells may suggest a defective negative selection checkpoint. B cell development in the bone marrow is an antigen independent and tightly regulated process and BCR expression enables negative selection of autoreactive B cells and their subsequent elimination by apoptosis (Keenan et al. 2008). Surviving B cells subsequently become transitional B cells (CD19+, CD38++, IgM+, IDG+) and travel via the blood into secondary lymphoid organs (e.g. spleen) where complete maturation occurs [Verma et al. 2007]. Generally, only 10-20% of immature B cells produced in the bone marrow reach the spleen, as a large number are depleted via the negative selection checkpoint because of the expression of defective autoreactive BCRs [Bradley et al. 2013]. Therefore, the authors postulated a defective negative selection checkpoint to lead to a subtle tendency towards autoimmunity in the CFS/ME cohort.

Interestingly, increased numbers of transitional B cells have also been reported in a number of other patient groups that exhibit humoral immunity, including patients with systemic lupus erythematosus [Cuss et al. 2006] X linked lymphoproliferated disease and patients recovering from hematopoietic transplantation [Lee et al. 2009]. Nevertheless, it is important to interpret the findings with caution, as it cannot be ascertained as to whether the changes exhibited are the cause of CFS/ME symptoms or simply the result of patient inactivity, sleep disturbance or raised stress. However, in a recent large placebo controlled clinical trial, symptomatic benefit was shown in 67% of CFS/ME patients after receiving two infusions of rituximab versus 13% of CFS/ME patients receiving placebo [Fluge et al. 2011]. Rituximab has many mechanisms in addition to depleting CD20⁺ cells (B cells) down-regulating CD40L and CD80 on B cells, decreasing CD4 effector cells, reducing NK cell no and activation inducing macrophage maturation and reducing tumor necrosis factor (TNF) [Kessel et al. 2008]. Thus, indicating the involvement of B-cells in the pathology or perpetuation of CFS/ME or at least in a subset of patients.

When examining the evidence base, it is clear that CFS/ME is underlined by a complex cascade of immune abnormalities, resulting in a loss of innate immune function and chronic immune stimulation.

1.2.4 Oxidative stress

Reactive species and free radicals are molecules that due to their electronic instability (e.g. unpaired electron) promote oxidation reactions with other molecules such as proteins, lipids and DNA to become stabilised [Gomes et al. 2012]. Many reactive species are O₂ centred (e.g. H₂O₂) and are denominated reactive oxygen species (ROS). Some ROS are also free radicals e.g. superoxide anion (O₂⁻) and nitric oxide anion (NO) because they have an unpaired electron [Zadak. 2009]. One important source of ROS/free radical production is believed to be the result of the leakage of electrons in the mitochondrial respiratory chain, due to inadequate coupling of the electron transfer between complexes I and III [Vollard et al. 2005; Xu et al. 2009]. The movement of electrons through the electron transport complex (ETC) and subsequent sites of O₂⁻ production are illustrated in Figure 1.2 . It has been suggested that for every molecule of ATP generated by the mitochondria, one molecule of superoxide is generated [Jason et al. 2009]. O₂⁻ then combines with nitric oxide to form

peroxynitrite which breaks down to release a hydroxyl radical that can induce genetic damage. Peroxynitrite (ONOO^-) production also leads to an increase in the generation of both nitric oxide and superoxide, which act to produce more peroxynitrite, creating a self-sustaining cycle known as lipid peroxidation [Jason et al. 2009].

Interestingly, enhanced oxidative stress has been reported in CFS/ME patients. For example, studies have demonstrated that CFS/ME patients exhibit excessive production of ROS following physical exertion [Brkic et al. 2010; Jammes et al. 2012] as well as altered resting blood oxidant to antioxidant status [Brkic et al. 2010; Jammes et al. 2012; Maes et al. 2011].

Additionally, bio-chemical markers associated with oxidative stress play a pivotal role in skeletal muscle fatigue [Finsterer et al. 2012], which is often cited as a debilitating symptom experienced by CFS/ME patients [Van Oosterwijck et al. 2010]. Oxidative and nitrosative stress involves the enhanced production of ROS and reactive nitrogen species (RNS), in addition to other free radicals. These reactive species have the potential to disrupt cell membrane function through lipid peroxidation, as well as damage to functional proteins and DNA. This can ultimately lead to alterations in cell structure and disease initiating mutations [Bloomer et al. 2005].

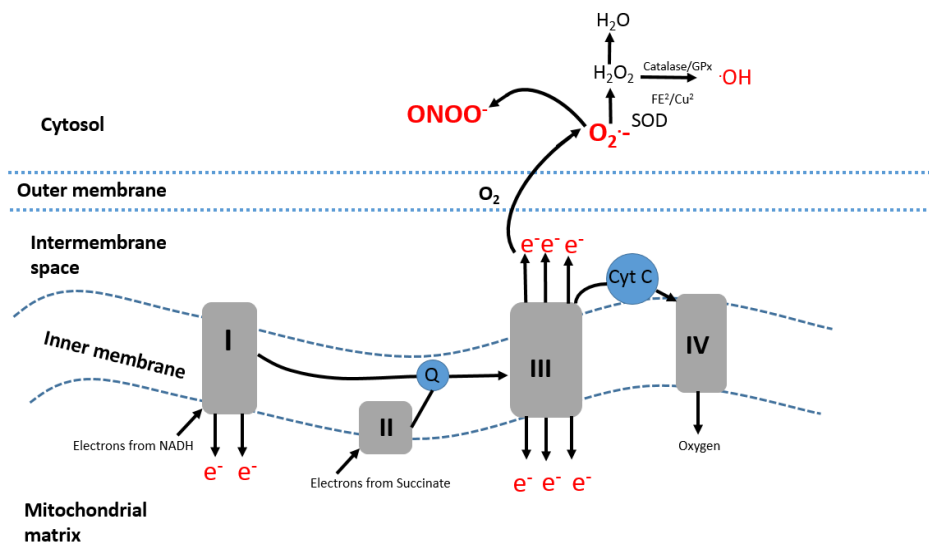


Figure 1.2: Complex I and II have both been accepted as major sites of electron leakage and O_2^- production. If O_2^- enters the cytosol it may further react with NO and redox ions to form additional reactive oxygen species e.g. H_2O_2 and ONOO^- .

Additionally, elevated ROS/RNS exhibit the capacity to profoundly impair mitochondrial function, this has been proposed to be due to the accumulation of oxidative modified mitochondrial proteins, lipids and DNA [Crane et al. 2013]. With the potential of these factors to induce electron transport chain dysfunction, an impairment in cellular bioenergetics and ultimately skeletal muscle fatigue. Furthermore, skeletal muscle is a post-mitotic tissue so is extremely susceptible to mitochondrial oxidative damage, due to being terminally differentiated and because of a slow cellular turn over and high metabolic rate [Crane et al. 2013].

Mitochondria are a major source of ROS generation in cells and are therefore highly susceptible to oxidative damage. For example, they exhibit reduced levels of antioxidants such as glutathione, in comparison to levels found in the cytosol [Fernandez-Checa. 1998]. This relative lack of protection enables mitochondrial DNA (mtDNA) to be damaged, leading to major changes in polypeptide synthesis. Finally, mt DNA repair enzyme activity is considerably lower than found in the nucleus [Wan et al. 2009]. The combination of the effects lead to a reduced electron transfer rate with subsequent reduction in the rate of ATP synthesis [Genova et al. 2004].

In relation to the impact of elevated oxidative stress on muscle dysfunction, muscle specific symptoms of fatigue have been reported to be proportional to the blood levels of a marker of ROS induced lipid peroxidation, named thiobarbituric acid reactive substances (TBARS) [Vecchiet et al. 2003]. TBARS occurs in the serum as a result of lipid peroxidation of low-density lipoproteins and oxygen mediated injury of myocyte membranes [Hulbert et al. 2005]. Lipid peroxidation of skeletal muscle fibres induces a loss of membrane excitability as a result of altered activation of K^+ channels [Jammes et al. 2012; Luin et al. 2011]. Additionally, muscle biopsies from healthy adults indicated that the intensity of membrane excitation was proportional to K^+ efflux measured in plasma [Marcos et al. 1995], with an increase in ROS generation acting to inhibit Na^+-K^+ pump activity, thus reducing the K^+ outflow and muscle membrane excitability [Juel et al. 2006]. Furthermore, in another study [Fulle et al. 2003] CFS/ME patients were reported to exhibit a reported loss of Na^+/K^+ and Ca^{2+} -ATPase pump regulation, in addition to alterations in the ryanodine channels within the sarcoplasmic reticulum membrane. This was related to increased fluidity of the sarcoplasmic membrane as a result of ROS induced formation of lipid hydroperoxides, which the authors

suggested to support the hypothesis that sarcolemma conduction system and some aspects of Ca^{2+} transport are negatively influenced in CFS/ME.

Furthermore, in another study [Jammes et al. 2012] blood oxidant status and muscle membrane excitability were measured pre and post exercise. The case control study compared CFS/ME patients (n=55) and healthy matched controls (n=40). However, within the CFS/ME cohort sub groups emerged, firstly those who had reported severe infection (e.g. Pneumonia, Septis, encephalomyelitis, H1N1 influenza) within 3-7 months preceding onset of CFS/ME symptoms . Secondly, those who had practiced sport to a high level (>6hrs per week) for 6 years prior to the onset of CFS/ME symptoms and with no history of severe infection. Thirdly, a combination group who had practiced sport to a higher level and had experienced an infection prior to the onset of symptoms. Finally, the last group of CFS/ME patients exhibited no relevant pre-illness history. Participants were required to complete a maximal incremental cycle based protocol to reach the point of maximal oxygen uptake. In relation to markers of oxidative stress, blood samples were obtained at pre, during and post exercise time points, enabling plasma concentration of TBARS and endogenous antioxidant (reduced ascorbic acid) to be measured. Additionally, action potential (M-wave) was evoked in the vastus lateralis to explore muscle excitability.

Results demonstrated that all CFS/ME patients to exhibit abnormal biochemical and electrophysiological measures indicated by elevated TBARS levels prior to exercise and an altered M-wave configuration during and after exercise. These findings are in agreement with other studies [Jammes et al. 2009 and 2005] which also reported an elevated blood oxidant status at rest, which was accentuated by exercise in addition to reduced muscle excitability. For example, one study described enhanced exercise induced oxidative stress, in CFS/ME patients indicated by early changes in TBARS and reduced ascorbic acid in response to incremental exercise. Additionally, CFS/ME patients also exhibited marked alterations in muscle membrane excitability; indicate by lengthened M-wave duration during the recovery period [Jammes et al. 2005].

However, a pivotal finding of the more recent study [Jammes et al. 2012] was that CFS/ME patients who had a history of infection exhibited significant accentuation of blood oxidant status at rest and muscle hypoexcitability at work, in addition to a significantly reduced potassium outflow in response to maximal exercise in this group. Therefore, CFS/ME patients with a history of previous severe infection exhibited greater biological and EMG

disorders in comparison to those who reported completing a high level of physical activity before the onset of fatigue related symptoms. The authors concluded that severe infection could act as a stressor responsible for the alteration in blood oxidant status, which may help to explain impaired exercise-induced K^+ outflow and altered membrane excitability. However, it is important to acknowledge that the CFS/ME patients self-reported physical activity level for the 6 years prior to the onset of CFS/ME symptoms. Therefore, it is possible CFS/ME patients overestimated their physical activity habits prior to developing CFS/ME symptoms.

1.2.5 Mitochondrial dysfunction

There is evidence to suggest that mitochondrial dysfunction plays a key role in CFS/ME aetiology. Lowered ATP production, impaired oxidative phosphorylation and mitochondrial damage has been reported in patients with CFS/ME [Filler et al. 2014; Myhill et al. 2009]. Moreover, these CFS/ME patients share common skeletal muscle symptoms associated with diseases linked to mitochondrial dysfunction, for example muscle pain, fatigue and cramping [Morris & Maes. 2014; Fulle et al. 2007].

Additionally, there is accumulating evidence to suggest that abnormally high lactate levels and intracellular acidosis exhibited in patients with CFS/ME are the result of impaired mitochondrial function [Morris & Maes. 2014; VanNess et al. 2010]. For example, CFS/ME patients exhibit profound and sustained intracellular acidosis of the peripheral musculature following relatively low-level exercise, resulting in a decreased ATP as a result of an overutilization of the lactate dehydrogenase pathway [Jones et al. 2010; Jones et al. 2012]. Upon the point of exhaustion CFS/ME, patients have been found to have intracellular ATP concentrations that are lower than those found in non-diseased controls. This would be indicative of disorders relating to oxidative metabolism. Moreover, in a recent review [Morris & Maes. 2014] the authors concluded the response to exercise in CFS/ME patients to be similar to that typically exhibited in individuals with mitochondrial disease. Additionally, there were also a number of similarities between symptoms of mitochondrial disease and the physio-somatic symptoms of CFS/ME. For example, muscle pain, cramps, weakness and myalgia's [Morris & Maes. 2014; Fulle et al. 2007; Nijs et al. 2004].

Mitochondrial dysfunction in CFS/ME may be explained not only by elevated oxidative and nitrosative stress but also increased immune-inflammatory stress pathways [Morris & Maes. 2012]. For example, chronic low grade inflammation in CFS/ME has been demonstrated through increased levels of pro-inflammatory cytokines (IL-1, TNF α) and a movement towards a Th2 dependant immune response, in addition to inflammatory mediators including nuclear factor- κ B (NF- κ B) and elastase [Nijs et al. 2004]. Further, evidence of elevated oxidative and nitrosative stress is demonstrated by increased isoprostane levels, peroxides and protein carbonyl levels, indicating damage to lipids and mitochondrial protein as previously discussed [Jammes et al. 2012].

In relation to immune dysfunction a study was conducted to examine cytokine networks in 40 female CFS/ME patients and 40-case matched controls [Broderick et al. 2010]. The authors examined a total of 16 cytokines and results revealed a diminution of Th1 and Th17 function and a movement towards Th2 type immunity. Similarly, several other groups have reported a shift for a Th1 to Th2 cytokine profile in CFS/ME patients [Brenu et al. 2011; Fletcher et al. 2009. Skowera et al. 2004]. For example, Skowera et al [2004] examined the frequency of type 1 and 2 regulator CD4 and CD8T cells in 35 patients with CFS. Results illustrated a bias towards a Th2 immune response.

Elevated levels of the inflammatory mediator NF- κ B [Maes et al. 2011] have also been reported in the blood samples of CFS/ME patients. NF- κ B is a major upstream intracellular mechanism, which regulates inflammatory and oxidative stress mediators [Maes et al. 2007]. For example, it functions to trigger inducible nitric oxide synthetase (iNOS) expression, which promotes the production of nitric oxide (NO) by monocytes and macrophages [Paludan. 1998].

Maes and colleagues [2007] examined the production of NF- κ B P50 in unstimulated 10ng/mL TNF- α and 50ng/mL phorbol 12-myristate 13-acetate (PMA) stimulated peripheral blood lymphocytes in 18 CFS/ME patients and 18 age-matched controls. Results demonstrated both unstimulated (10ng/mL) TNF- α (P=0.0009) and PMA (0.008) stimulated production of NF- κ B to be significantly higher in CFS/ME patients compared to controls. Additionally, positive correlations were reported between the production of NF- κ B and severity of illness in CFS/ME patients (as measured by fibro fatigue scale) and with symptoms, including muscular fatigue and tension. Interestingly, NF- κ B signals the function of p53 is pivotal in the regulation of glycolysis and mitochondrial respiration as it reduces the

activity of the glycolytic pathway and stimulates mitochondrial O₂ consumption and aerobic respiration. However, when inhibited there is a shift to anaerobic glycolysis and reduced O₂ consumption [Morris and Maes. 2012].

Aside from immune dysfunction, several studies have reported mitochondrial dysfunction to be caused by abnormal levels of key mitochondrial enzymes. For example, in a paper by Smit and colleagues [2011] a significant reduction in citrate synthase in quadriceps biopsies from patients with CFS/ME was reported when compared to healthy control samples. Citrate synthase is an enzyme located in the mitochondrial matrix, which plays a critical role in the tricarboxylic cycle [Tymoczko. 2010]. Similarly, the McArdle group [1996] reported a decrease in citrate synthase in addition to succinate reductase and cytochrome- C oxidase (Complex IV), which are two of the four mitochondrial transmembrane enzyme complexes of the electron transport chain. However, in contrast to the McArdle group [1996], Smit and colleagues [2011] attributed the decrease in transmembrane enzymes to be the result of reduced physical activity levels frequently present in CFS/ME patients, as opposed to underlying mitochondrial dysfunction. Nevertheless, a paper by Edwards and colleagues [1993] reported there to be no significant difference in partial cytochrome-C oxidase in skeletal muscle biopsies between CFS/ME patients and healthy matched controls.

Evidence also exists to suggest that CFS/ME patients exhibit significantly reduced levels of Co-enzyme Q10, an important mitochondrial nutrient that functions as a co-factor for the production of ATP in the mitochondria and displays significant antioxidant activity [Jones et al. 2009]. In a study conducted by Maes and colleagues [2009], CFS/ME patients (n=58) displayed significantly lowered plasma co-enzyme Q10 concentration compared to healthy controls (n=22). Moreover, in CFS/ME patients there was a significant inverse relationship exhibited between plasma co-enzyme Q10 concentration and fatigue severity measured by means of the fibro fatigue scale.

Furthermore, CFS/ME patients may also exhibit alterations in L-carnitine and acyl carnitine homeostasis [Reuter et al. 2011]. L-carnitine is a ubiquitously occurring trimethylated amino acid that plays an important role in the transport of long chain fatty acids across the inner mitochondrial membrane, which is essential for energy production via fatty acid metabolism [Reuter et al. 2009]. Previous studies have reported a reduction in endogenous plasma L-carnitine and total carnitine levels in patients with CFS/ME [Karatsune et al.1998 and 1994]. Nevertheless, other studies have not always replicated these findings [Jones et al. 2005;

Majeed et al. 1995] . Reuter and colleagues [2011] postulated this to be related to the use of varying methodological approaches, with some studies solely focused on free carnitine and total carnitine rather than the level of each individual acyl carnitine, which may be ‘cancelled out’ by normal levels of other acyl carnitines in CFS/ME patients. To overcome this weakness Reuter and colleagues [2011] utilised tandem mass spectrometry to quantify individual acyl carnitine levels in plasma samples to provide a more detailed carnitine profile. Results demonstrated significant alterations in C8:1, C12DC, C14, C16:1, C18, C18:1, C18:2 and C18:1-Oh acyl carnitines. What is more, significant correlations between acyl carnitine and clinical symptomology were observed.

1.2.6 Post-exertional malaise and immune function

CFS/ME patients report a changeable pattern to their symptoms and physical and cognitive capabilities, often with severe symptom exacerbation following physical exercise [Fukuda et al. 1994; Whiteside et al. 2004]. This is termed PEM, with approximately 95% of CFS/ME patients experiencing PEM [Prins et al. 2007]. As regards the cause of PEM, it has been suggested that exercise may exhibit the ability to amplify pre-existing immune abnormalities, in addition to oxidative and nitrosative stress [Twisk. 2015]. Immunological abnormalities have been reported following exercise in CFS/ME. For example, observations in CFS/ME symptom flare after moderate intensity exercise have been reported to be directly linked to the levels of Interleukin 1 β (IL-1 β), IL-12, IL-8, IL-10 and IL-13, 8 hours post-exercise [White et al. 2012]. Additionally, sustained increase in plasma TNF α in CFS/ME patients and not in healthy controls has been observed post-exercise [White et al. 2012]. Moderate intensity exercise has also been reported to induce a larger 48-hour post exercise area under the curve for IL-10 [Light et al. 2012].

However, a recent systematic review [Nijs et al. 2014] compared 23 case control studies regarding exercise-induced immunological changes in CFS/ME patients verses healthy control participants. The authors reported in comparison to healthy participants, CFS/ME patients exhibited a more exaggerated response in the complement system, indicated by C4a split product level, enhanced oxidative stress, combined with a delayed and reduced antioxidant response. Finally, the authors also reported there to be an apparent alteration in immune cell gene expression profile, which was evidenced by an increase in post-exercise

IL-10 and toll like receptor 4 gene expression. Nonetheless, in contrast to previous work there was no reported change in circulating pro and/or anti-inflammatory cytokines. Effectively, the review confirmed CFS/ME patients to respond differently to an exercise-based stimulus, resulting in a more pronounced immune response.

1.2.7 Muscle bio-energetic dysfunction

1.2.7.1 Intracellular acidosis

Even a minimal decrease in muscle pH interferes with cross bridge binding and ATPase activity due to competitive binding and reduced enzyme function [Jones et al. 2009]. Decreased intracellular pH impairs oxidative enzyme activity and may adversely affect ryanodine receptor function [Bellinger et al. 2008]. Furthermore, recent studies confirm the presence of a peripheral bio-energetic abnormality in CFS/ME patients [Jones et al. 2010; VanNess et al. 2010; Jones et al. 2012].

In a cross, sectional study conducted by Jones et al [2010] novel ³¹P MRS techniques were utilised to investigate muscle acid handling following exercise in CFS/ME patients and the relationship with autonomic dysfunction. CFS/ME patients (n=16) and age and sex matched normal controls (n=8) performed an exercise protocol, which consisted of 3 minutes of plantar flexion at 35% load maximum voluntary contraction (MVC) at a rate of 0.5Hz, followed by 3 minutes recovery. After the period of exercise ³¹P MRS was utilised to investigate intramuscular acid handling. Results demonstrated, a significant suppression of proton efflux immediately post-exercise ($P<0.05$) in CFS/ME patients, in addition to a significantly ($P<0.05$) prolonged time taken to reach maximum proton efflux. In controls there was a strong inverse correlation between maximum proton efflux and nadir pH following exercise ($r^2=0.6$, $P<0.01$). However, in CFS/ME patients the significance of this relationship was lost ($r^2=0.003$; $P=ns$). Collectively, these findings demonstrated CFS/ME patients to exhibit abnormalities in the recovery of intramuscular pH following standardised exercise. Effectively, proton efflux is crucial for acidosis resolution, with the immediate post-exercise period associated with maximum proton efflux in healthy individuals; however this initial fast phase does not occur in CFS/ME patients [Jones et al. 2010]. Furthermore, the authors also acknowledged there to be a close relationship between the degree of intramuscular acidosis and proton efflux, demonstrating a closely regulated process, which

has been observed in healthy individuals [Kemp et al. 1997] in addition to the study control group. Nevertheless, they concluded this relationship to be lost in CFS/ME patients. However, the relatively small sample size of this study made it difficult to draw firm conclusions. Therefore, additional adequately powered studies are required to investigate the relationship further.

In contrast, Wong et al. [1992] reported no difference in intramuscular pH at rest, exhaustion and during early and late recovery, following a graded exercise test to exhaustion. Measurement of intramuscular pH of the gastrocnemius muscle was performed via ³¹P nuclear magnetic resonance (NMR) spectroscopy. However, the authors did report changes in PCr and pH to occur more rapidly at the onset of exercise in CFS/ME patients compared to controls, which was suggested to be indicative of accelerated glycolysis. Nevertheless, the authors postulated this finding to reflect a lower level of physical endurance due to inactivity in the CFS/ME patient cohort. Nonetheless, it is important to interpret this study with caution, as the CFS/ME patients were able to complete a maximal exercise test to exhaustion. Thus, suggesting the patients in this study were not severely physically incapacitated by the condition and therefore may not be representative of the wider CFS/ME population.

Alternatively, Jones et al. [2012] reported prolonged post-exercise recovery from acidosis. In this investigation CFS/ME, patients and age/sex matched healthy controls performed a similar exercise protocol (35% MVC plantar flexion for 180s, 390s recovery, repeated 3 times). In addition, participants were also required to perform a MVC assessment and a cycle based cardio-respiratory fitness test. Results revealed the ability to divide patients into two distinct groups; 8 (45%) demonstrated normal phosphocreatine (PCr) depletion in response to exercise at 35% MVC, with MVC strength values comparable to controls. In the second grouping, 10 CFS/ME patients exhibited low PCr depletion (generating abnormally low MVC values). Results demonstrated anaerobic threshold (AT), VO₂ and VO₂ peak to be significantly reduced in all CFS/ME patients compared to controls. Essentially, one implication of a reduced AT would be a reliance upon anaerobic as opposed to aerobic metabolism, with the predicted consequence of greater short-term acid generation within the muscle as a result of an over-utilisation of the lactate dehydrogenase pathway [Jones et al. 2010]. This was further confirmed by MRS demonstrating CFS/ME patients to exhibit markedly increased intramuscular acidosis compared to controls at a similar work rate

following each 3-minute bout, with prolongation (almost 4-fold) in the time taken for pH to recover to baseline, replicating previous findings [Jones et al. 2010].

Based on the findings the authors went on to conclude that the profound intramuscular acidosis exhibited with repeat exercise was at least in part related to poor aerobic capacity. This in relation to the physiology of fatigue closely mirrors that observed in patients with the autoimmune disease primary biliary cirrhosis (PBC). PBC exhibits a comparable peripheral pattern and a similar level to fatigue to CFS/ME [Hollingsworth et al. 2010]. In a study by Hollingsworth and colleagues [2010], PBC patients exhibited profound and comparable intramuscular acidosis to the CFS/ME patients in the Jones et al. [2012] study following the same repeat exercise protocol. However, one pivotal difference between the conditions, which may contribute to the severity of fatigue in CFS/ME, is related to acid homeostasis. In contrast to CFS/ME patients, when PBC patients undergo repeat exercise the extent of acidosis within the muscle decreases with each repeated exercise bout. This may suggest a compensatory mechanism, which operates to resolve excess acidosis. One potential mechanism that may account for this is increased proton flux, in addition to the speed of onset of maximum proton excretion with repeat exercise [Hollingsworth et al. 2010; Jones et al. 2012]. This mechanism also plays a role in mitochondrial disease whereby increased proton efflux post-exercise helps to compensate for decreased aerobic capacity [Trenell. 2006]. Nevertheless, it would seem that in comparison to other conditions that exhibit reduced aerobic capacity and acidosis, CFS/ME patients are unable to compensate for an increased reliance upon anaerobic energy pathways during exercise [Jones et al. 2012].

While the production of protons as a by-product of anaerobic metabolism is a feature of normal metabolism, the body requires mechanisms to effectively manage protons as even small changes in pH dramatically alter enzyme kinetics, decrease muscle function and cause fatigue [Allen et al. 1995]. Thus, slow recovery from acidosis in CFS/ME may relate to ineffective exporting of protons from the recovering muscle. Protons are actively transported out of the muscle by 3 main groups of proton transporters [Juel et al. 2006]; Na⁺/H⁺ anti-transporters, namely NHE1 [Street et al. 2001] sodium/bicarbonate co-transporters (NBCs) [Kristensen et al. 2004] and most predominantly monocarboxylate transporters (MCT), whereby in the latter group MCT-1 and MCT-4 isoforms seem to be of particular importance in human skeletal muscle [Wilson et al. 1998]. During rest, intramuscular pH is predominantly influenced by NHEs, with MCTs and NBCs playing a greater role during the

recovery from muscular contraction. These transporter systems are under autonomic regulation [Halenstrep & Prince. 1998]. It is therefore possible that the impaired function of acid transporters occurs in CFS/ME, which may be a consequence of autonomic dysfunction as previously discussed an abnormality found frequently in CFS/ME [De Becker et al. 2000; Newton et al. 2007; Anderson et al. 2008]. Additionally, it is also possible that reduced vascular run off, (related to autonomic dysfunction) resulting in decreased vascular flow into and out of the muscle following exercise, which may have an effect on O₂ delivery, potentially limiting the function of the three enzyme complex pyruvate dehydrogenase complex (PDC) [Anderson et al. 2008].

A sub group of patients (low PCr depletion) exhibited no excess acidosis, which appeared to be entirely the consequence of lower MVC values compared to normal PCr depletion controls. Interestingly, despite markedly lower MVC values the patients perceived themselves to be working maximally immediately following the MVC assessment. However, despite this perception the authors postulated that these findings related to a type of exercise avoidance behaviour. Kinesiophobia is defined as an excessive, irrational and debilitating fear of movement and activity resulting from a fear of vulnerability to painful injury or re-injury [Kori et al. 1990; Nijs et al. 2004] and has been reported to play a role in a variety of musculoskeletal disorders, including CFS/ME patients who experience widespread pain [Silver et al. 2002; Vlaeyen et al, 1995]. Therefore, the fear of the consequence of an action such as exercise may lead to avoidance behaviour in patients with CFS/ME patients [Jones et al. 2012] However, the study was limited, as it did not include a repeat assessment. Therefore, it is impossible to ascertain whether the groups were stable i.e. avoiding the first exercise session and consistently doing so.

Interestingly, previous studies have also reported the existence of sub-groups within CFS/ME patient cohorts in relation to glycolytic metabolism and intramuscular pH regulation [Lane et al. 1998a; Wong et al. 1997; Barnes et al. 1993]. However, unlike the studies conducted by Jones et al [2012 and 2010], the earlier studies have reported an absence in abnormal glycolytic metabolism in the majority of the CFS/ME patients. For example, Barnes et al [1993] explored intramuscular pH regulation in 46 CFS/ME patients via ³¹P MRS. Results demonstrated no consistent abnormalities in glycolysis or pH regulation at rest or following exercise when the group was taken as a whole. Nonetheless, 12 patients did exhibit abnormal PCr depletion following exercise, with 6 patients within this group displaying increased

intramuscular acidification in relation to PCr depletion and the other 6 demonstrating reduced acidification. This study illustrates the heterogeneity within the CFS/ME patient population and suggests sub-groups do exist in CFS/ME that display abnormal glycolytic metabolism and intramuscular pH. Similarly, in Lane's studies [1998a and 1998b] CFS/ME patients completed a sub anaerobic threshold exercise protocol. Results revealed only a small sub-group (8%) of CFS/ME patients to have an increased blood lactate response to exercise and muscle biopsies revealed a relative increase in type 2 glycolytic fibres for this sub-group.

1.2.7.2 Acidosis as a consequence of impaired PDC function

It is possible that the previously demonstrated muscle cell acidosis in CFS/ME is the consequence of down-regulated PDC function and a concomitant increase in the metabolism of pyruvate to lactic acid (over-utilisation of lactate dehydrogenase (LDH) pathway). PDC is a 3 protein complex responsible for a series of reactions that convert pyruvate to acetyl coA during aerobic respiration. Principally, when the function of this complex is reduced, pyruvate that has been generated by glycolysis accumulates within the cells and is metabolised anaerobically to lactic acid. This accumulation causes a drop in pH and concurrent deterioration in muscle function [Forque et al. 2003].

The phenotype of fatigue exhibited by CFS/ME patients closely mirrors that seen in fatigue associated PBC. For example, Hollingsworth et al [2010] reported that PBC patients exhibited significant acidosis because of an over-utilisation of the lactate dehydrogenase pathway, following a low-level repeat exercise protocol [Hollingsworth et al. 2010]. Furthermore, the authors postulated that the increased dependence on anaerobic pathways of energy production resulted in the fatigue associated with PDC.

The idea that impaired PDC function leads to an over-utilisation of the lactate-dehydrogenase pathway is in agreement with other studies. For example, Murrough et al [2009] reported significantly higher levels of lactate in ventricular cerebrospinal fluid in CFS/ME patients in when compared to healthy controls. Similarly, Constantin-Teodosiu and colleagues [2009] in an experimental exercise model using rats, demonstrated that when PDC function was decreased via the use of PPAR modulating drugs which up-regulated PDK function, lactate accumulated intramuscularly which led to decreased muscle function.

Therefore, impaired energy generation in muscle, an increase in the lactate/pyruvate ratio in CFS/ME patients and a propensity towards excess intra-muscular acidosis following limited

exercise suggests PDC dysfunction in the muscles of CFS/ME patients, which has implications in relation to the expression of fatigue. Furthermore, as previously discussed CFS/ME patients exhibit significant intramuscular abnormalities relating to both acid generation and clearance from tissue, which has been postulated to relate to a centrally-perceived “stop signal”, leading to a disproportionate perception of fatigue [Jones et al. 2009]. Figure 1.3 illustrates the effect of PDC downregulation, leading to an over-utilisation of the lactate dehydrogenase pathway.

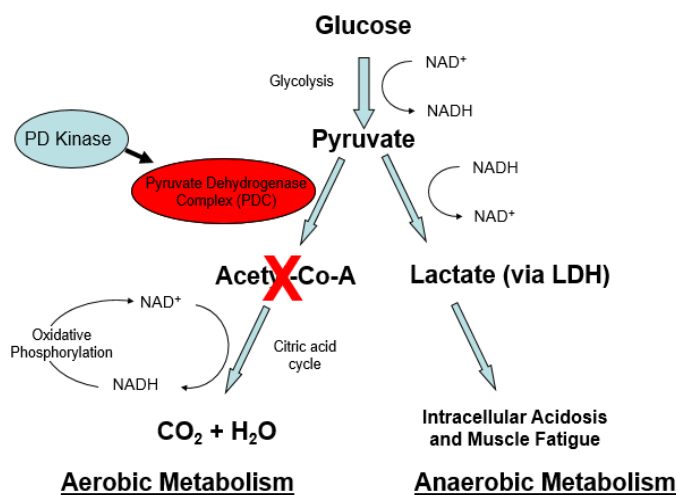


Figure 1.3: Diagram outlining PDC function when down-regulated, leading to an over utilisation of the lactate dehydrogenase pathway.

1.2.8 Abnormal AMPK activation and glucose uptake

A recent study [Brown et al. 2015] reported striking biochemical differences in skeletal muscle cultures established from 10 CFS/ME patients and 7 age-matched controls. Samples were subjected to EPS for 24-hours and examined for exercise associated changes. Key differences emerged, in the basal state there was increased myogenin expression in CFS/ME samples but a decrease in IL-6 secretion during differentiation when compared to control samples. Following 16 hours EPS there was a significant increase ($P < 0.006$) in AMP-activated protein kinase (AMPK) phosphorylation and glucose uptake ($P < 0.0001$) in control samples when compared to unstimulated control cultures. Alternatively, CFS/ME samples demonstrated no increase in AMPK phosphorylation or glucose uptake. Nevertheless, glucose

uptake remained responsive to insulin, suggesting exercise related dysfunction. Furthermore, IL-6 secretion on response to EPS was significantly reduced ($P < 0.05$ vs corresponding control) across all time points measured.

AMPK is a phylogenically-conserved fuel-sensing enzyme, consisting of a heterotrimeric complex composed of a catalytic α subunit and regulatory β and γ subunits [Richter et al. 2009]. During exercise under normal physiological conditions, AMPK is activated in the skeletal muscle of healthy humans, with exercise suggested to be the most powerful physiological activator of AMPK [Chen et al. 2003; Winder et al. 2000]. Upon activation AMPK sets into motion processes that increase ATP production such as glucose transport and fatty acid oxidation [Richter et al. 2009], while decreasing others that consume ATP, for example lipid and protein synthesis and cell growth and proliferation [Hardie et al. 2007; Kahn et al. 2005; Richter et al. 2009]. Additionally, evidence also suggests AMPK to have a broader range of actions including mitochondrial bio-genesis [Winder et al. 2000; Jorgensen. 2005] and skeletal muscle angiogenesis [Ouchi et al. 2005]. Suggesting AMPK activation to play a key role in peripheral muscle function during exercise.

However, it is important to consider the role of physical activity on AMPK activation. For example, trained subjects have been reported to express higher levels of $\alpha 1$ AMPK in comparison to untrained individuals [Nielsen. 2002]. Furthermore, a 3-week endurance training intervention with young male participants resulted in increases in $\alpha 1$ and $\alpha 2$ AMPK protein expression in addition to ACC- β phosphorylation, which suggested basal activity of AMPK to be, increased [Frosig et al. 2004]. Therefore, it should be considered that the decreased AMPK activation reported in CFS/ME muscle samples after EPS may be the result of lowered physical activity levels of the CFS/ME sample donors, when compared to control donors. As regards study recruitment criteria, although participants were age matched it was not specified whether any measures had been taken to ensure donors were matched in terms of physical activity habits. Future work is required with patients and controls who are matched in terms of physical activity.

In addition to impaired activation of AMPK, the study also reported reduced IL-6 secretion in response to EPS. Interestingly, previous studies have reported IL-6 to activate AMPK in skeletal muscle by increasing the concentration of cAMP and secondly by increasing the AMP:ATP ratio [Kelly. 2009].

The inability of CFS/ME muscle cells to activate AMPK and glucose uptake in addition to reduced IL-6 secretion in response to EPS is suggestive of underlying peripheral muscle dysfunction in CFS/ME. However, further work is required to investigate the mechanisms that lead to impaired activation of AMPK in those with CFS/ME.

1.3 Conclusion

There is increasing evidence to suggest muscular bio-chemical abnormality to play a major role in CFS/ME associated fatigue. Patients have been reported to exhibit profound intramuscular dysfunction regarding acid generation and clearance, with a tendency towards an over-utilisation of the lactate dehydrogenase pathway following relatively low-level activity. However, the precise mechanisms underlying the dysfunction are yet to be fully elucidated but may relate to impaired function of PDC. Future work is required to examine PDC function *in vitro*, to determine the mechanisms responsible for muscle cell acidosis in and explore the capacity of drugs to normalise bio-energetic function and ultimately treat peripheral fatigue.

1.4 Aims

The aim of this thesis is to improve understanding of the mechanisms underlying peripheral muscle dysfunction and the associated perception of fatigue in patients with CFS/ME through the development of an *in vitro* muscle cell culture testing platform.

Preliminary work has demonstrated an aberrantly low intracellular pH in CFS/ME patients, which was subsequently normalised following treatment with PDK inhibitor DCA. Which was revealed when pH was measured using a novel pH sensing platform [Boulton. 2012]. Therefore, a key aim of this thesis is to validate and further develop this *in vitro* model as a pre-clinical testing system, to firstly determine the presence of acidosis in CFS/ME and secondly the extent in which pH is modulated by bio-energetic enzyme inhibition. The identification of therapeutic targets within the biological muscle system are warranted to enable the development of appropriate therapies to inform clinical trials in CFS/ME.

Specific chapter aims are stated below.

Chapter 2 will further validate and develop the fluorescent pH responsive nanosensor previously reported by Boulton [2012]. Additionally, PDK inhibitor DCA was added to the cells to assess the capacity of drugs to normalise intracellular acidosis *ex vivo*.

Chapter 3 will investigate O_2^- generation in CFS/ME patient myoblasts *ex vivo*, performed following chemical stimulation with ethanol or incubation with lactic acid. Specific experimental hypotheses are (1) CFS/ME myoblasts exhibit elevated O_2^- generation following ethanol stimulation, compared to controls. (2) O_2^- elevated in CFS/ME patient samples compared to controls following incubation with lactic acid.

Chapter 4 will measure cytosolic pH via the application of the widely used free dye 2',7'-bis(2-carboxyethyl)-5(6) carboxyfluorescein (BCECF) in CFS/ME myoblasts and differentiated myotubes at rest and following electrical pulse stimulation (EPS), performed *ex vivo* experimental work performed. The specific experimental hypotheses are (1) CFS/ME myoblasts and differentiated myotubes exhibit significantly lower intracellular pH at rest and following EPS, when compared to controls. (2) Treatment with PDK inhibitor DCA normalises intracellular pH in CFS/ME samples at rest and following EPS

Chapter 5 will measure glycolytic function in CFS/ME patient myoblast and myotube samples via extracellular flux analysis, in addition to extracellular lactate quantification performed *ex vivo*. Which will be performed using extracellular flux glycolytic stress testing and L-lactate measurements via fluorometric assay. The specific experimental hypotheses proposed are (1) Increased glycolytic activity in CFS/ME patient myoblasts and myotubes when compared to controls. (2) Normalisation of glycolytic function comparable to controls following treatment with PDK inhibitor DCA.

Chapter 6 will investigate CFS/ME myoblast and myotube mitochondrial function *ex vivo* via XF analysis. Function will be assessed following the addition of key inhibitors of the mitochondrial electron transport chain. Further investigation into CFS/ME myoblast and myotube function will be performed by varying substrate availability (glucose) during the mitochondrial stress test. Specific experimental hypotheses are (1) CFS/ME myoblasts and myotubes exhibit impaired mitochondrial function. (2) CFS/ME samples exhibit a greater impairment in mitochondrial function compared to controls when substrate availability is reduced.

The conclusions of each chapter are summarised in **Chapter 7**.

References

- Action for ME (2012) An investigation into NHS specific service provision for people with ME/CFS. 1-34
- Allen, D, G. Lannergren, J. Westerblad, H. (1995) Muscle cell function during prolonged activity: Cellular mechanism of fatigue. *Experimental Physiology*. 8 (4) 497-527
- Amann, M. Dempsey, J, A. (2008) Locomotor muscle fatigue modifies central motor drive in healthy humans and imposes limitations on exercise performance. *Journal of physiology*. 586, 161-175
- Anderson, E, B. Boesen, F. Henricksen, O. (2008) Local and central sympathetic reflex control of blood flow in skeletal muscle and subcutaneous tissue in normal man. *Clinical Physiology Functional Imaging*, 11. 451–458
- Baker, J, C. Yan, X. Peng, T. Kasten, S. Roche, T, E. (2000) Marked differences between two isoforms of human pyruvate dehydrogenase kinase. *J. Biol. Chem*. 275, 15773–15781
- Barnes, P, R. Taylor, D, J. Kemp, G, J. Radda, G, K. (1993). Skeletal muscle bioenergetics in chronic fatigue syndrome. *J Neurol Neurosurg Psychiatry*. 56, 679-683
- Befroy, D, E. Shulman, G, I. (2011) Magnetic resonance spectroscopy studies of human metabolism. *Diabetes*. 60, 1361-1369
- Bellinger, A, M. Mongillo, M. Marks, A, R. (2008) Stressed out: the skeletal muscle ryanodine receptor as a target of stress. *Journal of Clinical Investigation*. 118:445-53.
- Bloomer, R, J. Goldfarb, A, H. Wideman, L. McKenzie, M, J. Consitt, L,A. (2005) Effects of acute aerobic and anaerobic exercise on blood markers of oxidative stress. *Journal of Strength and Conditioning Research*. 19, 276-285
- Blomstrand, E. Andersson, S. Hassmen, P. Ekblom, B. Newsholme, E, A. (1995) Effect of branched-chain amino acid and carbohydrate supplementation on the exercise-induced change in plasma and muscle concentration of amino acids in human subjects. *Acta Physiologica Scandinavica*. 153, 87–96

Boneva, R, S. Decker, M, J. Maloney, E, M. Lin, J, M. Jones, J, F. Helgason, H, G.(2007) Higher heart rate and reduced heart rate variability persist during sleep in chronic fatigue syndrome: a population based study. *Autonomic Neuroscience Basic Clinical*. 13, 94–101

Bonnet, S. Archer, S, L. Allalunis-Turner, J. Haromy, A. Beaulieu, C. Thompson, R. Lee, C,T. Lopaschuk, G, D. Puttagunta, L. Bonnet, S. Harry, G. Hashimoto, K. Porter, C, J. Andrade, M, A. Thebaud, B. Michelakis, E, D. (2007) A mitochondria-K⁺ channel axis is suppressed in cancer and its normalization promotes apoptosis and inhibits cancer growth. *Cancer Cell* 11: 37 – 51

Boulton, S, J. (2012) Integrated free radical sensor systems for investigation of cellular models of disease. PhD thesis, Newcastle University. Identifier: <http://hdl.handle.net/10443/1427>

Bowker-Kinley, M, M. Davis, W, I. Wu, P. Harris, R, A. Popov, K, M. (1998) Evidence for existence of tissue-specific regulation of the mammalian pyruvate dehydrogenase complex. *Biochem. J.* 329.191–196

Bradley, A, S. Ford, B. Bansal, A, S. (2013) Altered functional B-cell subset populations in patients with chronic fatigue syndrome compared to healthy controls. *Clinical and Experimental Immunology*. 172 (1) 73-80

Brand-Saberi, B. (2005) Genetic and epigenetic control of skeletal muscle development. *Ann Anat.* 187, 199-207

Brenu, E,W. van Driel, M, L. Staines, D,R. Ashton, K,J. Ramos, S, B. Keane, J. Klimas, N, G. Marshall-Gradisnik, S, M. (2011). Immunological abnormalities as potential biomarkers in Chronic Fatigue Syndrome/Myalgic Encephalomyelitis

Brkic S, Tomic S, Maric D, Novakov Mikic A, Turkulov V.(2010) Lipid peroxidation is elevated in female patients with chronic fatigue syndrome. *Medical Science Monitor*. 16(12) 628–632

Broderick,G. Fruite, J. Kreitz, A. Vernon, S, D. Kilmas, N. Fletcher, M-A. (2010) A formal analysis of cytokine networks in CFS. *Brain Behaviour and Immunity*. 24 (7) 1209-1217

Brown,A,E. Jones, D,A. Waker,M. Newton. J,L. (2015) Abnormalities of AMPK activation and glucose uptake in Chronic Fatigue Syndrome. *PLOS ONE*. 10 (4)

- Buckley, T.M. Schatzberg, A.F. (2005). Review: On the interactions of the hypothalamic-pituitary-adrenal (HPA) axis and sleep: Normal HPA axis activity and circadian rhythm, exemplary sleep disorders. *The Journal of Clinical Endocrinology and Metabolism*, 90(5), 3106-3114
- Cairns, R. Hotopf, M. (2005) systematic review describing the prognosis of chronic fatigue syndrome. *Occupational Medicine*, 20–31
- Calderon-Montano, J. Burgos-Moron, E. Perez-Guerrero, C. Salvador, J. Robles, A. Lopez-Lazaro, M. (2011) Role of the Intracellular pH in the Metabolic Switch between Oxidative Phosphorylation and Aerobic Glycolysis - Relevance to Cancer. *CANCER*.2 (3)
- Carruthers, B, M. Jain, A,K. De Meirlier, K, L. Peterson, D,L. Basted, A, C. Flor-Henry, P. Joshi, P. Powles, P,A,C. Sherkey, J,A. Vande Sande, M, I. (2003) Myalgic encephalomyelitis/ chronic fatigue syndrome: Clinical working case definition, diagnostic and treatment protocols. *Journal of Chronic Fatigue Syndrome*. 11 (1) 7-36
- Cavelaars, M. Tulen, J, H. Van Bommel, J,H. Borg, M, J. Mulder, P, G. Van den Meiracker, A, H.(2002) Determinants of ambulatory blood pressure response to physical activity. *Journal of Hypertension*. 22 (1) 89-96
- Chen, Z, P. Stephens, T, J. Murthy, S. Canny, B, J. Hargreaves, M. Witters, L, A. Kemp, B, E. McConell, G, K. (2003) Effect of exercise intensity on skeletal muscle AMPK signaling in humans. *Diabetes*. 52, 2205–2212.
- Christ, B. Bran-Saberi, B. (2002) Limb muscle development. *International dev bio*. 46, 405-914
- Constatin-Teodosiu, D. Baker, D, J. Constantin, D. Greenhaff, P, L. (2009) PPAR-delta agonism inhibits skeletal muscle PDC activity, mitochondrial ATP production and force generation during prolonged contraction. *Journal of Physiology*. 587 (1) 231-239
- Cooke, W, H. Hoag, J, B. Crossman, A, A. Kuusela, T, A. Tahvanainen, K, U, O. Eckberg, D, L (1999) Human responses to upright tilt: A window on central autonomic regulation. *The Journal of physiology*.517, 617-628

Cooper, G, M. (2000) *The Cell: A Molecular Approach*. 2nd edition. Sunderland (MA): Sinauer Associates; 2000. *The Mechanism of Oxidative Phosphorylation*. Available from: <http://www.ncbi.nlm.nih.gov/books/NBK9885/>

Courtois, I. Cools, F. Calsius, J. (2015) Effectiveness of body awareness interventions in Fibromyalgia and Chronic Fatigue Syndrome: A systematic review and meta analysis. *Journal of body work and movement therapies*. 19, (1) 35-56

Crane, J, D. Abadi, A. Hettinga, B, P. Ogbourn, D, I. MacNeil, L, G. Steinberg, G, R. (2013) Elevated mitochondrial oxidative stress.

Cuss, A, K. Avery, D, T. Cannons, J, L. Yu, L, J. Nichols, K, E. Shaw, P, J. (2006) Expansion of functionally immature transitional B cells is associated with human immunodeficient states characterised by impaired humoral immunity. *Journal of Immunity*. 176; 1506-1516

De Becker, P. Roeykens, J. Reynders, M. McGregor, N. De Meirier, K. (2000) Exercise capacity in chronic fatigue syndrome. *Archives of Internal Medicine*. 27, 160, 3270-3277

Department of Health (2002) CFS/ME Working Group. A report of the CFS/ME Working Group: Report to the Chief Medical Officer of an Independent Working Group. London: Department of Health

Duprez, D, A. Debuyzere, M, L. Drieghe, B. Vanhaverbeke, F. Taes, Y. Michelson, W. (1998) Long- and short-term blood pressure and RR-interval variability and psychosomatic distress in chronic fatigue syndrome. *Clinical Science*. 94, 57–63.

Edmonds, M. McGuire, H. Price, J, R. (2004) Exercise therapy for chronic fatigue syndrome. *Cochrane Database of Systematic Reviews*. 3.

Edwards, R, H. Gibson, H. Clague, J, E. Helliwell, T. (1993) Muscle histopathology and physiology in chronic fatigue syndrome, *Symposium*. 173. 102–117

Fernandez-Checa, J, C. García-Ruiz, C. Colell, A. Morales, A. Marí, M. Miranda, M, Ardite E. (1998) Oxidative stress: role of mitochondria and protection by glutathione. *Biofactors*. 8 (1-2) 7-11

- Filler, K. Lyon, D. Bennet, J. McCain, N. Elswick, R. Lukkahatai, N. Saligan, L. N. (2014) Association of mitochondrial dysfunction and fatigue: A review of the literature. *BBA Clinical*. 1, 12-23
- Finsterer, J. (2012) Biomarkers of peripheral muscle fatigue during exercise. *BMC Musculoskeletal Disorders*. 13, (218), 1-13
- Fletcher, M, A. Zeng, X, R. Maher, K. Levis, S. Hurwitz, B. Antoni, M. Broderick, G. Kumas, N, G. (2009) Biomarkers in chronic fatigue syndrome: Evaluation of natural killer cell function and dipeptidyl peptidase IV: CD26. *PLOS ONE*. 5 (5) 1-7
- Fluge, Ø. Bruland, O. Risa, K. Storstein, A. Kristoffersen, E, K. (2011) Benefit from B-Lymphocyte Depletion Using the Anti-CD20 Antibody Rituximab in Chronic Fatigue Syndrome. A Double-Blind and Placebo-Controlled Study. *PLoS ONE* 6(10): e26358
- Forque, F, O. Brivet, M. Boutron, A. Vequaud, C. Marsac, C, C. Zabet, A, N, D, M. Benelli, C. (2003) Differential effect of DCA treatment on the pyruvate dehydrogenase complex in patients with severe PCHC deficiency. *Paediatric Research*. 53 (5), 793-799
- Frith, J. Watson, S. Bolton-Maggs, P, H, B. Newton, J, L. (2012) Cognitive symptoms are common in immune thrombocytopenia and associate with autonomic symptom burden. *European Journal of Haematology*. 83 (3) 224-228
- Frosig, C. Jorgensen, S, B. Hardie, D, G. Richter, E, A. Wostaszewski, J, F. (2004) 5'-AMP-activated protein kinase activity and protein expression are regulated by endurance training in human skeletal muscle. *Amateur Journal Physiology Endocrinology Metabolism*. 286, 411-417
- Fujita, H. Nedachi, T. Kanzaki, M. (2007) Accelerated de novo sarcomere assembly by electric pulse stimulation in C2C12 myotubes. *Exp Cell Res*. 313(9):1853–65.
- Fukuda, K. Straus, S, E. Hickie, I. Sharpe, M, C. Dobbins, J, G. Komaroff, A. (1994) The chronic fatigue syndrome: a comprehensive approach to its definition and study. *Annals of Internal Medicine*. 121, 953–9.
- Fulle, S. Belia, S. Vecchiet, J. Morabito, C. Vecchiet, L. Fano, G. (2003) Modification of the functional capacity of sarcoplasmic reticulum membranes in patients suffering from chronic fatigue syndrome. *Neuromuscular Disorders*, 13, 479-484.

- Fulle, S. Pietrangelo, T. Mancinelli, R. Saggini, R. Fano, G. (2007) Specific correlations between muscle oxidative stress and chronic fatigue syndrome: a working hypothesis. *Journal of Muscle Research Cell Motility*. 28: 355-362
- Genova, M, L. Pich, M, M. Bernacchia, A. Bianchi, C. Biondi, A. Bovina, C. Falasca, A.I. Formiggini, G. Castelli, P. Lenza, G. (2004) The mitochondrial production of reactive oxygen species in relation to ageing and pathology. *Annals of the New York Academy of Science*. 1011, 86-100
- Gomes, E, C. De Oliveira, M, R. Silva, A, N. (2012) Oxidants, antioxidants and the beneficial roles of exercise-induced production of reactive species. *Oxidative medicine and cell longevity*. 755, 132
- Gupta, S, Aggarwal, S. Rathanravan, B. Lee, T. (1998) Th1- and Th2-like cytokines in CD4+ and CD8+ T cells in autism. *Journal of Neuroimmunology*. 85(1)106–109
- Hagglund, H. Uusitalo, A. Peltonen, J, E. Koponen, A, S. Aho, J. Tiianen, S. Seppanen, T. Tuippo, M. Tikkanen, H, O. (2012) Cardiovascular autonomic nervous function and aerobic capacity in type 1 diabetes. *Frontiers Physiology*. 7 (3) 1-8
- Halenstrup, A, P. Price, N, T. (1998) The proton- linked monocarboxylate transporter (MCT) family: structure, function and regulation. *Biochemical Journal*. 343, 281-299
- Hardie, D,G. (2007) AMP-activated/SNF 1 protein kinases: conserved guardians of cellular energy. *Nature Reviews Molecular Cell Biology*. 8 (10) 774-785
- Harris, R, A. Bowker-Kinley, M, M. Wu, P. Jeng, J. Popov, K, M. (1997) Dihydrolipoamide dehydrogenase-binding protein of the human pyruvate dehydrogenase complex. DNA-derived amino acid sequence, expression, and reconstitution of the pyruvate dehydrogenase complex. *J Biol Chem*. 272(32):19746–19751
- Harvey, L. (2008) The effect of developmental vitamin D3 deficiency on brain development, behaviour and immune function in the Sprague-Dawley rat. *Biomedical science*. 1-6
- Hollingsworth, K, G. Jones, D, E, J. Taylor, R, Blamire, A, M. and Newton, J, L. (2010) Impaired cardiovascular response to standing in Chronic Fatigue Syndrome. *European Journal of Clinical Investigation*. 40, 608–615.

Hossenbaccus, Z. White, P. D. (2013) Views on the nature of CFS: Content analysis. *JRSM Short Report*. 4 (1) 1-6

Hulbert, A. J. (2005) On the importance of fatty acid composition of membranes for aging. *Journal of Theoretical Biology*. 234, 277-88.

IOM institute of medicine. (2015) Beyond myalgic encephalomyelitis/chronic fatigue syndrome: redefining the illness. Washington DC. National academies

Jammes, Y., Steinberg, J. G., Delliaux, S. Bregeon, F. (2009) Chronic fatigue syndrome combines increased exercise-induced oxidative stress and reduced cytokine and Hsp responses. *Journal of Internal Medicine*, 266, 196- 206

Jammes, Y. Steinberg, J. G. Delliaux, S. (2012) Chronic fatigue syndrome: Acute infection and history of physical activity affect resting levels and response to exercise of plasma oxidant/antioxidant status and heat shock proteins. *Journal of Internal Medicine*, 272, 74-84.

Jammes, Y. Steinberg, J. G. Guleu, R. Delliaux, S. (2012) Chronic fatigue syndrome with history of severe infection combined altered blood oxidant status and reduced potassium efflux and muscle excitability at exercise. *Open Journal of Internal Medicine*. 3, 98-105

Jammes, Y. Steinberg, J. G. Delliaux, S. and Bregeon, F. (2009) Chronic fatigue syndrome combines increased exercise-induced oxidative stress and reduced cytokine and Hsp responses. *Journal of Internal Medicine*, 266, 196- 206

Jammes, Y. Steinberg, J. G. Delliaux, S. (2011) Chronic fatigue syndrome. Acute infection and history of physical activity affect resting levels and response to exercise of plasma oxidant/antioxidant status and heat shock proteins. *Journal of Internal Medicine*, 266, 196-206. *Journal of Internal Medicine*, 257, 299-310

Jason, L. A. Sunnquist, M. Brown, A. Newton, J. L. Stranf, E. S. Vernon, S. D. (2015) Chronic fatigue syndrome versus systemic exertion intolerance disease. *Fatigue: Biomedicine, health and behaviour*. 3 (3) 127-141

Jason, L. A. Porter, N. Herrington, J. Sorenson, M. Kubow, S. (2009) Kindling and oxidative stress as contributors to myalgic encephalomyelitis/ Chronic fatigue syndrome. *Journal of Behaviour Research and Neuroscience Research*. 1 (2) 1-17

Jha, M, K. Jeon, S. Suk, K. (2012). Pyruvate Dehydrogenase Kinases in the Nervous System: Their Principal Functions in Neuronal-glia Metabolic Interaction and Neuro-metabolic Disorders. *Current Neuropharmacology*, 10 (4) 393–403.

<http://doi.org/10.2174/157015912804143586>

Jones, D, E, J. Hollingsworth, K. Blamire, A, M. Taylor, R. Newton, J, L.(2010) Abnormalities in pH handling by peripheral muscle and potential regulation by the autonomic nervous system in chronic fatigue syndrome. *Journal of Internal Medicine*. 26, 394–401

Jones, D, E. Hollingsworth, K, G. Jakovljevic, D, G. Faltakhova, G. Pairman, J. Blamire, A, M. Trennel, M, I. Newton, J, L.(2012) Loss of capacity to recover from acidosis on repeat exercise in chronic fatigue syndrome: A case control study. *European Journal of Clinical Investigation*. 42 (2) 184-194

Jones, D, A. Turner, D, L. McIntyre, D, B. Newham, D, J. (2009) Energy turnover in relation to slowing of contractile properties during fatiguing contractions of the human anterior tibialis muscle. *Journal of Physiology*. 587. 4329-4338

Jorgensen, S, B. Wojtaszewski, J, F. Viollet, B. Andreelli, F. Birk, J, B. Hellsten, Y. Schjerling, P. Vaulont, S. Neufer, P, D. Richter, E, A. Pilegaard, H. (2005) Effects of alpha-AMPK knockout on exercise-induced gene activation in mouse skeletal muscle. *FASEB Journal*. 19, 1146-1148

Juel, C. (2006) Muscle fatigue and reactive oxygen species. *The Journal of Physiology*, 576, 279-288 *Physiology*, 71, 207-214.

Kahn, B, B. Alquier, T. Carling, D. Hardie, D,G. (2005) AMP-activated protein kinase: ancient energy gauge provides clues to modern understanding of metabolism. *Cell Metabolism*. 1 (1), 15-25

Kuratsune, K. Yamaguti, M. Takashi, H. Misaki, S. Tagawa, T. (1994) Acylcarnitine deficiency in chronic fatigue syndrome. *Clinical Infect Dis*. (1) 62-67

Kuratsune, H. Yamaguti, K. Lindh, G. (1998) Low-levels of serum acyl-carnitine in chronic fatigue syndrome and chronic hepatitis type C but not other disease. *Int J mol med*. 51-56

Keenan, R, A. De riva, A. Corleis, B. Hepburn, L. Licence, S. Winkler, T, H. Martensson, I-L. (2008) Censoring of autoreactive B cell development by the pre-B cell receptor. *Science*. 321 (5889) 696-699

Kelly, M. Gauthier, M,S. Saha, A, K. Ruderman, N, B. (2009) Activation of AMP-activated protein kinase by interleukin-6 in rat skeletal muscle: association with changes in cAMP, energy state, and endogenous fuel mobilization. *Diabetes*. 58(9):1953–60

Kemp, G, J. Thompson, C, H. Taylor D, J. Radda, G, K.(1997) Proton efflux in human skeletal muscle during recovery from exercise. *European Journal of Applied Physiology*. 76: 462–71

Kennedy, G. Spence, V, A. McClaren, M. Hill, A. Underwood, C. Belch, J, J, F. (2005) Oxidative stress levels are raised in chronic fatigue syndrome and are associated with clinical symptoms. *Free Radical Biology and Medicine*. 39, 584-589

Kessel, A. Rosner, I. Toubi, E.(2008) Rituximab: beyond simple B cell depletion. *Clinical Reviews in Allergy and Immunology*. 34 (1) 74–79

Kitzmann, M. Fernandez, A. (2001) Crosstalk between cell cycle regulators and the myogenic factor MYOD in skeletal muscle myoblasts. *Cell mol life sci*, 58, 57-579

Knoechel, T, R. Tucker, A, D. Robinson, C, M. Phillips, C. Taylor, W. Bungay, P, J. Kasten, S, A. Roche,T, E. Brown, D, G. (2006) Regulatory roles of the N-terminal domain based on crystal structures of human pyruvate dehydrogenase kinase 2 containing physiological and synthetic ligands. *Biochemistry*. 45, 402–415

Kori, S, H. Miller, R, P. Todd, D, D. (1990). Kinesiophobia: a new view of chronic pain behaviour. *Pain Management*. 35-43

Kristensen, J, M. Kristensen, M. Juel, C. (2004) Expression of Na⁺/HCO₃⁻ co-transporter proteins (NBCs) in rat and human skeletal muscle. *Acta Physiologica Scandinavia*. 182: 69–76

Kulkarni, S, S. Salehzadeh, F. Fritz, T. Zierath, J, R. Krook, A. Osler, M, E. (2012) Mitochondrial regulators of fatty acid metabolism reflect metabolic dysfunction in type 2 diabetes mellitus. *Metabolism*.61,175–185.

- La Manca, J, J. Peckerman, A. Walker, J. Kesil, W. Cook, S. Taylor, A. (1999) Cardiovascular response during head-up tilt in chronic fatigue syndrome. *Clinical Physiology*. 19,111–20
- Lancet (Editorial) (1998) 2, 546- 548. *Fatigue*
- a) Lane, R, J, Barrett, M, C. Taylor, D, J. Kemp, G, J. Lodi, R. (1998). Heterogeneity in chronic fatigue syndrome: evidence from magnetic resonance spectroscopy of muscle. *Neuromuscul Disord*. 8, 204-209.
- b) Lane, R, J. Barrett, M, C. Woodrow, D. Moss, J. Fletcher, R. Archard, L, C. (1998). Muscle fibre characteristics and lactate responses to exercise in chronic fatigue syndrome. *J Neurol Neurosurg Psychiatry*. 64, 362-367
- Lee, J. Kucher, S. Fischer, R. Cheng, S. Lipsky, P, E. (2009) Identification and characteristics of a human CD5+ pre-naïve B-cell population. *The Journal of Immunology*. 182 (7) 4116-4126
- Light, A, R. Bateman, L. Jo, D. Huguen, R, W. Vanhaisma, T, A. White, A, T. (2012) Gene expression alterations at baseline and following moderate exercise in patients with chronic fatigue syndrome, and fibromyalgia syndrome. *Journal of Internal Medicine*. 271(1): 64-81
- Lorusso, L. Mikhaylova, S ,V. Capelli, E. Ferrari, D. Ngonga, G, K. Ricevvti, G. (2009) *Autoimmunity Reviews*. 8 (4) 287-291
- Luin, E. Giniatullin, R. Sciancalepore, M. (2011) Effects of H₂O₂ on electrical membrane properties of skeletal myotubes. *Free Radical Biology & Medicine*, 50, 337- 344
- Macintyre A. (1992) CFS, post-viral fatigue syndrome; how to live with it. London: Thorsons. (27-33)
- MA, M. Mihaylova, I, M. Bosmans, E.(2007) Not in the mind but in the cell: increased production of cyclo-oxygenase-2 and inducible NO synthase in chronic fatigue syndrome. *Neuro Endocrinolgy Letter*. 28 (4):463–9.
- Maes, M. Twisk, F, N, M. Kubera, M. Ringel, K. (2011) Evidence for inflammation and activation of cell-mediated immunity in Myalgic Encephalomyelitis/Chronic Fatigue

- Syndrome (ME/CFS): Increased interleukin-1, tumor necrosis factor- α PMN-elastase, lysozyme and neopterin. *Journal of Affective Disorders*. 136(3):933–9
- Maher, K, J. Klimas, N, G. Fletcher, M, A. (2005) Chronic fatigue syndrome is associated with diminished intracellular perforin. *Clinical Experimental Immunology*. 142 (5) 505-511
- Majeed, T. De Simone, C. Famularo, G. Marcellini, S. Behan, P,O. (1995) Abnormalities of carnitine metabolism in chronic fatigue syndrome. *European Journal of Neurology*. 2, 425-428
- Malouff, J, M. Thornsteinsson, E, B. Rooke,S,E. Bhullar,N. Schutte,N,S. (2008) Efficacy of cognitive behavioural therapy for chronic fatigue syndrome: A meta-analysis. *Clinical Psychology Reviews*. 28 (5) 736-745
- Marcos, E. Ribas, J. (1995) Kinetics of plasma potassium concentrations during exhausting exercise in trained and untrained men. *European Journal of Applied*
- McArdle, A. McArdle, F. Jackson, M, J. Page, S, F. Fahal, I. Edward, R, H. (1996) Investigation by polymerase chain reaction of enteroviral infection in patients with chronic fatigue syndrome, *Clinical Science*.90 (4) 295–300
- Meeus, M. Rousell, N. Truljens, S. Nijs, J. (2010) Reduced pressure pain thresholds in response to exercise in chronic fatigue syndrome but not in chronic lower back pain: an experimental study. *Journal of rehabilitation medicine*. 42, 884-890
- Meyer, R, A. Campbell, J, N. Raja, S, N. (1995) Peripheral neural mechanisms of nociceptors in: wall P.D Meizack, R. Editors Textbook of pain. 3rd edition. Edinburgh, Churchill, Livingston, 13-144
- Michelakis, E, D. Sutendra, G. Dromparis, P. Webster, L. Haromy, A. Niven, E. Maguire, C. Gammer, T, L. Mackey, J, R. Fulton, D. Abdulkarim, B. McMurtry, M, S. Petruk, K, C. (2010) Metabolic modulation of glioblastoma with dichloroacetate. *Sci Transl Med*. 2, 31-44
- Morris, G. Maes, M. (2012) Increased nuclear factor KB and loss of p53 are key mechanisms in Myalgic encephalomyelitis and Chronic fatigue syndrome. *Medical Hypotheses*. 79, 607-613

- Morris, G. Maes, M. (2014) Mitochondrial dysfunction in myalgic encephalomyelitis/Chronic fatigue syndrome, explained by activated immune-inflammatory, oxidative and nitrosative stress pathways. *Metabolic Brain Disease*. (1) 19-36
- Murrough, J, W. Mao, X. Collins, K, A. Kelly, C. Andrade, G. Nestadt, P. Levine, S, M. Matthew, S, J. (2009) Increased ventricular lactate in chronic fatigue syndrome measured by ¹H MRS imaging at 3.0T Comparison with major depressive disorder. *NMR Biomedicine*. 23, 643-650
- Myhill, S. Booth, N, E. McLaren-Howard, J. (2009) Chronic Fatigue Syndrome and mitochondrial dysfunction. *International Journal Clinical Experimental Medicine*. 2: 1-16
- Nacul, L, C. Lacerda, E, M. Pheby, D. (2011) Prevalence of myalgic encephalomyelitis/ chronic fatigue syndrome (ME/CFS) in three regions of England: a repeated cross-sectional study in primary care. *BMC Medicine*. 9, 1–12.
- Nedachi, T. Fujita, H. Kanzaki, M. (2008) Contractile C2C12 myotube model for studying exercise-inducible responses in skeletal muscle. *Amateur Journal of Physiology Endocrinology Metabolism*. 295(5):1191–204
- Nellemann, B. Vendelbo, M, H. Nielsen, T, S. Bak, A, M. Hogild, M. Pedersen, S, B. Bienso, R, S. Pilegaard, H. Moller, N. Jessen, N. Jorgensen, J, O. (2013). Growth hormone-induced insulin resistance in human subjects involves reduced pyruvate dehydrogenase activity. *Acta Physiol*.
- NICE- National Institute for Health and Clinical Excellence. (2007) Chronic Fatigue/Myalgic Encephalomyelitis (or encephalopathy): Diagnosis and Management of CFS/ME in adults and children. NICE Clinical Guideline, 53
- Nijs, J. Meeus, M. Van Osterwijk, J. Ickmans, K. Moorkens, H. Hans, G. De Clerck, L, S. (2012) In the mind or in the brain? Scientific evidence for central sensitisation in chronic fatigue syndrome. *European Journal of Clinical Investigation*. 42 (2) 203-212
- Nijs, J. Nees, A. De Kooning, M. Ickmans, K. Meeus, M. Van Oosterwijk, J. (2014) Altered immune response to exercise in patients with chronic fatigue syndrome/ myalgic encephalomyelitis: A systematic review. *Exercise Immunology Review*. 20, 94-116

- Nikolic, N. Bakke, S, Kase, T, E, Rudberg I. Halle, F, I. Rustan, A, C. (2012) Electrical pulse stimulation of cultured human skeletal muscle cells as an in vitro model of exercise. *PLoS ONE*. 12 / 14 7(3)
- Nielsen, J, N. Mustard, K,J. Graham, D, A. Yu, H. Macdonald,C,S. Pillegaard, H. Goodyear, L, J. Hardie, D, G. Richter, E,A. Wojtaszewski, J, F. (2002) 5 'AMP-activated protein kinase activity and subunit expression in exercise-trained human skeletal muscle. *Journal of Applied Physiology*
- Newton, J, L. Sheth, A. Shin, J. Pairman, J. Wilton, K. Burt, J, A. Jones, D, E, J. (2009) Lower Ambulatory Blood Pressure in Chronic Fatigue Syndrome. *Psychosomatic Medicine*. 71(3), 361-365.
- Newton, J, L. Okonkwo, O. Sutcliffe, K. Seth, A. Shin, J. Jones, D.E. (2007) Symptoms of autonomic dysfunction in chronic fatigue syndrome. *QJM* 100, 519–526
- Nijs, J. Meirleir, K. Meeus, M. McGregor, N, R. Englebienne, P. (2004) Chronic fatigue syndrome: intracellular immune deregulations as a possible etiology for abnormal exercise response. *Medical Hypotheses*. 62, 759-765
- Ouchi, N. Shibata, R. Walsh, K. (2005) AMP-activated protein kinase signalling stimulates VEGF expression and angiogenesis of skeletal muscle. *Circulatory Research*. 96 (8) 838-846
- Pan, J, G. Mak, T, W. (2007) Metabolic targeting as an anticancer strategy: dawn of a new era? *Sci STKE* pe14
- Paludan, S, R. (1998) Interleukin-4 and Interferon- γ : The Quintessence of a Mutual Antagonistic Relationship. *Scandinavian Journal of Immunology*. 48 (5) 459-468
- Patarca, R. (2006) Cytokines and chronic fatigue syndrome. *Annals of New York Academy of Sciences*. 933 (1) 505-511
- Perrin, R, N. Richards, J, D. Pentreath, V. Percy, D, F. (2011) Muscle fatigue in Chronic fatigue syndrome/myalgic encephalomyelitis CFS/ME an its response to a manual therapeutic approach: A pilot study. *International Journal of Osteopathic Medicine*. 1-6
- Piao, L. Sidhu, V, K. Fang, Y, H. Ryan, J, J. Parikh, K, S. Hong, Z. Toth, P, T. Morrow, E. Kutty, S. Lopaschuk, G, D. Archer, S, L.(2013) FOXO1-mediated upregulation of pyruvate dehydrogenase kinase-4 (PDK4) decreases glucose oxidation and impairs right ventricular

function in pulmonary hypertension: therapeutic benefits of dichloroacetate. *J Mol Med (Berl)* 91, 333–346

Price, J, R. Mitchell, E. Tidy, E. Hunot, V. (2008) Cognitive Behavioural Therapy for Chronic Fatigue Syndrome. *Cochrane Database of Systematic Reviews*. 3, 1-23

Prins, J, B. Knopp, H. Bleijenberg, G.(2007) The effect of cognitive behaviour therapy for CFS on self- reported cognitive impairments and neuropsychological test performance. *Journal of Neurology and Neurosurgery Psychiatry*. 78 (4) 434-436

Prins, J, B. Van der Meer, J, W, M. Bleijenberg, G. (2006) Chronic fatigue syndrome. *Lancet* 367, 346-355

Reed, L, J. Hackert, M, L. (1990) Structure-function relationships in dihydrolipoamide acyltransferases. *J Biol Chem*. 265 (16)8971–8974

Reuter, S, E. Evans, A, M. (2011) Long-chain acylcarnitine deficiency in patients with chronic fatigue syndrome. Potential involvement of altered palmitoyltransferase activity. *Journal of internal medicine*. 76-84

Richter, E, A. Ruderman, N, B. (2009) AMPK and the biochemistry of exercise implications for human health and disease. *Biochemical Journal*. 418 (2) 261-275

Ridgeway, A, G. Petropoulos, H. Wilton, S. (2000) Wnt signalling regulates the function of MYOD and myogenin. *Journal of biological chemistry*. 277, 32398-32405

Robinson, M. Gray, S, R. Watson, M, S. Kennedy, G. Belch, J, J. Nimmo, M, A. (2010) Plasma IL-6, its soluble receptors and F2-Isoprostanes at rest and during exercise in Chronic fatigue syndrome. *Scandinavian Journal of Medicine and Science in Sport*. 20 (2) 282-290

Robson-Ansley, P, J. Milander, L. Collins, M. Noakes, T, D. (2004) Acute interleukin-6 infusion impairs athletic performance in healthy, trained male runners. *Canadian Journal of Applied Physiology*. 29, 411–418.

Rowe, P, C. Calkins, H. (1998) Neurally mediated hypotension and chronic fatigue syndrome. *Am J Med*.105, 15–21.

- Sameen, S. Khalid, Z. Malik, S, I.(2011) Role of pyruvate dehydrogenase kinases (PDK's) and their respective microRNA's in human ovarian cancer. *J Med Genet Genomics*. 3, 115–121
- Sanderson, S, J. Miller, C. Lindsay, J, G. (1996) Stoichiometry organisation and catalytic function of protein X of the pyruvate dehydrogenase complex from bovine heart. *Eur J Biochem*. 236 (1) 68–77
- Shepherd, C. (2006) The debate: Myalgic encephalomyelitis and Chronic fatigue syndrome. 15, (12) 662-669
- Silver, A. Haeney, M. Vijayadurai, P. Wilks, D. Pattrick, M. Main, C, J. (2002) The role of fear of physical movement and activity in chronic fatigue syndrome. *Journal of Psychosomatic Research* 52, 485-493.
- Skowera, A. Cleare, A. Blair, D. Bevis, L. Wessely, S, C. (2004) High levels of type 2 cytokine producing cells in chronic fatigue syndrome. *Clinical and Experimental Immunology* . 135 (2) 295-302
- Smits, B. van den Heuvel, L. Knoop, H. (2011) Mitochondrial enzymes discriminate between mitochondrial disorders and chronic fatigue syndrome. *Mitochondrion*. 11(5)735-738
- Smolle, M. Prior, A, E. Brown, A, E. Cooper, A. Byron, O. Lindsay, J, G. (2006) A new level of architectural complexity in the human pyruvate dehydrogenase complex. *J. Biol. Chem*. 281, 19772–19780
- Stacpoole, P, W. (1989) The pharmacology of dichloroacetate. *Metabolism*. 38 (11) 1124
- Street, D. Bangsbo, J. Juel, C. (2001) Interstitial pH in human skeletal muscle during and after dynamic graded exercise. *Journal of Physiology*. 537, 993-998
- Tapscott, S, J. Weintraub, H. (1991) MYOB and the regulation of myogenesis by helix-loop-helix protein. *Journal of clinical investigation*. 87, 1183-1138
- Torres-Harding, S. Sorenson, M. Jason, L. Reynolds, N. Brown, M. Maher, K. Fletcher, M-A. (2008) The associations between basal salivary cortisol and illness symptomatology in chronic fatigue. *IACFS/ME*. 13 (3) 157-180
- Trenell, M, I. Sue, C, M. Kemp, G, J. Sachinwalla, T. Thompson, C. (2006) Aerobic exercise and muscle metabolism in patients with mitochondrial myopathy. *Muscle Nerve*. 33, 524–31

Twisk, F, N, M. (2015) The 4I hypothesis: A neuro-immunological explanation for characteristic symptoms of myalgic encephalomyelitis/chronic fatigue syndrome. *Int Journal of Neurol Res.* 8 (2) 20-38

Tymoczko, J. Berg, J. Stryer, L. (2010) *Biochemistry: A short course*. W.H Freeman and Company. New York, NY

VanNess, J, M, Stevens, S, R. Bateman, L. Stiles, T, L. Snell, C, R. (2010) Postexertional malaise in women with chronic fatigue syndrome. *Journal Womens Health* 19, 239-244

Van Oosterwijck, J. Nijs, J. Meeus, M. Lefever, I. Huybrechts, L. Lambrecht, L. (2010). Pain inhibition and post-exertional malaise in myalgic encephalomyelitis/chronic fatigue syndrome: an experimental study. *Journal of Internal Medicine*. 268, 265–78

Vecchiet, J. Cipollone, F. Falasca, K. Mezzetti, A. Pizzigallo, E. Bucciarelli, T. De Laurentis, S. Affaitati, G. De Cesare, D. Giamberardino, M, A. (2003) Relationship between musculoskeletal symptoms and blood markers of oxidative stress in patients with chronic fatigue syndrome. *Neuroscience Letters*. 335(3) 151–154

Vollaard, N, B, J. Shearman, J, P. Cooper, C, E. (2005) Exercise- induced oxidative stress: myths, realities and physiological relevance. *Sports Medicine*, 35 (12) 1045–1062

Verma, A. Anand, V. Verma, N, P. (2007) Sleep disorders in chronic traumatic brain injury. *Journal of Clinical Sleep Medicine*. 3(4) 357-362.

Vlaeyen, J, N. Kole-Sniders, A, M. Boeren, R, G. VanEek, H. (1995) Fear of movement / (re) injury in chronic lower back pain and it's relation to behavioural performance. *Pain*. 62 (3) 363-372

Wan, Y. Zou, Q, Zi, Y. (2009) High frequency of mitochondrial DNA D-loop mutations in Ewing's sarcoma. *Biochemical and Biophysical Research Communities*. 390 (3) 447-450

Wessley, S. Chalder, T. Hirsch, S. Wallace, P. Wright, D. (1997) The prevalence and morbidity of chronic fatigue syndrome. A prospective primary care study. *Amateur Journal of Public Health*, 87:1449-1455

White, P, D. Goldsmith, K, A. Johnson, A, L. Potts, L. Walwyn, R. DeCesare, J, C. Baber, H, L. Burgess, M. Clark, L, V. Cox, D, L. Bavinton, J. Angus, B, J. Murphy, G. Murphy, M. O'Dowd, H. Wilks, D. McCrone, P. Chalder, T. Sharpe, M. (2011) Comparison of adaptive pacing therapy, cognitive behaviour therapy, graded exercise therapy, and specialist medical care for chronic fatigue syndrome (PACE): a randomised trial. *Lancet*. 377, 823-836

Whiteside, A. Hansen, S. Chaudhuri, A. (2004) Exercise lowers pain threshold in chronic fatigue syndrome. *Pain* 109: 497–9

Wilson, M. C., Jackson, V. N., Heddle, C., Price, N. T., Pilegaard, H., Juel, C., Bonen, A. Motgomery, I. Hutter, o, F. Halestrap, A, P. (1998) Lactic acid efflux from white skeletal muscle is catalysed by monocarboxylate transporter MCT3. *Journal of Biological Chemistry*. 273, 15920-15926

Winder, W, W. Holmes, B, F. Rubink, D, S. Jensen, E, B. Chen, M. Holloszy, J, O. (2000) Activation of amp-activated protein kinases increases mitochondrial enzymes in skeletal muscle. *Journal of applied physiology*. 88, 2219-2226

Winkler, A, S. Blair, D. Marsden, J, T. Peters, T, J. Wessely, S. Cleare, A, J. (2004) Autonomic function and serum erythropoietin levels in chronic fatigue syndrome. *Journal of Psychosomatic Research*. 56, 179–83

Wong, R. Lopaschuk, G. Zhu, G. Walker, D. Catellier, D. Burton, D. Teo, K. Collins-Nakai, R. Montague, T. (1992). Skeletal muscle metabolism in the chronic fatigue syndrome. In vivo assessment by ³¹P nuclear magnetic resonance spectroscopy. *Chest* 1992, 102, 1716-1722

World Health Organisation (1992). The ICD-10 Classification of Mental and Behavioural Disorders; Clinical Descriptions and Diagnostic Guidelines. Geneva: World Health Organisation

Wyller, V, B. Saul, J, P. Walløe, L. Thaulow, E. (2008) Sympathetic cardiovascular control during orthostatic stress and isometric exercise in adolescent chronic fatigue syndrome. *European Journal of Applied Physiology*. 102, 623–632.

Wyller, V, B. Barbieri, R. Saul, J, P. (2011) Blood pressure variability and closed-loop baroreflex assessment in adolescent chronic fatigue syndrome during supine rest and orthostatic stress. *European Journal of Applied Physiology*, 111, 497–502

Xu, X. Arriaga, E, A. (2009) “Qualitative determination of superoxide release at both sides of the mitochondrial inner membrane by capillary electrophoretic analysis of the oxidation products of triphenylphosphonium hydroethidine,” *Free Radical Biology and Medicine*. 46 (7) 905–913,

Yamamoto, Y. LaManca, J, J. Natelson, B, H.(2003) A measure of heart rate variability is sensitive to orthostatic challenge in women with chronic fatigue syndrome. *Experimental Biology and Medicine*. 228, 167–174

Yoshiuchi, K. Quigley, K, S. Ohashi, K. Yamamoto, Y. Natelson, B, H. (2004) Use of time-frequency analysis to investigate temporal patterns of cardiac autonomic response during head-up tilt in chronic fatigue syndrome. *Autonomic Neuroscience*, 113, 55–62.

Zadak, Z. Hyspler, A. Ticha, M. Hronek, P. Fikrova, J. Rathouska, D. Hrciarikova, R. Stetina, R. (2009) Antioxidants and vitamins in clinical conditions. *Physiology research*. 58, 13-17

Zheng, J. (2012). Energy metabolism of cancer: Glycolysis versus oxidative phosphorylation (Review). *Oncology Letters*, 4(6), 1151–1157.

Chapter 2

Application of a Novel pH Sensing Nanosensor Platform to Measure Intracellular pH in CFS/ME Primary Myoblasts

2.1 Introduction

Previous research has demonstrated that CFS/ME patients exhibit profound and sustained intracellular acidosis with repeat exercise, compared to controls [Jones et al. 2012]. In addition to abnormality in the recovery of intramuscular pH following exercise [Jones et al. 2010]. The authors suggested that these findings result from an over-utilisation of the lactate dehydrogenase energy-producing pathway, pointing towards a bio-energetic abnormality, which may offer the potential of therapeutic intervention. Furthermore, Boulton [2012] utilised a novel *in vitro* drug pre-testing platform to measure intracellular pH in CFS/ME muscle, to determine whether the PDK enzyme inhibitor DCA had the potential to modify intracellular pH. Results demonstrated that CFS/ME patient myoblasts exhibit an aberrantly low intracellular pH when compared to controls. Remarkably, this effect was completely normalised following treatment with PDK inhibitor DCA.

Briefly, PDK functions to inhibit PDC a 3-enzyme complex which is responsible for the conversion of pyruvate to acetyl-coA during aerobic respiration. However, when PDC functionality is decreased an increase in pyruvate generated by glycolysis accumulates in the cell and is metabolised to lactic acid, which due to ineffective oxidative phosphorylation can cause a decrease in pH and a concurrent reduction in muscle function. The compound DCA is a pyruvate analogue and functions to inhibit PDK, an enzyme which acts to inhibit PDC function therefore downregulating aerobic metabolism. DCA exhibits the capacity to reverse intracellular acidosis by inducing the active state of PDC and promoting the clearance of lactic acid by functioning to convert it back to pyruvate aerobically [Boulton, 2012; Forque, 2003].

The primary aims of this chapter were [1] to validate and develop the *in vitro* muscle pH sensing system reported by Boulton [2012] and further confirm the presence of abnormal pH in CFS/ME myoblasts. [2] To apply PDK inhibitors into the system in order to investigate the ability of drugs to modify intracellular acidosis.

2.1.1 Intracellular pH and Cell Function

Intracellular pH plays a pivotal role in nearly all aspects of cell function, including regulation of cell volume, vesicle trafficking, cellular metabolism, cell membrane polarity, growth and proliferation [Dennis et al. 2012; Loisel et al. 2003; Busa et al. 1984]. The disruption of intracellular pH is associated with serious physiological consequences and an alteration in pH of as little as 0.1-0.2 pH units can induce metabolic depression [Gibbin et al. 2014].

Eukaryotic cells therefore exhibit mechanisms to prevent any significant fluctuations in pH, for example acute alterations as a consequence of metabolic reactions are neutralised via weak acids and bases located in the cytosol [Gibbin et al. 2014; Casey et al. 2010]. However, more significant long-term fluctuations involve the use of more permanent mechanisms such as transmembrane exchangers [Gibbin et al. 2014]. Cellular dysfunction is often associated with an abnormally low intra compartmental pH, which can function to denature proteins or activate enzymes, which are usually inactive at neutral pH [Han and Burgess, 2010].

Additionally, low intracellular pH may negatively influence upon other aspects of human physiological functioning particularly the nervous system and has been implicated in the pathophysiology of cancer [Izumi et al. 2003] and Alzheimer's disease [Dennis et al. 2012]. Typically, cytosolic pH should be between 7.2-7.4, with even subtle alterations inducing cellular dysfunction [Dennis et al. 2012].

Given the central role, that intracellular pH plays in cell function it is not surprising that practically all cell types operate to regulate intracellular pH and ensure it remains within the optimal physiological range [Valli et al. 2005]. This steady state intracellular pH is determined by the balance between the rate of acid extruding processes and acid loading processes [Boron et al. 2004]. In terms of acid loading processes, this includes the uptake of HCO_3^- and CO_3 by the Na^+ -coupled members of the solute carrier family (SLCF) family, Na^+ - H exchange, vacuolar H^+ pumps in the plasma membrane, in addition to lactate efflux. Alternatively, acid loading processes involve HCO_3^- efflux, which is aided by the Cl^- - HCO_3^- exchangers in the SLC4 family with help from the anion channels.

2.1.2 Acidosis and fatigue development

The role of pH and the precise physiological mechanisms that contribute to fatigue remain relatively elusive and the subject of intense debate and investigation [Lancha Junior et al.

2015]. However, evidence does exist to suggest several physiological mechanisms associated with acidosis contribute to the development of muscle fatigue. For example, competition between H^+ and Ca^{2+} ions for the troponin binding site leads to an impairment in the ability of the contractile components to function effectively [Donaldson et al. 1978; Fabiato et al. 1978]. In addition, excessive H^+ ions function to inhibit phosphorylcreatine resynthesis [Sahlin et al. 1975]. In addition to inhibiting enzymes involved in the glycolytic pathway such as glycogen phosphorylase and phosphofructokinase, limiting the ability of the muscle to deal with energetic demand [Sutton et al. 1981]. *In vitro* muscle cell pH homeostasis is maintained by the flux of H^+ out of the cell and into the extracellular environment, this is achieved through the monocarboxylate transporters (MCT), particularly MCT-1 and MCT-4 [Juel. 2008]. These transport proteins carry monocarboxylates across the cell membrane. Additionally H^+ ions are also transported out of the cell via the sodium hydrogen exchanger and the sodium bicarbonate co-transporter [Lancha Junior et al. 2015].

2.1.2 Intracellular sensing techniques

Conventional intracellular sensing techniques have included the use of fluorescent dyes [Bkaily et al. 1999], optochemical sensors, NMR and surface enhanced Raman scattering (SERS) [Desai et al, 2014]. NMR can effectively discriminate between cytoplasmic and vacuolar pH. However, a major drawback associated with this technique is the inability to measure pH at the single cell level, as larger tissue sections are required [Sondergaard et al. 2014]. Alternatively, SERS may be used to measure the pH of single cells following the internalisation of metal nanoparticles, which is promising, however presently the resolution of SERS when performing live cell imaging does not compare to fluorescent-based measurement [Sondergaard et al. 2014]. In relation to the use of fluorescent dye, there are a diverse range of fluorophores commercially available, which provide a rapid response, which is measureable via confocal microscopy or spectrophotometry [Han and Burgess. 2009]. The use of fluorescent dye enables the real-time measurement of various analytes, including pH. The small size of the free dye molecules provide the benefit of high spatial resolution and allows information throughout the cell to be collected *en masse* [Coupland et al. 2009].

Nevertheless, the technique is not without limitation. For example, the direct contact between the dye and the intracellular environment may be associated with cytotoxicity, through the

induction of biochemical processes within the cell [Desai et al. 2014]. There is also the potential for non-specific protein binding within the cell leading to false positive results and sequestration [Srivastava. 1997]. Furthermore, simply retaining the dye within the cellular environment throughout the duration of the experiment is another difficult problem as many dyes are prone to leeching due to their low molecular weight [Coupland et al. 2009].

Alternatively, optochemical sensors (optodes), overcome some of the inherent weaknesses associated with the use of free dye (graphic representation of an optode displayed in Figure 2.1). For example, the tip of the optical fibre consists of a bio-compatible matrix protecting the cell from cytotoxicity associated with the dye. Nevertheless, there are crucial limitations associated with the use of the optochemical sensor. For example, the technique requires a fibre with a modified tip to be inserted directly into an individual cell [Buhlman et al. 1998; Vo-Dinh. 2003]. The large size of the fibre in comparison to a single cell causes damage to the cell membrane, which can trigger apoptosis. Further, the physical size of the probe bodies prevents more than two or three sensors being used per cell. This limits resolution of the of the intracellular sensing capabilities [Coupland et al. 2009].



Figure 2.1: Graphic representation of an 'optode' used for intracellular analysis

2.1.3 PEBBLE Nanosensors

The PEBBLE (Probes Encapsulated By Biologically Localised Embedding) nanosensor represents a major development within sensor-based technology, overcoming many of the inherent weaknesses associated with optochemical and free-dye sensing techniques. For example, due to their sub-micron diameter, inert matrix, signal intensity and ratiometric ability they can be used to accurately characterise intracellular compartments and allow real-time measurement in sub-cellular environments [Aylott et al. 2003]. Effectively, PEBBLE is a term, which can be used to describe a wide range of matrices and nano-fabrication techniques that have been used to miniaturise optical sensing technologies [Monson et al. 2014]. Their structure is spherical and they are around 30-500nm in size [Desai et al. 2014], taking up approximately 1ppb of the internal volume of a mammalian cell, resulting in minimal perturbation and ‘passive’ (non-destructive) analytical observations [Buck et al. 2004; Clarke et al. 1999]. The most common matrices used to fabricate the nanosensors are, polyacrylamide, sol gel silica and cross-linked methacrylate [Monson et al. 2014]. This chapter will focus upon the use of polyacrylamide nanosensors. See Figure 2.2 for a simplified illustration of nanosensor structure and function.

The nanosensor exhibits a wide range of benefits over conventional sensing techniques. For example, they consist of an inert matrix, which prevents any non-specific interaction between fluorophores and cellular components, which reduces potential cytotoxic effects exhibited by the dye. [Desai et al, 2014].

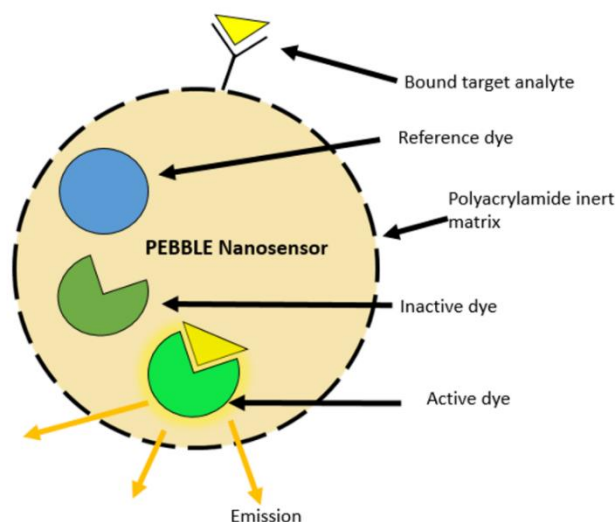


Figure 2.2: Schematic representing a PEBBLE nanosensor

A major limitation of traditional free fluorescent dyes is uneven dye loading within the cell. During the loading process, each cell will take up an arbitrary amount of fluorophore. This means that when performing single cell analysis variations in fluorescence between cells may be dependent on the concentration of fluorescent dye in each cell rather than the concentration of the analyte of interest. Nanosensors routinely contain two types of fluorophore; an indicator and a reference probe. The indicator functions to generate a signal, which is directly proportionate to the concentration of the analyte of interest within the cell. The reference dye does not respond to the analyte of interest and exhibits a constant signal at a different wavelength to the indicator dye. Although there may still be considerable variation in the number of nanosensors take up by individual cells, the analyte-dependent fluorescent signal can be 'normalised' with respect to the reference signal. Absolute fluorescent values may vary but the ratio of indicator to reference signal will be constant for a given concentration of analyte.

The combination of these dyes allows for accurate and ratiometric measurements to be performed. It is possible to add multiple pH sensitive dyes to the nanosensor matrix during production to allow for an extended range of pH measurements to be obtained across the physiological range [Chauhan et al. 2011; Sun et al. 2011]. The fluorophores used in this chapter were selected in reference to the Desai et al. [2013] protocol. This included the use of two pH sensitive dyes with identical emission spectra but with varying pKa values (5'-carboxyfluorescein [FAM]) pKa 6.5, Oregon green pKa 4.8. In addition to a reference probe (5-(and-6)-carboxy-tetramethylrhodamine (TAMRA). Essentially, the optimal responsiveness of Oregon green is within the acidic range (3.5-5.5) whereas FAM is optimally stimulated in the neutral range (5.5-7.5). Therefore, at low pH levels Oregon green responds to pH, while FAM is largely inactive [Desai et al. 2013].

2.1.4 Nanosensor delivery

The cellular cytoplasm is separated from the external environment by a plasma membrane, in addition to lipid bilayer with membrane proteins, lipids and carbohydrates embedded. Before a nanosensor can effectively interpret sub-cellular pH it must be capable of first crossing the cell membrane, which can be challenging [Chou et al. 2011].

It is possible to aid intracellular delivery by bio-chemically engineering the synthetic nanosensor to aid passage through the plasma membrane into the intracellular environment. One method involves functionalising the nanosensor with specific ligands, which are capable of binding to the surface of the cell membrane, enabling receptor-ligand interaction and leading to receptor mediated endocytosis of the nanosensor [Chou et al. 2011]. Alternatively, cationic coating of the nanosensor is another internalisation strategy. Effectively, cationic molecules are able to interact with the negatively charged plasma membrane, to promote membrane permeability [Chou et al. 2011]. It has been hypothesised that increased permeability is due to the formation of nanoscale holes within the plasma membrane following interaction with cationic species [Al-Jamal et al. 2008; Al-Jamal et al. 2008^b]. A number of cationic coatings have been used in the transfection process and include; cationic liposomes, polypeptides and amine-containing polymers [Herrero et al. 2009; Chatterjee et al. 2008]. An example of a popular liposomal transfection reagent is lipofectamine. This reagent is able to complex with negatively charged, water-soluble quantum dots through simple electrostatic interaction during co-incubation in culture media. This delivery technique involves pinocytosis, a process which enables the cell to take in the surrounding extracellular environment as a result of vaginating and pinching off the plasma membrane into vesicles containing the extracellular fluid [Derfus et al. 2004]. A major benefit of liposomal delivery is that nanosensors can be delivered to a large number of cells simultaneously [Monson et al. 2014]. Figure 2.3 illustrates the various endocytic pathways into the cell, in addition to the possible transport routes the nanosensor could take through the endosomal network.

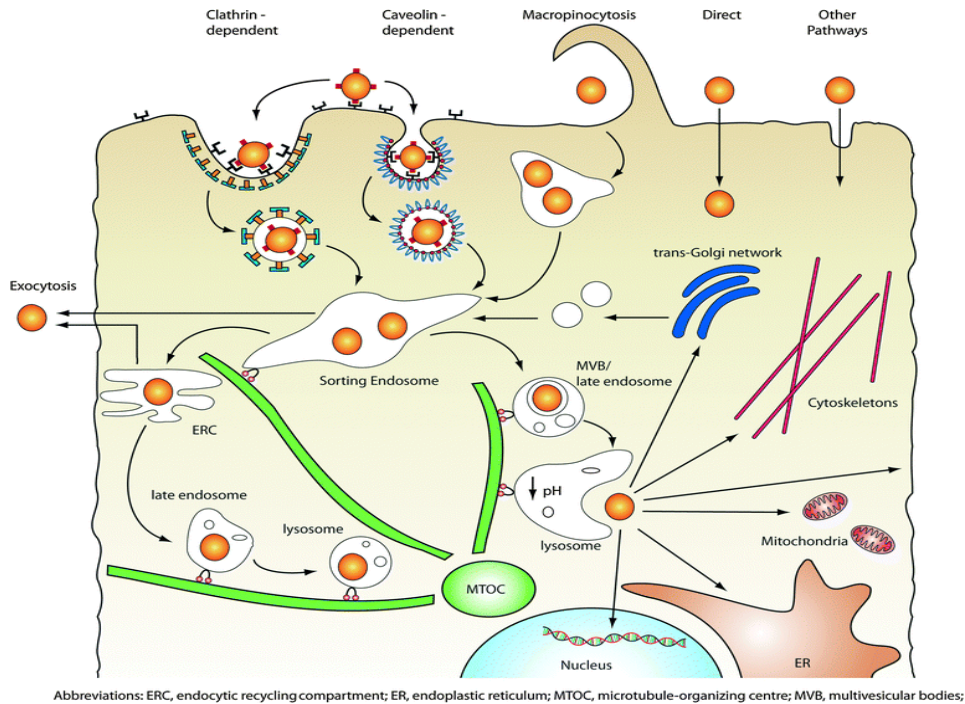


Figure 2.3: Graphical representation of the different endocytic pathways that provide entry into the mammalian cell. The possible transport routes through the endosomal network following internalisation are also depicted.

2.1.5 pH sensitive nanosensor application

Pilot work conducted by Boulton [2012] investigated the ability of the novel pH sensing nanosensor system incorporating to provide pH measurements in CFS/ME patient myoblasts. The nanosensors consisted of a polyacrylamide matrix and incorporated the free dyes Fluorescein isothiocyanate (FITC) and Alexa Fluor 568. The aim of the investigation was to use the nanosensors to confirm the presence of intracellular acidosis in CFS/ME patients, which has been previously reported via MRS techniques [Jones et al. 2010].

Boulton [2012] investigated the ability to successfully deliver the pH nanosensors to the intracellular environment of the myoblasts using the transfection reagent Lipofectamine 2000. Confocal microscope imaging was reported to confirm the nanosensor distribution throughout the intracellular environment (displayed in Figure 2.4) Nevertheless, it is important to interpret these images with caution, as higher quality imaging is required to confirm the sub-cellular location of the nanosensor or simply whether they were bound to the outer cell membrane.

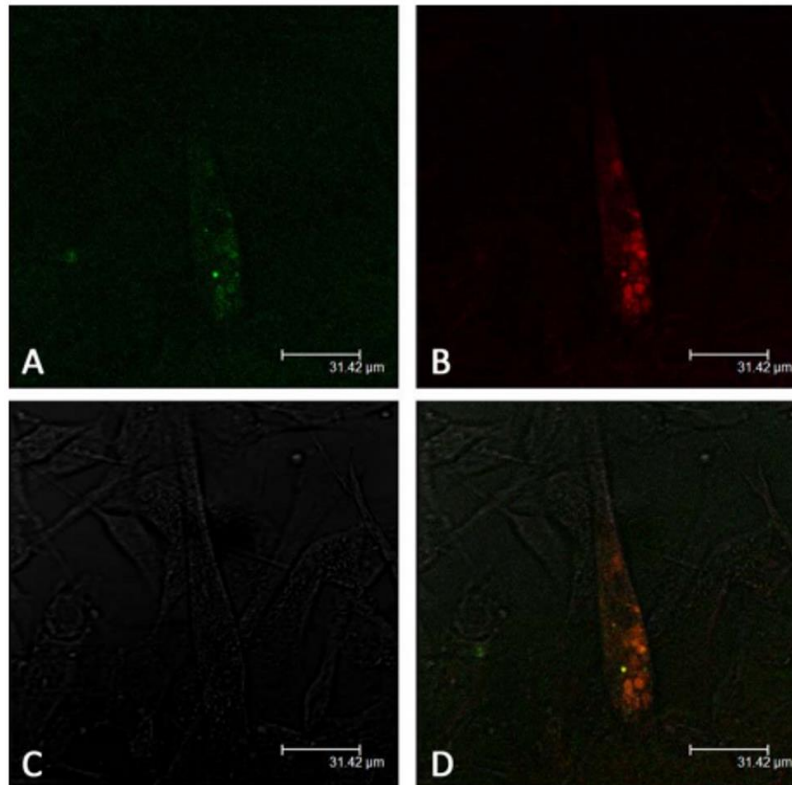


Figure 2.4 Preliminary data generated by Boulton [2012], depicting confocal imaging of discrete z-slice in a control myoblast. A fair distribution of nanosensors throughout the cell was observed. FITC fluorescence A, Alexafluor568 fluorescence B, Bright field C and merged D.

Additionally, the nanosensors were also reported to quantify intracellular pH via fluorimetric measurement. CFS/ME myoblasts loaded with pH responsive nanosensors exhibited significantly lower intracellular pH compared to controls. The acidosis was reversed when the cells were treated with the PDK inhibitor DCA (See Figure 2.5). These findings suggested that CFS/ME related acidosis could be reversible and potentially treatable with drug intervention. Therefore, a primary aim of this chapter was to reproduce this pilot data to further confirm the presence of aberrantly low pH in CFS/ME myoblasts via the nanosensor system and the extent in which it could be manipulated following DCA treatment.

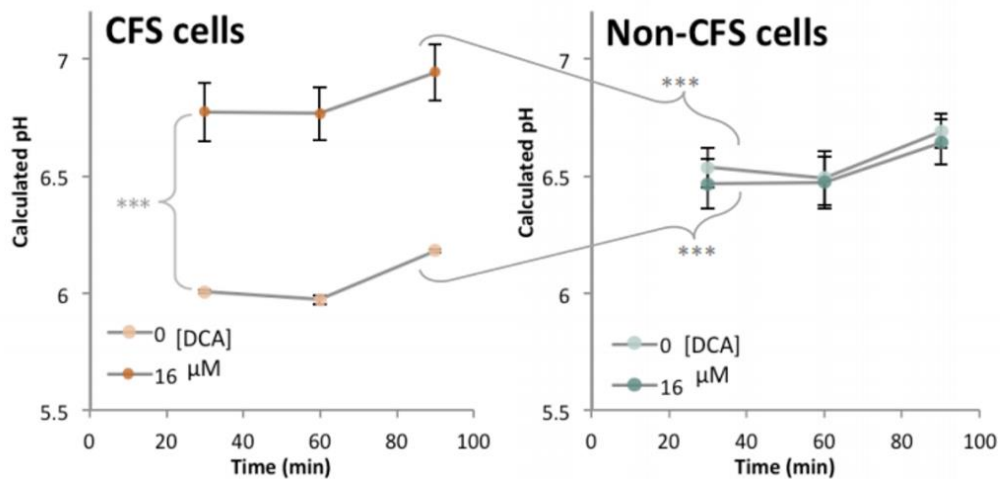


Figure 2.5 Preliminary data generated by Boulton [2012]. Myoblasts were treated with 16 μ M DCA. No change in pH between treated and untreated control myoblasts. DCA boosted pH beyond the baseline level of normal myoblasts. Untreated CFS/ME exhibited a significantly lower pH. Data presented \pm SEM, N=4, *** denotes $p < 0.005$

2.1.6 Hypotheses

The experimental hypotheses were (1) CFS/ME myoblasts exhibit intrinsic intracellular acidosis compared to controls. This could represent a major advance in the understanding of mechanisms that underpin a major phenotypic characteristic of this condition. (2) A normalisation in CFS/ME intracellular pH to control levels could be achieved in response to the PDK inhibitor DCA. This could represent a novel treatment strategy in the management of symptoms associated with CFS/ME.

2.2 Materials and Methods

All diseased (CFS/ME) and non-diseased primary myoblasts were supplied by Dr Audrey Brown at Newcastle University.

All tissue culture reagents were purchased from Sigma-Aldrich (Poole, Dorset, UK) with the exception of Ham's F10 myoblast growth media (Lonza, SLS, East Riding of Yorkshire, UK) and chick embryo extract (Seralab, West Sussex, UK). Tissue culture flasks, 24-well plates and serological pipettes were supplied by Greiner bio-one (Stonehouse, UK). Resazurin (7-Hydroxy-3H-Phenoxazin-3-one10-oxide) dye was purchased from Sigma-Aldrich.

pH responsive dyes and TAMRA were purchased from Life Technologies (Glasgow, UK).

Inhibitors of enzyme PDK (Potassium Dichloroacetate, Sodium Iodoacetate, Dehydroabietylamine) were purchased from Sigma Aldrich.

The delivery reagent Lipofectamine 2000 was purchased from Thermo Fisher Scientific (Paisley, UK)

2.2.1 Study participants

Muscle biopsy samples were obtained from patients with CFS/ME and healthy control participants. The CFS/ME and control individuals were gender and age matched, for example in this chapter the CFS/ME patient was a female aged 65 years and the control participant was a female aged 66 years. Recruitment was achieved through the NHS CFS clinical service within the Newcastle Upon Tyne Hospital Foundation Trust. The CFS/ME patients all met the Fukuda (1994) criteria for CFS/ME. All participants agreed to complete the study via formal written consent. Ethical approval for the study was provided by the Newcastle and North Tyneside joint ethics committee.

2.2.2 Cell culture and preparation

Muscle biopsies from both CFS/ME patients and control participants were obtained and isolated as previously described by Brown et al. [2015]. Briefly, samples were collected from

the vastus lateralis (Location illustrated in Figure 2.6) via fine needle biopsy. The precursor cells were then isolated via the Blau and Webster method [1981]. The biopsies were collected in medium designed for proliferation (Ham's F10 supplemented with 20% (v/v) FBS, 2% chick embryo extract,1% penicillin-streptomycin). The samples were then transferred into a petri dish and washed with PBS. Any adipose or connective tissue was removed with a scalpel before the samples were again washed in PBS. The samples were then added to a falcon tube which contained 5mL 0.05% trypsin-EDTA and spin-digested at 37°C for 15 minutes. The trypsin was then removed and 5mL of media added before centrifuging at 448 G for 5 minutes. The pellet containing the satellite cells was then re-suspended in medium and the spin dissociation process was repeated an additional 3 times. The pellets were then plated into a T25 culture flask with Ham's F10 growth medium. The media was changed after 24hours to remove any cellular debris. Cells were expanded via routine culture and proliferating myoblasts were passaged multiple times before performing experimental work.

Diseased (CFS/ME) and non-diseased primary human myoblasts were routinely cultured using Ham's F-10 medium supplemented with 20% FBS 2% chick embryo extract , 500U/mL penicillin streptomycin and 1% amphotericin B. Cells were grown in a humidified environment 5% (v/v) CO₂ at 37.5°C throughout. Cells were grown to 80% confluence before passaging. Prior to experimentation growth media was removed and replaced with experimental medium which was unsupplemented Dulbecco's modified eagles medium.

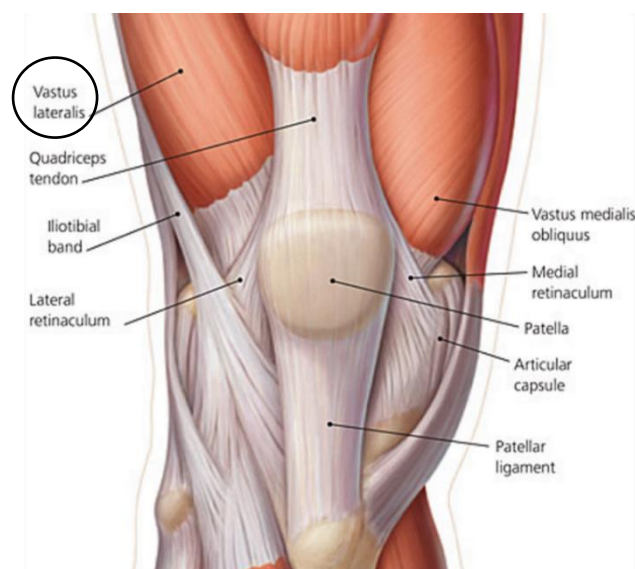


Figure 2.6 Schematic of the lower limb anatomy as depicted by Dixit et al. [2007]

2.2.3. Intracellular optical sensing

2.2.3.1 pH responsive nanosensor production

PEBBLE (Probes Encapsulated by Biologically Localised Embedding) Nanosensors were synthesised during a multi-stage process developed by Chauhan et al. [2011]. The method involved dissolving acrylamide (7.6mM) and N,N Methylene bisacrylamide (1.3mM) in 1.5mL of deionised water by sonication to create a monomer solution. Dextran linked reference fluorophore TAMRA-D and indicator dyes FAM-D and Oregon green-D were added to the monomer solution at 10mg/mL and covered to avoid exposure to light as they are photosensitive. A surfactant mixture was prepared consisting of Dioctyl sulphosuccinate (3.6mM) and Brij 30 (8.5mM) and deoxygenated. The surfactant was added to 42mL of deoxygenated hexane by perfusion with argon gas to form a micro emulsion. The monomer/fluorophore solution was then added to the surfactant mixture and left for 10 minutes. The polymerisation process was then initiated by the addition of 30µL of ammonium persulphate (10% w/v) and 15µL of -N,N,N',N'tetramethylethylenediamine. Following 2 hours of polymerisation hexane was removed by rotary evaporation in the absence of oxygen and the remaining nanosensors washed 5 times in absolute ethanol, which was removed by rotary evaporation during the final wash. The remaining sensors were stored in an airtight container at 4°C.

2.2.3.2 pH sensitive nanosensor calibration

The pH nanosensor calibration was performed following the Desai et al. [2013] protocol. Buffer stock solutions were prepared before completing the calibration. A 0.2M stock of sodium phosphate dibasic was prepared by adding 7.098g of sodium dibasic to 250mL of deionised water into a volumetric flask before sonicating. A 0.1M stock solution of citric acid monohydrate was also prepared by adding 5.524g of citric acid monohydrate to 250mL deionised water and then sonicated. Buffer solutions between pH 4-8 and the volumes of sodium diphosphate and citric acid monohydrate were added to 50mL Falcon tubes as detailed in Table 1.1. A pH meter was then used to confirm the pH of each solution.

Table 1.1 . The volumes required of the stock concentrations of sodium phosphate dibasic (0.2M) and citric acid monohydrate (0.1M) required to make buffer solutions between pH 4-8.

pH	Volume (mL)	
	Sodium phosphate dibasic (0.2M)	Citric acid monohydrate (0.1M)
4	7.72	12.28
5	10.28	9.72
6	12.84	7.16
7	17.44	2.56
8	19.53	0.47

Nanosensor suspensions were prepared by dissolving nanosensors in buffer solutions over a range of pH values (4-8) in each buffer solution to achieve a final concentration of 10mg/mL. The nanosensors contained 3 dye probes OG-D, FAM-D and Tamra-D (reference dye). The nanosensor/buffer solution was then added (200 μ L) in triplicate to a 96-well plate, in addition to a control triplicate containing only buffer solution to ensure that background fluorescence did not interfere or overlap with the response obtained from the dye nanosensors. Fluorescent intensity (FI) measurements were performed as detailed in section

2.2.3.2 Fluorometric measurement strategy

FI measurements were obtained using a Tecan Infinite 200 fluorimeter (Tecan, Mannedorf, Switzerland). Data was attained using the companion Magellan software. The measurement settings for the active dyes OG-D and FAM-D were ($\lambda_{\text{ex}} = 490\text{nm}$, $\lambda_{\text{em}} = 525\text{nm}$) and for reference dye TAMRA-D ($\lambda_{\text{ex}} = 555$, $\lambda_{\text{em}} = 580$). The software was set to perform multiple reads per well and a gain value of 50 was selected remained constant across all experiments.

2.2.4 Resazurin cytotoxicity assay

Prior to all cytotoxicity assays CFS/ME and control myoblasts were routinely cultured and seeded into 96-well testing plates at a density of 1×10^4 cells per well. Following seeding cells were incubated in a humidified environment at 37.5°C and 5% CO_2 . Myoblast viability was measured by adding resazurin dye (concentration 0.03%) to each well. Resorufin produced as a result of resazurin bio-reduction was measured assessed using a Tecan-I fluorometric plate reader at $\lambda_{\text{ex}} 560\text{nm} / \lambda_{\text{em}} 590\text{nm}$. Essentially, resazurin is a none fluorescent dye, however in the presence of viable cells it is reduced by the mitochondria into highly fluorescent forms of the dye namely resorufin and dihydroresorufin.

2.2.4.1 Dye free nanosensor toxicity

To assess the biocompatibility of the polyacrylamide nanosensor matrix, nanosensors containing no fluorophores (blanks) were added to the wells of the testing plate at a 10mg/mL concentration. Resazurin dye was added at a concentration of (0.03% w/v) and fluorometric analysis were performed as described in section 2.2.4.

2.2.4.2 pH sensitive nanosensor cytotoxicity

Cell viability was also investigated following incubation with nanosensors containing pH responsive dyes OG-D and FAM. Briefly, nanosensors were added to the wells of the testing

plate at a 10mg/mL concentration in addition to resazurin dye (concentration 0.03% w/v). The plate was then read over the following 3,4,5,6 hours as detailed in section 2.2.4.

2.2.4.3 Free dye FAM and Oregon Green cytotoxicity

The nanosensor has been reported to provide a protective barrier between the cell and the potential cytotoxic effects of the dyes which are encapsulated during the fabrication process [Desai et al. 2013]. Therefore, the cytotoxicity of the pH responsive dyes FAM-D and OG-D was assessed as these dyes were incorporated into the nanosensors described in this chapter. Concentrations (5-20 μ g/mL) of FAM-D and OG-D were added to the cell culture plate. Viability was investigated following the addition of resazurin (concentration 0.03% w/v). The plate was monitored over the following 3 hours as described in section 2.2.4.

2.2.4.4 Lipofectamine 2000 cytotoxicity

In this chapter lipofectamine 2000 was transfection reagent used to deliver nanosensors into the intracellular environment. The cytotoxicity of the reagent was assessed at varying concentrations (0.003-0.3%) which were added to the wells of the testing plate, followed by 0.03% resazurin and incubated for 3 and 6 hours. Fluorescent intensity (FI) was then measured as detailed in section 2.2.4.

2.2.4.5 DCA cytotoxicity

The impact of PDK inhibitor DCA upon intracellular pH was investigated in this chapter. It was important to assess the cytotoxicity of the drug before applying it to the cell system. DCA was added to 96-well testing plates at varying concentrations (1 μ M-1mM). Resazurin (concentration 0.03% w/v) and plates were incubated for 3 and 6 hours. The plate was read as described in section 2.2.4.

2.2.4.6 pH measurement of DCA in a cell-free system

The impact of PDK inhibitor DCA upon myoblast intracellular pH was investigated in this chapter. Prior to applying the drug to a cell system it was essential to firstly determine the inherent pH of the drug in a cell-free system. To achieve this nanosensors at a concentration of 10mg/mL were added to the wells of a 96-well testing plate and then treated with varying concentrations of DCA (0-40 μ M). FI measurements were performed as described in section 2.2.3.2.

2.2.5 pH sensitive nanosensor internalisation with varying lipofectamine concentration

Primary myoblasts were routinely culture and seeded at a density of 1×10^4 cells per well, in triplicate into 96-well testing plates. Following 12-hours incubation in a humidified environment at 37°C and 5% CO₂ day, nanosensors at 10mg/mL were dissolved in experimental media containing lipofectamine 2000 at varying concentrations (0.003-3%). The nanosensor/lipofectamine mixture was allowed to complex for 30 minutes at 37.5°C. The culture media was then removed from the testing plates and the nanosensor/lipofectamine mixture was added to the wells and left for 3 hours at 37.5°C and 5% CO₂ to allow for nanosensor uptake. The plate was washed twice with PBS before replacing with experimental media and incubated for a further 30minutes at 37.5. Intracellular pH was then measured over the next for the next 6 hours. FI measurements were performed as described in section 2.2.3.2.

2.2.6 pH sensitive nanosensor internalisation and DCA treatment

Primary myoblasts were routinely cultured and seeded into 96-well testing plates at a density of 1×10^4 cells per well. Following attachment, a nanosensor (10mg/mL) and lipofectamine (0.03%) complex was allowed to complex for 30-minutes before being to the well and incubated at 37.5°C and 5% CO₂ for 3 hours to enable nanosensor uptake. The plate was washed twice with PBS before replacing with experimental media , which was then dosed with various concentrations of DCA (0-20 μ M). Intracellular pH was measured over the following 6 hours. FI measurements performed as described in section 2.2.3.2.

2.2.7 Data analysis

The statistical model used to analyse the data was Minitab 17 statistical software. Inferential statistics were performed to investigate intracellular pH in CFS/ME and control skeletal muscle samples. An independent sample T-test was used to examine intracellular pH differences between different samples (CFS/ME vs control). A paired sample T-test was utilised to investigate within group differences, for example pH at baseline verses DCA treatment. The descriptive statistics used were mean \pm SD.

2.3 Results

2.3.1 pH Sensitive nanosensor calibration curve in a cell-free system

pH responsive nanosensors at 10mg/mL were initially analysed in the absence of cells over a range of pH values. Fluorescent intensity (FI) ratio measurements for OG-D and FAM in relation to reference dye TAMRA-D were obtained. FI ratio values were shown to be linearly dependent on pH ($y=6.0624x$, $R^2=0.9885$, $N=3$). The linear regression of the calibration curve was then utilised to determine intracellular pH for nanosensor-doped myoblast samples. The data is presented in Figure 2.7.

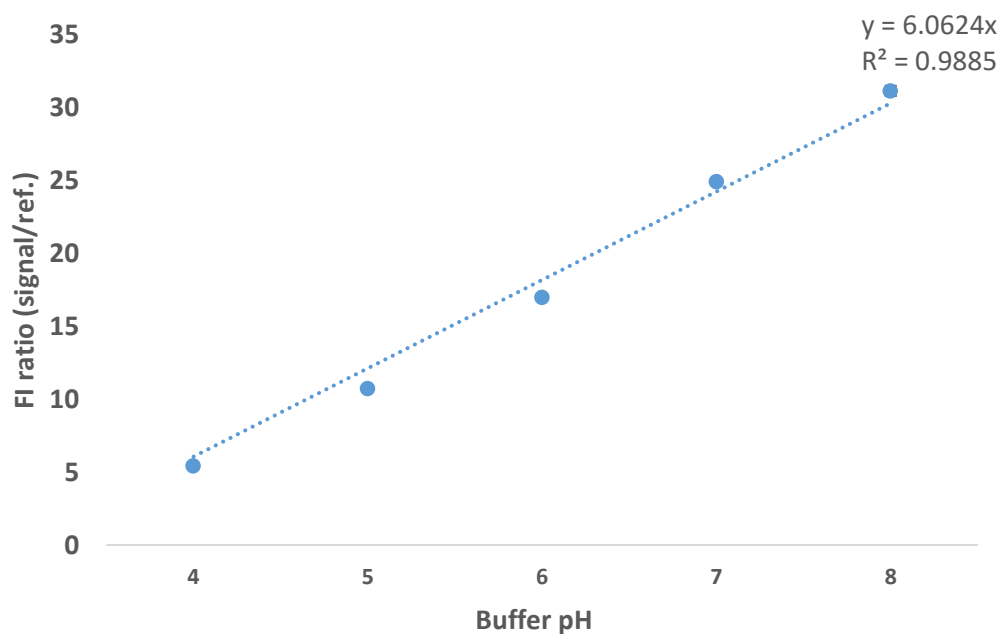


Figure 2.7 Calibration of pH responsive nanosensors containing FAM-D and OG-D. The Fluorescent ratio was shown to be linearly dependent upon pH ($y=6.0624x$). The data is presented as mean \pm SD, $n=5$, $R^2=0.9885$

2.3.2 pH responsive nanosensor optimisation

2.3.2.1 Myoblast viability following exposure to dye-free (blank) nanosensors

CFS/ME and control myoblast viability was assessed following the addition of dye-free nanosensors and was measured via the resazurin viability assay. Figure 2.8 demonstrated myoblast viability over time following incubation with 10mg/mL dye-free nanosensors. After 24-hours CFS/ME and control myoblast viability was significantly reduced (% of untreated control) when compared to all other time points ($P \leq 0.0005$). There was no significant difference between any other time points.

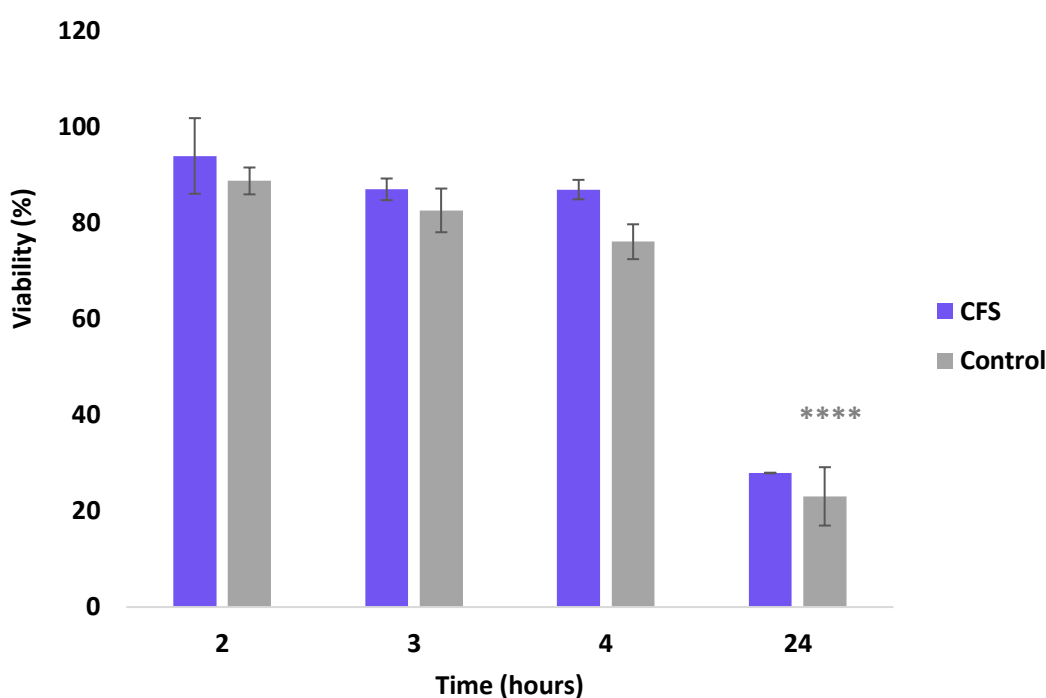


Figure 2.8 CFS/ME and Control myoblast viability (% of untreated control) following incubation with 10mg/mL of dye free nanosensors. Data presented as mean of 3 replicate measurements \pm SD. Significant difference in viability between 24 hours and all other time points denoted by **** ($P \leq 0.0005$), $n=2$

2.3.2.2 Myoblast viability following exposure to Oregon green and FAM

Figure 2.9 demonstrated CFS/ME myoblast viability following treatment with varying concentrations (5-20 μ g/mL) of pH responsive free dyes OG-D and FAM-D, simultaneously. Viability was decreased to less than 70% (of untreated control values) across all concentrations after 1 hour.

CFS/ME cell viability was significantly decreased ($P \leq 0.0005$) between 1 and 2 hours for a free dye concentration of 20 μ g/mL. Similarly, there was a significant decrease ($P \leq 0.0005$) between 2 and 3 hours, resulting in a final % viability of less than 40%. The higher the dye concentration and the longer the exposure period the higher the cell death. Cell death was only seen to be concentration dependent beyond 2h incubation.

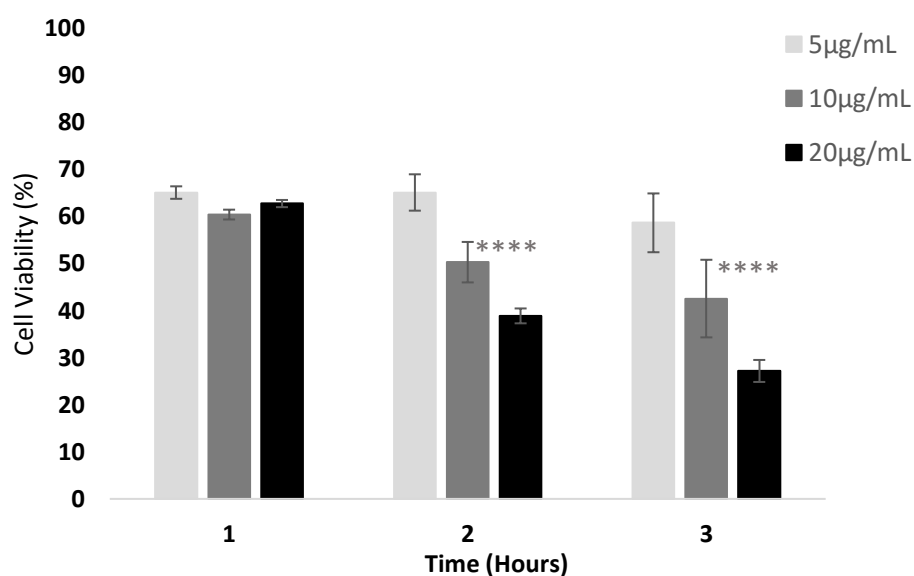


Figure 2.9 Control myoblast viability (%) after incubation with varying concentrations (5-20 μ g/mL) of pH sensitive Oregon green and FAM. Data presented as mean \pm SD, n=3. Significant difference in viability between 1 and 2 hours at 20 μ g/mL, and similarly between 2 and 3 hours as denoted by **** ($P \leq 0.0005$)

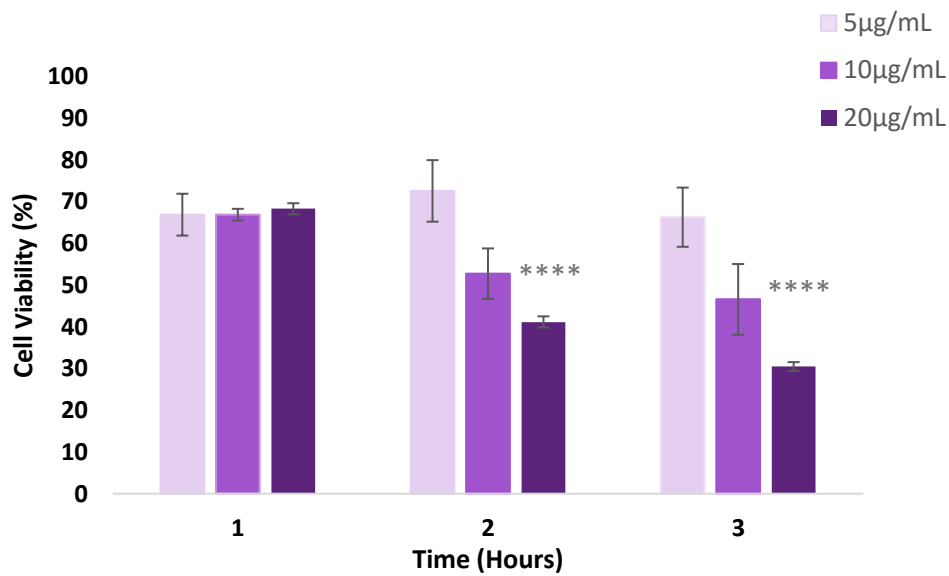


Figure 3.0 CFS/ME myoblast viability (%) after incubation in varying concentrations (5-20µg/mL) of pH sensitive Oregon green and FAM. Data presented as mean of triplicate measurements from n=2 donors \pm SD . Significant difference in viability between 1 and 2 hours at 20µg/mL, and similarly between 2 and 3 hours as denoted by **** (P \leq 0.0005)

2.3.2.3 Myoblast viability following treatment with Lipofectamine 2000

Following 3-hours incubation with varying concentrations of lipofectamine myoblast viability is shown in figure 3.1. During this time period CFS/ME myoblasts exhibited significantly reduced (P<0.005) viability at 3% versus 0.003% lipofectamine concentration, a decreased viability of 33%. Similarly, control myoblast viability was also significantly reduced at 3% versus 0.003% lipofectamine concentration (P<0.05) which resulting reduction in viability by 44%.

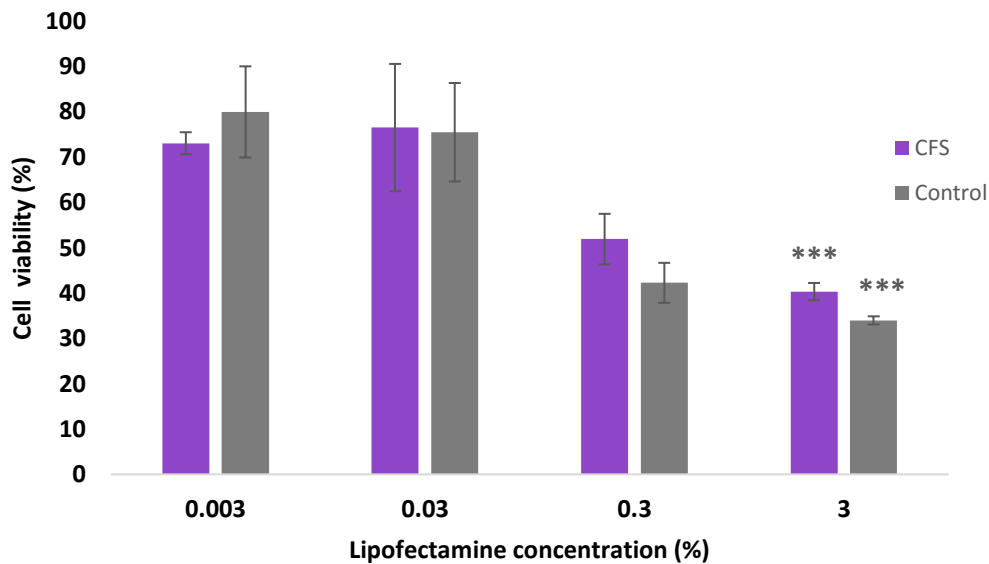


Figure 3.1 CFS/ME & control myoblast viability (%) following 3 hours incubation with varying concentrations (0.003-3%) of lipofectamine. Data presented as mean of triplicate measures for n=2 donors, \pm SD. Significant reduction in viability at 3% versus 0.003% concentration for both CFS/ME and control myoblasts, denoted by *** ($P < 0.005$), n=2

2.3.2.4 Myoblast viability following incubation with DCA

Myoblasts were treated with varying concentrations (1 μ M-1mM) of the PDK inhibitor DCA and viability was assessed via the resazurin assay. Figure demonstrated viability (% of untreated control) after 3-hours incubation and Figure 3.3 following 6-hours. Results demonstrated good viability at both 3 and 6 hours incubation, across all concentrations and in both CFS/ME and control samples (>88%).

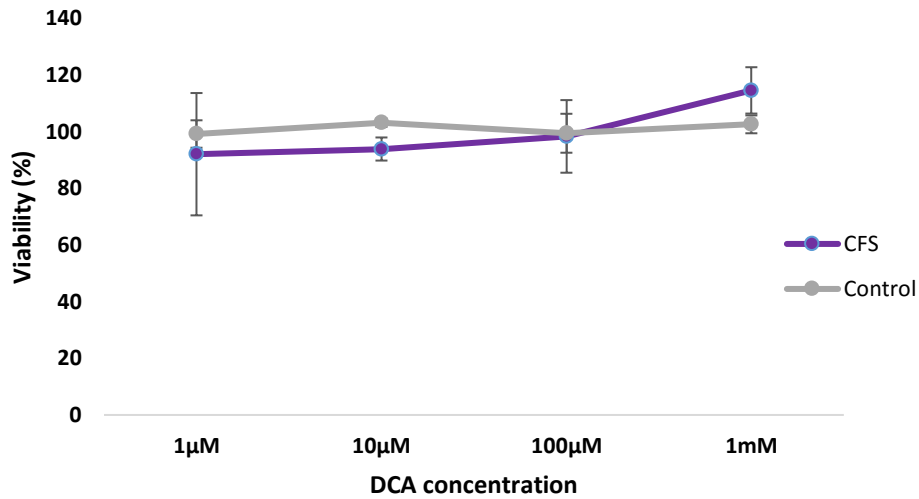


Figure 3.2 CFS/ME (n=2) and control (n=2) myoblast viability following 3-hours incubation with 1µM- 1mM DCA. Viability (% untreated control) was assessed following the addition of 0.03% resazurin. Myoblast viability remained high across all concentrations (>90%) in both CFS/ME and control sample groups. Data presented as mean ±SD.

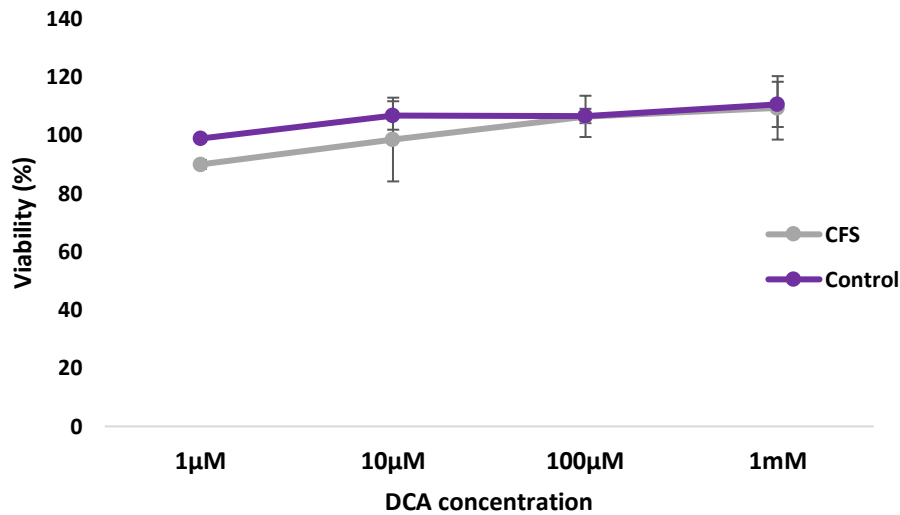


Figure 3.3 CFS/ME (n=2) and control (n=2) myoblast viability following 6-hours incubation with 1µM- 1mM DCA. Viability (% untreated control) was assessed following the addition of 0.03% resazurin. Myoblast viability remained high across all concentrations (>87%) in both CFS/ME and control sample groups. Data presented as mean ±SD.

2.3.2.4 pH measurement of DCA in a cell-free nanosensor system

Figure 3.4 demonstrated the calculated pH values for varying concentrations of DCA (0-40 μ M) measured by pH responsive nanosensors at a concentration of 10mg/ml. All concentrations of DCA maintained neutral pH during course of experiment.

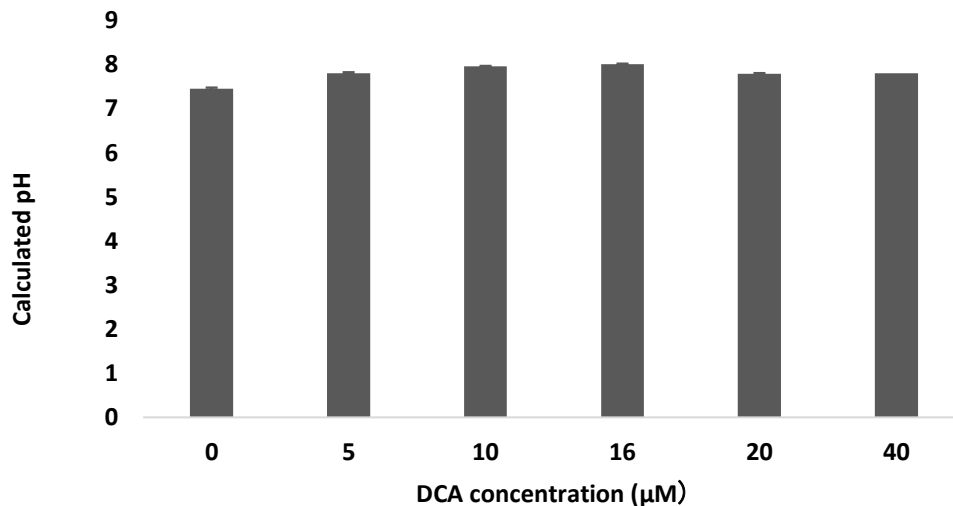


Figure 3.4 Calculated pH for varying concentrations of DCA (0 μ M-40 μ M). pH measured by nanosensors at 10mg/mL concentration. Data presented as mean of 3 replicate measures \pm SD

2.3.3 Nanosensor application

2.3.3.1 Myoblast pH with varied lipofectamine 2000 concentration

Figure 3.5 demonstrated CFS/ME and control myoblast intracellular pH measurements with varied lipofectamine 2000 concentration (0.003-3%). Control myoblast intracellular pH was significantly lower at all lipofectamine 2000 concentrations ($P < 0.005$) compared to CFS/ME samples.

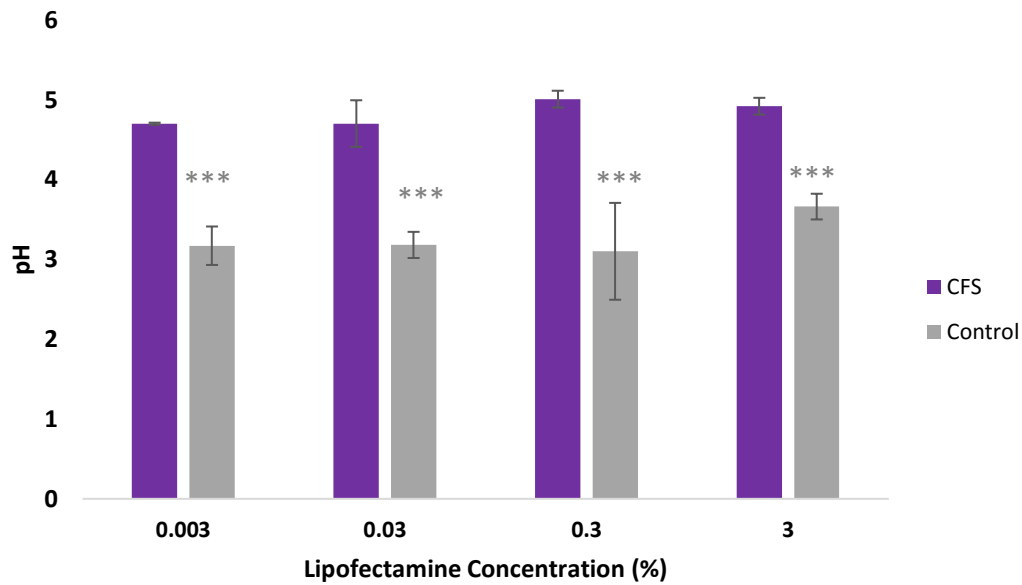


Figure 3.5 CFS/ME & control myoblast intracellular pH with varied lipofectamine concentration (0.003-3%). Data presented as mean of triplicate measurements \pm SD. Significantly lower intracellular pH for control myoblasts at across all lipofectamine concentrations. Denoted by *** ($P < 0.005$), $n = 2$ donors

2.3.3.2 Myoblast pH with varied DCA treatment

Intracellular pH was measured using nanosensors at a 10mg/mL concentration. Following nanosensor internalisation, cells were treated with varying concentrations of DCA (10-20 μ M) and incubated for 3-hours. pH was significantly lower in control compared to CFS/ME myoblasts at baseline (0 μ M DCA) and with all DCA concentrations. Displayed in Figure 3.6.

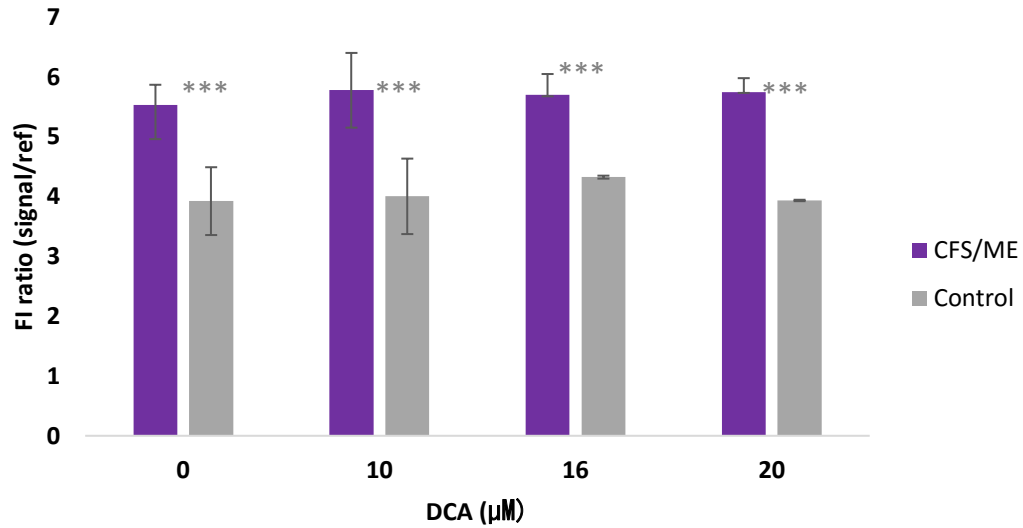


Figure 3.6 CFS/ME & control myoblast intracellular pH at baseline (0μM) and following treatment with DCA (10-20μM). pH measured with nanosensors at 10mg/mL concentration. Significantly lower intracellular pH for control compared to CFS/ME myoblasts at baseline and following treatment with all concentrations of DCA. P<0.005 denoted by ***, Data presented as mean of triplicate measurements ±SD, n=2 donors

2.4 Discussion

Existing literature has demonstrated the role of impaired bio-energetic function in CFS/ME patients. For example, MRS studies have reported patients to have a delayed recovery from intramuscular acidosis following a standardised exercise protocol [Jones et al. 2010], as well as profound and sustained intracellular acidosis with repeat exercise [Jones et al. 2012]. Furthermore, Boulton [2012] reported the presence of inherently low intracellular pH in CFS/ME myoblasts compared to controls when measuring using the novel intracellular nanosensor system. Additionally, the author also reported DCA to completely normalise intracellular pH in the CFS/ME patient samples. Thus, suggesting bio-energetic dysfunction in CFS/ME may be modifiable and therefore treatable.

In this chapter the intracellular pH of CFS/ME and control myoblasts was determined using pH responsive fluorescent nanosensors. Specific aims were [1] Repeat pilot work conducted by Boulton [2012] to confirm the presence of abnormal pH in CFS/ME myoblasts measured using pH responsive nanosensors. [2] Apply PDK inhibitors to the cells to investigate the ability of drugs to treat intracellular acidosis and potentially open a new route to therapeutic intervention.

The work carried out in this chapter was unable to reliably detect any acidosis in CFS/ME cells or any difference in intracellular pH between CFS/ME and control cells. Secondly, DCA did not modify intracellular pH in either CFS/ME or control myoblasts contrasting previously reported data. The following sections will contextualise the findings and suggest possible reasons for the conflicting results.

2.4.1 pH nanosensor optimisation

Optimisation work was required before the nanosensor experimental platform could be utilised to interpret intracellular pH in CFS/ME patient samples. This included varying dye ratios in order to optimise signal strength and investigating innate cellular toxicity associated with the nanosensors.

The nanosensors were successfully calibrated over a diverse pH range (4-8), however this was could only be achieved following chemical modification of the pH sensitive dyes FAM

and Oregon green. During the initial calibration process there was a large degree of fluctuation in the signal strength provided by the pH responsive dyes. Additionally, it was observed during the washing steps of the fabrication process that there was a substantial amount of dye leaking from the sensors with each wash. It was felt that the variation in signal strength could be linked to the apparent dye leeching observed during fabrication. Therefore, as suggested by Desai et al [2013] dextran linked fluorophores were incorporated into the fabrication process. Effectively, dextran is an inert molecule, which is large enough in size to entrap the fluorophores in the nanosensor matrix to prevent the low molecular weight dye leaking from the sensor.

The nanosensor has been reported to exhibit a wide range of benefits over the use of conventional free-dye based sensing techniques. For example, the polyacrylamide shell has been described as biologically compatible, preventing non-specific interaction between fluorophores and cellular components, therefore minimising cytotoxicity [Desai et al. 2014]. Thus, a key aim of the optimisation work was to investigate whether blank (dye-free) nanosensors exhibited a cytotoxic effect on the CFS/ME and control myoblasts. Interestingly, the nanosensors were found to be bio-compatible with short term incubation (≤ 6 hours), however after 24-hours viability in both CFS/ME and control samples was significantly reduced ($< 40\%$) when compared to other time points (See Figure 2.8 and 2.9). In contrast to this finding Lee et al. [2010] reported blank polyacrylamide nanosensors to exhibit a non-toxic effect ($> 90\%$ viability) in a glioblastoma cell line following 20-hours incubation. However, the nanosensor concentrations used (1-4mg/mL) were considerably lower than used in this chapter (10mg/mL). The higher sensor concentration was chosen to give a more clearly defined intracellular signal.

It is not clear why prolonged exposure caused substantial cell death in the present investigation. However, one possible explanation could relate to chemical residue left on the nanosensor surface following the manufacturing process. Following synthesis the nanosensors were washed in several changes of ethanol in order to remove plasticisers used during the fabrication process. Although the sensors were washed 7 times in ethanol as previously recommended [Desai et al. 2013], it is possible that residual contaminants may have remained on the surface and it may have taken prolonged exposure to these contaminated probes before significant cell death occurred.

Another potential factor that could be attributed to cell death with prolonged exposure could relate to contamination within the culture. When working with a primary cell culture the need for sterility is very important and the introduction of any nonsterile product to cell culture greatly increases the risk of contamination [Burns et al. 2011]. Nevertheless, contamination can usually be avoided through the use of conventional sterilisation techniques. However, the ability to sterilise the nanosensors via typical sterilisation techniques such as autoclaving and UV irradiation is not possible. For example, UV irradiation may photo bleach the fluorophores making them less responsive to changes in pH [Benjaminson et al. 2011]. Additionally, sterilisation via autoclaving is not possible as excessive heat exhibits the capacity to limit fluorophore function and disrupt the polyacrylamide structure of the nanosensor shell. Therefore, the inability to sterilise the nanosensors is an inherent weakness in the ability to use the platform to measure pH in cell cultures where sterility is a necessity.

Additional toxicity work was performed to investigate the impact of exposure to pH responsive dyes Oregon green and FAM. A key benefit of the nanosensor has been reported to be its ability of the polyacrylamide matrix to protect the cell from possible fluorophore cytotoxic effects. Following exposure to FAM and Oregon green both CFS/ME and control myoblasts exhibited a significant reduction in viability (<70% compared to untreated controls) after only 1 hour. Similarly, viability was also significantly reduced between 1 and 2 hours and again between 2 and 3 hours at the higher dye concentration (20µg/mL) and in both samples (See Figure 3.0). Therefore, it would appear that the higher the concentration of the dyes and the longer the exposure, the greater the cytotoxic effect. Interestingly, while blank nanosensors demonstrated biocompatibility during early measurements, it would appear the free dyes Oregon green and FAM are acutely cytotoxic (i.e. within 1 hour of exposure to the cells).

Toxicity work was also performed on the transfection reagent Lipofectamine 2000 (Displayed in Figure 3.1). It has been reported to exhibit negligible cytotoxicity in a wide variety of cell-lines [Cui et al. 2012]. Results demonstrated good viability (>70% compared to untreated controls) at the lower concentrations (0.003, 0.03%), however after 3-hours incubation at the highest concentration (3%) there was a significant reduction in viability (<40% cells still viable) in both CFS/ME and control samples. Therefore, concentrations below 3% were used in the nanosensor internalisation experiments.

The PDK inhibitor DCA was added to cells that were loaded with nanosensors to test the ability of DCA to ‘normalise’ CFS/ME myoblast intracellular pH. The cytotoxic profile of the inhibitor was investigated and it was associated with good viability (>89%) when measured over a 24-hour period (See Figure 3.2 and 3.3). This is in agreement with the data presented in a review by Papandreou et al. [2011], who reported clinically relevant concentrations of DCA (<1mM) to exhibit no direct cytotoxic effect *in vitro*.

Finally, it was also important to determine the innate acidity/alkalinity of the inhibitor and the potential effect it may have in relation to intracellular pH. pH was measured via the nanosensors and DCA maintained a neutral pH during the course of the experiment. Therefore, DCA was considered acceptable to use within the nanosensor experimental system.

2.4.2 pH Nanosensor application

The discovery that control myoblasts exhibited significantly lower intracellular pH compared to CFS/ME patient samples, contrasts previous findings [Jones et al. 2010, 2012; Boulton, 2012], which measured intracellular pH via MRS and using a pH responsive nanosensor platform, similar to the one reported in this chapter. However, the design incorporated only one pH responsive fluorophore (FITC), with a limited pH range (Pka 6.5). In contrast, in this chapter a dual-fluorophore approach to extend the dynamic pH range, with fluorophores exhibiting the same emission spectra but different PKa values, increasing the pH sensing range (3.5-7).

Importantly, unlike the aforementioned studies the data generated in this chapter demonstrated both CFS/ME and control myoblasts to exhibit intracellular pH readings outside the cytosolic physiological range of around 7.2 [Casey et al. 2010; Han and Burgess, 2009; Llopis et al, 1998]. For example, intracellular pH was <4.5 for both patient and control samples following incubation with varying concentrations of transfection reagent lipofectamine 2000 [Displayed in Figure 3.5]. Similarly, following treatment with 0-20µM DCA intracellular pH was <5.7 for both samples [See Figure 3.6].

When interpreting these findings it is important to consider the heterogeneity of the intracellular environment and the difficulty in delivering nanosensors to specific sub-cellular

compartments. For example, mitochondrial pH has been reported as high as 8, compared to 4.7 in lysosomes, which are significantly different to the value of 7.2 reported in the cytoplasm [Panariti et al. 2012].

Despite many studies being conducted in the intracellular drug-delivery field, the ability of a nanoparticle to reach a specific sub-cellular compartment remains a substantial barrier, largely due to the complex and dynamic nature of the intracellular environment [Kristl et al. 2013; Ruenraroengsak, 2010]. In the present investigation the sub-cellular component of interest was the cytoplasm, this is because with a greater glycolytic rate within the cell there is a concomitant increase in the release of protons in the cytoplasm [Robergs. 2001]. An increased rate of glycolysis is associated with a concomitant greater release in protons in the cytoplasm as a direct result of glycolysis increases greater glycolytic rate there is a concomitant increase in proton release in the cytoplasm as a direct result of glycolysis and ATP hydrolysis.

To understand why nanosensors provided a measurement outside the cytosolic range it is first important to consider how nanosized particles are trafficked within the cell. Intracellular trafficking processes are still not fully understood, however various internalisation pathways have been recognised [Zhang et al. 2012]. In the present study, cationic mediated delivery (Lipofectamine 2000) was utilised. This transfection approach has been reported to rely primarily on clathrin-dependent mediated pathways through the transmembrane [Cui et al. 2014]. Once endocytosed it has been suggested that nanosensors are encapsulated within transport vesicles which move through the endosomal pathway. It has been reported that nanoparticles taken up by clathrin-dependent endocytosis are typically marked for lysosomal degradation [Zhang. 2012; Bareford and Swan. 2007], which would explain the low pH values reported in the present study.

Although unpublished pilot work conducted by Boulton [2012] reported intracellular pH measurements within the cytosolic pH range, presently no published work has demonstrated the ability to deliver nanosensor to the cytosolic compartment. Interestingly, in agreement with the present study other authors have reported the nanosensor platform to provide pH measurements consistently outside the cytosolic range in a variety of cell lines. This finding has been associated with the endosomal and lysosomal localisation of the nanosensor once internalised [Sondergard et al. 2014; Benjaminson et al. 2011; Coupland et al. 2009; Burns et al. 2006]. For example, in a study conducted by Benjaminson et al. [2011] the authors

investigated the use of a polyacrylamide nanosensor, which covalently incorporated 2 pH responsive dyes (fluorescein and Oregon green) and reference probe rhodamine, to measure intracellular pH in a HepG2 cell line. The authors tracked pH using live cell imaging confocal microscopy and reported localisation of nanosensors to the endosome during early measurement time-points (1 hour: 5.1 ± 0.6 , 2 hours: 4.9 ± 0.6) and exclusively the lysosome after 24-hours (4.5 ± 0.4). Likewise, Coupland et al. [2009] reported pH values of 4.88 and 5.10 and combined with cell imaging confirmed endosomal localisation after 2-3 hours of uptake of a Tat conjugated polyacrylamide nanosensor in a CHO-K1 cell line. Furthermore, Burns et al. [2006] used an alternative nanosensor (matrix, silica gel), however similarly reported low pH values (5.11-6.6) an hour after uptake in a RBL-2H3 cell line. It is important to note that mildly acidic intracompartamental pH in the endosome and a significantly more acidic lysosomal pH is not an indication of cellular dysfunction. In terms of cell biology, the endosome plays a pivotal role in receptor recycling and the degradation of foreign material. Additionally, the lysosome is recognised as the principle site of intracellular digestion and is filled with hydrolytic enzymes that are used for controlled digestion of macromolecules involved in cellular metabolism [Han and Burgess. 2009; Alberts et al. 2002].

It is also important to note that the resting intracellular pH measurements reported by Boulton [2012] were lower (6.3-6.5 CFS/ME and 6.5-7.0 controls) than previously reported (7-7.1) by Jones et al. [2012] via MRS. Interestingly, even after exercise CFS/ME patients in the Jones et al. [2012] study exhibited an intracellular pH measurement of >6.6 which was not as acidic as the resting values reported by Boulton [2012]. It is therefore possible that the aberrantly low pH values reported in the present study and by Boulton [2012] were the result of nanosensor localisation within the acidic endosomal and lysosomal network. However, neither studies used live-cell imaging technology so it is difficult to draw firm conclusions.

An additional aim of this chapter was to investigate the capacity of the PDK enzyme inhibitor DCA to alter intracellular pH. Boulton [2012] reported DCA treatment to induce pH changes in CFS/ME myoblast samples, effectively normalising the highly acidic intracellular environment in CFS/ME cells to a level comparable to control samples, alternatively DCA did not exhibit any effect on control cells. The authors postulated the observed effect to be related to underlying abnormality in normal pyruvate metabolism. This could be either through reduced function PDH within multi-enzyme complex of PDC or due to over activity of PDK, leading to an over-reliance upon the lactate dehydrogenase energy-producing

pathway and localised acidosis. The data presented in this chapter showed that DCA did not alter intracellular pH in either CFS/ME or control myoblast samples (See Figure 3.4). However, the ability of this compound to modify cytosolic pH cannot be clearly defined as results would also suggest that the nanosensors were located in the endosomal and lysosomal intracellular compartments.

Aberrantly low pH values recorded in this and other work using intracellular pH responsive nanosensors would suggest that they are being sequestered by subcellular organelles. It is possible to release sensors from lysosomal entrapment but this is a complex task and requires chemical surface modification of the nanosensors. Benjaminson et al. [2013] suggested polyamines such as poly (ethylene imine) (PEI) which is positively charged to potentially enable the nanosensors to leave the lysosome via the ‘proton sponge effect’. This hypothesis suggests unprotonated amines of PEI to exhibit the ability to absorb protons while they are pumped into the lysosome. Subsequently, more protons are pumped into the lysosome, inducing an increased influx of Cl^- ions and water of the resulting osmotic swelling causes the lysosomal membranes to rupture and the contents are released into the cytoplasmic environment [Benjaminson et al. 2013; Nel et al. 2009; Behr et al. 1997]. Such an approach though potentially useful, was beyond the scope of the work presented in this chapter.

2.4.3 Limitations

The aim of this chapter was to repeat preliminary work conducted by Boulton [2012]. Therefore, care was taken to ensure the fabrication and internalisation methods performed were in line with pilot work. However, evidence suggested that nanosensor transfection via lipofectamine mediated delivery to be ineffective in delivering the nanosensor to the cytosolic compartment. This issue may have been rectified by incorporating a chemical surface modification step within the nanosensor fabrication process, to enable the nanosensors to break through the endosomal/lysosomal membrane and into the cytosolic environment.

Another potential limitation is that confocal microscopy was not used to confirm nanosensor internalisation in the present investigation. Previous studies using this imaging approach confirmed that lipofectamine was effective at internalising nanosensors into alveolar cell [Henderson et al. 2009]. It was felt that recorded pH values discussed in this chapter were so

far from physiological acceptable values that there were obvious limitations to the nanosensor approach that rendered imaging of little value.

In preliminary work conducted by Boulton [2012] images were provided to suggest the successful internalisation of the pH nanosensors. However, the image quality was limited and it was difficult to determine whether the nanosensors were internalised or bound to the outer membrane of the cell. Furthermore, it was impossible to determine the sub-cellular compartmental localisation of the nanosensors. Therefore in the present investigation the aforementioned imaging technique was not performed. To overcome this weakness a more sophisticated imaging technique could have been utilised. For example, Desai et al. [2014] reported fluorescence co-localisation via Wide field microscopy to enable the identification of the nanosensor sub-cellular location. This technique involves the genetic labelling of the nanosensor with fluorescent protein constructs.

2.4.4 Conclusion

The use of fluorescent-based pH responsive nanosensors revealed significantly lower pH in control myoblasts compared to those isolated from CFS/ME patient samples. This finding contrasted pilot work that reported CFS/ME samples to exhibit an aberrantly low intracellular pH, which could be returned to normal control levels following treatment with DCA.

However, the pH values reported in this chapter are in line with other studies that utilised a similar experimental protocol and confirmed the endosomal/lysosomal localisation of the nanosensors via live-cell confocal imaging [Sondergard et al. 2012; Benjaminson et al. 2011; Coupland. 2009]. Thus, it would seem that without chemical modification the nanosensors are unable to freely locate within the cell cytosol. Future work could centre on the investigation of different nanosensor surface modification strategies to promote cytosolic delivery and prevent lysosomal entrapment. Additionally, fluorescent co-localisation microscopy techniques should be used to investigate nanosensor intracellular trafficking.

2.5 References

- Alberts, B. Johnson, A. Lewis, J. (2002) Molecular biology of the cell. Transport from the golgi network to the lysosomes. New York garland science.
- Al-Jamal,W,T. Al-Jamal, K,T. Bomans, P,H. Fredrik, P,M. Kostarelos, K. (2008) Functionalized-Quantum-Dot-Liposome hybrids as multimodal nonparticles for cancer. *Small*,4, 1406-1415
- Al-Jamal, W, T. Al-Jamal, K, T . Tian, B. Lacerda, L Bornans, P. H. Frederik P. M. Kostarelos, K *ACS Nano*, 2008, **2**, 408–418
- Aylott J. W. (2003). Optical nanosensors-an enabling technology for intracellular measurements. *Analyst* 128, 309–312
- Babic, M. Horak, D. Trchova, P. Jendelova, P. Glogarova, P. Lesny, V. Herynek, M. Hajek, E. (2008) Sykova, *Bioconjugate Chem.*, 19, 740–750
- Bareford, L. M., & Swaan, P. W. (2007). Endocytic mechanisms for targeted drug delivery. *Advanced Drug Delivery Reviews*, 59(8), 748–758
- Behr, J (1997). The proton sponge: A trick to enter cells the viruses did not exploit. *Chimia* **51**: 34–36.
- Benjaminsen, R.V. Matthebjerg, M.A. Henriksen, J.R. Moghimi, S.M. Andresen, T.L. (2013)The possible “proton sponge” effect of polyethylenimine (PEI) does not include change in lysosomal pH. *Mol. Ther.* 21, 149–157
- b) Benjaminsen, R. V. Sun, H. Henriksen, J, R. Christensen, N, M. Almdal, K. Andresen, T, L. (2011) Evaluating nanoparticle sensor design for intracellular pH measurements. *ACS Nano*. 5, 5864–5873
- Bkaily, G. Jacques, D. Pothier, P. (1999) Use of confocal microscopy to investigate cell structure and function. *Methods in Enzymology*. 307:119–135
- Blau, H,M. Webster C. Isolation and characterization of human muscle cells. (1981) Proceedings of the National Academy of Sciences of the United States of America. 78(9):5623–7

- Boron, W, F. Regulation of intracellular pH.(2004) *Adv Physiol Educ* 28. 160–179
- Boulton, S, J. (2012) Integrated free radical sensor systems for investigation of cellular models of disease. PhD thesis, Newcastle University. Identifier:
<http://hdl.handle.net/10443/1427>
- Brown AE, Jones DE, Walker M, Newton JL (2015) Abnormalities of AMPK Activation and Glucose Uptake in Cultured Skeletal Muscle Cells from Individuals with Chronic Fatigue Syndrome. *PLoS ONE* 10(4):
- Buck, Y. Koo, E. Park, H. Xu, M. Philbert, M. Brausel. R. Kopelman,(2004) Current opinions in Chemical. Biology. 8, 540.
- Buhlman,P. Pretsch,E. Bakker, E. (1998) *Chem Rev*
- Busa, W, B. Nuccitelli, R.(1984) Metabolic Regulation via Intracellular pH. *Am J Physiol.* 246, 409– 438.
- Burns, A. Ow, H. Wiesner, U. (2006a). Fluorescent core-shell silica nanoparticles: towards “Lab on a Particle” architectures for nanobiotechnology. *Chem. Soc. Rev.* 35, 1028–1042
- Casey, J, R. Grinstein, S. Orlowski, J. (2010) Sensors and regulators of intracellular pH. *Nature reviews: molecular cell biology.* 11, 50-61
- Chatterjee,D,K. Ruffal, A,J. Zhang, Y.(2008) *Biomaterials*, **29**, 937–94
- Chauhan V. M. Burnett, G, R. Aylott, J, W. (2011). Dual-fluorophore ratiometric pH nanosensor with tuneable pKa and extended dynamic range. *Analyst.*136, 1799–1801
- Chou, L,Y. Ming, K. Chan,W, C, W. (2011) Strategies for the intracellular delivery of nanoparticles .*Chem Soc Rev.* 40 (1) 233-245
- Clark, H, A. Barker, S, L. Brasuel, M. Miller, M, T. Monson, E. Parus, S. (1998).Subcellular optochemical nanobiosensors: probes encapsulated by biologically localised embedding (PEBBLEs). *Sensor. Actuat. B Chem.* 51, 12–16
- Cui, S. Zhang, H. Chen,B. Wang, Y,Z. (2012) The mechanisms of lipofectamine 2000 mediated transmembrane gene delivery. *Engineering.* 4 (8) 172-175

- Coupland, P, G. Briddon, S, J. Aylott, J, W. (2009). Using fluorescent pH-sensitive nanosensors to report their intracellular location after Tat-mediated delivery. *Integr. Biol.* (Camb). 1, 318–323
- Davies, T,A. Fine, R,E. Johnson, R,J. Levesque, C,A. Rathbun, W,H. Seetoo,K, F. Smith,S,J. Strohmeier,G. Volicer,L. Delva,L. Simons, E,R. (1993) Non-age related differences in thrombin responses by platelets from male participants with advanced Alzheimer's disease. *Biochemistry biophysics research community.* 194, 537-543
- Dennis, A, M. Rhee,W,J. Sotto, D. Dublin, S, N. Bao, G. (2012) Quantum dot- fluorescent protein FRET probes for sensing intracellular pH. *ACS Nano.* 6 (4) 2971-2934
- Derfus, A, M. Chan, W, C, W. Bhatia, S, N. (2004) Probing the cytotoxicity of semiconductor quantum dots. *Nano Letters.* 4, 1–18.
- Desai, A. (2014) Development of optical pH nanosensors for biological insights into the intracellular trafficking of nanomedicines. PhD thesis. University of Nottingham.
- Desai, A. S. Chauhan, V, M. Johnston, A, P, R. Esler, T. Aylott, J, W. (2013). Fluorescent nanosensors for intracellular measurements: synthesis, characterization, calibration, and measurement. *Frontiers in Physiology,* 4, 401
- Dixit,S. Difiori,J,P. Burton, M. Mines,B. (2007) Management of patellofemoral pain syndrome. *Amateur family physician.* 75 (2) 194-202
- Donaldson, S, K. Hermansen, L. Bolles, L. (1978) Differential, direct effects of H⁺ on Ca²⁺-activated force of skinned fibers from the soleus, cardiac and adductor magnus muscles of rabbits. *Pflugers Arch.* 376:55–65
- Fabiato, A. Fabiato, F. (1978) Effects of pH on the myofilaments and the sarcoplasmic reticulum of skinned cells from cardiac and skeletal muscles. *J Physiol.* 276: 233–255.
- Forque, F, O. Brivet, M. Boutron, A. Vequaud, C. Marsac, C, C. Zabet, A, N, D, M. Benelli, C. (2003) Differential effect of DCA treatment on the pyruvate dehydrogenase complex in patients with severe PCHC deficiency. *Paediatric Research.* 53 (5), 793-799

- Gibbin, E, M. Putnam, H, M. Davy, S, K. Gates, R, D. (2014) Intracellular pH and its response to CO₂ in symbiotic and non-symbiotic cells. *Journal of experimental biology*. 214, 1963-1969
- Han, J. Burgess, K. (2010) Fluorescent indicators for intracellular pH. *Chemical reviews*. 110, 2709-2728
- Henderson, J, R. Swalwell, H. Boulton, S. Manning, P. McNeil, C, J. Birch-Machin, M, A. (2009) Direct, real-time monitoring of superoxide generation in isolated mitochondria. *Free Radical Res*. 43, 796–802
- Herrero, M, A. Toma, K, T. Al-Jamal, K. Kostarelos, A. Bianco, T. Da Ros, F. Bano, L. Scoles, C, G. Prato, J. (2009) *Journal Am Chem soc*. 131. 9843-9848
- Izumi, H. Torigoe. T. Ishiguchi, H. Uramoto, H. Yoshida, Y. Tanabe, M. Ise, T. Murakami, T (2003) Cellular pH regulators: Potentially promising molecular targets for cancer. *Chemotherapy cancer treatment reviews*. 29, 541-549
- Jones, D, E, J. Hollingsworth, K. Blamire, A, M. Taylor, R. Newton, J, L. (2010) Abnormalities in pH handling by peripheral muscle and potential regulation by the autonomic nervous system in chronic fatigue syndrome. *Journal of Internal Medicine*. 26, 394–401
- Jones, D, E. Hollingsworth, K, G. Jakovljevic, D, G. Faltakhova, G. Pairman, J. Blamire, A, M. Trennel, M, I. Newton, J, L. (2012) Loss of capacity to recover from acidosis on repeat exercise in chronic fatigue syndrome: A case control study. *European Journal of Clinical Investigation*. 42 (2) 184-194
- Juel C. (2008) Regulation of pH in human skeletal muscle: adaptations to physical activity. *Acta Physiol*. 193:17–24.
- Kristl, J. Plajnssek, K, T. Kreft, M, E. Janovic, B. Kocbek, P. (2013) Intracellular trafficking of solid lipid nanoparticles and their distribution between cells through tunnelling nanotubes. *European journal of pharmaceutical sciences*. 50, 1, 139-148
- Lancha Junior, A, H. Painelli, V, D. Saunders, B. Artioli, G, G. (2015) Nutritional strategies to modulate intracellular and extracellular buffering capacity during high-intensity exercise. *Sports medicine*. 45, 71-81

- Llopis, J. McCaffery, J. M. Miyawaki, A. Farquhar, M. G. Tsien, R. J. (1998) Measurement of cytosolic, mitochondrial and golgi pH in single living cells with green fluorescent proteins. *Proceedings of the national academy of sciences of the united states of america*. 95, 6803-6808
- Loiselle, F. B. Casey, J. R. (2003) Measurement of Intracellular pH. *Methods Mol Biol*. 227, 259–280
- Monson, E. Brasuel, M. Philbert, M.A. Kopelman, R. (2014) PEBBLE Nanosensors for *in vitro* bio-analysis. *Therapeutics and advanced biophotonics*. 22, 555-574
- Nel, A. E. Madler, L. Velego, D. Xia, T. Hoek, E. M. V. Somasundaran, P. Klaessig, F. Castranova, V. Thompson, M. (2009) Understanding biophysicochemical interactions at the nano-bio interface. *Nature Materials*. 8:543–55
- Panariti, A. Miserochi, G. Rivolta, I. (2012) The effect of nanoparticle uptake on cellular behaviour: disrupting or enabling functions. *Nanotechnology, Science, Applications*. 5, 87-100
- Papandreou, I. Goliassova, T. Denko, N. C. (2011) Anticancer drugs that target metabolism: is dichloroacetate the new paradigm. *International Journal of Cancer*. 128, 1001-1008
- Robergs, R. A. (2001) Exercise-induced metabolic acidosis: Where do the protons come from? *Sportscience*. 5 (2)
- Ruenraroengsak, J. Cook, J. M. Florence, A. T. (2010) Nanosystem drug targeting: facing up to complex realities. *Journal Control. Rel*. 141, 265-276
- Schulz, A. Wotschadlo, J. Heinze, T. Mohr, G. J. (2010). Fluorescent nanoparticles for ratiometric pH-monitoring in the neutral range. *J. Mater. Chem*. 20, 1475–1482
- Shahlin, K. Harris, R. C. Hultman, E. (1975) Creatine kinase equilibrium and lactate content compared with muscle pH in tissue samples obtained after isometric exercise. *Biochem J*. 152:173–180
- Sondergaard, R.V. Henriksen, J. R. Andresen, T. L. (2014) Design, calibration and application of broad-range optical nanosensors for determining intracellular pH. *Nature protocols*. 9, 2841-2858

- Srivastava, J. Barber, D, L. Jacobson, M, P. (2007). Intracellular pH sensors: design principles and functional significance. *Physiology (Bethesda)* 22, 30–39
- Sun, H. Almdal, K. Andresen, T, L. (2011) Expanding the dynamic measurement range for polymeric nanoparticle pH sensors. *Chem. Commun. (Camb)*. 47, 5268–5270
- Sutton, J, R, Jones, N, L. Toews, C, J. (1981). Effect of pH on muscle glycolysis during exercise. *Clinical Science*. 61. 331–338.
- Valli, M. Savier, M. Branduardi, P. Borth, N. Porro, D. Mattnovich, D. (2005) Intracellular pH distribution in *saccharomyces cerevisiae* cell populations, analysed by flow cytometry. *Appl environ microbial*, 71, 3, 1515-1521
- Vo-Dinh (2003) *Journal of cell biochemistry*. 87, 154
- Zhang, X. Allen, P, G. Grinstaff, M. (2012) Macropinocytosis is the major pathway responsible for DNA transfection in CHO cells by a charge-reversal amphiphile. *Mol Pharm*. 8, 758–766

Chapter 3

Direct, Real-time Electrochemical Detection of Superoxide Generation in CFS/ME Patient Myoblasts

3. 1 Introduction

The purpose of this chapter was to utilise a direct, real-time electrochemical sensing technique to investigate the potential role of elevated O_2^- production in the generation of the CFS/ME fatigue phenotype. For example, a series of *in vivo* investigations confirmed the elevation of blood oxidant status both pre and post-exercise, in a variety of CFS/ME patient cohorts [Jammes et al. 2012, 2009 and 2005]. Additionally, bio-markers associated with oxidative stress have been reported to play a pivotal role in skeletal muscle fatigue [Finsterer et al. 2012], which is regularly described as a debilitating symptom experience by CFS/ME patients [Van Oosterwijck et al. 2010]. Overproduction of ROS/RNS has been linked to impaired mitochondrial function. This may relate to the accumulation of modified mitochondrial proteins, lipid and DNA, which may interfere with the electron transport chain leading to cellular bio-energetic dysfunction. Presently, there have been no *in vivo* studies that have attempted to measure cellular superoxide generation directly and in real-time in CFS/ME patient muscle samples. This chapter will use an electrochemical superoxide sensor and myoblasts derived from CFS/ME patients.

Specifically, O_2^- generation was measured in response to ethanol stimulation, which has recognised as a key chemical stimulant of O_2^- in other cell lines (e.g. hepatocytes). Ethanol is metabolised by the enzyme cytochrome P450 2E1 (CYP2E1), which has been recognised as a key generator of oxidative stress (Gonzalez. 2007). While predominantly located in the liver, genes encoding CYP2E1 have been reported to be clearly expressed in human skeletal muscle [Molina-Ortiz et al. 2013], suggesting skeletal muscle to play a role in xenobiotic metabolism. Ethanol has also been reported to stimulate the mitochondria specific CYP2E1 enzyme [Bansal et al. 2010]. Given the presence of CYP2E1 in human skeletal muscle and as myoblasts contain a high volume of mitochondria, the use of ethanol as a chemical stimulant to assess the capacity of CFS/ME myoblasts to generate O_2^- was justified.

O_2^- generation was also measured in response to lactic acidification, to assess the impact of extracellular acidification on oxidative stress. As previously described CFS/ME patients have been reported to exhibit significant intracellular acidosis when measured via MRS [Jones et al. 2012; 2010], in addition an *in vitro* study reported aberrantly low intracellular pH in CFS/ME compared to control myoblasts [Boulton, 2012].

3.1.1 Free-radical overview

Oxygen-derived free radicals are produced as a result of a one electron reduction in molecular oxygen resulting in an extremely unstable configuration. Radicals rapidly react with other radicals or molecules to achieve stability (Displayed in Figure 3.7). Oxygen is a di-radical possessing two unpaired electrons. When oxygen gains an additional electron O_2^- is produced which is the precursor to other ROS and RNS. For example, the reaction of O_2^- with nitric oxide produces a highly aggressive oxidant, peroxynitrite ($ONOO^-$) which acts to greatly limit nitric oxide availability. Furthermore, in aqueous solutions O_2^- may also steadily dismutate to hydrogen peroxide (H_2O_2), which is catalysed by superoxide dismutase (SOD) in the body. Finally, in the presence of trace metals, including copper and iron, O_2^- and H_2O_2 can produce hydroxyl radical $\cdot OH$ which rapidly reacts with a wide variety of biological molecules. The hydroxyl radical has a particularly high affinity for lipid and is associated with lipid membrane degeneration via lipid peroxidation [Brandes and Janiszewski. 2005].

In terms of the function of ROS, under normal physiological conditions the cellular concentration of ROS is maintained at a constant level with this balance modulated by processes that both produce and eliminate free radicals. Effectively, the source of ROS can be separated into two categories. Firstly processes that release ROS through normal physiological processes as a waste product such as mitochondrial oxidative phosphorylation. Secondly, processes that generate ROS purposefully, in response to xenobiotics, cytokines and bacteria invasion, either through molecular synthesis or breakdown and as part of a signal transduction pathway, or functioning as part of cell defence mechanism [Finkel et al.2011; Zhang et al. 2016].

In terms of the impact of ROS on skeletal muscle cells, ROS have been reported to induce and promote mitochondriogenesis a key factor in muscle differentiation. This has been

reported to occur via peroxisome proliferator-activated-receptor-gamma-coactivator-1 α (PGC-1 α) activated signal transduction pathway. However, in excess ROS may target mt DNA effectively shutting down myogenic differentiation [Rochard and Sejtli, 2000]. The occurrence of each of these processes is determined by the level and duration of ROS targeting muscle cells, the antioxidant status of the cell (SOD content) and the DNA repair capability of the cell. The differentiating stage of the muscle cell (satellite cell, differentiating myoblast or myotube) also is capable of redirecting the cell through different signalling pathway and further modifying cellular response to limit damage [Barbieri et al. 2012]. Therefore, it would appear that while ROS generation can promote muscle cell differentiation and repair, in excess it exhibits the capacity to be highly detrimental to muscle cell growth and development [Barbieri and Sejtli, 2012].

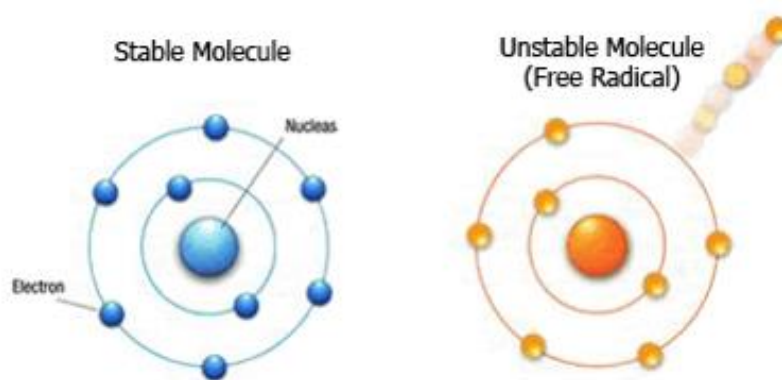


Figure 3.7 Free radicals are atoms that contain an unpaired electron in their outermost shell, resulting in a highly unstable configuration and radicals rapidly reacting with other molecules and radicals to achieve stable configuration.

3.1.2 O₂⁻ Detection techniques

3.1.2.1 Spectroscopic O₂⁻ measurement

Spectroscopic techniques have been used to measure O₂⁻ flux in real-time [Tarpey and Fridovich. 2001]. One method being the reduction of cytochrome *c*, which has been used to measure the rate of O₂⁻. generation from enzymes, tissue extracts and whole cells [Tarpey and Fridovich. 2001]. In terms of the reaction, it occurs at a constant of 1x5x10⁵mol/L⁻¹, pH8 and at room temperature, absorbance is then measured spectrophotometrically at λ 550nm

[Land and Swallow. 1971; Ballou et al. 1969]. During the reaction, ferricytochrome *c* is reduced to ferrocycytochrome *c* by receiving an electron from O_2^- . When ferricytochrome *c* is reduced its spectrophotometric absorbance is altered in a specific manner, with absorbance at 550nm increased, whereas at λ 540nm and λ 560nm absorption remains unchanged and serve as isobestic points [Dikalov et al. 2007].

The reduction of cytochrome *c* is considered by many researchers to be the ‘gold standard’ technique for the detection of O_2^- . However, while the technique is effective in measuring O_2^- when it is present in large amounts e.g. during respiratory burst in neutrophils and in isolated enzyme reactions, it may not be as effective at detecting O_2^- in tissues that produced lower levels such as endothelial and muscle cells [Dikalov et al. 2007]. Tarpey and Fridovich [2001] outlined further precautions to consider when using the technique to measure O_2^- . For example, tissue extracts contain compounds such as ascorbate and glutathione that can reduce cytochrome *c*, in addition to reductases that enzymatically catalyse cytochrome *c* reduction. What is more, reduced cytochrome *c* can be reoxidised by cytochrome oxidases, peroxidases and oxidants, which include H_2O_2 and ONOO-. This reoxidation by diminishing apparent rates of cytochrome *c* reduction, which can lead to the underestimation of O_2^- formation.

Nitroblue tetrazolium (NBT) is another technique commonly applied in spectroscopic O_2^- detection and is based upon the reduction of NBT dye in the presence of O_2^- . [Brandes and Janiszewski. 2005]. A limitation associated with this technique is that the reduction of NBT is not isolated to O_2^- . Other substances including cellular reductases can donate an electron to NBT, forming the NBT radical. The major problem is that under aerobic conditions the NBT radical is capable of reacting with environmental O_2 , which acts to generate O_2^- artificially [Warwar et al. 2011; Tarpey and Fridovich. 2001].

The NBT radical intermediate can react with molecular oxygen under aerobic conditions which acts to generate O_2^- artificially, which further reduces NBT and a false positive result [Warwar et al. 2011].

3.1.2.2 Electron spin resonance spectroscopy

Electron spin resonance spectroscopy (ESR) also referred to as electron paramagnetic resonance is a technique that detects paramagnetic species with one or more unpaired

electrons [Hogg. 2010]. ESR exhibits a number of benefits when compared to other superoxide detection techniques because of its unique ability to detect either short or long lived free radicals with specificity and sensitivity [Tarpey and Fridovich. 2001]. ESR is capable of taking advantage of the paramagnetic state of $O_2^{\cdot-}$, however the low steady-state concentration, short lifetime as well as the rotational angular momentum of the relatively small diatomic molecule limits the ability to direct detection, requiring the need for spin-trapping [Warwar et al. 2011]. Spin traps are molecules that react with $O_2^{\cdot-}$ to produce a relatively stable paramagnetic species [Warwar et al. 2011; Khan et al. 2003]. The spin-trapping technique utilises a nitron or nitroso compound to react with a free radical to produce a nitroxide (spin adduct), which exhibits substantially greater stability than the parent free radical [Ledoux et al. 2004; Gornicki et al. 2001]. Traditionally, the most common spin trap used for superoxide detection has been $O_2^{\cdot-}$ -5,5 dimethyl-1-pyrroline-N-Oxides (DMPO). However, DMPO-OOH (DMPO/ $O_2^{\cdot-}$) adduct is incredibly unstable and decays rapidly with a half-life of approximately 60 seconds at pH7. Due to this limitation, more recently other spin-traps have been synthesised including ester group 5-tert-butoxycarbonyl-5-methyl-pyrroline-N-oxide (BMPO). BMPO exhibits an increased rate constant for spin trapping $O_2^{\cdot-}$ compared to DMPO and BMPO-OOH exhibits a greater half-life than DMPO-OOH [Rana et al. 2010].

Nevertheless, even with improvements in spin-trapping capability, due the low-levels of $O_2^{\cdot-}$ *in vivo* makes detection via ESR techniques incredibly difficult. Furthermore, ESR has been primarily used to measure $O_2^{\cdot-}$ in cell lysates and purified proteins and lacks the ability to detect $O_2^{\cdot-}$ in whole cell systems [Rana et al. 2010; Tarpey and Fridovich et al. 2001]

3.1.2.3 Amperometric extracellular $O_2^{\cdot-}$ monitoring

Electrochemical techniques for the detection of free radicals exhibit a key benefit over other free radical detection methods by enabling the direct, real-time measurement of free radicals within a biological system, with negligible disruption to the sample throughout experimentation [McNeil and Manning. 2002]. Amperometric $O_2^{\cdot-}$ detection devices are a type of electrochemical sensor, which continuously measure current resulting from redox reactions occurring at the electrode surface [Grieshaber et al. 2008]. The electrodes that are commonly used are produced from conductive materials such as gold, platinum and graphite

[Ramirez et al. 2009]. In the 1970s it was realised that electrode surfaces following functionalisation were capable of interacting with proteins, to provide stable and direct electrochemistry that was not disturbed by artefacts [McNeil and Manning. 2002; Armstrong et al, 1990]. Cooper et al. [1993] first described the use of a gold electrode with immobilised cytochrome *c* on the surface. The covalent attachment of cytochrome *c* on the modified surface was achieved through a carbodiimide initiated condensation reaction, with cytochrome *c* forming an integral part of the amperometric $O_2^{\cdot -}$ sensor.

Manning et al. [1998] described a simplified protocol for cytochrome *c* immobilisation at a gold electrode surface in comparison to previously described methods [Cooper et al. 1993]. In this method the $O_2^{\cdot -}$ electrode was functionalised via a two-step process (See Figure 3.8)

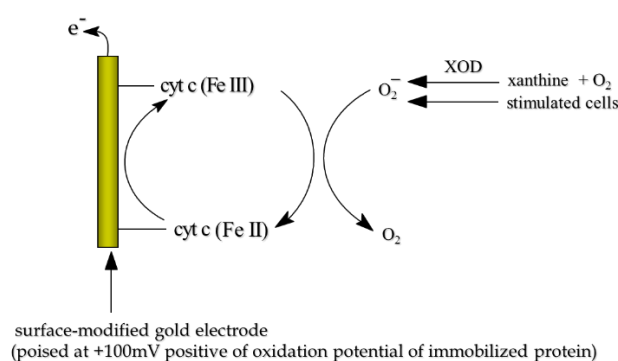


Figure 3.8: Schematic representation of the electrochemical superoxide sensor described by Manning et al. [1998].

Firstly, the link molecule 3-3'-dithiobis (sulfosuccinimidyl-propionate) (DTSSP) was attached to the gold surface of the electrode, which was possible as DTSSP possesses a disulphide group to enable covalent attachment to gold surface. Once attached the molecule exhibits two carboxyl groups which undergo amide linkage with cytochrome *c*. The electrode was then poised at a working potential of +100mV versus a silver/silver chloride reference electrode [McNeil and Manning. 2002]. In a study conducted by Tammeveski et al. [1998] the authors reported the use of a gold surface electrode functionalised with cytochrome *c* to be effective in detecting $O_2^{\cdot -}$ generated through the enzymatic breakdown to xanthine to uric acid by xanthine oxidase. Furthermore, Manning et al. [1998] utilised the cytochrome *c* functionalised electrode to measure *in vitro* extracellular flux of $O_2^{\cdot -}$ from phorbol-12 myristate-13 acetate (PMA) stimulated astrocytes. This demonstrated the ability of the technique to measure $O_2^{\cdot -}$ production

directly and in real-time from a cellular system. More recent studies have also reported cytochrome *c* functionalised electrodes to be effective in measuring $O_2^{\cdot-}$ generated in live cells as well as isolated mitochondria [Aitken et al. 2007; Henderson et al. 2009]. Other functionalisation methods have been reported, for example, Shleev et al. [2006] described an $O_2^{\cdot-}$ electrode that utilised azurin rather than cytochrome *c*. However, this method exhibited a crucial limitation in that the stability period of the electrode was reduced when compared to that described by Manning et al. [1998].

Recent studies have also reported cytochrome *c* functionalised electrodes to be effective in measuring $O_2^{\cdot-}$ generation in various *in vitro* biological systems [Aitken et al. 2007; Henderson et al. 2009; Manning et al. 2001]. Other functionalisation methods have been reported, for example, Shleev et al. [2006] described an $O_2^{\cdot-}$ electrode that utilised azurin rather than cytochrome *c*. However, this method exhibited a crucial limitation in that the stability period of the electrode was reduced when compared to that described by Manning et al. [1998]. Despite a more prolonged functionalisation process.

3.1.3 Hypotheses

The aim of the chapter was to examine $O_2^{\cdot-}$ generation in CFS/ME patient myoblasts, performed following chemical stimulation with ethanol or incubation with lactic acid.

Specific experimental hypothesis were:

- (1) CFS/ME myoblasts exhibit elevated $O_2^{\cdot-}$ generation following ethanol stimulation, compared to controls.
- (2) $O_2^{\cdot-}$ elevated in CFS/ME patient samples compared to controls following incubation with lactic acid.

3.2 Materials and Methods

CFS/ME and control myoblast samples were provided by Dr Audrey Brown from the diabetes research group, Newcastle University. In this chapter the myoblast samples were derived from a female CFS/ME patient aged 65 years and a female control participant aged 66 years.

Tissue culture reagents were supplied by Sigma-Aldrich (Poole, Dorset), apart from Ham's F10 growth medium (Lonza, SLS, East Riding, Yorkshire) and chick embryo extract (Sera Lab, West Sussex, UK).

Plastic consumables such as tissue culture flasks, serological pipettes, 24-well plates, falcon tubes and cell scrapers were supplied by Greiner Bio-one (Stonehouse, UK).

Superoxide dismutase (SOD), Xanthine, Xanthine oxidase (XOD), cytochrome c and lactic acid were purchased from Sigma Aldrich. DTSSP was supplied by Pierce (Chester, UK). Ethanol was purchased from Fisher (Cramlington, UK).

3.2.1 Cell culture and preparation

CFS/ME and control muscle samples were collected and processed as described in chapter 2. Myoblast samples were cultured in Ham's F10 growth medium, which the addition of 20% FBS, 2% chick embryo extract, 500U/mL penicillin streptomycin and 1% amphotericin B. Cells were grown to 80% confluence prior to experimentation in a T75 flask. Cells were maintained in a humidified incubator at 5% (v/v) CO₂ at 37° C .

3.2.1.1 Direct real-time electrochemistry

3.2.1.2 Preparation of superoxide specific electrode

The electrode was prepared as detailed by Manning et al. [1998]. A 2 mm O.D. solid gold electrode (BioAnalytical Systems, Cambridgeshire, UK) was polished with a 0.2µm aluminium oxide slurry bound to a micro-cleaning cloth (BioAnalytical Systems, Cambridgeshire, UK). The electrode surface was then cleaned by sonicating in 100% ethanol for 5 minutes, before rinsing with deionised water. Subsequently, the electrode was incubated

with 50mM of the thiol linker DTSSP and incubated for 5 minutes at room temperature before rinsing with deionised water. The electrode was then treated with a 2mM of cytochrome *c* prepared in PBS and incubated over night at 4 °C. Prior to experimentation, the electrode was once again rinsed with deionised water to remove any unbound protein.

3.2.1.3 Electrode calibration

An enzyme-based reaction (Xanthine/ XOD) was used to calibrate the electrode. See Figure 3.9.

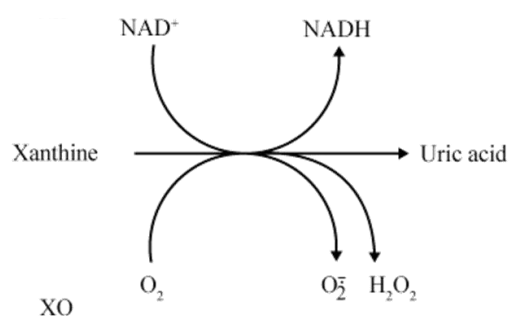


Figure 3.9: Superoxide production by the action of xanthine oxidase (XOD) on xanthine.

Throughout the calibration the electrode was poised at +100mV and used in conjunction with an Ag/AgCl electrode which acted as a combined reference and counter electrode. The working electrode and the Ag/AgCl reference electrode were both placed in a 24-well plate containing 1.5mM xanthine in PBS. Following the achievement of a stable baseline varying concentrations of XOD (0,0.25, 0.5, 0.75, 1 U/mL) were added to the reaction volume and the resultant change in current was observed. To ensure XOD was equally and rapidly distributed throughout the well a magnetic based stirring system was applied. To test the specificity of the electrode to O_2^- the scavenger superoxide dismutase (SOD) radical was added to the well at a concentration of 500U/mL to quench any responses at the electrode surface. Measurements were obtained using a 2-channel potentiostat and data was acquired using UiEchem software (Buxton, UK).

Following routine culture cells were seeded into a clear, 24-well plate at a density of 1×10^5 cells per well and placed in an incubator overnight to attach. Cells were maintained in a humidified environment at 5% CO_2 at a temperature of 37.5°C .

During experimentation the working and reference electrode were connected to the potentiostat and suspended just above the cell later. A steady baseline current was achieved before adding $50\mu\text{L}$ of PBS (control), or varying concentrations of ethanol (2-5%). The chemicals were used to induce the generation of O_2^- radicals by the myoblasts. Current was produced at a rate that was directly proportional to the rate of O_2^- production by the cell. The specificity of the electrode response to O_2^- was assessed by using the superoxide specific scavenger, SOD (500 U/mL) was added to scavenge superoxide after a clear maximal current value had been obtained following the addition of the chemical stimulant.

3.2.1.4 Cellular superoxide measurement following ethanol stimulation of myoblasts

CFS/ME and control myoblasts were seeded into 24-well testing plates at a density of 1×10^5 cells per well in triplicate and were allowed to attach overnight. The following day, ethanol was added to the wells of the testing plate at the concentration 2, 3, 4 and 5%. To confirm the presence of superoxide the enzyme superoxide dismutase (SOD) was subsequently added at a concentration of 500 U/mL to scavenge any superoxide radicals present.

3.2.1.5 Cellular superoxide measurement following acidification of myoblasts

CFS/ME and control primary myoblasts were seeded into 24-well testing plates at a density of 1×10^5 per well in triplicate. Following overnight attachment, cell culture media was acidified by adding 2 mM lactic acid directly to each well, which corresponded to $\text{pH } 5.36$ (determined prior to the experiment using a pH meter (Hanna, Bedfordshire, UK)). Cells were incubated in a humidified environment at 5% CO_2 and at a temperature of 37.5°C for 30 minutes, 5 hours and 24 hours.

Following achievement of a maximal response (indicated by a stable plateau in current values) 500 U/mL of SOD was added to the well to scavenge any superoxide radicals.

3.2.2 Cell viability in response to lactic acidification

The role of lactic acidification as a potential stimulator of O_2^- generation was investigated in this chapter. Therefore, it was necessary to assess the cytotoxicity of lactic acid following 24-hours incubation. Briefly, myoblasts were seeded at a density of 1×10^4 cells per well and allowed to attach overnight. The following day, growth medium was removed, cells were washed once with PBS and replaced with DMEM and varying concentration of lactic acid (0.5mM- 2mM). The plate was then incubated for 24-hours.

3.2.3 Data analysis

Minitab statistical software was the statistical model used to examine the data. The descriptive statistics used were mean \pm SD. Inferential statistics were used to investigate CFS/ME and control O_2^- generation in response to ethanol stimulation and lactic acidification. Specifically, the statistical tests used were paired samples T-test and independent T-test. Significance was accepted at the $P < 0.05$ level.

3.3 Results

3.3.1 Direct real-time electrochemistry

3.3.1.1 Xanthine/XOD calibration curve

Figure 4.0 demonstrated a that current recorded at the electrode was directly proportional to the concentration of XOD added to the system (in the presence of excess xanthine) ($R^2=0.9582$).

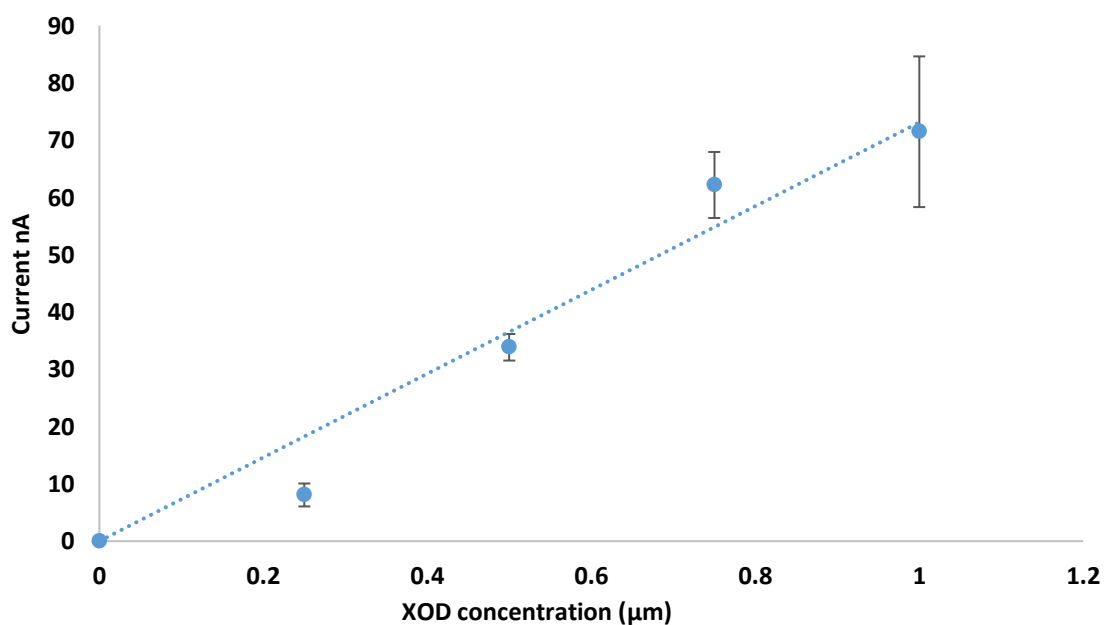


Figure 4.0: Superoxide calibration curve with varying concentrations of xanthine oxidase (0.25-1.0 μM) in the presence of constant xanthine (1.5mM) produced a linear increase in current ($R^2=0.9582$, $n=4 \pm\text{SD}$)

3.3.1.2 Cellular superoxide response to ethanol in myoblasts

Figure 4.1 (a) showed there to be a slight linear relationship ($R^2= 0.7007$) between increased ethanol concentration and a greater recorded current in CFS/ME myoblasts. Similarly, Figure

4.1 (b) also demonstrated control myoblasts to exhibit a small linear increase ($R^2=0.6814$) in current with a rise in ethanol concentration. Additionally, responses were quenched with (500U/mL) SOD which was added directly to the well, confirming the presence of O_2^- . There was no significant difference in current for CFS/ME compared to control myoblasts at any of the ethanol concentrations tested when each sample. Statistical analyses were performed by comparing triplicate measures for CFS/ME and control samples for each of the ethanol concentrations.

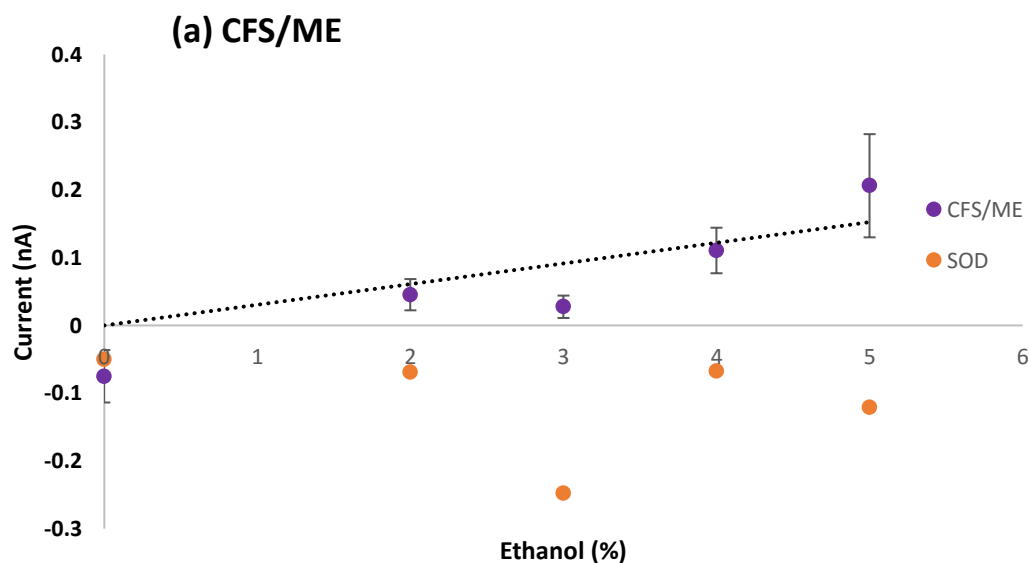


Figure 4.1 (a): Superoxide generation in CFS/ME myoblast cells following stimulation with varying concentrations (2-5%) of ethanol. There was a small linear relationship between ethanol concentration and recorded current ($R^2=0.7007$). The response was inhibited with 500U/mL of SOD. Data presented as Mean \pm S.D of 3 replicate measures, n=2.

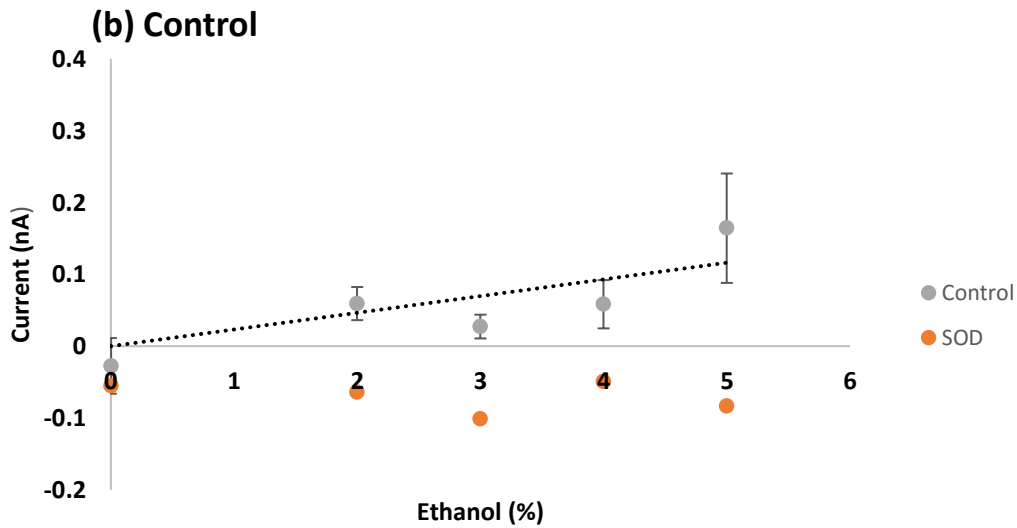


Figure 4.1 (b): Superoxide generation in CFS/ME myoblasts cells following stimulation with varying concentrations (2-5%) of ethanol. There was a small linear relationship between ethanol concentration and recorded current ($R^2=0.6814$). The response was inhibited with 500U/mL of SOD. Data presented as Mean \pm S.D of 3 replicate measures, $n=2$.

3.3.1.3 Superoxide generation following acidification in myoblasts

Figure 4.2 showed acidification of the medium to pH 5.36 (2mM lactic acid) over-time to induce no significant difference in superoxide generation (nA) in either CFS/ME or control myoblasts at any of the time points.

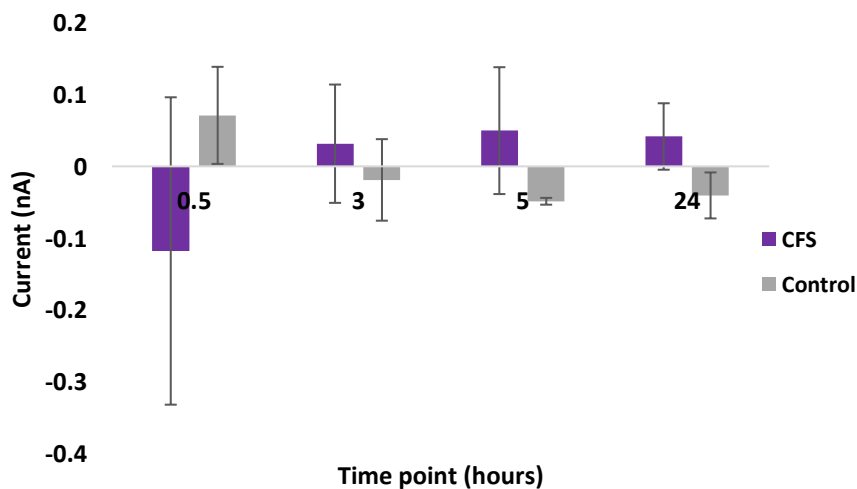


Figure 4.2: Lactic acidification (2mM, pH 5.36) over time (30 minutes-24 hours) did not induce any meaningful change in superoxide generation over-time in CFS/ME or control myoblasts samples. Data presented as Mean \pm S.D of 3 replicate measures, $n=2$

3.3.2 Cytotoxicity with lactic acidification

Figure 4.3 demonstrated both CFS/ME and control myoblast cell viability measured with 0.03% resazurin following 24-hour incubation with varying concentrations of lactic acid (0.5mM-2mM) . CFS/ME cells exhibited significantly greater viability when compared to control cells following 2mM acidification (pH 5.36 (P<0.0005), 1.5mM (pH 6.11 (P<0.0005) and 1mM(pH 6.61 (P<0.005). There was no significant difference following 0.5mM (pH 7.09) acidification.

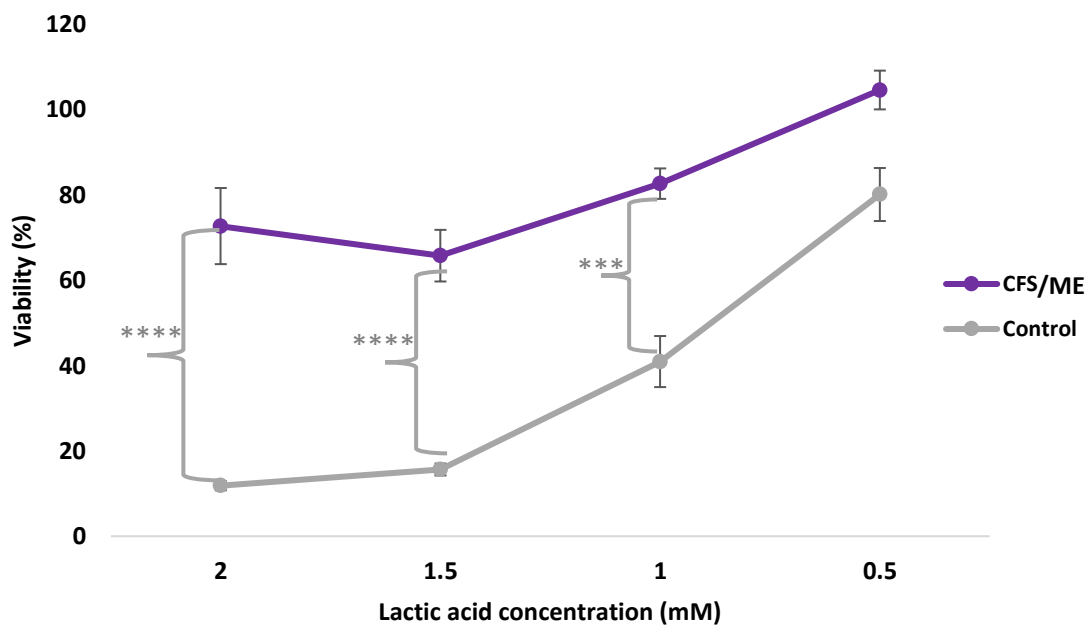


Figure 4.3: Lactic acidification of CFS/ME and control myoblasts over 24-hours resulted in significantly lower viability in control compared to CFS/ME cells following treatment with 1mM, 1.5mM and 2mM Lactic acid (pH 6.61, 6.11 and 5.36 respectively). There was no significant difference between CFS/ME and control cells following 0.5mM acidification (pH 7.09). Data presented as mean \pm SD of 3 replicate measures, n=2. **** denotes $P \leq 0.0005$, *** denotes $P \leq 0.005$ as determined by independent t-test.

3.4 Discussion

Previous studies have confirmed CFS/ME patients to exhibit increased oxidative stress and decrease antioxidant status at rest, which was related to the extent of symptomology. In these studies blood oxidant markers such as TBARS and ascorbic acid were measured [Jammes et al. 2005; Fulle et al. 2000; Keenoy et al. 2001; Richards et al. 2000]. More recently, *in vivo* exercise based investigations have reported accentuated oxidative stress and altered muscle membrane excitability, which the authors suggested to explain muscle pain and PEM experienced by individuals with CFS/ME [Jammes et al. 2012; 2009 and 2005]. Elevated ROS has been reported to impact upon skeletal muscle function by inducing lipid peroxidation, which may lead to a loss of membrane excitability as a consequence of altered activation of K^+ channels within skeletal muscle [Luin et al. 2011].

In this chapter, a direct, real-time approach to monitoring $O_2^{\cdot-}$ generation in CFS/ME patient muscle samples was used. The electrochemical sensing technique was first reported by McNeil et al. [1992] and later developed by Manning et al. [1998]. Briefly, the method involved the covalent attachment of cytochrome *c* to the surface of a gold working electrode through surface modification with DTSSP. The generation of $O_2^{\cdot-}$ by Xanthine/XOD resulted in the one electron reduction of cytochrome c^3 to cytochrome c^2 , with the reduced protein then reoxidised at the electrode surface (poised at 100mV against Ag/AgCl reference electrode). The current rates recorded were found to be directly comparable to $O_2^{\cdot-}$ production by XOD [Manning and McNeil. 2011]. The electrochemical technique has been reported to successfully detect $O_2^{\cdot-}$ in a number of *in vitro* studies including, isolated mitochondria, cultured glial cells, human glioblastoma and B16 mouse melanoma [Henderson et al. 2009; Valverde et al. 1996; Manning et al. 2001; Manning et al. 1998].

In this chapter $O_2^{\cdot-}$ generation was measured in CFS/ME myoblast samples following ethanol stimulation or lactic acidification. The work performed in this chapter did not confirm the presence of elevated $O_2^{\cdot-}$ generation in CFS/ME muscle samples. Firstly, stimulation with ethanol was associated with a small linear increase in $O_2^{\cdot-}$ generation in both CFS/ME and control samples, however no significant difference in $O_2^{\cdot-}$ generation between sample groups was found (Figure 4.1 a and b). Secondly, following lactic acidification of the assay medium, $O_2^{\cdot-}$ generation did not significantly differ between CFS/ME and control muscle samples (displayed in Figure 4.2). However, cytotoxicity work did reveal CFS/ME myoblasts viability to be significantly higher than controls following incubation with lactic acid (See Figure

4.3), suggesting CFS/ME myoblasts to be better able to buffer the effects of extracellular acidification.

3.4.1 Ethanol stimulation

In this chapter O_2^- generation was not elevated in CFS/ME muscle samples following ethanol stimulation. It is difficult to contextualise this finding as presently no other studies have used electrochemical sensing approaches to directly measure O_2^- in the muscle of CFS/ME patients.

However, this finding contrasts previous *in vivo* studies that have alternatively reported CFS/ME patients to exhibit enhanced oxidative stress at rest, which was accentuated during exercise [Jammes et al. 2012, 2009 and 2005]. Nevertheless, it is important to acknowledge the differing methodological approaches used. Free-radicals exist for a limited period *in vivo* and cannot be measured directly [Halliwell and Whiteman, 2004]. Therefore, previous studies have measured blood-based markers associated with oxidative stress. These have included TBARS and endogenous antioxidant such as RAA and erythrocyte reduced glutathione [Jammes et al. 2012, 2009]. These markers give an indication of the degree of systemic oxidative stress. Unlike, the aforementioned *in vivo* studies a key benefit of the electrochemical sensing approach reported in this chapter is its ability to directly measure O_2^- at the cellular level. Nevertheless, it is important to recognise that *in vitro* effects may not be representative of the wider biological system as a whole. For example, *in vitro* cell systems lack the *in vivo* microenvironment, communication and direct contact with other cells and bio active substances [Aas et al. 2013].

It is also important to note that previous studies measured blood oxidant markers at rest and following exercise, representing a normal biological state [Jammes et al. 2012, 2009] However, in this chapter myoblast cells were chemically manipulated to induce oxidative stress. Ethanol is metabolised by the CYP2E1 enzyme, with this process recognised as a key generator of O_2^- [Bansal et al. 2010; Gonzalez, 2007; Jimenez-Lopez and Cederbaum. 2005]. While the expression of CYP2E1 has been reported in the skeletal muscle of adults and children [Molina-Ortiz et al. 2013]. It is accepted that the enzyme is predominantly located in the liver and the levels found in the muscle are substantially lower [Jimenez-Lopez

and Cederbaum. 2005]. Therefore, ethanol stimulation may not have been the most effective way to promote oxidative stress in skeletal muscle cells.

3.4.2 Extracellular acidification

This chapter also investigated O_2^- generation in response to lactic acidification, to assess whether extracellular acidification impacted upon oxidative stress. As previously described, several *in vivo* studies have revealed excessive intramuscular acidosis in CFS/ME patients, suggestive of bio-energetic dysfunction and an over utilisation of the lactate dehydrogenase pathway. In addition, intracellular pH has also been reported to be significantly lower in CFS/ME myoblasts compared to controls [Boulton. 2012].

Nevertheless, in this chapter lactic acidification of the assay medium did not lead to increased O_2^- generation in CFS/ME myoblasts when compared to healthy controls. Contrary, to previous investigations that have reported elevated blood-oxidant status in CFS/ME patients and concurrent muscle dysfunction [Jammes et al. 2012, 2009 and 2005]. Thus, extracellular acidification does not appear to induce oxidative stress.

However, it is important to note that chemical manipulation to induce extracellular acidification may not be representative of intracellular acidosis that has been reported in CFS/ME patients following exercise, which may alternatively be related to bio-energetic dysfunction [Jones et al. 2012 and 2010]. Therefore, in this chapter it would have been advantageous to simulate exercise *in vitro* through the EPS of muscle samples, to investigate the impact of muscle contraction on O_2^- generation in CFS/ME. However, it was not possible to use EPS in conjunction with the electrochemical sensor as the device function to electrically stimulate muscle samples to contract. As the electrode measures current in the well it would have been difficult to decipher between artefacts due to EPS and changes in the current caused by O_2^- generation.

Although, lactic acidification work did not impact upon O_2^- generation, a cytotoxicity assay revealed CFS/ME myoblasts to exhibit greater viability than control cells following treatment with lactic acid. This was an interesting finding as it suggests the CFS/ME patient cells to tolerate substantial acidification, although it is difficult to determine the mechanism behind this occurrence. However, as previously described several studies have revealed profound

intramuscular acidosis in CFS/ME patients [Jones et al. 2012; 2010], it is possible as a consequence that cells have developed an improved buffering capacity to cope with excessive acidification.

3.4.3 Limitations

It is important to acknowledge a number of limitations associated with this technique. For example, the concentration of ROS at the site of production is very high. However, as $O_2^{\cdot-}$ was measured in the extracellular medium and was required to diffuse out of the cell it is possible that the amount of $O_2^{\cdot-}$ measured by the electrode was not reflective of the intracellular environment. Additionally, the presence of trace metals in the extracellular medium may potentially function to decrease cellular $O_2^{\cdot-}$ generation. For example, copper has been reported to serve an essential co-factor for several oxidative stress related enzymes such as superoxide dismutase which quenches cellular $O_2^{\cdot-}$ generation [Tchounwou et al. 2012].

An enzyme based reaction (Xanthine/XOD) was performed to calibrate the $O_2^{\cdot-}$ electrode, this process was carried out in a stirred system to ensure equal diffusion of the enzyme and substrate throughout the well. However, when $O_2^{\cdot-}$ was measured *in vitro*, cells were attached to the surface at the bottom of the well. It was therefore not possible to use a magnetic stirrer without disturbing the cell layer. This was a limiting factor as following the addition of the chemical stimulants (i.e. ethanol/lactic acid) it was not possible to achieve equal diffusion across the well. It could have been possible to incorporate stirrers from above, however as the $O_2^{\cdot-}$ electrode also was positioned above the cell layer such equipment risked disturbing the electrode.

Additionally, although each well was seeded at the same density (1×10^5 cells), following attachment cells did not provide even coverage across the well. Consequently, it was impossible to position the probe in an area of exactly the same coverage during each measurement, bringing the reliability of the technique into question.

3.4.4 Conclusion

The direct real-time electrochemical sensing approach used in this chapter enabled the measurement of $O_2^{\cdot-}$ generation in CFS patient myoblast cells. Contrary, to previous *in vivo* studies that have reported evidence of elevated oxidative stress in CFS/ME patients this study alternatively revealed CFS/ME patient myoblasts to exhibit $O_2^{\cdot-}$ generation comparable to healthy control cells following chemical stimulation. Therefore, oxidative stress does not appear to contribute towards the muscle dysfunction and fatigue phenotype associated with CFS/ME.

3.5 References

- Aas, V. Bakke, S, S. Feng, Y, Z. Tranheim, E, K. Jensen, J. Bajpeyi, S. Thoresen, H. Rustan, A, C. Are culture myotubes far from home? Institute of pharmacy and Biomedical laboratory Science, Faculty of Health Science, Oslo and Akerhus University College of Applied Sciences, Oslo, Norway. Identifier <https://oda.hio.no/jspui/bitstream/10642/1936/10447post>
- Aitken, G, R. Henderson, J, R. Chang, S, C. McNeil, C, J. Birch-Machin, M, A. (2007) Direct monitoring of UV-induced free radical generation in HaCaT keratinocytes. *Clinical Experimental Dermatology*. 32, 722-727.
- Armstrong, F.A. (1990) Probing metalloproteins by voltammetry. *Struct. Bond*. 72, 137-22
- Bansal, S. Liu, C-P. Sepuri, N, B, V. Anandatheerthavarada, H, K. Selvaraj, V. Hoek, J. Milne, G, L. Guengerich, P, F. Avandhani, N, G. (2010) Mitochondria-targeted cytochrome P450 2E1 induces oxidative damage and augments alcohol mediated oxidative stress. *The Journal of Biological Chemistry*. 285, 2409-2469
- Ballou, D. Palmer, G. Massey, V. (1969) Direct demonstration of superoxide anion production during the oxidation of reduced flavin and of its catalytic decomposition by erythrocuprein. *Biochem Biophys Res Commun*. 36, 898–904.
- Barbieri, E. Sejtli, P. (2012) Reactive oxygen species in skeletal muscle signalling. *Journal of signal transduction*. 17
- Boulton, S, J. (2012) Integrated free radical sensor systems for investigation of cellular models of disease. PhD thesis, Newcastle University. Identifier: <http://hdl.handle.net/10443/1427>
- Brandes, R, P. Janiszewski, M. (2005) Direct detection of reactive oxygen species ex vivo. *Kidney International*. 67, 1662-1664
- Brown, A, E. Jones, D, A. Waker, M. Newton. J, L. (2015) Abnormalities of AMPK activation and glucose uptake in Chronic Fatigue Syndrome. *PLOS ONE*. 10 (4)
- Cooper, J, M. Greenough, K, R. McNeil, C, J. (1993) Direct electron transfer reactions between immobilised cytochrome c and modified gold electrodes. *Journal of Electroanalytical Chemistry* 347(1-2), 7-275

- Dikalov, S. Griending, K, K. Harrison, D, G. (2007) Measurement of reactive oxygen species in cardiovascular disease studies. *Hypertension*. (4) 717-727
- Finkel, T. (2011) Signal transduction by reactive oxygen species, *Journal of Cell Biology*. 194, (1) 7–15
- Finsterer, J. (2012) Biomarkers of peripheral muscle fatigue during exercise. *BMC Musculoskeletal Disorders*. 13, (218), 1-13
- Fulle, S. Mecocci, P. Fano, G. (2000) Specific oxidative alterations in vastus lateralis muscle of patients with the diagnosis of chronic fatigue syndrome. *Free Radic Biol Med*. 29, 1252–1259
- Gonzalez, F, J. (2007) CYP2E1. *Drug metabolism and disposition*. 35, 1-8
- Gornicki, A. Gutsze, A. (2001) Erythrocyte membrane fluidity changes in psoriasis: An EPR study. *J Dermatol Sci*. 27, 27-30
- Grieshaber, D. MacKenzie, R. Voros, J. Reimhuit, E. (2008) Electrochemical biosensors- sensor principles and architectures. *Sensors (Basel)*. 8 (3) 1400-1458
- Halliwell, B. Whiteman, M. (2004) Measuring reactive species and oxidative damage in vivo an in cell culture: how should you do it and what do the results mean. *British Journal of Pharmacology*. 142 (2) 231-255
- Halliwell, B. Gutteridge, J, M, C. (1999) Free radicals in biology and medicine. 3rd edition. Oxford University press. New York.
- He, W. Liu, Y. Warner, W, G. Yin, J-J. (2014) Spectroscopy for the study of nanomaterial-mediated generation of reactive oxygen species. *Nanomaterials- Toxicology and medical applications*. 22 (1) 49-63
- Henderson, J, R. Swalwell, H. Boulton, S. Manning, P. McNeil, C, J. Birch-Machin, M, A. (2009) Direct, real-time monitoring of superoxide generation in isolated mitochondria. *Free Radical Res*. 43, 796–802.
- Hogg, N. (2010) Detection of Nitric Oxide by Electron Paramagnetic Resonance Spectroscopy. *Free Radical Biology & Medicine*, 49 (2) 122–129.

Jammes, Y. Steinberg, J, G. Mambrini, O. Bregeon, F. Delliaux, S. (2005). Chronic fatigue syndrome: assessment of increased oxidative stress and altered muscle excitability in response to incremental exercise. *J Int Med.* 257, 299-231.

Jammes, Y. Steinberg, J, G. Delliaux, S. Bregeon, F. (2009) Chronic fatigue syndrome combines increased exercise-induced oxidative stress and reduced cytokine and Hsp responses. *Journal of Internal Medicine*, 266, 196- 206

Jammes, Y. Steinberg, J, G. Delliaux, S. (2012) Chronic fatigue syndrome. Acute infection and history of physical activity affect resting levels and response to exercise of plasm oxidant/antioxidant status and heat shock proteins. *Journal of Internal Medicine*, 266, 196-206

Jammes, Y. Steinberg, J, G. Guieu, R. Delliaux, S. (2012) Chronic fatigue syndrome with history of severe infection combined altered blood oxidant status, and reduced potassium efflux and muscle excitability at exercise. *Open Journal of Internal Medicine.* 3, 98-105

Jimenez-Lopez, J, M. Cederbaum, A, I. (2005) CYP2E1-dependent oxidative stress and toxicity: role in ethanol-induced liver injury. *Expert Opin Drug Metab Toxicol.* 1(4) 671-85

Jones, D, E, J. Hollingsworth, K. Blamire, A, M. Taylor, R. Newton, J, L.(2010) Abnormalities in pH handling by peripheral muscle and potential regulation by the autonomic nervous system in chronic fatigue syndrome. *Journal of Internal Medicine.* 26, 394–401

Jones, D, E. Hollingsworth, K, G. Jakovljevic, D, G. Faltakhova, G. Pairman, J. Blamire, A, M. Trennel, M, I. Newton, J, L. (2012) Loss of capacity to recover from acidosis on repeat exercise in chronic fatigue syndrome: A case control study. *European Journal of Clinical Investigation.* 42 (2) 184-194

Keenoy, M, Y. Moorkens, G. Vertommen, J. De Leeuw, I.(2001) Antioxidant status and lipoprotein peroxidation in chronic fatigue syndrome. *Life Sci.* 68, 2037–2049

Khan, N. Wilmot, C, M. Rosen, G, M. Demidenko, E. Sun, J. Joseph, J. O’Hara, J, Kalyanaraman B, Swartz HM (2003). Spin traps: *in vitro* toxicity and stability of radical adducts. *Free Radic Biol Med.* 34. 1473–1481.

Land, E, J. Swallow, A, J. (1971) One electron reactions in biochemical systems as studied by pulse radiolysis, V cytochrome C. *Arch biochem, biophys.* 143, 365

- Ledoux, F. Zhilinskaya, E, A. Courcot, D. Aboukais, A. Puskaric, E. (2004) EPR investigation of iron in size segregated atmospheric aerosols collected at Dunkerque, Northern France. *Atmos Environ.* 38. 1201–10.
- Luin, E. Giniatullin, R. Sciancalepore, M. (2011) Effects of H₂O₂ on electrical membrane properties in myotubes. *Free Radical Biology and Medicine.*50, 337-344
- Mashirin, A, A. Hillhouse, E.W. Manning, P. McNeil, C, J, 1. (1998). Superoxide electrode based on covalently immobilised cytochrome c: Modelling studies. *Free Radical Biology & Medicine* 25(8) 973-978.
- Manning, P. Cookson, M, R. McNeil, C, J. Figlewicz, D. Shaw, P, J. (2001) Superoxide induced nitric oxide from cultured glial cells. *Brain Res.* 911, 203–210.
- Manning, P. McNeil, C, J. Cooper, J, M. Hillhouse, E, W. (1998) Direct, real-time sensing of superoxide and nitric oxide production by activated human glioblastoma cells. *Free Radical Biol Med.* 24,1304–1309.
- McNeil, C, J. Manning, P. (2002) Sensor-based measurements of the role and interactions of free radicals in cellular systems. *Rev. Mol. Biotechnol.* 82, 443–455.
- McNeil, C, J. Greenough, K, R. Weeks, P, A. Self, C, H. Cooper, J, M. (1992) Electrochemical sensors for direct reagentless measurement of superoxide production by human neutrophils. *Free Radical Research Commun.* 17, 399-406
- Molina-Ortiz, D. González-Zamora, J. Camacho-Carranza, R. Lopez-Acosta, O. Colin-Martinez, O. Domínguez-Ramírez, A. Vences-Mejía, A. [2013] Xenobiotic-Metabolizing Enzymes in Skeletal Muscle of Children and Adolescents. *Pharmacology & Pharmacy.* 4 (2) 231-239
- Ramirez, B, N, I. Salgado, A, M. Valdman, B. (2009) The Evolution and Developments of Immunosensors for Health and Environmental Monitoring: Problems and Perspectives. 26, 227-249
- Richards, R, S. Roberts, T, K. McGregor, N, R. Dunstan, R, H. Butt, H, L.(2000) Blood parameters indicative of oxidative stress are associated with symptom expression in chronic fatigue syndrome. *Redox Rep.* 5, 35–41. 26

Rochard, P. Rodier, A. Casas. F. (2000) Mitochondrial activity is involved in the regulation of myoblast differentiation through myogenin expression and activity of myogenic factors," *Journal of Biological Chemistry*, 275, (4), 2733–2744,

Shleev, S. Wetterö, J. Magnusson, K.-E. Ruzgas, T. (2006) Electrochemical characterization and application of azurin-modified gold electrodes for detection of superoxide. *Biosensors & Bioelectronics*. 22(2) 213-219

Sudha, R. Raman, C. Raj, K. Shefali, S. Antoaneta, Z. Yanka, D. Veselina, G. Rajesh, A. Sarwat, S. Kumar, S, R. (2010) Electron paramagnetic resonance spectroscopy in radiation research: Current status and perspectives. *Journal of Pharmacy and BioAllied Sciences* 2 (2) 80-87

Tammeveski, K. Tenno, T, T. Mashirin, A, A. Hillhouse, E,W. Manning, P. McNeil, C, J. (1998). Superoxide electrode based on covalently immobilised cytochrome c: modelling studies. *Free Radical Biology & Medicine* 25(8) 973-978.

Tchounwou, P, B. Yedjou, C, G. Sutton, S, J. (2012) Heavy metals and the environment. *EXS*. 101, 133-164

Tarpey, M, M. Fridovich, I. (2001) Methods of detection of vascular reactive species Nitric oxide, superoxide, hydrogen peroxide and peroxynitrite. *Circ res*. 89, 224-236

Valverde, P. Manning, P. McNeil, C, J. Thody, A, J. (1996) Activation of tyrosinase reduces the cytotoxic effects of the O₂⁻ anion in B16 mouse melanoma cells. *Pigment Cell Res*. 9, 77–84.

Van Oosterwijck, J. Nijs, J. Meeus, M. Lefever, I. Huybrechts, L. Lambrecht, L. (2010). Pain inhibition and post-exertional malaise in myalgic encephalomyelitis/chronic fatigue syndrome: an experimental study. *Journal of Internal Medicine*. 268, 265–78

Warwar, N. Mor, A. Fluhr, R. Pandian, R, P. Kuppusamy, P. Blank, A. (2011) Detection and imaging of superoxide in roots by electron spin resonance spin-probe method. *Biophys J*. 101 (6) 1529-1538

Zhang,J. Wang, Z. Vikash,V. Ye, Q. Wu,D. Liu, Y. Dong, W. (2016) ROS and ROS-mediated cellular signalling. *Oxidative Medicine and Cellular Longevity*. 18

Chapter 4

Application of 2'7'-bis (2-carboxyethyl)-5 (6) Carboxyfluorescein to Measure Intracellular pH in CFS/ME Myoblasts and Myotubes

4.1 Introduction

Chapter 2 investigated intracellular pH in CFS/ME myoblasts using a novel pH sensing nanosensor platform. However, the nanosensor system was unable to reliably determine the cytosolic pH. It was therefore determined that the technique required further development, which was beyond the scope of this thesis. The aim of this chapter was to investigate variations in cytosolic pH using the well characterised, pH responsive fluorophore 2'7'-bis (2-carboxyethyl)-5 (6) carboxyfluorescein (BCECF) in CFS/ME myoblasts and differentiated myotubes at rest and following electrical pulse stimulation (EPS).

Evidence exists to suggest CFS/ME patients exhibit profound acidosis following low-level exercise, when measured via MRS [Jones et al. 2010]. Additionally, pilot work using the fluorescent nanosensor system (detailed in Chapter 2) to measure intracellular pH showed that CFS/ME myoblasts exhibited a significantly lower pH at rest compared to non-diseased control cells. Further, this innate acidosis could be normalised following addition of the PDK inhibitor, DCA [Boulton. 2012]. This represented the first *in vitro* analysis of pH in myoblasts derived from CFS/ME patients and suggested that these cells were intrinsically acidic which could have a significant influence on the CFS/ME phenotype. Importantly, this acidosis could be reversed by PDK inhibition. This observation, if correct, could open up novel treatment strategies for CFS/ME patients. However, in the absence of subsequent reliable nanosensor data it was decided free fluorescent dye would be used in an attempt to measure intracellular myoblast pH and further examine these initial observations.

This chapter developed also upon Chapter 2 by investigating intracellular pH in myoblasts and differentiated myotubes. Multinucleated myotubes represent the best alternative to intact human skeletal muscle and have been reported to exhibit the morphological, metabolic and biochemical properties of intact adult muscle cells [Gaster et al. 2001; Henry et al. 1995; Nikolic et al. 2012].

4.1.1 Intracellular sensing

Techniques that can accurately and precisely measure intracellular pH under physiological conditions are highly advantageous as intracellular pH plays a pivotal role in cell function, with organelle metabolic processes directly affected by H^+ ion concentration [Han and Burgess. 2010; Orkan et al. 2002]. Even slight deviations in cytosolic pH (typically 7.2-7.4) are associated with a reduction in cell function, growth and division, which is observed in diseases such as cancer and Alzheimer's disease [Izumi et al. 2003; Davies et al. 1993].

As discussed in Chapter 2 a number of pH intracellular sensing techniques exist, including the use of optochemical sensors, fluorescent dye, NMR, SERS and PEBBLE nanosensors. This chapter utilised the fluorophore 2',7'-bis (2-carboxyethyl)-5 (6) carboxyfluorescein (BCECF) to investigate intracellular pH. BCECF was introduced in 1982 [Rink et al. 1982] for the measurement of cytoplasmic pH and has since been widely used for pH measurement in mammalian cells, living tissues and individual organelles [Han and Burgess. 2010]. In terms of intracellular delivery, chemical modification of BCECF can occur to incorporate acetoxymethyl ester (AM), which is synthesised from carboxyfluorescein by the addition of two extra carboxylate groups via short alkyl chains. BCECF-AM is therefore a no charge, non- fluorescent form of BCECF. In terms of function, the presence of AM ester enables BCECF to rapidly diffuse through the cell membrane into the cell, once inside the cell hydrolysis of the acetyl ester linkage by enzymatic cleavage regenerates the less permeable and fluorescent original compound BCECF [Gdovin et al. 2010] (Displayed in Figure 4.4) which is capable of generating a fluorescent signal in relation to intracellular pH [Gdovin et al. 2010; Han and Burgess. 2010; Orkan et al. 2002].

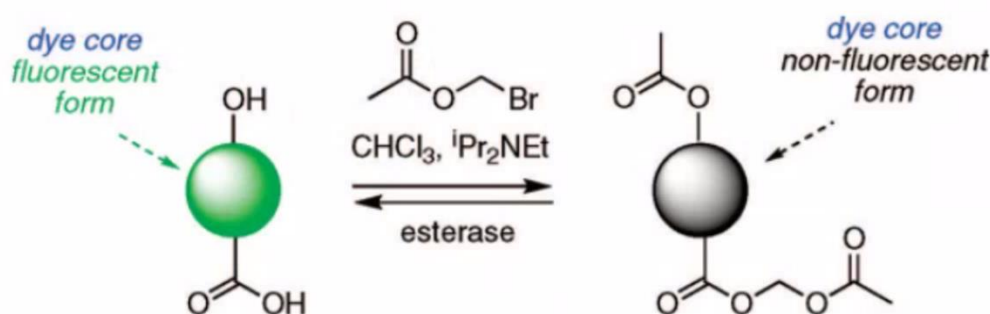


Figure 4.4: The synthesis and hydrolysis of AM and acetate ester as illustrated by Han and Burgess [2010].

BCECF remains one of the most widely used fluorophores for intracellular pH measurement. Its popularity is due to it exhibiting a number of benefits when compared to other dyes, which were detailed in a review conducted by Han and Burgess [2010], regarding the use of fluorescent indicators for intracellular pH measurement. For example, the dye is retained well inside the cell as at physiological pH it exhibits 4-5 negative charges. BCECF also exhibits a pK_a of 7.0 which makes it well suited for the measurement of cytosolic pH which is typically in the 7.2-7.4 range. Additionally, BCECF AM esters are membrane permeable enabling non-destructive dye loading into the cell. Furthermore, non-fluorescent BCECF-AM esters are converted into fluorescent BCECF acid in a highly efficient manner, so much so it may be used for cell viability assays [Perez-Sala et al. 1995]. Finally, BCECF is a ratiometric fluorophore, which enables fluorescence to be measured at two excitation wavelengths. For example, when excited at 440nm (isosbestic point) the dye is pH insensitive and when excited at 495nm the dye is pH sensitive [Gdovin et al. 2010]. Effectively, ratiometric dyes correct for a number of shortcomings inherently associated with the use of free-dye, including variable dye loading, dye leakage and detector sensitivity [Grant & Acosta.1997].

Although BCECF remains the most widely used intracellular pH indicator, other popular fluorophores for pH measurement include fluorescein and fluorescein derivatives (carboxyfluorescein). However, without additional modification these dyes are able to leak through the cell membrane allowing for erroneous pH measurement [Han and Burgess. 2010]. For example, at 37°C intracellular concentrations of 5- and 6-carboxyfluorescein have been reported to be decreased 30-40% after the first 10 min following washing [Rink et al. 1982]. Alternatively, although BCECF-AM has been reported to leach from the cell, the rate is around 10% 20 minutes after washing, which is a lot lower than other commercially available dyes. Therefore, it would seem that in terms of approaches to measure intracellular pH, BCECF-AM combined with fluorescent spectroscopy is a popular choice, exhibiting high sensitivity, good spatial and temporal observation of pH change as well as being relatively operationally simple [Han and Burgess et al. 2010].

4.1.2 Electrical pulse stimulation

In this chapter electrical pulse stimulation (EPS) was applied to enable the contraction of skeletal muscle cells in vitro as a strategy to investigate the effect of physical activity on intracellular pH in CFS/ME patient muscle samples. The EPS protocol that was used has previously been described by Brown et al. [2015] and EPS was performed using the C-pace EP cell culture pacer (Ion Optix, Dublin), Displayed in figure 4.5.



Figure 4.5: EPS was performed using the C-pace EP cell pacer (Ion Optix, Dublin)

A number of studies have reported the use of EPS to induce muscle contraction in skeletal muscle cells. For example, Fujita et al. [2007] reported EPS to accelerate *de novo* sarcomere assembly, in addition to the induction of Ca^{2+} transients in C2C12 mouse skeletal muscle myotubes. Additionally, Nedachi et al. [2008] utilising the same experimental model reported EPS to induce AMPK activation, increase glucose transport and enhance the release of chemokines such as IL-6. Interestingly, other papers have detailed the use of EPS to investigate human skeletal muscle myotube function [Lambernd et al. 2012; Nikolic et al. 2012], with these studies reporting the model to enhance sarcomere assembly, increase AMPK activation, glycolysis and glucose uptake as well as chemokine expression. Interestingly, Brown et al. [2015] demonstrated EPS to simulate exercise in cultured CFS/ME and control myotubes. For example, the authors reported alternating frequency (low/high)

EPS to be successful in enabling muscle contraction and inducing metabolic changes associated with exercise. In healthy cells, EPS induced myotube contraction and increased AMPK activation whereas in the CFS/ME patient group AMPK activation and glucose uptake were impaired. The authors therefore concluded the *in vitro* use of EPS be effective strategy to investigate metabolic and bio-chemical exercise associated dysfunction in cultured cells.

The cytotoxic effects of EPS on skeletal muscle cells have also been investigated. For example, Nikolic et al. [2012] reported acute high frequency and chronic low frequency EPS to exhibit no significant alteration in lactate dehydrogenase [LDH] concentration, when measured in the experimental medium following 24 and 48-hours stimulation. Furthermore, Brown et al. [2015] also reported there to be no significant increase in the release of LDH into the assay medium following 24-hours EPS, in CFS/ME myotubes compared to controls. Therefore, suggesting both acute and chronic EPS of myotubes to not exhibit any notable toxic effect on skeletal muscle cells.

4.1.3 Hypotheses

The aim of this chapter was to investigate the intracellular pH of CFS/ME myoblasts and differentiated myotubes at rest and following (EPS) to mimic exercise. Intracellular pH was measured via fluorescent spectrophotometry following treatment with fluorophore BCECF-AM. The PDK inhibitor DCA was utilised to investigate whether PDC function impacts upon intracellular pH

The experimental hypotheses were:

- (1) CFS/ME myoblasts and differentiated myotubes exhibit significantly lower intracellular pH at rest and following EPS, when compared to controls.
- (2) Treatment with PDK inhibitor DCA normalises intracellular pH in CFS/ME samples at rest and following EPS.

4.2 Materials and Methods

CFS/ME and control myoblasts were supplied by Dr Audrey Brown from the diabetes research group at Newcastle University. Myoblasts were obtained from a total of 5 (4 females, 1 male) CFS/ME patients which consisted of 4 females and 1 male aged 43 ± 12.73 years. A total of 4 myoblast samples were obtained from control participants (3 females, 1 male) who were aged 50.14 ± 12.81 years.

All tissue culture reagents apart from Ham's F10 growth medium (Lonza, SLS, East Riding, Yorkshire) and chick embryo extract (Sera Lab, West Sussex, UK) were purchased from Sigma-Aldrich (Poole, Dorset).

Plastic tissue culture flasks, serological pipettes, 6-well plates, falcon tubes and cell scrapers were purchased from Greiner Bio-one (Stonehouse, UK).

pH responsive dye BCECF-AM was purchased from Abcam (Cambridge, UK). Intracellular pH calibration kit was purchased from Thermo Fisher Scientific (Loughborough, UK). PDK inhibitor potassium DCA was purchased from Sigma-Aldrich.

4.2.1 Cell culture and preparation

As described in Chapter 2, CFS/ME and control muscle cell samples were collected and isolated as detailed in the study by Brown et al (2015). The myoblast samples were routinely cultured in Ham's F10 medium, supplemented with 20% FBS, 2% chick embryo extract, 500 U/mL penicillin-streptomycin and 1% amphotericin B. Myoblasts were grown to 80% confluence in a T75 flask before being trypsinised and seeded into the vessel of choice. Cells were grown and maintained in a humidified incubator at 5% (v/v) CO₂ at 37° C .

Myoblasts were seeded into 6-well testing plates at a density of 2×10^5 cells per well and left overnight to attach. BCECF-AM pH calibration or experimentation was performed the following day. Growth media was removed and replaced with Minimum Essential Medium (MEM), which was supplemented with 2% (V/V) FBS and 1% Penicillin-streptomycin. MEM was replaced every 48-hours over a 7 day period.

4.2.2 Intracellular pH calibration

To enable the accurate determination of intracellular pH in cells treated with BCECF-AM an *In situ* pH calibration was performed for both myoblast and myotube samples. The calibration was conducted using reagents provided by a commercially available pH calibration kit (Thermo Fisher Scientific, Loughborough).

Myoblasts were seeded into 96-well testing plates at a density of 3×10^4 cells per well and at 2×10^5 cells per well in 6-well plates to promote differentiation into myotubes. Immediately prior to the calibration, cells were washed once with PBS. To ensure equilibration of extracellular and intracellular pH, cell-loading solution was prepared by dissolving ionophores nigericin and valinomycin in DMSO at a stock concentration of $100 \mu\text{M}$ before adding them to each pH buffer solution (4-7) at final concentration in the well of $10 \mu\text{M}$ at 37°C . Following 5-minutes incubation BCECF-AM was added to the wells at a final concentration of $2 \mu\text{M}$ and further incubated at 37°C for 30 minutes, before FI measures were performed.

FI measurements were then acquired using the Tecan-I 200 fluorimeter and data was provided by using the compatible Magellan software. Fluorescence was determined by measuring excitation at 440nm (non-pH dependent) and 490nm (pH dependent), with emission detected at 535nm. FI data was then analysed to provide FI ratios, this was achieved by dividing the FI at $\lambda 490$ by FI at $\lambda 440$. A standard curve was then produced to display the relationship between pH and FI ratio. A polynomial second-order curve was then applied to determine the pH of cells treated with BCECF-AM.

4.2.3 Myoblast viability following treatment with BCECF-AM

It was necessary to investigate the biocompatibility of BCECF-AM before using the fluorophore to measure intracellular pH in skeletal muscle samples. To assess the level of cytotoxicity, varying concentrations of the pH responsive dye ($0.5\text{-}2 \mu\text{M}$) were incubated with CFS/ME and control myoblasts. Briefly, myoblasts were seeded into 96-well plates at a density of 1×10^4 cells per well. BCECF-AM was then added to the plate and incubated for 3, 6 and 24-hours. Viability was measured following the addition of resazurin (0.03%) and fluorescence was interpreted at $\lambda_{\text{ex}}=560\text{nm}$, $\lambda_{\text{em}}=590\text{nm}$, via the Tecan- I 200 fluorimeter.

4.2.4 BCECF-AM intracellular pH measurement

Intracellular pH measurements were acquired for myoblast and myotube samples following the internalisation of fluorophore BCECF-AM.

Prior to experimentation culture medium was removed and testing plates were washed once with PBS. Assay medium (DMEM) in addition to BCECF-AM was then added to the wells at a final concentration of 2 μ M. The plate was then incubated for 35 minutes at 37°C. The assay media was aspirated and the plate was washed once before adding fresh assay medium or assay medium supplemented with DCA (40 μ M).

Fluorescence was measured using the Tecan 2000 fluorimeter and measurement settings were $\lambda_{ex}440\text{nm}$ (non-pH dependent) and $\lambda_{ex}490\text{nm}$ (pH dependent) / $\lambda_{em} 535\text{nm}$.

4.2.5 Electrical pulse stimulation

EPS was performed to simulate exercise in CFS/ME and control myotube samples. The ability of EPS to model exercise *in vitro* has previously been confirmed, with a number of studies utilising the technique to investigate cellular metabolic function [Orfanos et al. 2016; Brown et al. 2015].

The EPS protocol that was used has previously been described by Brown et al. [2015]. EPS was performed using the C-pace EP cell culture pacer (Ion Optix, Dublin). Myoblasts were plated into 35mm culture dishes at a density of 2×10^5 . The cells were differentiated for 7 days before stimulation was initiated for 24-hours at alternating frequencies, with one hour low frequency (5 volts, 24ms, 2Hz) followed by one hour high frequency (5 volts, 24ms, 0.2Hz).

4.2.6 Data analysis

The statistical model used to analyse the data was Minitab 17 statistical software. Inferential statistics were carried out to examine intracellular pH in CFS/ME and control skeletal muscle

samples. The statistical tests used were the paired samples T-test and independent T-test and statistical significant was accepted at $P < 0.05$. The descriptive statistics used were mean \pm SD.

4.3 Results

4.3.1 BCECF-AM pH *In Situ* Calibration

Cultured primary myoblasts and differentiated myotubes were treated with pH responsive free-dye BCECF-AM (2 μ M). To ensure intracellular and extracellular pH equilibration cells were incubated with varying pH buffer solutions (4-7), which were doped with ionophores valinomycin and nigericin (10 μ M). FI measurements were obtained and ratios were calculated (490/440nm) for all samples. A second-order polynomial curve fitting was applied to generate the calibration curve. The polynomial fitting was successful in determining the buffer pH within the pH range tested in both myoblast ($y=0.3758x^2 - 3.4706x + 9.4155$, $R^2=0.999$, $n=3$) and myotube ($y=0.4119x^2 - 3.8228x + 10.10^2$, $R^2=0.995$, $n=3$) cell samples. Data presented for myoblast samples in Figure 4.6 and myotube samples in Figure 4.7.

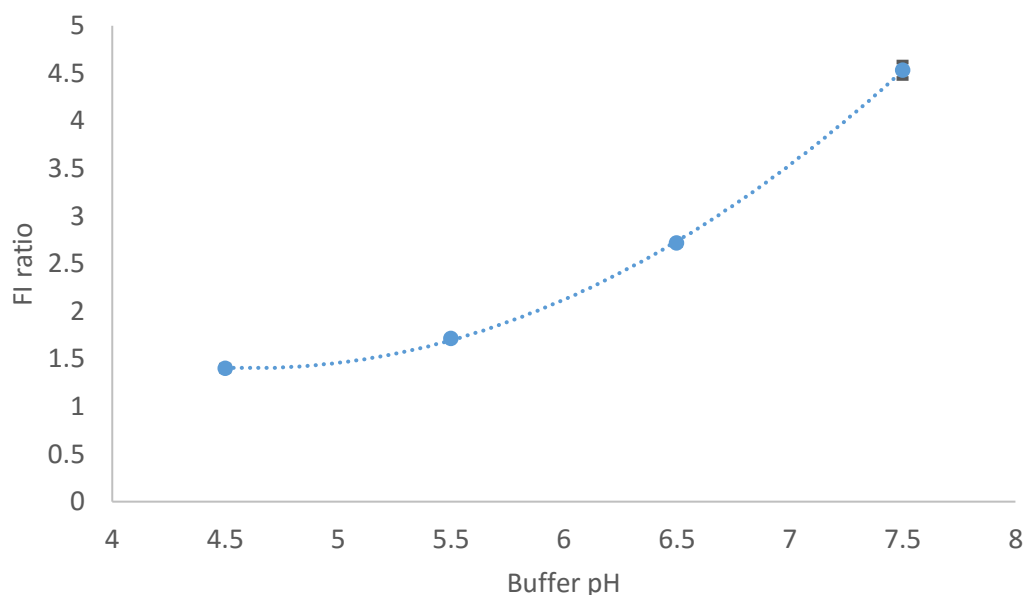


Figure 4.6: *In situ* calibration curve conducted in myoblast samples following incubation with BCECF-AM. A polynomial second-order fitting enabled the successful determination of pH within the physiological range from the FI ratio measures provided ($=0.3758x^2 - 3.4706x + 9.4155$, $R^2=0.999$). The data is presented at mean \pm SD ($n=3$).

4.3.2 Myoblast viability following exposure to BCECF-AM

Figure 4.8 a, b and c demonstrated CFS/ME and control myoblast viability following incubation with BCECF-AM for 3,6 and 25-hours respectively. Viability remained high for both samples across all time-points and dye concentrations (>70%). No significant differences in viability were exhibited (% untreated control) between samples, across time-points or as a result of varied BCECF-AM concentration.

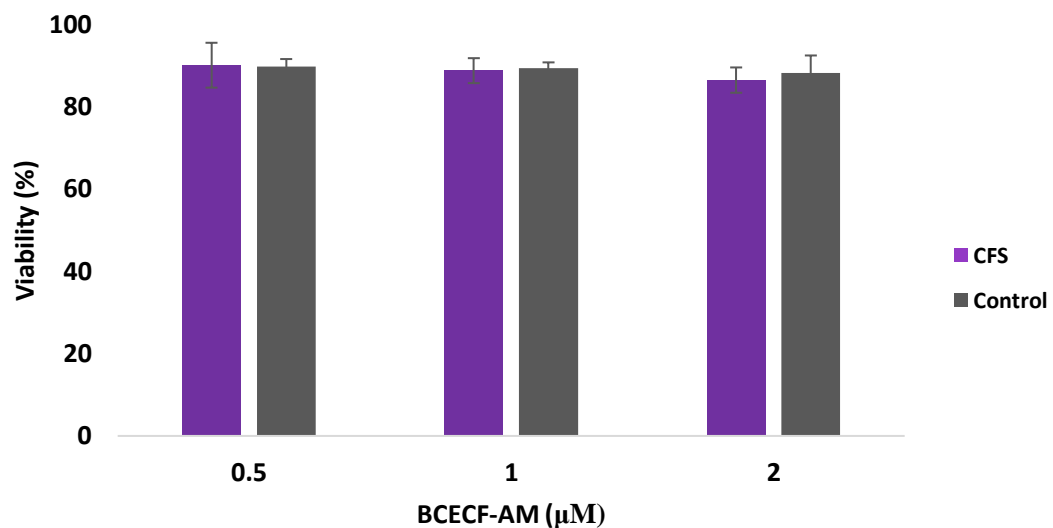


Figure 4.8 (a): CFS/ME & control myoblast viability after 3-hours incubation with BCECF-AM at 0.5-2μM concentrations. No significant differences in viability was observed between samples or with varying concentrations of BCECF-AM. Data presented as mean ±SD, n=4)

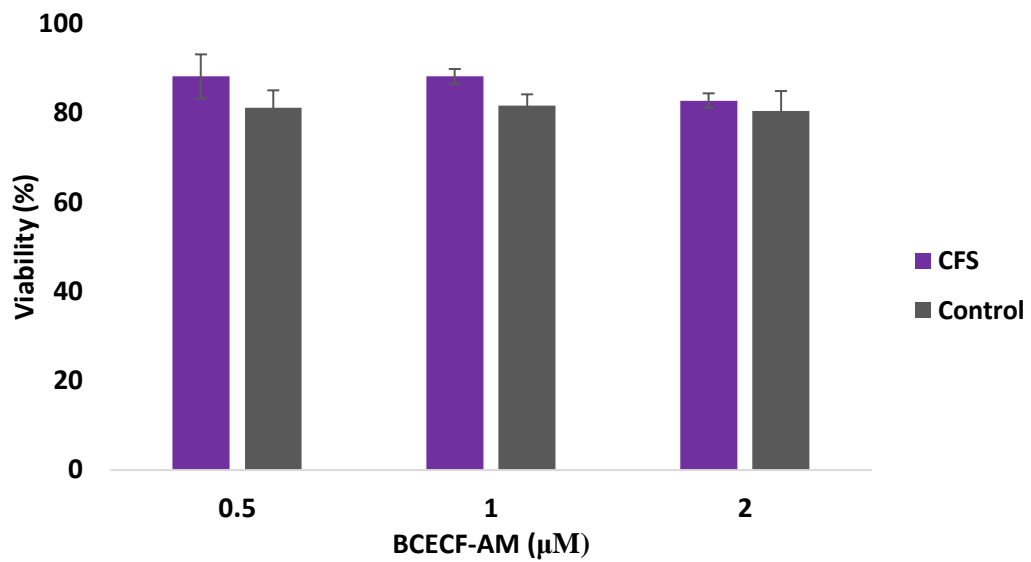


Figure 4.8 (b): CFS/ME and control myoblast viability after 6-hours incubation with 0.5-2μM BCECF-AM concentrations. No significant differences in viability was observed between samples or with varying concentrations of BCECF-AM. (Data presented as mean ± SD, n=4)

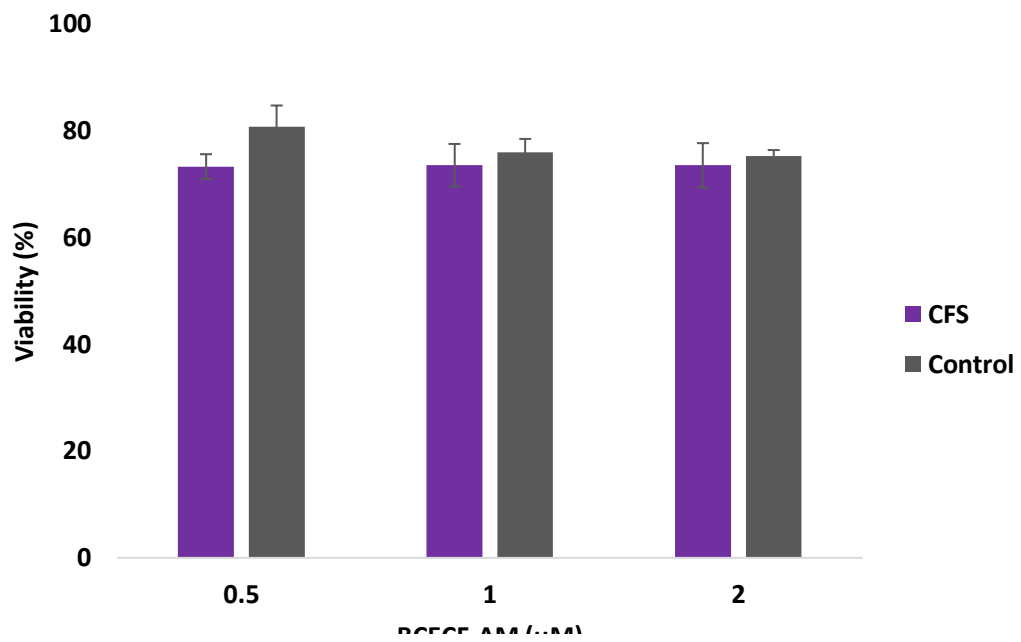


Figure 4.8 (c): CFS/ME and control myoblast viability after 24-hours treatment with 0.5-2μM concentrations of BCECF-AM. No significant differences in viability was observed between samples or with varying concentrations of BCECF-AM. (Data presented as mean ± SD, n=4)

4.3.3 Myoblast intracellular pH determination with DCA treatment

Figure 4.9 demonstrated intracellular pH measurements for CFS/ME (n=5) and control (n=4) myoblast samples following the internalisation of free-dye BCECF-AM (2 μ M). Intracellular pH did not significantly differ between the CFS/ME and control group samples at baseline or following DCA treatment across all time-points. In terms of within group effects, DCA did not induce any significant alteration in pH in both samples across any of the time-points.

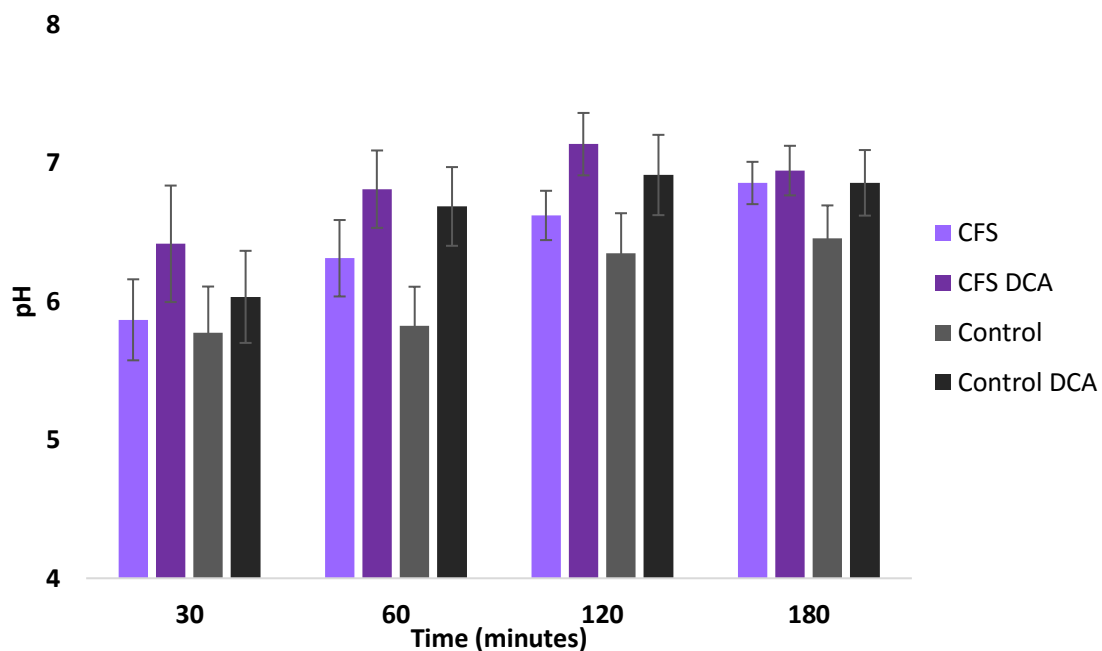


Figure 4.9 : CFS/ME & control myoblast intracellular pH measurements following BCECF-AM internalisation. No significant differences in pH were observed between CFS/ME & control samples at baseline or following incubation with DCA ,across any of the time-points. Additionally, no significant within group differences in pH for both samples were exhibited following treatment with DCA (40 μ M). Data presented as mean \pm SD, n=9

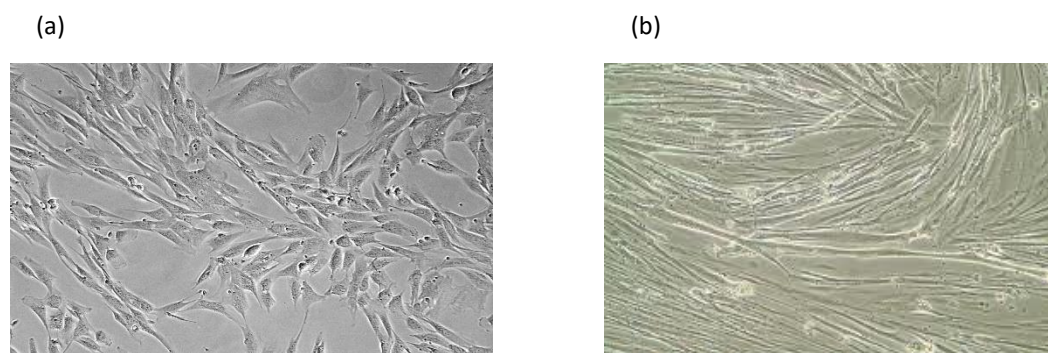


Figure 5.0 : (a) myoblasts in culture, (b) Myotubes 7-days differentiation

4.3.4 Myotube intracellular pH measurement at rest and post-EPS

The intracellular pH of CFS/ME (n=4) and control (n=4) myotubes was investigated at rest, following 24-hours EPS and in conjunction with DCA treatment. In resting samples, the intracellular pH of both CFS/ME and control samples did not significantly differ at baseline or following incubation with DCA (40 μ M). Moreover, there was no significant difference in the intracellular pH measurements within sample groups at baseline or following DCA treatment, displayed in Figure 5.1 a.

In terms of EPS, myotubes were stimulated for 24-hours at alternating frequencies. When compared to resting pH measurements there was no significant alteration in pH immediately post-exercise or throughout the recovery period for CFS/ME (see Figure 5.1 a and b) and control samples (see Figure 5.1 a and c) and DCA did not exhibit any effect on pH in either sample at any of the time points measured (CFS/ME samples see Figure 5.1a and 5.1b, Controls see figure 5.1 a and c). Furthermore, post EPS there was no significant difference in pH following DCA treatment compared to baseline for CFS/ME (see Figure 5.1c) and control samples (see Figure 5.1 c) immediately post-exercise and throughout recovery. Finally, when comparing CFS/ME to control samples there was no difference in the pH exhibited immediately post-EPS or throughout recovery at baseline and with DCA treatment (see Figure 5.1b and 5.1c).

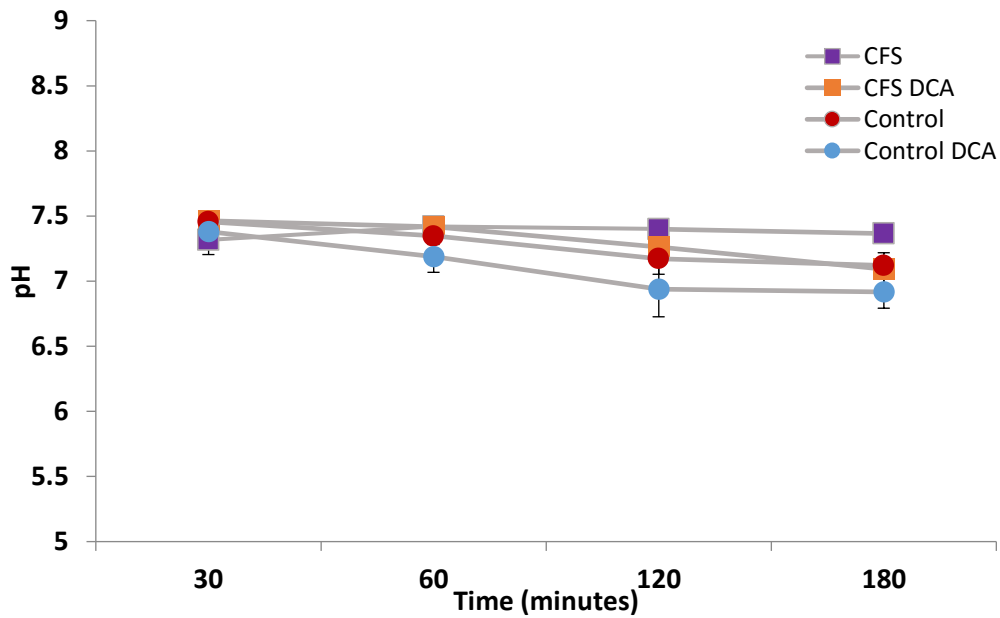


Figure 5.1a: CFS/ME (n=4) & control (n=4) resting myotube pH at baseline and following treatment with DCA (40 μ M). No significant difference in pH between groups at baseline or following DCA treatment. DCA did not exhibit any within group differences in pH when

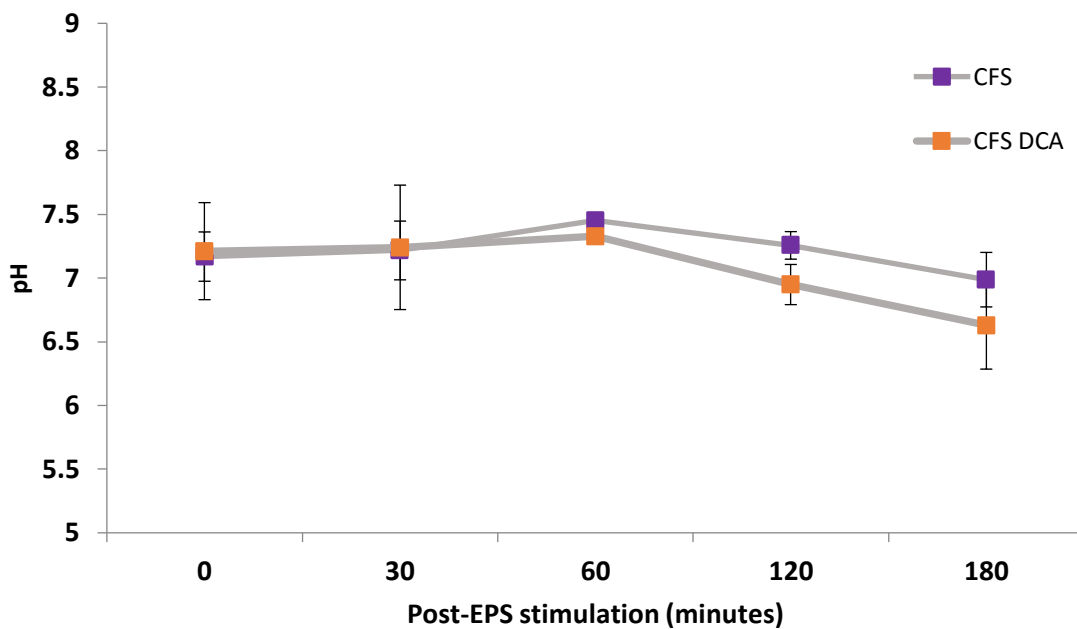


Figure 5.1b: CFS/ME myotube intracellular pH measurements post-EPs stimulation at baseline and following treatment with DCA (40 μ M). DCA did not induce any significant alteration in pH at any point during the recovery period. Data presented as mean \pm SD, n=4

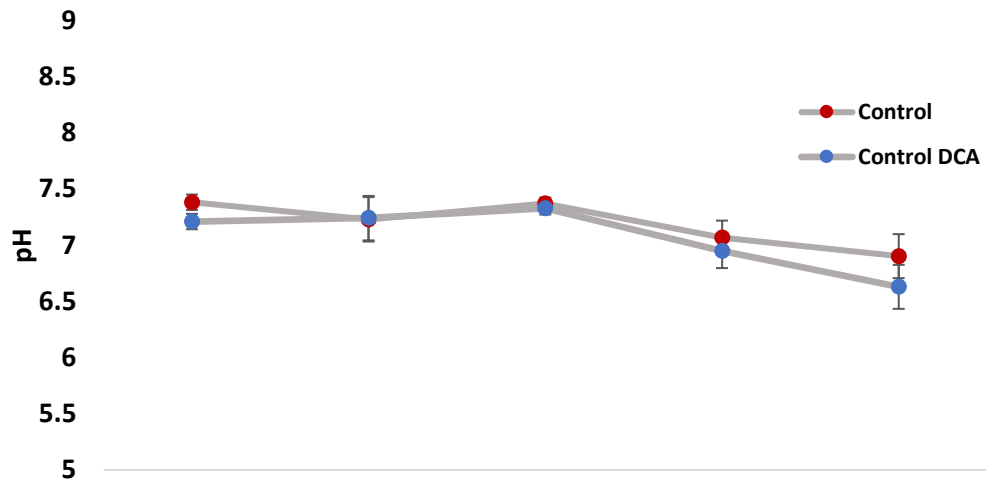


Figure 5.1 c: Control myotube intracellular pH measurements post-EPS stimulation at baseline and following treatment with DCA (40 μ M). DCA did not induce any significant alteration in pH at any point during the recovery period. Data presented at mean \pm SD, n=4

4.4 Discussion

Previous research has described intracellular pH abnormalities in the muscle of patients with CFS/ME. In a MRS study conducted by Jones et al. [2012] patients were reported to exhibit profound and sustained acidosis, following a relatively low-level repeat exercise protocol.

The authors postulated the findings to be evidence of underlying bio-energetic abnormality, due to an over-utilisation of the lactate dehydrogenase energy-producing pathway.

Intracellular pH dynamics were investigated in more detail in pilot work performed by Boulton [2012]. As described in Chapter 2, a novel pH sensing nanosensor system was utilised to investigate intracellular pH in patient myoblast samples. The primary finding was the presence of aberrantly low intracellular pH in CFS/ME myoblasts compared to controls. Secondly, intracellular pH was normalised to a level comparable to control samples following treatment with the PDK inhibitor DCA. These findings suggested bio-energetic abnormality in CFS/ME patient muscle as a consequence of impaired PDC function.

A pivotal aim of Chapter 2 in this thesis was to repeat the preliminary work of Boulton [2012], as well as further validating and developing the pH nanosensor system. However, it was not possible to reproduce the findings and the intracellular pH of CFS/ME myoblasts was not found to be significantly lower than controls. Additionally, DCA did not exhibit any significant effect on intracellular pH in either CFS/ME or control myoblast samples. Moreover, the pH measurements obtained for both myoblast samples were outside the cytosolic pH range and were suggestive of endosomal/lysosomal intracellular pH localisation. Work presented here therefore suggested that rather than being free to passively register pH changes in the cytoplasm, nanosensors may have been sequestered into subcellular organelles. Interestingly, this finding is in agreement with others who have also reported a low intracellular pH measurement following the internalisation of polyacrylamide nanosensors albeit in alternative cell-lines [Benjaminson et al. 2011; Coupland et al. 2009].

A primary aim of this chapter was to therefore utilise an alternative intracellular sensing technique to investigate the pH dynamics in CFS/ME skeletal muscle samples. In addition, as Jones et al. [2012] reported CFS/ME patients to exhibit acidosis following low-level exercise, EPS was used to stimulate muscle cells in an attempt to mimic physical activity in an *in vitro* setting. Specific aims were:

- a) To measure the intracellular pH of CFS/ME myoblasts at rest and differentiated myotubes at rest and following electrical pulse stimulation (EPS).
- b) To investigate the ability of PDK enzyme inhibitor DCA to impact upon intracellular pH at rest and post-EPS in myoblasts and differentiated myotube samples.

The results of this chapter showed that there was no significant difference in intracellular pH levels in CFS/ME myoblasts compared to controls (Figure 5.0a). Similarly, pH did not significantly differ between CFS/ME and control myotubes at rest and post-EPS (Figure 5.0b and 5.0c). Moreover, treatment with DCA did not significantly alter intracellular pH at rest in myoblast samples or at rest and following EPS in myotube samples (Figure 4.9 and 5.0a). These findings contrast the experimental hypotheses detailed in Section [4.1.3].

4.4.1 Optimisation

The toxicity profile of BCECF-AM was investigated before the dye was utilised to determine intracellular pH. Encouragingly, the pH responsive dye was well tolerated in the myoblast samples and cell viability remained high (>70%), even following 24-hours incubation (Figure 4.8c). BCECF-AM is a derivative of fluorescein which has also been reported as a low-toxic compound [Richo et al. 2013]. Alternatively, in high doses the dye purportedly exhibits a toxic effect in cell culture and *in vivo* [Alford et al. 2009]. BCECF-AM was deemed suitable to apply to the *in vitro* assessment of myoblast and myotube intracellular pH.

In terms of additional optimisation work, two *in situ* calibration curves were produced for both myoblast and myotube cell samples. BCECF-AM was successfully calibrated over the physiological pH range (Figure 4.6 and 4.7).

4.4.2 Intracellular pH determination

CFS/ME resting muscle samples did not exhibit lower intracellular pH when compared to control samples which contrasts previous work [Boulton. 2012], which reported aberrantly

low pH in CFS/ME myoblasts, which was subsequently normalised to control level following treatment with DCA.

A possible reason for the discrepancy may relate to the varying sample sizes utilised. In the present study n=5 CFS/ME myoblasts and n=4 control samples were investigated, compared to n=1 CFS/ME and n=1 control in the Boulton [2012] study. It is important to realise that failing to test multiple CFS/ME patient samples is methodological weakness as the sample tested may not be representative of the wider CFS/ME patient population. Furthermore, distinct sub-groups within patient population have been reported in terms of intracellular acidification following exercise. For example, Barnes et al. [1993] measured intramuscular pH via ³¹P-MRS in 46 CFS/ME patients. Results demonstrated no significant abnormality in pH when the group were taken as a whole following exercise, however 6 patients did exhibit intramuscular acidification. Considering the heterogeneity of the CFS/ME patient population it is clear that the study conducted by Boulton [2012] was statistically underpowered due to low sample size, effectively low statistical power negatively impacts the likelihood of a nominally statistical significant finding reflects a true effect [Button et al. 2013]. Thus, any conclusions drawn from the data must be interpreted with caution.

An additional aim of the present chapter was to investigate the impact of physical activity on intracellular pH in an *in vitro* muscle culture system. This was achieved through the application of EPS and myotubes were stimulated for 24-hours at alternating high and low frequencies to produce skeletal muscle contraction and to induce metabolic changes associated with physical activity. Results demonstrated EPS to exhibit no significant effect on either CFS/ME or control myotube intracellular pH when each group when post-EPS measures were compared to rest [Figure 5.0a, b and c]. In addition, no difference in pH was observed between CFS/ME and control myotubes immediately post-EPS or during the recovery period [Figure 5.0b and c]. The findings contrast with earlier *in vivo* studies, which demonstrated when exercising to a comparable level to control participants CFS/ME patients exhibited significant intramuscular acidosis and a 4-fold increase in the time taken to recover from acidosis [Jones et al. 2010; 2012]. Nevertheless, in agreement the work presented here other studies have reported limited evidence of reduced intramuscular pH in patients [Barnes et al.1993; Wong et al. 1992; Lane et al. 1998; 1998^b]. For example. Wong et al. [1992] reported there to be no difference in pH at rest or the recovery phase following graded exercise to exhaustion and measured by NMR. Similarly, Barnes et al. [1993] found no

evidence of abnormality at rest or following exercise when CFS/ME patients (n=46) were taken as a whole. However, 6 patients were reported to exhibit increased acidification in response to exercise. Likewise, in studies conducted by Lane [1998^a;1998^b], following sub-anaerobic threshold exercise CFS/ME only 8% of the group were reported to exhibit an elevated blood lactate response. All the studies compared CFS/ME patients to control participants and measured intramuscular pH via NMR or MRS. Importantly; the contrasting findings illustrate the heterogeneity of the CFS/ME patient population and the differing response to exercise.

It is important to note that contrasting patient bio-energetic responses to exercise exhibited with *in vivo* studies may be due to the level of patient engagement, which is a key limitation of that mode of investigation. For example, Jones et al. [2012] reported CFS/ME patients to fall into 2 distinct categories in relation to Phosphocreatine (PCr) depletion in response to exercise. The first group demonstrated normal bio-energetic dysfunction, exhibiting PCr depletion to a comparable level to controls when exercising at the same level of MVC. Conversely, the second group exhibited low-level PCr depletion and no exercise induced acidosis as a consequence. The authors postulated this effect to be evidence of some form of exercise avoidance behaviour. In contrast, the *in vitro* exercise model utilised in the present study eliminates the need for patient compliance in the exercise protocol and enables the bio-energetic function of all patient muscle samples to be examined equally following the same EPS strategy.

Nevertheless, it is important to acknowledge limitations associated with *in vitro* bio-energetic assessment for example, culture conditions are not homeostatic as there is a continuous depletion of nutrients and the generation of waste products within the culture medium. Additionally, oxygen supply is not always sufficient with dissolved oxygen typically consumed during the first few hours or medium replacement resulting in a diffusion limited supply which can induce anaerobic culture conditions (glycolysis) [Hartung and Daston, 2009; Coecke et al. 2006] Furthermore, while myotubes have been reported to closely resemble mature human skeletal muscle in terms of morphological, biochemical and metabolic characteristics [Olsson et al. 2015; Aas et al. 2013; Berggren et al. 2007]. However, when compared to intact skeletal muscle, myotube contractile force during EPS has been reported as lower. In addition, fused tetani is achieved at a reduced stimulating frequency and kinetic parameters are slower [Madden et al. 2015; Olsson et al. 2015].

Further, it is difficult to directly compare effects exhibited *in vivo* when the whole organism is exercising as a system compared to the localised effects occurring *in vitro* with cultured muscle samples. Similarly, Aas et al. [2013] suggested *in vitro* myotube systems to lack the *in vivo* microenvironment and communication with other cells, as well as the associated direct contact with other bioactive substances. Additionally, Brown et al. [2015] suggested monolayer cultures to be a good model to investigate exercise *in vitro*. However, it was recognised that the 2D nature of the culture environment was a potential limitation, as it did not enable the complete alignment of myotubes, which can impair intracellular signalling. To overcome this issue the authors suggested the development of a 3D cell culture exercise model. Interestingly, 3D cultures have been reported in primary human skeletal muscle [Martin et al. 2013] and differentiated C212 myoblasts [Player et al. 2014; Sharples et al. 2012], with these models reporting the 3D structure to closely mirror the structural, functional and myogenic characteristics associated with native skeletal muscle. Although, presently no studies have investigated the application of EPS in 3D muscle cultures, which Brown et al. [2015] suggested to be an important consideration for future studies.

However, a number of studies have validated the use of EPS and have demonstrated the model to improve lipid oxidation, increase glycolysis, glucose metabolism, AMPK activation, glucose transport and IL-6 release [Brown et al. 2015; Nikolic et al. 2012; Nedachi et al. 2008], which are well known effects exhibited with *in vivo* exercise. Therefore, confirming the application of *in vitro* muscle culture platforms combined with EPS to be an advantageous experimental platform to investigate metabolic disease and dysfunction.

Data generated in this chapter demonstrated intracellular pH to be substantially lower in CFS/ME and control myoblast samples compared to resting myotube samples. Interestingly, this finding is in line with findings from other researchers [Wagatsuma et al, 2013; Barberi et al. 2011; Leary et al, 1998; Moyes et al. 1997]. For example, Wagatsuma et al. [2013] reported there to be a gradual shift in the dominant energy producing pathways utilised due to myogenic differentiation. Additionally, Leary et al. [1998] investigated metabolic rates during various stages of myogenic differentiation. The authors reported that in proliferating myoblasts approximately 30% of the ATP utilised by the cells was generated via oxidative phosphorylation. Alternatively, in terminally differentiated myotubes oxidative phosphorylation was reported to account for approximately 60% of ATP production and thus the primary source of metabolic energy. It therefore appears that throughout the

differentiation process there is a steady increase in the movement from glycolysis to oxidative phosphorylation as the primary energy source. Moreover, from a molecular perspective mitochondrial enzyme activity (e.g. citrate synthase, cytochrome-c-reductase, succinate dehydrogenase and cytochrome C oxidase) has been reported to dramatically increase during myogenic differentiation. Additionally, respiratory chain complex content have also been reported to be increased in myotubes compared to myoblasts [Barberi et al. 2011; Moyes et al. 1997].

4.4.3 Limitations

Differentiated myotubes have been reported to closely resemble mature human skeletal muscle, in relation to morphological, biochemical and metabolic characteristics [Berggren et al. 2007]. However, as recognised by Brown et al. [2015] monolayer culture systems do not enable complete alignment of myotubes. To overcome this issue, it would be beneficial for future studies to develop novel 3D *in vitro* culture platforms which incorporate EPS stimulation, to enable *in vitro* studies to more accurately replicate *in vivo* investigations.

4.4.4 Conclusion

The *in vitro* muscle culture system developed in this chapter enabled the determination of intracellular pH in CFS/ME skeletal muscle samples. In contrast to Boulton [2012] the pH-sensing technique applied in this chapter revealed there to be no significant difference in muscle cell pH for CFS/ME patients compared to controls. Similarly, in terms of differentiated myotubes, both sample groups displayed comparable intracellular pH measurements following EPS, which was applied to simulate exercise *in vitro*. Finally, the PDK inhibitor DCA did not exhibit any significant effect on intracellular pH in any of the muscle samples tested.

This work has highlighted the importance of using significant patient numbers when investigating a heterogeneous population. It has also highlighted the difficulties of comparing *in vitro* and *in vivo* data. Taking these limitations into consideration it is still possible to

conclude that, based on current findings, there is no evidence for the role of impaired PDK enzyme function in the peripheral muscle of patients with CFS/ME.

4.5 References

- Alford, R. Simpson, H, M. Duberman, J. Hill, G, C. Ogawa, M. Regino, C. Kobayashi, H. Choyke, P, L. (2009) Toxicity of organic fluorophores used in molecular imaging: Literature review. *Mol Imaging*. 8 (6) 341- 354
- Aas, V. Bakke, S, S. Feng, Y, Z. Kase, E, T, Jensen, J. Bajpeyi, S. (2013). Are cultured human myotubes far from home? *Cell Tissue Res*.354 (3):671–82
- Barbieri, E. Battistelli, M. Casadei, L. Vallorani, L. Piccoli, G. Guescini, M. Falcieri, E. (2011). Morphofunctional and Biochemical Approaches for Studying Mitochondrial Changes during Myoblasts Differentiation. *Journal of Aging Research*.
- Barnes, P, R. Taylor, D, J. Kemp, G, J. Radda, G, K. (1993). Skeletal muscle bioenergetics in chronic fatigue syndrome. *J Neurol Neurosurg Psychiatry*. 56, 679-683
- Benjaminsen, R. V. Sun, H. Henriksen, J, R. Christensen, N, M. Almdal, K. Andresen, T, L. (2011) Evaluating nanoparticle sensor design for intracellular pH measurements. *ACS Nano*. 5, 5864–5873
- Berggren, J, R. Tanner, C, J. Houmard, J, A. (2007) Primary cell cultures in the study of human muscle metabolism. *Exerc Sport Sci Rev*. 35(2) 56–61
- Boulton, S, J. (2012) Integrated free radical sensor systems for investigation of cellular models of disease. PhD thesis, Newcastle University. Identifier: <http://hdl.handle.net/10443/1427>
- Brown, A, E. Jones, D, A. Waker, M. Newton. J, L. (2015) Abnormalities of AMPK activation and glucose uptake in Chronic Fatigue Syndrome. *PLOS ONE*. 10 (4)
- Button, K, S. Ioannidis, J, P, A. Mokrysz, C. Nosek, B, A. Flint, K. Robinson, E, S, J. Munafo, M, R. Power failure: Why small sample size undermines the reliability of neuroscience. *Nature reviews neuroscience*. 14, 365-376
- Coeck, S. Ahr, H. Blauuboer, B, J. Bremer, S. Casati, S. Castell, J. Combes, R. Corvi, R. Crespi, C, L. Cunningham, M, L. (2006) Metabolism a bottle neck in vitro toxicological test development. *Altern. Lab. Anim*. 34, 49-8

- Davies, T, A. Fine, R, E. Johnson, R, J. Levesque, C, A. Rathbun, W, H. Seetoo, K, F. Smith, S, J. Strohmeier, G. Volicer, L. Delva, L. Simons, E,R. (1993) Non-age related differences in thrombin responses by platelets from male participants with advanced Alzheimer's disease. *Biochemistry biophysics research community*. 194, 537-543
- Fujita, H. Nedachi, T. Kanzaki, M. (2007) Accelerated de novo sarcomere assembly by electric pulse stimulation in C2C12 myotubes. *Exp Cell Res*. 313 (9) 1853–65
- Gaster, M. Kristensen, S, R. Beck-Nielsen, H. Schroder, H, D. (2001) A cellular model system of differentiated human myotubes. *Apmis* 109: 735–744.
- Gdovin, M, J. Zamora,D,A. Ravindran, M,C,R. Leiter,J,C. (2010) Optical recording of intracellular pH in respiratory chemoreceptors. *Ethnicity and disease*. 20, 33-38.
- Grant, R, L. Acosta,R. (1997) Ratiometric measurement of intracellular pH of cultured cells with BCECF in a fluorescent multi-well plate reader. *In vitro cellular and developmental biology-animal*. 33, 256-260
- Han, J. Burgess, K.(2010) Fluorescent indicators for intracellular pH. *Chemical reviews*. 110, 2709-2728
- Hartung,T. Daston, G. (2009) Are in vitro tests suitable for regulatory use. *Toxicol Sci*. 111 (2) 233-237
- Henry, R, R. Abrams, L. Nikoulina, S. Ciaraldi, T, P. (1995) Insulin action and glucose metabolism in nondiabetic control and NIDDM subjects. Comparison using human skeletal muscle cell cultures. *Diabetes*. 44, 936–946
- Izumi,H. Torigoe.T. Ishiguchi,H. Uramoto,H. Yoshida, Y. Tanabe,M. Ise,T. Murakami,T (2003) Cellular pH regulators: Potentially promising molecular targets for cancer. *Chemotherapy cancer treatment reviews*. 29, 541-549
- Jones, D, E, J. Hollingsworth, K. Blamire, A, M. Taylor, R. Newton, J, L.(2010) Abnormalities in pH handling by peripheral muscle and potential regulation by the autonomic nervous system in chronic fatigue syndrome. *Journal of Internal Medicine*. 26, 394–401
- Jones, D, E. Hollingsworth, K, G. Jakovljevic, D, G. Faltakhova, G. Pairman, J. Blamire, A, M. Trennel, M, I. Newton, J, L. (2012) Loss of capacity to recover from acidosis on repeat

exercise in chronic fatigue syndrome: A case control study. *European Journal of Clinical Investigation*. 42 (2) 184-194

Lambernd, S. Taube, A. Schober, A. Platzbecker, B. Gorgens, S, W. Schlich, R. (2012) Contractile activity of human skeletal muscle cells prevents insulin resistance by inhibiting pro-inflammatory signalling pathways. *Diabetologia*. 55(4) 1128–1139

(a) Lane, RJ; Barrett, MC; Woodrow, D; Moss, J; Fletcher, R; Archard, LC. (1998). Muscle fibre characteristics and lactate responses to exercise in chronic fatigue syndrome. *J Neurol Neurosurg Psychiatry*. 64, 362-367

(b) Lane, R, J. Barrett, M, C. Taylor, D, J. Kemp, G, J. Lodi, R. (1998). Heterogeneity in chronic fatigue syndrome: evidence from magnetic resonance spectroscopy of muscle *Neuromuscul Disord*. 8, 204-209.

Leary, S, C. Battersby, B, J. Hansford, R, G. Moyes, C, D. (1998) Interactions between bioenergetics and mitochondrial biogenesis. *Biochim Biophys Acta* 1365: 522–530

Madden, L. Juhas, M. Kraus, W, E. Truskey, G, A. Bursac, N. (2015) Bioengineered human myobundles mimic clinical responses of skeletal muscle to drugs. *eLife*. 4.

Nedachi T, Fujita H, Kanzaki M.(2008) Contractile C2C12 myotube model for studying exercise-inducible responses in skeletal muscle. *Am J Physiol Endocrinol Metab*. 295(5): 191–204

Martin, N, R. Passey, S, L. Player, D, J. Khodabukus, A. Ferguson, R, A. Sharples, A, P. Mudera, V. Baar, K. Lewis, M, P. (2013) Factors affecting the structure and maturation of human tissue engineered skeletal muscle. *Biomaterials*. 34 (24) 5759- 5765

Moyes, C, D. Mathieu-Costello, O, A. Tsuchiya, N. Filburn, C. Hansford, R, G.(1997) Mitochondrial biogenesis during cellular differentiation. *American Journal of Physiology*. 272(4)1345–1351

Nedachi, T. Fujita, H. Kanzaki, M.(2008) Contractile C2C12 myotube model for studying exercise-inducible responses in skeletal muscle. *Am J Physiol Endocrinol Metab*. 295(5) 191–204

Nikolic, N. Skaret Bakke, S. Tranheim Kase, E. Rudberg, I. Flo Halle, I. Rustan, A, C. (2012). Electrical pulse stimulation of cultured human skeletal muscle cells as an in vitro model of exercise. *PLoS ONE*. 14 (7)

- Olsson, K. Cheng, A. J. Alam, S. Al-Ameri, M. Rullman, E. Westerblad, H. Gustafsson, T. (2015). Intracellular Ca²⁺-handling differs markedly between intact human muscle fibers and myotubes. *Skeletal Muscle*, 5, 26
- Orfanos, Z. Godderz, M, P, O. Soroka, E. Godderz, T. Rummyantseva, A. van der Ven, P, F, M. Hawke, T, J. Furst, D, O. (2016) Breaking sarcomeres by in vitro exercise. *Scientific reports*. 6, 1-9
- Orkan, P. Mutharasan, R. (2002) A rapid method for measuring intracellular pH using BCECF-AM. *Biochimica et Biophysica (BBA)- General subjects*. 1572 (1) 143-148
- Perez-Sala, D. Collado-escobar, D. Mollinedo, F. (1995) *Journal of biological chemistry*. 270, 6235
- Player, D, J. Martin, N, R. Passey, S, L. Sharples, A, P. Mudera, V. Lewis, M, P. (2014) Acute mechanical overload increases IGF-I and MMP-9 mRNA in 3D tissue-engineered skeletal muscle. *Biotechnology letters*. 36 (5):1113–24.
- Richoz, O. Gatziofias, Z. Francois, P. Schrenzel, J. Hafezi, F. (2009) Impact of fluorescein on the antimicrobial efficacy of photoactivated riboflavin in corneal collagen cross-linking. *J Refract surg*.
- Rink, T, J. Tsien, R, Y. Pozzan, T. (1982) *Journal of cell biology*.
- Sharples, A, P. Player, D, J. Martin, N, R. Mudera, V. Stewart, C, E. Lewis, M, P. (2012) Modelling in vivo skeletal muscle ageing in vitro using three-dimensional bioengineered constructs. *Aging cell*. 11(6) 986–95
- Wagatsuma, A. Sakuma, K. (2013) Mitochondria as a potential regulator of myogenesis. *The Scientific World Journal*. 593267
- Wong, R. Lopaschuk, G. Zhu, G. Walker, D. Catellier, D. Burton, D. Teo, K. Collins-Nakai, R. Montague, T. (1992). Skeletal muscle metabolism in the chronic fatigue syndrome. *In vivo* assessment by ³¹P nuclear magnetic resonance spectroscopy. *Chest* . 102, 1716-1722

Chapter 5

An Exploration of Glycolytic Function in CFS/ME Primary Myoblasts and Myotubes via Extracellular Flux Analysis and L-lactate Quantification

5.1 Introduction

The purpose of this chapter was to investigate glycolytic function in the skeletal muscle of patients with CFS/ME via extracellular flux (XF) analysis and through the measurement of cellular L-lactate concentration. Previous *in vivo* studies have reported CFS/ME patients to exhibit excessive acidosis following relatively low level physical activity, which was postulated to be the result of an over-utilisation of the lactate dehydrogenase energy-producing pathway [Jones et al. 2010; Jones et al. 2012]. Additionally, a pilot *in vitro* study revealed CFS/ME skeletal muscle samples to exhibit aberrantly low intracellular pH in culture, which was normalised following treatment with DCA, further supporting the presence of heightened anaerobic glycolysis in CFS/ME [Boulton. 2012].

5.1.1 Overview of cellular glycolysis

Glycolysis occurs in the cytoplasm and functions as an intracellular bio-chemical energy producing pathway, which acts to convert a single molecule of glucose into two molecules of pyruvate, with a parallel generation of two molecules of ATP (Teslaa & Teitell. 2014). The molecule ATP is the primary source of cellular energy and acts to capture and transfer free energy within biological systems (Pelletier et al. 2014) . ATP is generated by both glycolysis and oxidative phosphorylation (mitochondrial respiration). It is important to note that oxidative phosphorylation and glycolysis are tightly coupled and operate as a molecular interconversion system. Under normal conditions, cells are able to consume energy supplied primarily by oxidative phosphorylation, however in hypoxic situations glycolysis is dramatically increased to maintain the energetic balance [Zheng. 2012] .During anaerobic conditions pyruvate is reduced to lactic acid in the cytosol by the enzyme lactate dehydrogenase, in aqueous solutions lactic acid almost completely dissociates into lactate and H^+ . Effectively, acidosis occurs if there is an impairment in oxidative phosphorylation capacity, leading to a net gain in H^+ [Winer et al. 2014; Zheng, 2012]. Protons are pumped

out of the cell via various mechanisms to maintain intracellular pH [Winer et al. 2014; Casey et al. 2010] and it is the efflux of protons into the extracellular space or medium that results in extracellular acidification (Hochachka et al. 1983; Lane et al. 2009) which can be readily measured via a number of techniques. Overview of the glycolytic pathway demonstrated in figure 5.2

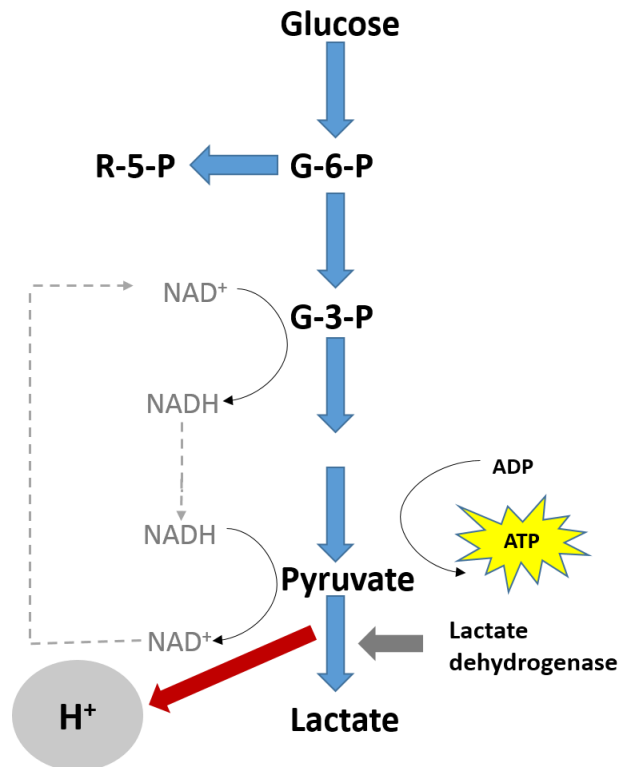


Figure 5.2: Schematic illustration of cellular glycolysis, adapted from Winer et al [2011].

5.1.2 Techniques to measure cellular glycolytic flux

Cellular glycolytic function can be measured via glucose uptake and lactate excretion. Effectively, glucose is transported into the cell via glucose transporters Glut 1-4. Alternatively, lactate excretion occurs through monocarboxylic transporters 1-4. A number of techniques are available to quantify extracellular lactate and glucose in the cell culture media (Teslaa & Teitell. 2014).

One method is via the entrapment of radioactive isotopes, this generally involves the uptake of glucose analogues to measure glycolytic flux. Typically, cells are seeded into culture dishes and then treated with radiolabelled deoxyglucose, which is then phosphorylated in the cytosol of the cell trapping the radioactivity, which is deemed proportional to glycolytic rate of the cell (Bittner et al. 2010). However, this technique does exhibit limitations as noted by Bittner et al (2010). For example, glucose analogues are treated differently by hexokinase than glucose and also may be acutely toxic to the cell even in low doses (Kurtoglu et al. 2007). Additionally, the accumulation of glucose is not only determined by metabolism but is also controlled by the ability of glucose to be transported via the transporters. Furthermore, isotopic measurement provides low spatio-temporal resolution, which makes it impossible to quantify the contribution of individual cells or the detection of rapid phenomena. Finally, Bittner et al. (2010) concluded the technique to be relatively insensitive and exhibit a need for radioactive isotope manipulation which makes them inadequate for the purposes of high throughput analysis.

Glucose and lactate may also be measured through the use of commercially available kits, which function to quantify the amount of the substrate in the cell culture media. Measurement is made via calorimetric or fluorometric detection via standard laboratory spectrophotometry (Teslaa & Teitell. 2014).

Cellular glycolytic function may also be assessed via extracellular flux analysis (Seahorse Bioscience). The XF analyser was introduced in 2006/2007 and was developed to address the need for a high-throughput system for the determination of mitochondrial dysfunction. (Horan et al. 2012). In terms of measurement of cellular acidification, the XF analyser builds upon probe technology developed during the late 1980's and early 1990's which resulted in the production of the microphysiometer, which functioned to measure proton excretion in culture (Parce et al. 1989; Owicki et al. 1992). However, the instrument overcomes many of the weaknesses associated with the microphysiometer and exhibits increased sensitivity, improved throughput and is capable of measuring in real-time the uptake and excretion of metabolic end products, with the additional option of compound injection (Ferrick et al. 2008; Wu et al. 2007). The flux analyser operates on a 24 or 96-well microplate format and a key benefit is that the assay is based on a single plate which containing multiple samples which can be analysed with high resolution, therefore providing sensitivity and high-throughput capability (Horan et al. 2012). The system consists of a novel fluorescent sensor

probe, which fits over the culture plate and is submerged in the wells of the plate [Horan et al. 2011] (Figure 5.3) . Proton extrusion from the cells into the surrounding medium causes rapid and measurable alterations in pH, which is reported as extracellular acidification rate (ECAR), and is measured in milli-pH units per minute (mpH) (Wu et al. 2007). The sensor probe also contains 4 delivery ports, which enable key reagents to be transferred into the culture media to manipulate cellular metabolism.

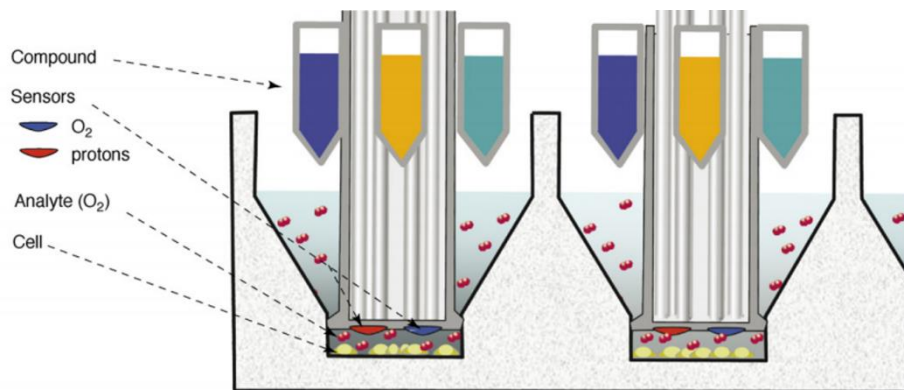


Figure 5.3: An illustration of an XF microplate and sensor cartridge as depicted by Ferrick et al. [2008]

The XF analyser enables glycolytic stress testing by the sequential delivery of glucose, oligomycin and 2-Deoxy-D-glucose (2-DG). Glucose is supplied to feed glycolysis and the difference between ECAR prior and after injection of glucose is a measure of glycolytic rate. Oligomycin acts to inhibit ATP synthase in the electron transport chain (ETC) which causes a reduction in the ATP/ADP ratio, thus stimulating glycolysis. The difference between ECAR before and after oligomycin addition is equal to the glycolytic capacity. The difference between the glycolytic capacity and glycolysis defines glycolytic reserve capacity. 2-DG glucose acts to inhibit glycolysis through competitive binding with glucose hexokinase and therefore provides baseline ECAR measurement. ECAR after the addition of 2-DG represents non-glycolytic acidification (Teslaa & Tietell, 2014; Wu et al. 2007). Glycolytic flux in response to the injection of key glycolytic stress test reagents is displayed in Figure 5.4.

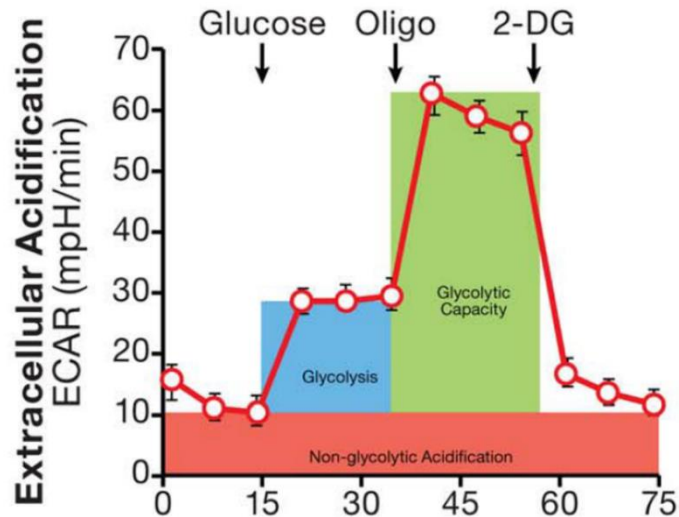


Figure 5.4: Schematic illustration of glycolytic flux following the addition of stress test reagents to provide the parameters glycolysis, glycolytic capacity and non-glycolytic acidification.

5.1.3 Hypotheses

The aim of this chapter was to thoroughly investigate glycolytic function in CFS/ME skeletal muscle cells. Specifically, by utilising XF stress testing to reveal key glycolytic parameters, in addition to quantifying L-lactate concentration at rest and following exercise simulation. In each experiment cells were also treated with PDK inhibitor DCA to explore the capacity of the compound to alter cellular glycolytic function.

The specific experimental hypotheses proposed were (1) Increased glycolytic activity in CFS/ME patient myoblasts and myotubes when compared to controls. Evidenced by elevated ECAR for each glycolytic parameter obtained via XF analysis. (2) Elevated cellular L-lactate concentration in CFS/ME muscle samples compared to controls. (3) Normalisation of glycolytic function and L-lactate concentration comparable to controls following treatment with PDK inhibitor DCA.

5.2 Materials and Methods

CFS/ME and non-diseased primary myoblasts and myotubes were supplied by Dr Audrey Brown at Newcastle University. A total of 5 (4 females, 1 male) CFS/ME patient myoblast samples were used for experimentation with a donor age of 43.83 ± 12.73 . Control samples were obtained from 3 females participants and 1 male aged 50.14 ± 12.81 .

All tissue culture reagents for myoblast and myotube routine culture were purchased from Sigma-Aldrich (Poole, Dorset, UK) with the exception of Ham's F10 myoblast growth media (Lonza, SLS, East Riding of Yorkshire, UK) and chick embryo extract (Seralab, West Sussex, UK).

Tissue culture flasks, 6 well culture plates and serological pipettes were supplied by Greiner bio-one (Stonehouse, UK).

XF-96 (V3) polystyrene cell culture plates, sensor cartridge and cartridge calibration buffer were supplied by Seahorse Bioscience (North Billerica). Glycolysis stress test reagents glucose, oligomycin and 2DG were supplied by Sigma-Aldrich, in addition to Dulbeccos modified eagles medium DMEM which was used as experimental assay medium and L glutamine.

L-lactate assay kit (calometric/fluorometric) was purchased from Abcam (Cambridge, UK).

PDK enzyme inhibitor Potassium Dichloroacetate was purchased from Sigma-Aldrich.

PierceTM Bicinchoninic acid assay (BCA) protein quantification kit was purchased from Thermo Fisher scientific (Cramlington, UK) and complete Lysis-M buffer from Roche diagnostics (Risch-Rotkreuz, Switzerland).

5.2.1 Study participants

Muscle biopsy samples were obtained from patients with CFS/ME and healthy control participants. The CFS/ME and control individuals were gender and age matched and both groups included both male and female volunteers. Recruitment was achieved through the NHS CFS clinical service within the Newcastle Upon Tyne Hospital Foundation Trust. The

CFS/ME patients all met the Fukuda (1994) criteria for CFS/ME. All participants agreed to complete the study via formal written consent. Ethical approval for the study was provided by the Newcastle and North Tyneside joint ethics committee.

5.2.2 Cell culture and preparation

As previously described in chapter 2, CFS/ME and control muscle cell samples were collected and isolated as detailed in the Brown et al. (2015) study. The myoblast samples were routinely cultured in Ham's F10 medium, supplemented with 20% FBS, 2% chick embryo extract, 500 U/ML Penicillin-streptomycin and 1% amphotericin B. Myoblasts were grown to 80% confluence in a T75 before being trypsinised and seeded into the vessel of choice. Cells were grown and maintained in a humidified incubator at 5% (v/v) CO₂ at 37°C.

For XF glycolysis stress testing myoblasts were seeded at a density of 3×10^4 cells per well into XF-96 culture plates and allowed to attach overnight, assays were performed the following day. For L-lactate experimental work myoblasts were seeded at a density of 2×10^5 cells per well and tested the following day.

Differentiation was induced by replacing Ham's F10 medium with MEM supplemented with 2% (V/V) FBS and 1% Penicillin-streptomycin. Cells were allowed to differentiate over 7 days and experimentation was performed on day 7 differentiation. Media was replaced every two days and all myotubes were tested at passage 6-7.

5.2.3 Electrical pulse stimulation

Electrical pulse stimulation (EPS) was carried out using the C-pace EP cell culture pacer (Ion Optix, Dublin). Following 7 days differentiation EPS stimulation was initiated for 24-hours at alternating frequencies, with one hour low frequency (volts, 24ms, 2Hz) followed by one hour high frequency (5 volts, 24ms, 0.2Hz).

5.2.4.1 L-lactate assay

The commercially available L-lactate kit (Abcam) was used to assess L-lactate concentration in myoblast and myotube samples. Additionally, L-lactate was also measured in stimulated myotubes following EPS.

5.2.4.2 Standard curve and sample preparation

A standard curve was prepared using the L-lactate standard concentrations supplied by the manufacturers. Briefly, standards were diluted in assay buffer to achieve a final L-lactate concentration range of between 0-100pmol/well, which were then seeded into a 96-well plate in duplicate. Fluorescent measurements were performed at 535/587nm. The linear regression of the curve was then utilised to determine the L-lactate concentration in cell samples.

In terms of sample preparation cellular supernatant was diluted 10,000-30,000x in assay buffer as directed by the manufactures. A series of dilutions were performed until the samples readings were within the range of the standard curve.

5.2.4.3 Assay procedure

Prior to running the assay growth medium was removed from the myoblast and resting myotube samples and replaced with DMEM for untreated cells and DMEM supplemented with 40 μ M DCA for cells receiving treatment. Media was replaced in EPS myotubes after 23.5 hours stimulation. DMEM was removed 30-minutes later in all samples and replaced with lactate assay buffer. The cells were then scraped from the culture vessel and transferred into eppendorfs for sonication (30-seconds) and centrifugation (2000rpm, 5-minutes, 2°C). Supernatant was removed (50 μ l) and added to the well of a 96-well plate in addition to 50 μ l of reaction mix. The plate was incubated for 30 minutes, at room temperature and protected from light, before fluorometric measurement.

5.2.4.4 L-lactate fluorometric measurement setup

Fluorescent intensity measurements were performed using the TECAN I 200 fluorimeter and data was obtained using the compatible Magellan software. In terms of set up, the L-lactate kit recommended the following measurement settings, $\lambda_{ex}= 535\text{nm}$, $\lambda_{em}= 587\text{nm}$, additionally gain was set to 70 throughout all experiments and multiple reads (4x4) per well option was selected.

5.2.5 Extracellular flux analysis

5.2.5.1 Assay preparation

The day prior to running the assay myoblasts were seeded into XF-96 culture plates, myotubes were seeded into plates 7 days prior to the assay. The day before testing the XF sensor cartridge was hydrated by adding 100 μl of calibrant (Seahorse Bioscience) to the utility plate. The cartridge was then incubated overnight at 37.5°C without CO₂.

On the day of the assay, growth media was removed from culture plates and replaced with DMEM supplemented with 2mM L-glutamine and pH adjusted to 7.35 +/- 0.05 and warmed to 37.5°C. Cells were washed twice with experimental media before the addition of DCA (40 μM). The culture plate was then placed in an incubator at 37°C and no CO₂ for 60 minutes before initiating the assay to allow for media temperature and pH to reach equilibrium.

5.2.5.2 Compound injection

All glycolytic stress test stock reagents stored at -20°C were defrosted and warmed to 37°C prior to loading the sensor cartridge. Each port of the sensor cartridge was loaded with 25 μl of the required compound. Glucose was added to port A for a final well concentration of 10mM. Oligomycin was added to port B for a final well concentration of 3 μM and 2-deoxyglucose was added to port C for a final concentration within the well of 100mM.

5.2.5.3 Glycolytic stress test

A glycolysis stress test assay was created on the XF controller, the template incorporate a calibration step for the sensor cartridge carried out without the cell culture plate. Once calibrated the utility plate was removed and replaced with the culture plate and the assay was initiated. The default template involves mix-wait- measure with timings 3min-0min-3 min, with 3 basal rate measurements performed prior to the first injection, followed by 3 rate measurements after each injection.

5.2.5.4 Normalisation

Normalisation for total protein concentration in the well was performed after each glycolytic stress test via the BCA assay. Following the stress test media was removed from the culture plate and cells were washed once with PBS, before the addition of lysis buffer (Thermo fischer) to each well. The wells were then scraped and the contents of the well removed and placed into a new 96-well plate. A 50:1 solution of BCA reagent A to BCA reagent B (Thermofischer) was added to the wells as per manufacturer's instructions. The plate was agitated for 30s on a plate shaker and then incubated at 37°C for 30 minutes and protected from light. Absorbance was measured at 562nm on the Tecan Infinite 200.

5.2.6 Data analysis

Results are presented as mean \pm standard deviation. Data was analysed via independent and paired T-test. Statistical analysis was performed using Minitab 17 statistical software (Coventry, UK)

5.3 Results

5.3.1.1 L-Lactate standard curve

L-lactate standards were diluted in assay buffer to achieve a final concentration range of 0-100pmol/well. An increase in mean FI exhibited a linear relationship with L-lactate concentration ($y=99.613x$, $R^2=0.973$, $n=5$). The linear regression of this standard curve was utilised to determine the L-lactate concentration in the myoblast and myotube samples. (Figure 5.5).

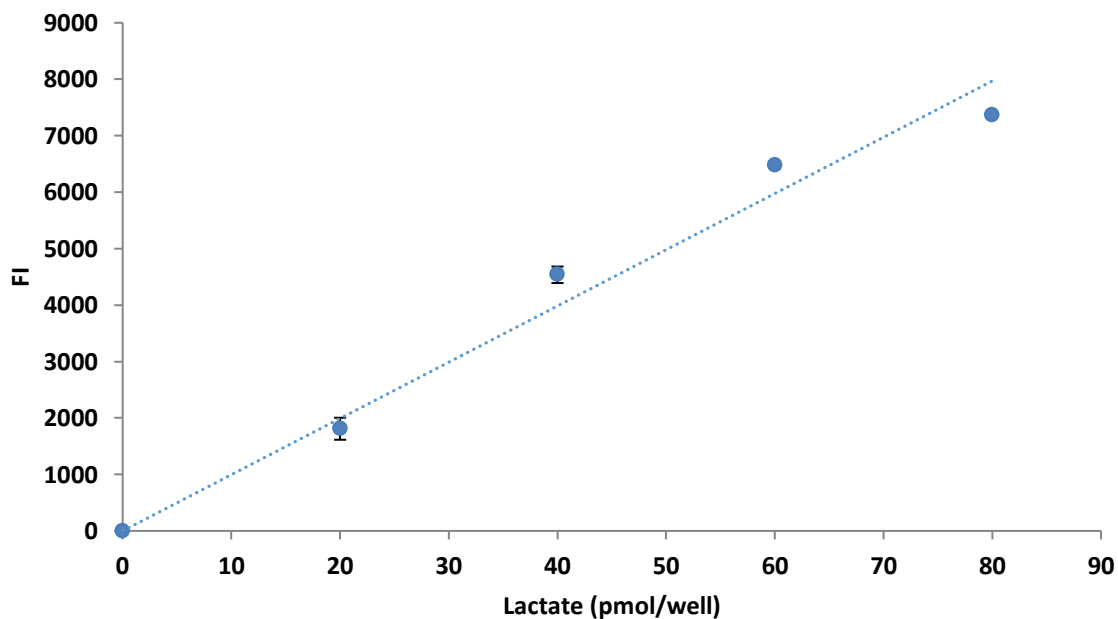


Figure 5.5 : Standard curve conducted with varying L-lactate standard concentrations. Mean FI was linearly dependent upon the L-lactate concentration ($y=99.613x$, $R^2=0.973$, $n=5$). The data is presented as mean \pm SD, $n=5$

5.3.1.2 Myoblast L-lactate measurement

L-lactate concentration was measured in CFS/ME ($n=5$) and control ($n=4$) myoblast samples. At baseline ($0\mu\text{M}$ DCA) CFS/ME and control myoblasts, samples did not exhibit significantly different L-lactate concentrations. Similarly, DCA treatment ($40\mu\text{M}$) did not induce any significant effect on either group. Displayed in Figure 5.6.

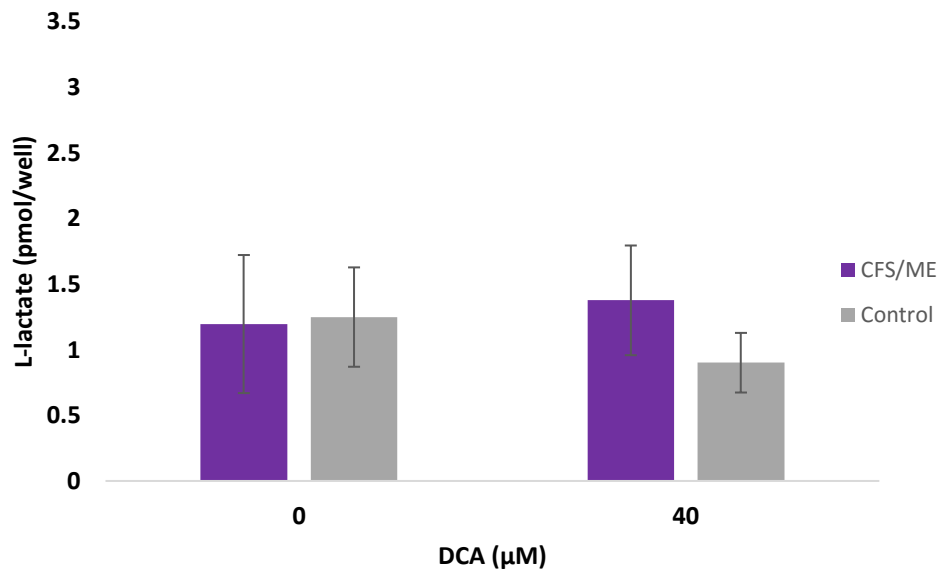


Figure 5.6 : L-lactate concentration in CFS/ME versus control myoblasts at baseline (0μM) and following treatment with 40μM DCA. No significant difference in L-lactate concentration was observed when the groups were compared. Additionally, no significant within-group effects were observed as a consequence of DCA treatment. Data is presented as mean ±SD, n=9

5.3.1.3 Myotube L-lactate measurement at rest and post-EPS

L-lactate concentration was measured in CFS/ME (n=4) and control myotubes (n=3) at rest and following 24-hours EPS. When CFS/ME myotubes were compared to controls at rest and following EPS there was no significant difference in L-lactate concentration at baseline (0μM) or following DCA (40μM) treatment. Similarly, EPS stimulation exhibited no significant alteration in L-lactate concentration when compared to resting levels in both samples at baseline and following DCA treatment. See figure 5.7.

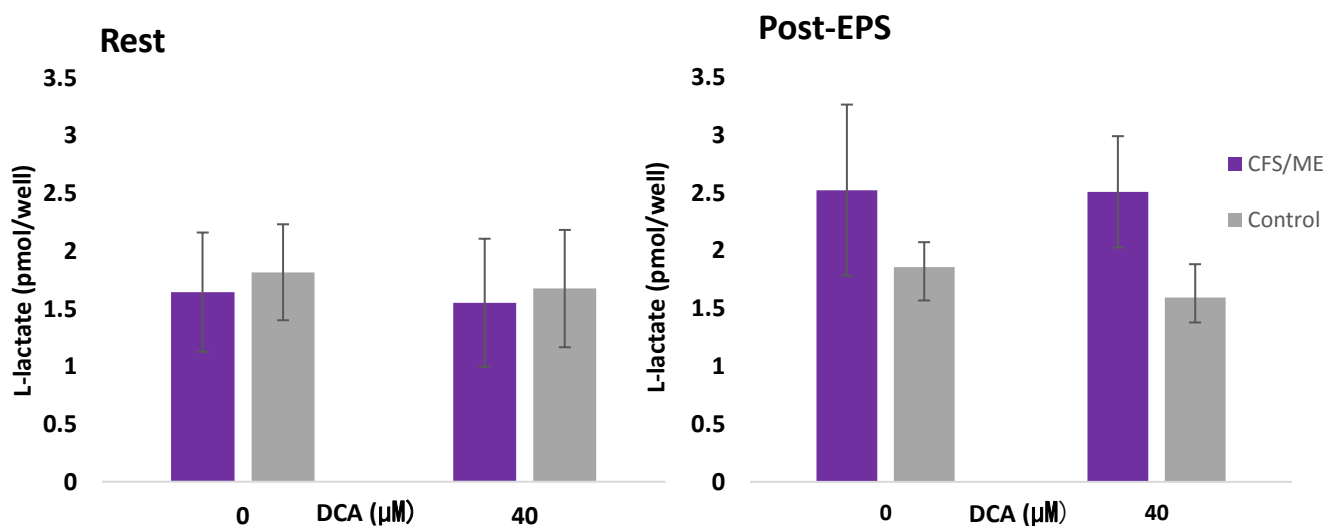


Figure 5.7 : L-lactate concentration in CFS/ME and control myotubes at rest and following 24-hours EPS. L-lactate concentration did not significantly differ for CFS/ME myotubes compared to controls at rest or following EPS at both 0μM and 40μM DCA conditions. The data is presented as mean ± SD, n=7

5.3.2 Extracellular Flux Analysis

5.3.2.1 Myoblast glycolytic stress testing with DCA treatment

Extracellular flux analysis provided a glycolytic profile for CFS/ME and control myoblasts. The sequential injection of inhibitors glucose, oligomycin and 2-DG enabled the measurement of glycolysis and glycolytic capacity and allowed the calculation of glycolytic reserve capacity.

Figure 5.8 demonstrated glycolysis measurements in CFS/ME (n=5) and control (n=4) myoblasts. ECAR was not significantly different in CFS/ME and control myoblasts at baseline (0μM), however was significantly lower in control compared to CFS/ME samples following 40μM DCA treatment. No within group (0μM vs 40μM DCA) effects as a consequence of DCA treatment were observed for either sample.

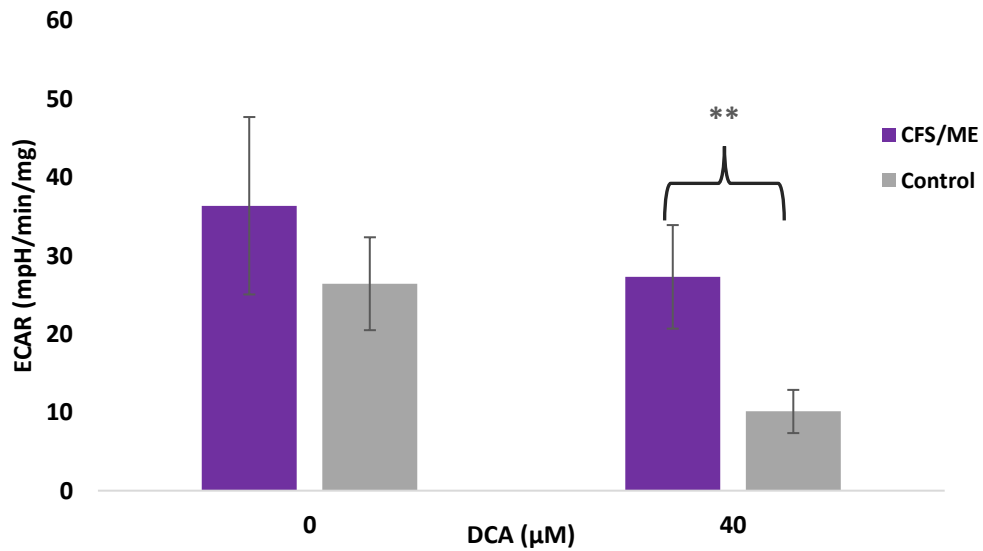


Figure 5.8: Glycolysis ECAR in CFS/ME and control myoblasts following treatment with DCA (40μM). No significant difference in ECAR at baseline (0μM) between samples, however ECAR significantly reduced in control compared to CFS/ME samples following DCA treatment. No within-group effects as a result of DCA treatment were observed. Data presented as mean ±SD, n=8, ** denoted P<0.05

The glycolytic capacity of the myoblast samples was demonstrated in Figure 5.9. ECAR at baseline (0μM) and following DCA treatment (40μM) was not significantly different between CFS/ME and control myoblasts. In terms of within-group effects, DCA treatment exhibited no significant alteration in ECAR for either the CFS/ME or control sample groups.

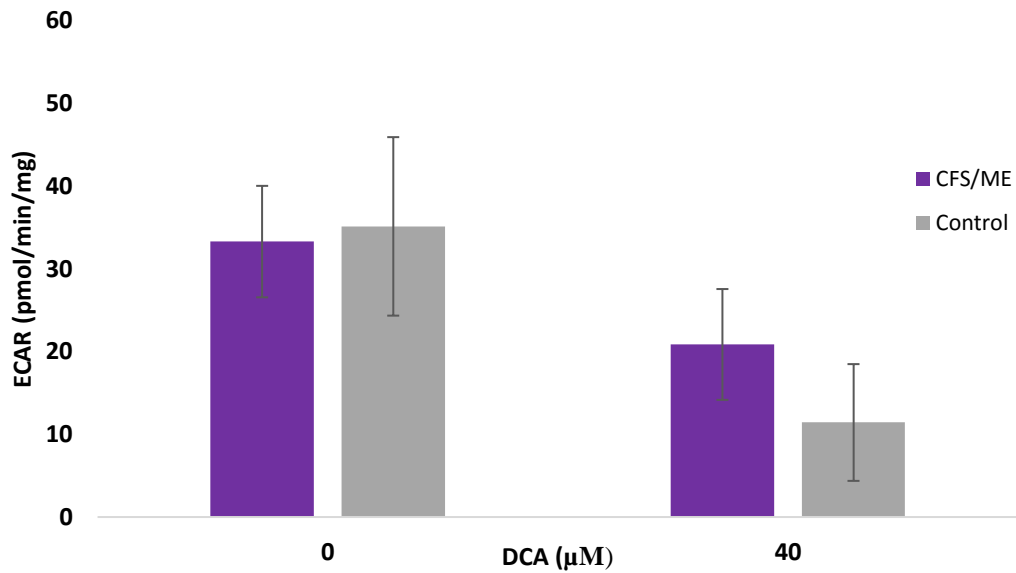


Figure 5.9 : Glycolytic capacity ECAR in CFS/ME and control myoblast samples. No significant difference was exhibited at baseline or following DCA treatment for the CFS/ME verses control myoblast samples. No within group effects were observed for either group following DCA treatment. Data presented as mean \pm SD, n=8

Figure 6.0 demonstrated myoblast glycolytic reserve capacity. CFS/ME and control myoblast ECAR did not significantly differ at baseline (0μM) or following treatment with DCA (40 μM). In terms of within-group effects there was no significant alteration in ECAR from baseline following DCA treatment in either group.

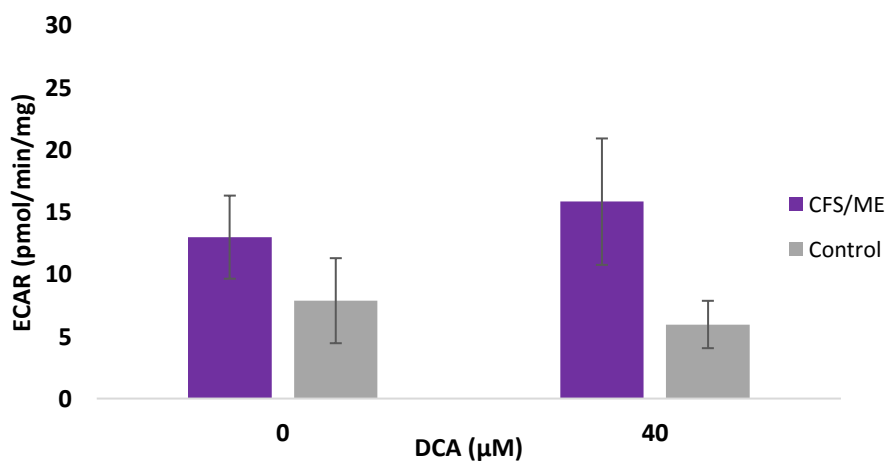


Figure 6.0: Glycolytic reserve capacity ECAR in CFS/ME and control myoblast samples. No significant difference was exhibited at baseline and following DCA treatment for the CFS/ME verses control myoblast samples. No within group effects were observed for either group following DCA treatment. Data presented as mean \pm SD, n=8

5.3.2.2 Myotube glycolytic stress testing with DCA treatment

Extracellular flux analysis was also performed to assess the glycolytic profile of differentiated myotube samples.

Glycolysis ECAR was not significantly different for CFS/ME (n=3) samples compared to controls (n=3) at baseline (0 μ M) or following incubation with DCA (40 μ M). Similarly, DCA treatment did not induce any significant alteration in ECAR in comparison to baseline measures in either group. Displayed in Figure 6.1.

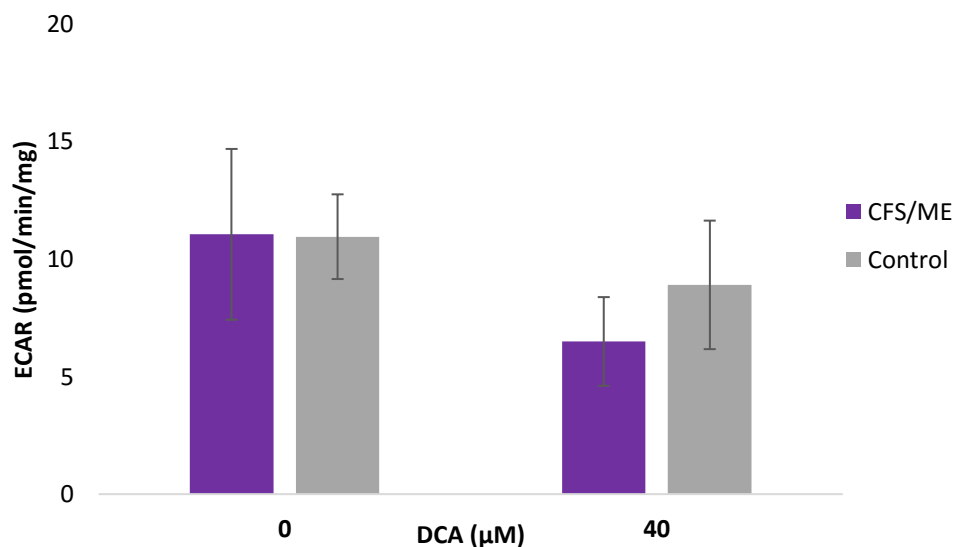


Figure 6.1: Glycolysis ECAR in myotube samples. No significant difference was exhibited at baseline and following DCA treatment for the CFS/ME versus control myotube samples. No within group effects were observed for either group following DCA treatment. Data presented as mean \pm SD, n=8

Glycolytic capacity ECAR is displayed in Figure 6.2. There was no significant difference in ECAR exhibited at 0 μ M or following 40 μ M DCA treatment in CFS/ME compared to control myotubes. Additionally, there was no significant alteration in ECAR following DCA treatment compared to baseline (0 μ M) in either sample group.

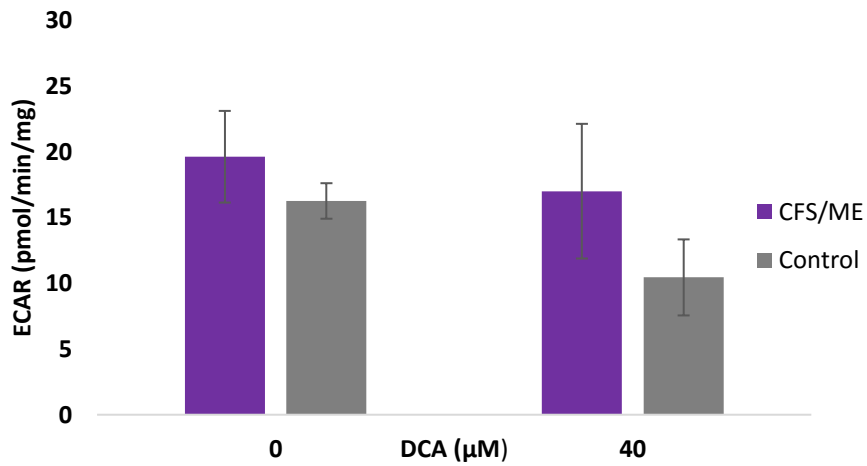


Figure 6.2 : Glycolytic capacity ECAR in myotube samples. No significant difference in ECAR at 10µM and 40µM in CFS/ME compared to control myotubes. No significant alteration in ECAR as consequence of DCA treatment in either group samples. Data presented as mean ±SD, n=8

Glycolytic reserve capacity is displayed in Figure 6.3. ECAR was significantly lower (P<0.05) in control myotubes at baseline compared to CFS/ME samples. However, following treatment with 40µM DCA this significant relationship was lost. No other significant effects were observed.

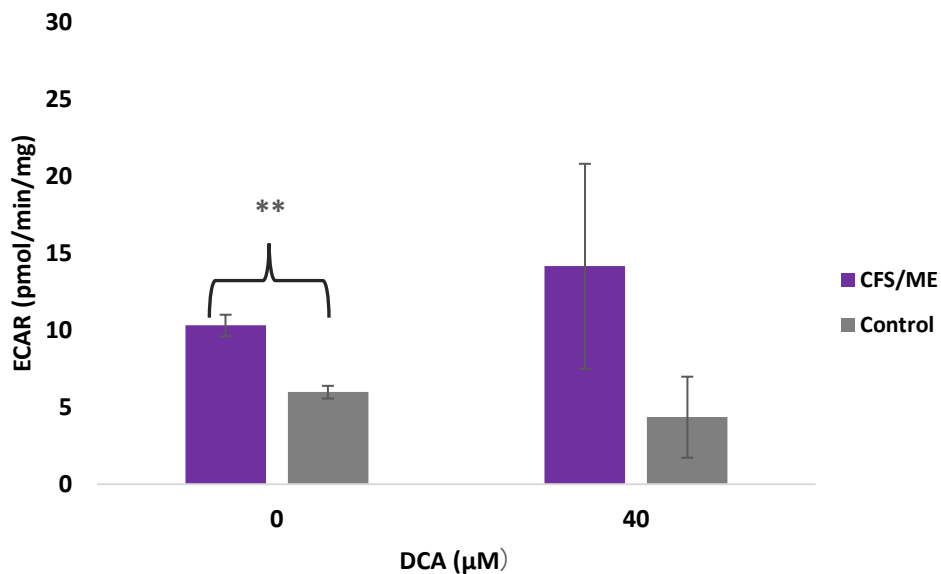


Figure 6.3: Glycolytic reserve capacity ECAR in CFS/ME and control myotube samples. Significantly lower ECAR at baseline in control samples. No other significant effects observed. Data presented as mean ± SD, ** denoted p<0.05

5.4 Discussion

CFS/ME patients frequently report the perception of generalised muscle fatigue, which is exacerbated following relatively low-level physical activity [Jones et al. 2010; Fukuda et al. 1994; MacIntyre et al. 1992]. *In vivo* studies have supported this assertion and have demonstrated the presence of profound intramuscular acidosis, a slowed time to recovery from acidosis post-exercise and a reduced anaerobic threshold in patients [Jones et al. 2010; 2012]. The authors postulated the findings to be related to an over-utilisation of the lactate dehydrogenase energy-producing pathway, even at relatively low exercise intensities. An *in vitro* pilot study also reported CFS/ME patient muscle samples to exhibit an aberrantly low intracellular pH compared to control samples. Nevertheless, this effect was completely normalised following treatment with PDK inhibitor DCA [Boulton. 2012].

The aim of chapter 2 in this thesis was to validate and further develop the *in vitro* muscle pH sensing system reported by Boulton [2012] and to confirm the presence of abnormal pH in CFS/ME myoblasts. However, the technique exhibited a number of weaknesses and it was not possible to accurately measure cytosolic pH. Therefore, in chapter 4 an alternative intracellular pH sensing technique was performed. Contrary to previous findings, CFS/ME muscle samples exhibited an intracellular pH comparable to controls at rest and following exercise simulation.

The aim of this chapter was to build upon chapter 2 and 4 and investigate cellular glycolytic function in more detail. Glycolytic function was assessed in myoblast and myotube samples via XF analysis, in addition to cellular L-lactate concentration, which was measured in resting samples and following exercise simulation. The results of this chapter demonstrated, firstly in terms of L-lactate concentration, levels were comparable for CFS/ME and control muscle samples at rest and following EPS, which contrasts the experimental hypotheses detailed in section 5.1.3. Additionally, contrary to the experimental hypothesis myoblast XF analysis revealed ECAR measurements for all glycolytic parameters to be comparable for both sample groups. However, glycolysis was reduced in control samples following DCA treatment. Finally, in contrast to the experimental hypothesis glycolytic reserve capacity was lower in control myotubes.

5.4.1 L-lactate concentration

In this chapter, cellular glycolytic function was investigated *in vitro*. This is the first study to measure L-lactate concentration in CFS/ME patient skeletal muscle samples at rest and following EPS. Lactate concentration is typically interpreted as a marker of anaerobic metabolism [Rogatzi et al. 2015]. Under anaerobic conditions, pyruvate is converted to lactic acid by the enzyme lactate dehydrogenase, which then dissociates to produce lactate and H^+ . If there is an impairment in oxidative pathways during lactate production, there is a net increase in hydrogen ions, resulting in a reduction in pH and the end point of acidosis [Phypers and Pierce. 2006].

The discovery that L-lactate concentration was not elevated in CFS/ME skeletal muscle samples at rest and following 24-hours EPS (Figure 5.6) is in agreement with the findings reported in chapter 4 of this thesis. Chapter 4 as previously described investigated intracellular pH as an alternative marker of anaerobic glycolysis and reported no evidence of elevated intracellular acidosis in CFS/ME muscle samples. Likewise, as discussed in earlier chapters several *in vivo* studies have measured intracellular pH dynamics using MRS at rest and post-exercise. These studies have reported a lack of evidence to suggest all CFS/ME patients exhibit excessive intracellular acidosis as a consequence of enhanced glycolytic function [Wong et al. 1992]. Additionally, Barnes et al. [1993], proposed the presence of a sub-group within the CFS/ME patient cohort which exhibit intramuscular acidification, however suggested this finding to not be uniform across the whole patient population.

In contrast, Boulton [2012] reported a decreased intracellular pH in CFS/ME myoblasts, which could be interpreted as an over-utilisation of lactate dehydrogenase energy-producing pathway. The reason for the discrepancy may relate to the previously described weaknesses associated with this study.

5.4.2 Glycolytic parameters

Skeletal muscle glycolytic function was assessed via XF analysis, with the technique enabling the determination of glycolytic parameters through the measurement of ECAR in the surrounding culture medium. Quite simply ECAR is a measurement of the excretion of lactic acid per unit of time following its conversion from pyruvate [Wu et al. 2007].

Glycolysis was the first parameter obtained and was measured following the injection of glucose, which was added to promote glycolytic metabolism [Das. 2013]. Glycolysis was not found to be elevated in CFS/ME skeletal muscle samples and DCA treatment did not alter ECAR (Figure 5.7 and 6.0). In contrast, control myoblast ECAR was reduced following the addition of DCA (Figure 5.7). It is difficult to ascertain the reason why ECAR was not similarly reduced in CFS/ME samples, however the finding does suggest control myoblasts to be more sensitive to DCA.

Glycolytic capacity was measured following the injection of oligomycin, which functioned to inhibit mitochondrial ATP production and shift energy production to glycolysis, with increases in ECAR revealing the maximal glycolytic capacity of the cells. CFS/ME muscle samples did not exhibit enhanced glycolytic capacity compared to controls and DCA treatment did not meaningfully alter ECAR in either group (Figure 5.8 and 6.1).

Finally, glycolytic reserve capacity was determined as the difference between glycolytic capacity (maximal in the presence of glucose + glucose) and glycolysis in the presence of glucose [Das, 2013]. Cells with a reduced reserve capacity have been reported to be more dependent upon glycolysis, with a higher reserve capacity indicative of greater tolerance to metabolic stress [Zheng et al. 2012]. Unexpectedly, in the present study control myotubes exhibited a reduced reserve capacity, however following treatment with DCA this effect was normalised (Figure 6.2). Suggesting, CFS/ME muscle samples to have an enhanced tolerance to metabolic stress.

Crucially, the findings suggest CFS/ME skeletal muscle samples to display normal cellular glycolytic function when under metabolic stress, which is in agreement with the previous section, which reported normal L-lactate concentration at rest and following 24-hours of EPS in CFS/ME muscle samples. Similarly, chapter 4 also reported no evidence of enhanced intracellular acidosis at rest and following EPS. However, the results do contrast previously described *in vivo* studies that measured intracellular pH following exercise [Jones et al. 2012; Jones et al. 2010]. Nevertheless, it is important to acknowledge this is the first *in vitro* study to directly measure glycolytic function in CFS/ME patient muscle samples, thus it is not possible to directly compare the findings to previous research.

If glycolytic function is not enhanced in CFS/ME, it is possible that other pathophysiological mechanisms may contribute to the muscle fatigue phenotype frequently reported. For

example, Allen et al [1995] suggested low pH and elevated intracellular lactate to impact upon the contractile apparatus of the muscle to a limited degree. In addition, Bogdanis et al. [2012], conducted isolated animal muscle and single fibre experiments and reported fatigue to be in part caused by increased inorganic phosphate leading to a reduction in force production and K^+ accumulation inside the T-tubules. With this effect negatively influencing upon action potential propagation.

Alternatively, in a CFS/ME specific study, Brown et al. [2015] reported several bio-chemical differences in CFS/ME muscle samples following EPS. These were impaired AMPK activation, impaired stimulation of glucose uptake and diminished release of IL-6. Interestingly, AMPK is a key regulator of cellular energy homeostasis, through increased AMP/ATP and ADP/ATP ratios [Jenkins et al. 2013]. It functions both acutely and chronically to restore and maintain cellular ATP levels. In the first instance AMPK stimulates glucose transport and fatty acid oxidation in skeletal muscle [Smith et al. 2005; Balon et al. 2001]. Chronically, AMPK functions to up-regulate proteins involved in substrate availability and oxidation capacity [Winder et al, 2000; Zheng et al. 2001]. Importantly, it acts to maximise mitochondrial function by promoting mitochondrial biogenesis [Jenkins. 2013; Hardie. 2011]. Given the role AMPK in promoting mitochondrial oxidative phosphorylation, reduced activation may contribute to mitochondrial dysfunction, which may contribute to skeletal muscle fatigue in CFS/ME patients

5.4.3 Conclusion

Glycolytic function in CFS/ME patient skeletal muscle samples was assessed by L-lactate measurement and XF analysis. Contrary to previous reports [Jones et al. 2012; 2010] there was no evidence of increased glycolytic function in CFS/ME samples in the basal state, following 24-hours EPS, or when metabolically stressed. Peripheral muscle fatigue experienced by CFS/ME does not appear to be the result of an impaired bio-energetic function and a concurrent over-utilisation of the lactate dehydrogenase energy-producing pathway as previously considered.

5.5 References

- Allen, D, G. Lannergren, J. Westerblad, H. (1995) Muscle cell function during prolonged activity: Cellular mechanism of fatigue. *Experimental Physiology*. 8 (4) 497-527
- Balon, T,W. Jasman, A, P. (2001) Acute exposure to AICAR increases glucose transport in mouse EDL and soleus muscle. *Biochem Biophys Res Commun*. 282, 1008-1011
- Barnes, P, R. Taylor, D, J. Kemp, G, J. Radda, G, K. (1993). Skeletal muscle bioenergetics in the chronic fatigue syndrome. *Journal of Neurology, Neurosurgery, and Psychiatry*, 56 (6) 679–683.
- Bittner, C, X. Loiza, A. Ruminot, I. Larenas, V. Sotelo-Hitschfeld, T. Gutierrez, R. Cardova, A. Valdebenito, R. Frommer, W, B. Barros, L, F. (2010) High resolution measurement of the glycolytic rate. *Front Neuroenergetics*. 2, 1-26
- Bogdanis, G, C. (2012). Effects of Physical Activity and Inactivity on Muscle Fatigue. *Frontiers in Physiology*, 3, 142.
- Boulton, S, J. (2012) Integrated free radical sensor systems for investigation of cellular models of disease. PhD thesis, Newcastle University. Identifier: <http://hdl.handle.net/10443/1427>
- Brown,A,E. Jones, D,A. Waker,M. Newton. J,L. (2015) Abnormalities of AMPK activation and glucose uptake in Chronic Fatigue Syndrome. *PLOS ONE*. 10 (4)
- Casey, J, R. Grinstein, S. Orlowski, J. (2010) Sensors and regulators of intracellular pH. *Nature reviews: molecular cell biology*. 11, 50-61
- Das, K, C. (2013) Hyperoxia decreases glycolytic capacity, glycolytic reserve and oxidative phosphorylation in MLE-12 cells and inhibits I and II function, but not complex IV in isolated mouse lung mitochondria. *PLoS ONE*. 8 (9) 1-59
- Ferrick, D, A. Neilson, A. Beeson, C. (2008) Advances in measuring cellular bioenergetics using extracellular flux. *Drug Discovery Today*. 12 (516) 268-274
- Fukuda, K. Straus, S, E. Hickie, I. Sharpe, M, C. Dobbins, J, G. Komaroff, A. (1994) The chronic fatigue syndrome: a comprehensive approach to its definition and study. *Annals of Internal Medicine*. 121, 953–9

- Hardie, D, G. (2011) AMP-activated protein kinase- an energy sensor that regulates all aspects of cell function. *Genes and Dev.* 1895-1908
- Hochachka, P,W. Mommsen, T, P. (1983) Protons and anaerobiosis. *Science.* 219, 1391-1397
- Horan, M, P. Pichaud, N. Ballard, J, W, O. (2012) Review: Quantifying mitochondrial dysfunction in complex diseases and aging. *J Gerontol A Biol Med Sci.* 1-13
- Jenkins, Y. Sun, T, Q. Markovtsov, V. Foretz, M. Li, W. (2013) AMPK Activation through Mitochondrial Regulation Results in Increased Substrate Oxidation and Improved Metabolic Parameters in Models of Diabetes. *PLoS ONE* 8(12)
- Jones, D, E, J. Hollingsworth, K. Blamire, A, M. Taylor, R. Newton, J, L.(2010) Abnormalities in pH handling by peripheral muscle and potential regulation by the autonomic nervous system in chronic fatigue syndrome. *Journal of Internal Medicine.* 26, 394–401
- Jones, D, E. Hollingsworth, K, G. Jakovljevic, D, G. Faltakhova, G. Pairman, J. Blamire, A, M. Trennel, M, I. Newton, J, L. (2012) Loss of capacity to recover from acidosis on repeat exercise in chronic fatigue syndrome: A case control study. *European Journal of Clinical Investigation.* 42 (2) 184-194
- Joynayvaz, F, R. Shulman,G, I. (2010) Regulation of mitochondrial bio-genesis. *Essays in biochemistry.* 47,10
- Kumuda, D, C. (2013) Hyperoxia decreases glycolytic capacity, glycolytic reserve and oxidative phosphorylation in MLE-12 cells and inhibits complex I and II function but not complex IV in isolated mouse lung mitochondria. *PLOS ONE*, 9, (9)
- Kurtoglu, M. Maher, J, C. Lampidis, J, L. (2007) Differential toxic mechanisms of 2-Deoxy-D-Glucose versus 2-Fluorodeoxy-D-Glucose in hypoxic and normoxic tumour cells. *Antioxidants & Redox Signalling.* 9 (9) 1382-1390
- Lane, A, N. Fan, T,W. Higashi, R, M. (2009) Metabolic acidosis and the importance of balanced equations. *Metabolomics.* 8-12
- Macintyre A.(1992) CFS, post-viral fatigue syndrome; how to live with it. London: Thorsons. (27-33)

- Owicki, J, C. Parce, J,W. (1992) Biosensors based on the energy metabolism of living cells: The physical chemistry and cell biology of extracellular acidification. *Biosens Bioelectron.*7. 255–72
- Parce, J,W. Owicki, J, C. Kercso, K, M. Sigal, G, B. Wada, H, G. Muir, V, C. Bousse, L, J. Ross, K, L. Sikic, B, I. McConnell, H, M. (1989) Detection of cell-affecting agents with a silicon biosensor. *Science.* 246, 243
- Phypers, B. Pierce, J, M, T. (2006) Lactate physiology in health and disease. *Contin Educ Anaesth Crit Case Pain.* 6 (3) 128-132
- Pelltier, M. Billingham, L, K. Ramaswamy, M. Siegel, M, A. (2014) Extracellular flux analysis to monitor glycolytic rates and mitochondrial O₂ consumption
- Rogatzki, M, J. Guson, B, S. Goodwin, M, L. Gladden, L, B. (2015) Lactate always the end product of glycolysis. *Front Neurosci.* 9, 1-6
- Smith, J, L. Patil, P, B. Fisher, J, S. (2005) AICAR and hyperosmotic stress increase insulin-stimulated glucose transport. *J Appl Physiol.* 99, 877-883
- TeSlaa,T. Teitell, M, A. (2014) Techniques to monitor glycolysis. *Methods Enzymol.* 542, 91-114
- Winder, W, W. Holmes, B, F. Rubink, D, S. Jensen, E, B. Chen, M. Holloszy, J, O. (2000) Activation of amp-activated protein kinases increases mitochondrial enzymes in skeletal muscle. *Journal of applied physiology.* 88, 2219-2226
- Winer, L, S. Wu, M. (2014) Rapid analysis of glycolytic and oxidative substrate flux of cancer cells in a microplate. *PLOS One,* 1-14, 9 (10)
- Wong, R. Lopaschuk, G. Zhu, G. Walker, D. Catellier, D. Burton, D. Teo, K. Collins-Nakai, R. Montague, T. (1992). Skeletal muscle metabolism in the chronic fatigue syndrome. In vivo assessment by ³¹P nuclear magnetic resonance spectroscopy. *Chest.*102, 1716-1722
- Wu, M. Neilson, A. Swift, A, L. Moran, R. Tamagnine, J. Parslow, D. (2007) Multiparameter metabolic analysis reveals a close link between attenuated mitochondrial bioenergetic

function and enhanced glycolysis dependency in human tumor cells. *American Journal of Physiology Cell Physiology*. 292 (1) 125–136.

Zheng, D. MacLean, P, S. Pohnert, S, C. Knight, J, B. Olson, A, L. (2001) Regulation of muscle GLUT-4 transcription by AMP-activated protein kinase. *J Appl Physiol*. 91, 1073-1083

Zheng, J.(2012) Energy metabolism of cancer: Glycolysis versus oxidative phosphorylation (Review). *Oncology Letters*. 4(6) 1151-11111

Chapter 6

An Investigation of Mitochondrial Function in CFS/ME Patient Myoblast and Myotube samples via Extracellular Flux Analysis

6.1 Introduction

The work reported in this chapter centred on assessing mitochondrial function in myoblasts and myotubes isolated from CFS/ME patient samples. Evidence suggests mitochondrial dysfunction may play a pivotal role in CFS/ME aetiology. Lowered ATP production, impaired oxidative phosphorylation and mitochondrial damage have been reported in patients with CFS/ME [Filler et al. 2014; Myhill et al. 2014]. Moreover, CFS/ME patients share common skeletal muscle symptoms associated with diseases linked to mitochondrial dysfunction, for example muscle pain, fatigue and cramping [Morris & Maes. 2014; Fulle et al. 2007]. However, presently no *in vitro* studies have been conducted to investigate mitochondrial function in CFS/ME muscle samples via extracellular flux analysis, therefore experimentation using this novel technique to measure cellular mitochondrial function under stress is required.

6.1.1 Oxidative phosphorylation overview

In chapter 5 the first pathway of breaking down glucose into pyruvate was discussed. Glycolysis occurring in the cytosol produces only a small amount of ATP. In contrast the oxidation of pyruvate in the mitochondria results in approximately 15 times more ATP produced compared to glycolysis [Huttemann et al. 2007]. The metabolic reactions involved in oxidative phosphorylation are energy-transducing processes, whereby the oxidation-reduction reactions are essential for the synthesis of ATP. During these reactions electrons are removed by the oxidation of fuel molecules and are transferred to the electron carrier coenzymes nicotinamide adenine dinucleotide (NAD^+) in addition to Flavin adenine dinucleotide (FAD) converting them to their reduced form (NADH and FADH_2). The electrons are then transferred to from NADH to O_2 through a series of protein complexes that form the electron transport chain [Hutteman et al. 2007]. The electron transport chain (ETC) is the site of oxidative phosphorylation and comprises the NADH-dehydrogenase (complex I), succinate dehydrogenase (complex II), ubiquinone, bc1 complex (III), cytochrome C and

cytochrome C oxidase (Complex IV). Effectively, electrons derived from NADH are carried through the ETC and enter the chain via complex I. Complex II passes electrons to the ubiquinone/ubiquinone pool and these electrons are transferred through the chain to molecular oxygen. The movement of electrons causes an exergonic reaction that is utilised to pump protons out of the mitochondrial matrix and in doing so generating a membrane potential across the intermembrane space in addition to electrochemical energy in the form of a proton-motive force in the intermembrane mitochondrial space. This process drives the synthesis of ATP as protons (H^+) are able to move passively to the mitochondrial matrix via a pore which is associated with ATP-synthase (complex V), thus driving ATP synthesis [Huttemann et al. 2007; Yong-Ling et al. 2008] (Displayed in Figure 6.3).

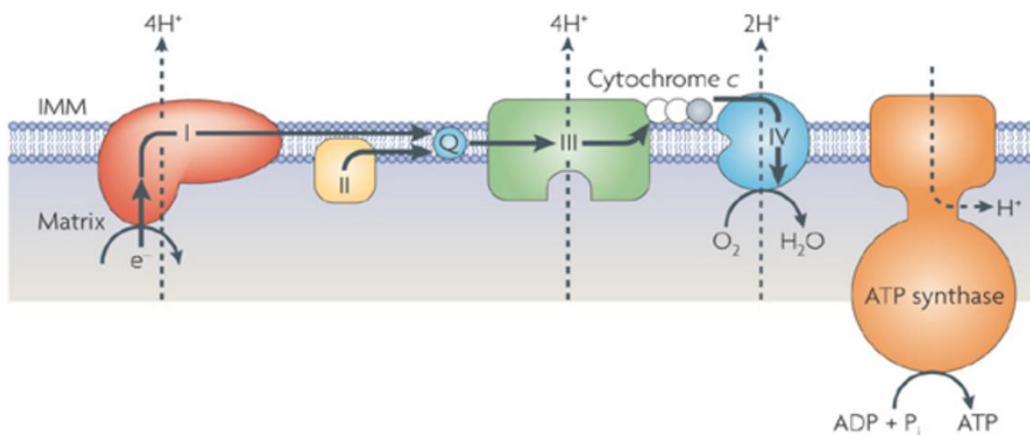


Figure 6.3: Created by Yong-ling et al [2008]. The electron transport chain with 4 membrane bound complexes (I-IV) Electrons pass through the complexes with assistance from electron carrier Ubiquinone (Q) and cytochromes. The movement of electrons is associated with proton (H^+) pumping from the mitochondrial matrix to the intermembrane space. This creates a proton motive force, which drives ATP synthesis.

6.1.2 Evidence of mitochondrial dysfunction in CFS/ME

Increasing evidence exists to suggest mitochondrial dysfunction plays an underlying role in CFS/ME pathophysiology [Filler et al. 2014; Morris and Maes. 2014]. For example, Booth et al. [2012] investigated mitochondrial function in a large cohort of CFS/ME patients. The authors conducted an ATP profile test, which incorporated a variety of biochemical tests to yield 6 numerical factors that described the availability of ATP, and the efficiency of oxidative phosphorylation in mitochondria located in neutrophils. Additionally, all patients were reported to exhibit measurable mitochondrial dysfunction, which correlated with severity of illness.

Although the mitochondrial investigations were performed in neutrophils the authors suggested the findings to be transferable to other cells in the body.

A variety of studies have investigated mitochondrial function in CFS/ME patient muscle biopsies. Interestingly, a number of these studies have reported the presence of structural abnormalities, which have included mitochondrial degeneration, atrophy of Type II fibres as well as fusion and branching of the cristae [Morris and Maes 2014; Behan et al. 1991]. Further, evidence also exists to demonstrate the presence of key skeletal muscle bio-energetic abnormalities including a reduction in the rate of ATP production and re-synthesis following exercise, when measured via ^{31}P MRS [Lane et al. 1998; 2003]. Additionally, studies utilising the same methodological approach have also reported an impairment in the bio-energetic function of cardiac muscle [Hollingsworth et al. 2010].

Nevertheless, the alterations in mitochondrial bioenergetics do not appear to be uniform across the CFS/ME patient population, with Barnes et al. [1993] reporting evidence of impaired mitochondrial function in only a sub-group of patients. Alternatively, McCully et al. [2003] reported no evidence of mitochondrial bioenergetic abnormality despite utilising the same methodology. Similarly, Vermeulen et al. [2010] reported CFS/ME patients to exhibit a normal oxidative phosphorylation capacity in the muscle. In this study, patients and control participants completed a controlled repeat exercise intervention to exhaustion. Results demonstrated CFS/ME patients in response to exercise to exhibit a reduced anaerobic threshold, despite an abnormal oxidative phosphorylation capacity. This finding lead the authors to suggest the impairment in anaerobic threshold to be linked to impaired oxygen transport capacity rather than mitochondrial dysfunction.

6.1.3 Mitochondrial respiration measurement techniques

The synthesis of ATP is a key function of the mitochondria and is typically determined experimentally in an in-direct manner through the measurement of mitochondrial O_2 consumption or respiration rate [Perry et al. 2013]. Traditional approaches to the investigation of mitochondrial respiration have predominantly utilised amperometric techniques. Perhaps the most common amperometric approach being the application of the Clarke-type electrodes. Perry et al. [2013] and Gnaiger et al. [2008] described the Clarke electrode as consisting of either a gold or platinum cathode and a Ag/AgCl anode, which are separated via a KCl solution.

Voltage can be applied to both half-cells, which kept apart from the experimental medium via an O₂ permeant material (polyvinylidene difluoride). O₂ diffuses through the membrane and is reduced by electrons at the cathode, generating hydrogen peroxide. This causes the oxidation of the Ag/AgCl anode, which acts to generate an electrical current, which is representative of the partial pressure in addition to the concentration of O₂ in the experimental medium. The changes in the concentration of O₂ in the medium inversely relate to respiratory rate of the cell and allow for the quantification of O₂ consumption. However, classical Clark-type O₂ electrodes are associated with a number of limitations including, the potential of the electrode to consume O₂, the sensitivity to mass exchange as a result of stirring requirements that may prove damaging to the cell and the need for a large assay volume, thus the electrode is positioned at quite a distance from the cell monolayer [Diepart et al. 2010].

Two systems have been developed to overcome the weaknesses associated with the use of traditional O₂ electrodes. The systems enable subtle changes in mitochondrial respiration to be determined. These systems include the high-resolution oxygraph- 2K (O₂K, Oroboros instruments, Austria) and the sensitive high-throughput extracellular flux analyser (Seahorse bioscience). The O₂K was produced during the 1990's and has since been extensively used in the field of mitochondrial respiratory analysis. In terms of set-up, the system combines two separate 2-mL chambers, which contain polarographic O₂ sensors, which enable the real-time measurement of O₂ concentration in (nanomoles/millilitre) and O₂ consumption (picomoles/second/millilitre) within each chamber. The system works by measuring both concentration and consumption of O₂ while injecting key substrates directly to the cells in suspension in the testing chamber, to stimulate various components of the electron transport chain [Gnaiger et al. 1995; Horan et al. 2012]. The O₂K exhibits a number of benefits over the conventional use of Clark-type electrodes. For example, one key advantage is that O₂ concentration in the measurement chambers can remain elevated throughout the duration of the assay, or until functional stability of the sample is reduced. This can enable extended substrate-uncoupler-inhibition-titration protocols to be completed, which is incredibly advantageous as such protocols allow for the evaluation of mitochondrial coupling and respiratory control measurements to be performed and as each substrate can be manually injected into the testing chamber each component of the electron transport chain can be investigated independently [Gnaiger, 2009; Horan et al. 2012]. However, the O₂K does exhibit some crucial limitations. For example, there is a high level of operator input required during experimentation, as there is a need for constant monitoring of the assay and adjustment of concentrations of the injectable

reagents to obtain an optimal signal intensity, thus a fairly labour intensive procedure. Additionally, the system is not capable of high-throughput analysis as only two samples can be tested at one time, with each experiment lasting approximately 1 hour, meaning only 16 samples can be tested in an 8-hour period [Horan et al. 2012].

The extracellular flux analyser (Seahorse Bioscience) overcomes a number of the weaknesses associated with Clark-type electrodes and the O₂K. For example, the XF analyser exhibits high-throughput unlike the Clark-type electrode and O₂K, as the platform is available in a 96-well format, enabling the measurement of mitochondrial bioenergetics in up to 96 samples per plate [Salabei et al. 2014; Ferrick et al. 2008]. Thus, it is possible to test up to 96 samples in one experiment. Additionally, the system is fully automated so requires minimal operator input so proves less labour intensive than the O₂K. Additionally, the XF analyser is capable of measuring O₂ levels in very small volumes of media, just above the cell monolayer, which was not possible with Clark-type electrodes [Wang et al. 2013].

As previously discussed in chapter 5 the XF analyser has now become a mainstream technique to measure cellular bioenergetics (Salabei et al. 2014). Through the use of the previously described optical sensors it is capable of measuring both ECAR and oxygen consumption (OCR) simultaneously. OCR is measured in picomoles/minute and is a determination of the rate of mitochondrial oxidative phosphorylation [Horan et al. 2012]. In terms of function, the sensor probe contains specific fluorophores sensitive to O₂, the piston like sensor is injected into the wells of the plate periodically to form a transient microchamber slightly above cell monolayer (200 microns). To measure OCR fibre optic bundles are injected into the sensor probe to provide excitation and emission light for the fluorophore [Perry et al. 2013]. O₂ levels are measured over a couple of minutes and provide an indication of the extent of cellular O₂ consumption [Perry et al. 2013].

Reagents that inhibit components of the electron transport chain can be added to the sensor cartridge to perform a mitochondrial ‘stress testing’ technique and the inhibitors allow for the determination of 6 mitochondrial parameters. These are, basal OCR, proton leak OCR, maximal OCR, reserve capacity OCR and non-mitochondrial OCR. The parameters are obtained following the sequential delivery of oligomycin (to inhibit ATP synthase), carbonylcyanide p-trifluoromethoxyphenylhydrazone (FCCP, to uncouple the mitochondrial inner membrane and allow for uninhibited electron flow through the ETC) and a combination of antimycin a and rotenone (to inhibit complex I and III) [Dranka et al. 2011], which is

displayed in Figure 6.4 . The difference between basal OCR and oligomycin- insensitive OCR determines the amount of O₂ consumption that is ATP-linked [Dranka et al. 2011; Jekabsons et al. 2004]. The FCCP injection allows for protons to move uninhibited across the mitochondrial inner membrane, leading to maximal electron flow through the ETC, which results in an increase in O₂ consumption and enables a determination of maximal OCR [Drank et al. 2011; Jekabsons et al. 2004; Nicholls et al. 2002]. The difference between FCCP OCR and basal OCR provides a measure of cellular respiratory reserve capacity. Finally, a combination of inhibitors antimycin A and rotenone act to completely halt electron movement by acting upon complex I and III, preventing electron movement through complex IV and therefore providing a measure of O₂ consumption from non-mitochondrial sources [Dranka et al. 2011; Jekabsons et al. 2004].

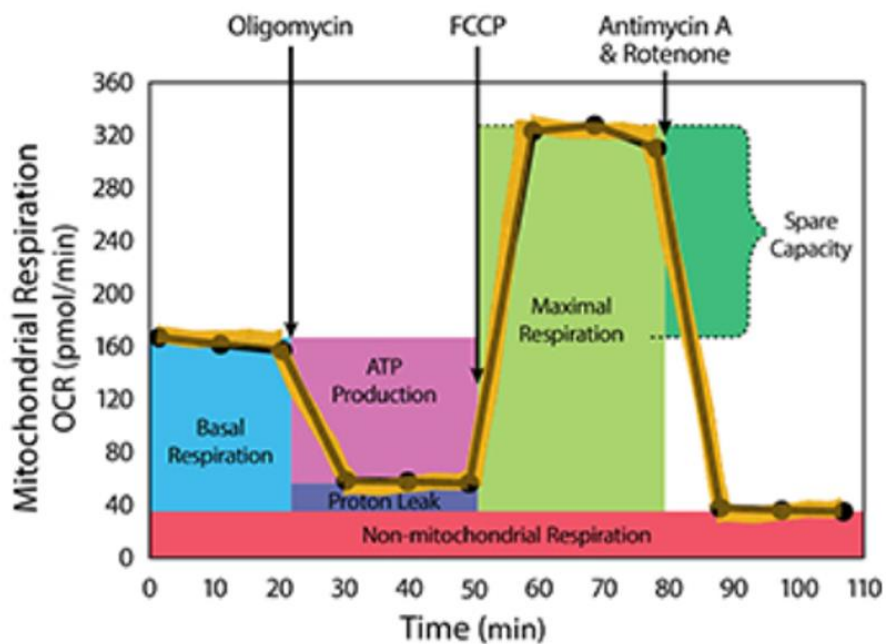


Figure 6.4: Mitochondrial respiration OCR during XF stress test. Mitochondrial parameters depicted in relation to substrate injection. Image provided by Seahorse Bioscience.

However, as with the techniques previously described the XF analyser also exhibits some limitations. Firstly, the injectable compounds are expensive to purchase and require optimisation prior to use. Additionally, the fluorescent plates, which are costly, can only be used in one assay [Horan et al. 2012]. Finally, it is possible that the injectable compounds may

interact with the fluorescent probe or plastic plate generating inaccurate results [Sauerbeck et al. 2011].

6.1.4 Assessment of mitochondrial function

In this chapter CFS/ME skeletal muscle mitochondrial bioenergetics were investigated *in vitro* by manipulating the glucose substrate availability. The concentration of glucose in the assay media was altered to maximise oxidative phosphorylation. Interestingly, muscle cells have been reported to be highly glycolytic when grown and differentiated in high glucose conditions relative to muscle tissue *in vivo*, which complicates the accurate study of mitochondrial function [Aguer et al. 2011]. For example, myoblasts are routinely cultured in high glucose media, which has been reported to diminish mitochondrial function. Additionally, cancer cell lines have been reported to be highly glycolytic when grown in high glucose media, an occurrence referred to as the ‘Crabtree effect’, whereby excess glucose functions to impair oxidative phosphorylation [Marroquin et al. 2007; Shulga et al. 2010; Rossignol et al. 2004]. Furthermore, this effect is not limited to cancer cell-lines and has also been reported in primary human myotubes [Aguer et al. 2011], embryonic tissues and proliferative thymocytes [Aguer et al. 2011; Ibsen et al. 1961].

To combat the ‘Crabtree’ effect a number of studies have substituted glucose for galactose, with a goal to promote the utilisation of mitochondrial oxidative phosphorylation and enable a thorough investigation of mitochondrial function/dysfunction [Aguer et al. 2011; Elkalaf et al. 2013; Marroquin et al. [2007]. However, Elkalaf et al. [2013] reported galactose supplementation of the culture medium to impair parameters of mitochondrial function (maximal respiration and spare respiratory capacity) in C2C12 myoblast and myotube cell lines.

6.1.5 Hypotheses

The aim of this chapter was to examine CFS/ME myoblast and myotube mitochondrial function via XF analysis. Function was assessed following the addition of key inhibitors of the mitochondrial electron transport chain. Further investigation into CFS/ME myoblast and

myotube function was performed by varying substrate availability (glucose) during the mitochondrial stress test.

The specific experimental hypotheses were:

- (1) CFS/ME myoblasts and myotubes exhibit impaired mitochondrial function indicated by reduced OCR measurements for all mitochondrial parameters.
- (2) CFS/ME samples exhibit lower OCR for mitochondrial parameters compared to controls when substrate availability is reduced.

6.2 Materials and Methods

CFS/ME and control myoblasts were provided by Dr Audrey Brown at Newcastle University. Tissue culture reagents including penicillin streptomycin, amphotericin B, Fetal bovine serum, trypsin EDTA, phosphate buffered saline and modified Eagles medium were supplied by Sigma-Aldrich (Poole, Dorset, UK). Ham's F10 growth media was supplied by Lonza (SLS, East riding, Yorkshire). Chick embryo extract was supplied by Sera lab (West Sussex, UK).

Plastic consumables including serological pipettes, 96-well plates, graduated pipette tips, cell scrapers, falcon tubes and tissue culture flasks were supplied by Greiner Bio (Stonehouse, UK).

XF flux 96-well plates, sensor cartridge and calibration buffer was supplied by Seahorse Bioscience (North Billerica). Assay medium (DMEM), L-glutamine, glucose and mitochondrial stress test reagents oligomycin, FCCP, antimycin and rotenone were all purchased from Sigma-Aldrich.

Pierce™ BCA protein assay kit was supplied by Thermo scientific (MA, USA). Complete Lysis-M was purchased from Roche diagnostics (Switzerland).

6.2.1 Study participants

Muscle biopsy samples were obtained from the vastus lateralis of CFS/ME patients and healthy control participants (as previously outlined in chapter 2). Recruitment was conducted through the Newcastle Upon Tyne Hospital foundation trust. All CFS/ME patients met the Fukuda criteria for CFS/ME. All participants supplied formal written consent and ethical approval was granted from the Newcastle and North Tyneside ethics committee. A total of 4 CFS/ME patient samples were used for experimentation (3 females, 1 male) with an average donor age of 46.12 ± 10.1 years. The control sample group consisted of 3 females and 1 male with a donor average donor age of 46.13 ± 7 years.

6.2.2 Cell culture and preparation

CFS/ME and control myoblast samples were collected as detailed by Brown et al (2015). Myoblasts were grown in Ham's F10 medium, supplemented with 20% FBS, 2% chick embryo extract, 500U/mL Penicillin streptomycin and 1% amphoteric B. The cells were stored in a humidified CO₂ incubator (5% v/v) at 37°C.

For the mitochondrial stress test myoblasts were seeded at a density of 3×10^4 cells per well into XF-96 plates. This seeding density was determined during optimisation work. Myoblast experimentation was performed the following day. Differentiation was performed by replacing growth media with MEM supplemented with 2% FBS (v/v) and 1% penicillin-streptomycin. The cells were allowed to differentiate over a 7-day period; media was replaced every two days. Experiments were performed on day 7 differentiation. All assays were performed on myoblast and myotubes at passage 6-7.

6.2.3 Extracellular flux analysis

6.2.3.1 Assay preparation

Prior to experimentation myoblasts were seeded into XF-96 plates and allowed to attach overnight or differentiated into myotubes for 7-days. The sensor cartridge was hydrated overnight in 100µl calibrant per probe. The cartridge was incubated in a CO₂ free incubator at 37°C.

On the day of the assay the experimental medium was prepared by supplementing DMEM with pyruvate (1mM) and L-glutamine (2mM), before adding the desired concentration of glucose. The glucose concentrations tested were 2.5mM (hypoglycaemic) 5mM (normal) and 10mM (hyperglycaemic). The media was then pH adjusted to 7.35 +/- 0.05 and warmed to 37.5°C. The media of the cell culture plate was removed, the plate washed and DMEM added. The culture plate was then placed in a CO₂ free incubator for one hour to enable an equilibration in the pH and temperature of the experimental media.

6.2.3.2 Compound preparation

Prior to the loading the sensor cartridge, the mitochondrial stress test stock reagents stored at -20°C were defrosted. The ports of the sensor cartridge were loaded at a volume of 25µl. Port A was loaded with oligomycin at a final well concentration of 3µM, port B was loaded with FCCP at a final well concentration of 1µM and finally port C was loaded with 1.2µM antimycin A and rotenone.

6.2.3.3 Optimisation

A series of optimisation assays were required before completing experimental work. Firstly, cell seeding density was determined for both myoblast and myotube cell samples. The XF-96 manufacturers (Seahorse Bioscience) recommend an optimal seeding density to exhibit an OCR of 20-160pmol/min during the final basal measure during mitochondrial stress testing. Therefore, seeding densities between 1×10^4 and 5×10^4 were investigated to determine the optimal seeding density. In both myoblast and myotube samples 3×10^4 was found to exhibit an OCR within the recommended range and also provided a good signal and consistent response throughout the experiment.

The concentration of stress test inhibitors was also optimised. This involved titrating concentrations of each inhibitor and choosing the concentration which exhibited the greatest and most consistent response. The inhibitor concentrations that provided the best response in both myoblast and myotube samples were 3µM oligomycin, 1µM FCCP and 1.2µM rotenone and antimycin-A.

6.2.3.4 Mitochondrial stress test

The mitochondrial stress test assay template was created on the XF controller. The assay incorporated a pre-calibration step followed by a calibration of the sensor cartridge. Once complete the utility plate was removed and replaced with the cell culture plate. The default template mix-wait-measure with the timings 3min,0 min, 3min was utilised in addition to three basal measurements performed before injection 1 and 3 rate measurements after each injection.

6.2.3.5 Normalisation

The OCR for each well was normalised for total protein concentration per well after each mitochondrial stress test. This normalisation process was justified as a number of studies have reported this normalisation strategy to be capable of successfully revealing mitochondrial bioenergetic differences between different cell samples [Salabei et al. 2014; Dott et al. 2014].

This was performed via BCA assay and briefly involved removing assay medium from the culture plate and adding 25µl of lysis buffer to each well. The contents of the well was then removed and placed into a clean 96-well plate. BCA reagent A and B were added in a 50:1 solution to each well as per manufacturer's instructions. The plate was agitated for 30s on a plate shaker and then incubated at 37°C for 30 minutes while protected from light. Absorbance was measured at 562nm on the Tecan Infinite 200.

6.2.4 Data analysis

Results are presented as mean \pm standard deviation. Data was analysed via independent and paired T-test. Statistical analysis was performed using Minitab 17 statistical software (Coventry, UK).

6.3 Results

6.3.1 Mitochondrial stress testing with varied glucose

Cellular mitochondrial function was assessed by varying the availability of the substrate glucose in the experimental assay media. Extracellular flux analysis provided a measurement of mitochondrial function following treatment with key mitochondrial ETC inhibitors; oligomycin, FCCP and a mixture of rotenone and antimycin A.

6.3.2 Basal respiration

Figure 6.5 demonstrated CFS/ME (n=4) and control (n=4) myoblast basal OCR in response to varied glucose media concentration. At the 2.5mM glucose concentration OCR was significantly lower ($P<0.05$) in the CFS/ME sample group compared to controls. No other significant alterations in OCR were observed as a consequence of varied glucose concentration.

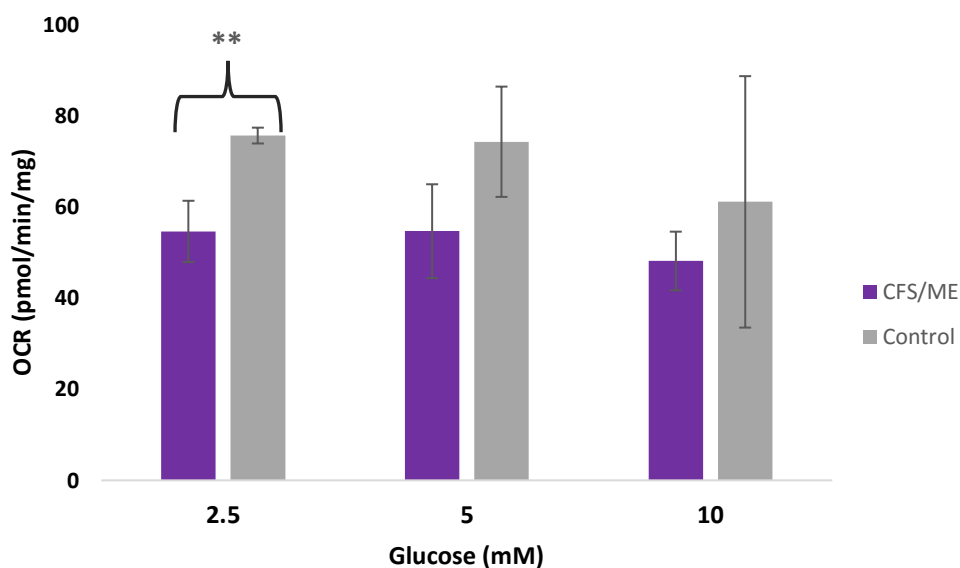


Figure 6.5: Basal OCR in myoblasts with varied glucose media concentration. CFS/ME samples exhibited significantly lower OCR compared to controls at 2.5mM glucose concentration. Data presented as mean \pm SD, n=8, ** denoted $P<0.05$

Figure 6.6 demonstrated myotube basal respiration OCR following the same glucose substrate treatment regime. No significant differences in OCR were exhibited with varying glucose concentration when CFS/ME (n=4) myotubes were compared to controls (n=4). Additionally, no significant within-group differences were observed.

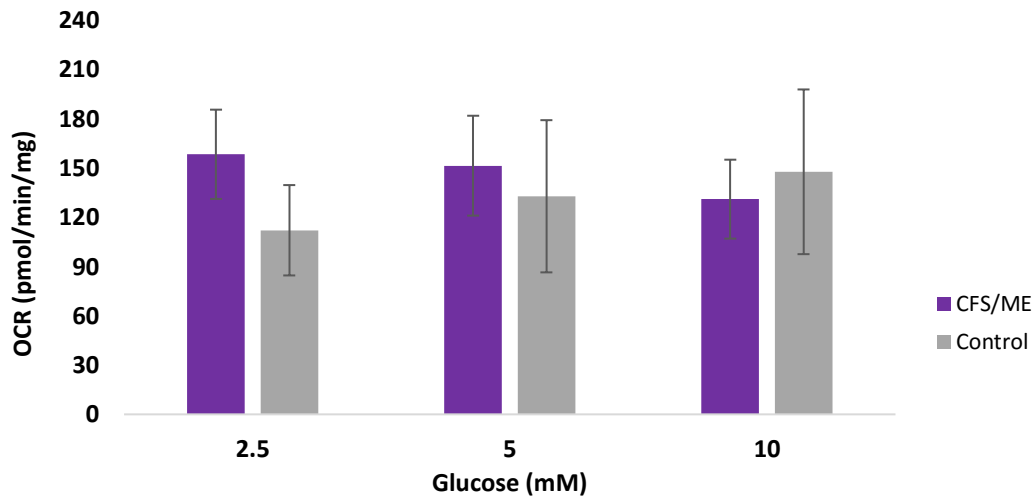


Figure 6.6: Basal OCR in myotubes with varied glucose media concentration. No significant difference in OCR for CFS/ME versus control myotubes was observed across the glucose concentrations. No significant within-group differences were found as a consequence of varied glucose concentration. Data presented as mean \pm SD, n=6

6.3.3 ATP-linked respiration

Myoblast ATP-linked respiration is demonstrated in Figure 6.7. CFS/ME (n=4) myoblasts exhibited significantly lower ($P<0.05$) OCR following incubation in 10mM glucose media when compared to controls (n=4). No other significant relationships were observed.

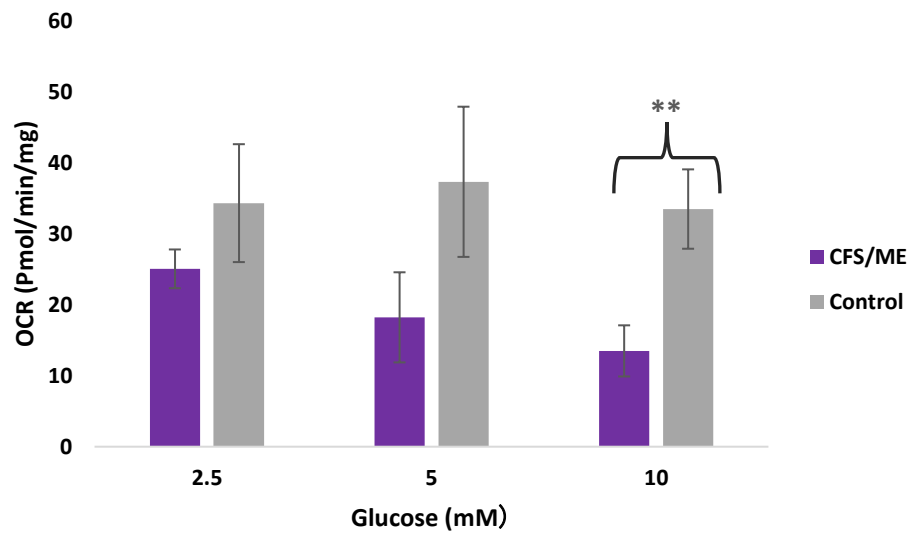


Figure 6.7: ATP-linked OCR in myoblast samples following incubation with varied concentrations of glucose media. At 10mM glucose, media concentration OCR was significantly lower in the CFS/ME sample group compared to controls. No significant within-group differences were found as a consequence of varied glucose concentration. Data presented as mean \pm SD, n=6, ** denoted $P < 0.05$

Myotube ATP-linked respiration is illustrated in Figure 6.8. There was no significant difference between CFS/ME and control samples associated with any of the glucose media concentrations. Similarly, there were no significant within-group differences as a consequence of varied glucose concentration.

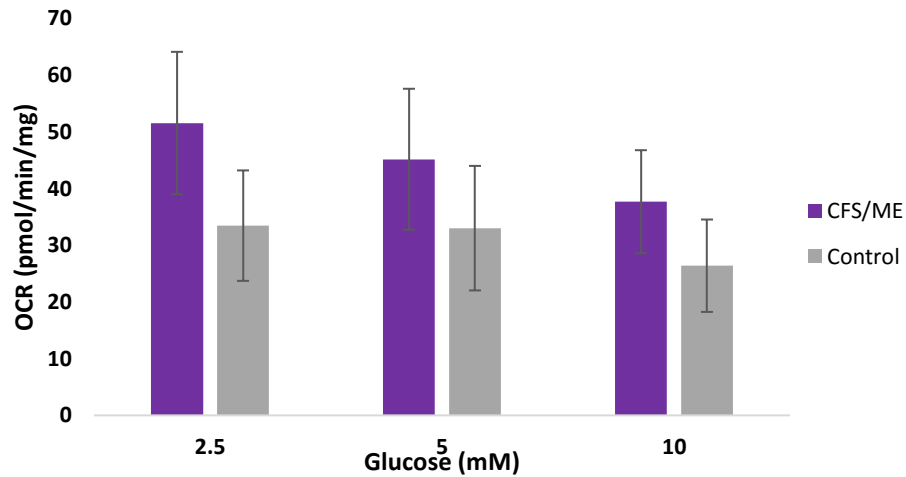


Figure 6.8: ATP-linked OCR in myotube samples following incubation with varied concentrations of glucose media. No significant difference in OCR for CFS/ME versus control myotubes at any glucose media concentration. No significant within-group differences were found as a consequence of varied glucose concentration. Data presented as mean \pm SD, n=6

6.3.4 Maximal respiration

Myoblast maximal respiration is displayed in Figure 6.9. No significant difference in OCR was exhibited between CFS/ME and control sample groups at any of the glucose media concentrations. No within-group differences were demonstrated as a consequence of varied glucose media concentration.

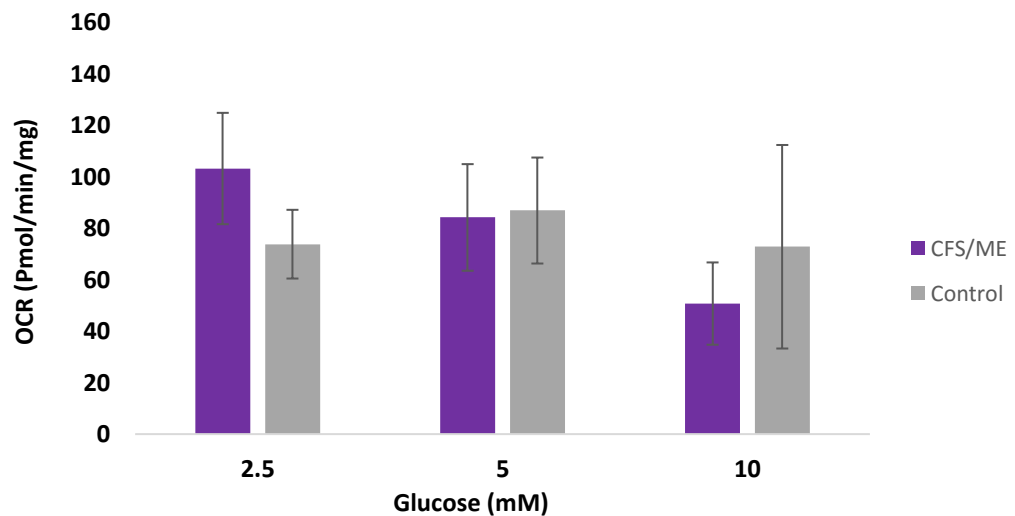


Figure 6.9: Myoblast maximal respiration with varied concentrations of glucose media. No significant difference in OCR for CFS/ME versus controls across glucose media concentrations. No significant within-group differences were found as a consequence of varied glucose concentration. Data presented as mean \pm SD, n=6

Myotube maximal respiration is demonstrated in Figure 7.0. OCR did not significantly differ between CFS/ME and control myotubes at any of the glucose media concentrations tested. Similarly, varied glucose media concentration did not result in any significant within-group differences.

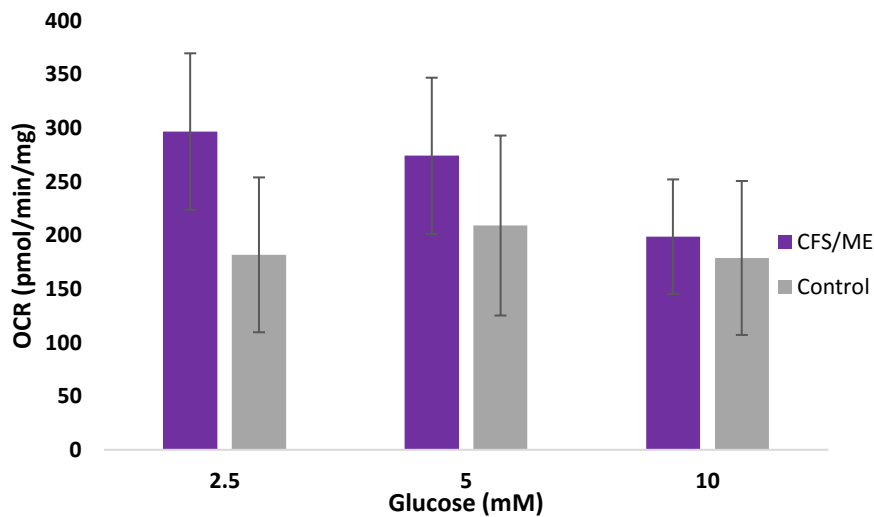


Figure 7.0: Myotube maximal respiration with varied concentrations of glucose media. No significant difference in OCR for CFS/ME versus controls across glucose media concentrations. No significant within-group differences were found as a consequence of varied glucose concentration. Data presented as mean \pm SD, n=6

6.3.5 Spare respiratory capacity

Myoblast spare respiratory capacity is demonstrated in Figure 7.1 . Spare capacity (%) in CFS/ME and control myoblasts did not significantly differ at any of the glucose media concentrations tested. Additionally, no within-group differences were observed across the concentration range tested.

Myotube spare respiratory capacity is demonstrated in Figure 7.2. As described in myoblast samples CFS/ME and control myotube spare respiratory capacity (%) did not differ significantly at any of the glucose media concentrations tested. Moreover, no within- group differences were observed at the media glucose concentrations investigated.

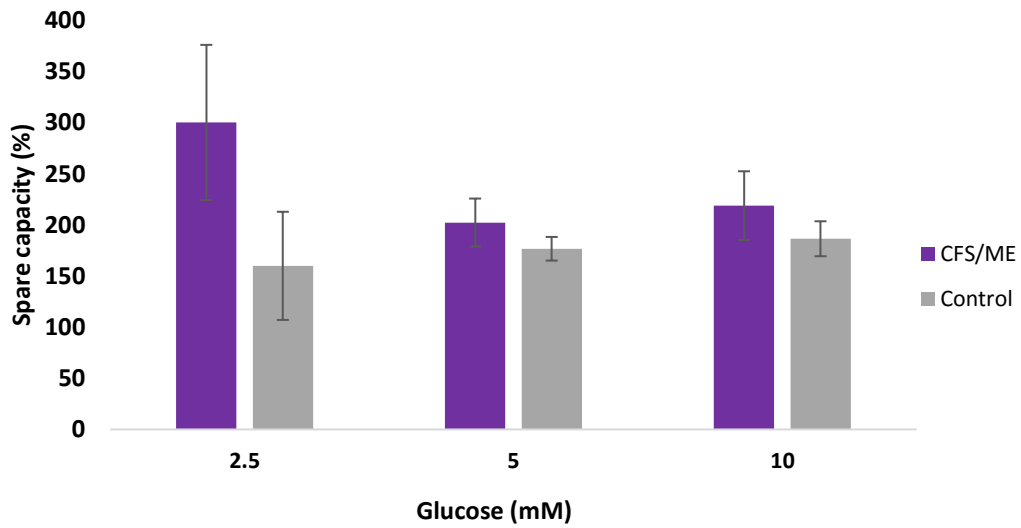


Figure 7.1: Myoblast spare respiratory capacity. OCR was not significantly different in CFS/ME compared to control myoblasts at any of the glucose media concentrations investigated. No within-group differences between any of the glucose concentrations was observed.

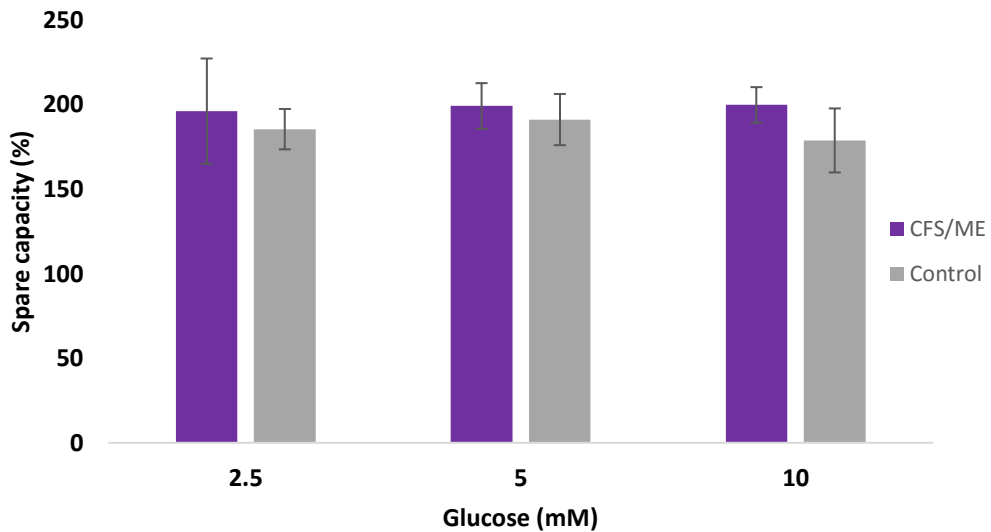


Figure 7.2: Myotube spare respiratory capacity. OCR was not significantly different in CFS/ME compared to control myoblasts at any of the glucose media concentrations investigated. No within-group differences between any of the glucose concentrations was observed.

6.4 Discussion

Previous research suggested that the peripheral muscle fatigue phenotype expressed in CFS/ME may be related to impaired bio-energetic function. This energetic abnormality subsequently leading to intracellular acidosis in response to exercise [Jones et al. 2012; 2010]. Likewise, *in vitro* assessment of muscle intracellular pH revealed CFS/ME myoblasts to exhibit an aberrantly low pH, which was later normalised following treatment with enzyme inhibitor DCA. Thus, taken together preliminary work hypothesised impaired function of the 3-enzyme complex PDC as the pathophysiological mechanisms underlying muscle fatigue in CFS/ME.

However, the data generated in previous chapters has not supported the assertion of impaired PDC function. This was evidenced following treatment with pH responsive dye BCECF-AM, which revealed CFS/ME skeletal muscle samples to exhibit an intracellular pH comparable to controls at rest and following EPS. Additionally, glycolytic capacity was investigated via extracellular flux analysis, revealing no abnormality in key glycolytic parameters when compared to controls. Finally, the compound DCA failed to modulate pH and ECAR in all of the *in vitro* assays performed.

The present chapter aimed to investigate the potential role of an alternative pathophysiological mechanism in CFS/ME that could be associated with muscle dysfunction and fatigue. Interestingly, a number of the muscle symptoms experienced by CFS/ME patients such as muscle pain, fatigue and cramping are also reported in disease states associated with mitochondrial dysfunction [Fulle et al. 2007; Morris and Maes. 2014]. Additionally, impaired oxidative phosphorylation, ATP production and mitochondrial damage have been reported in patients with CFS/ME (Filler et al. 2014; Myhill, 2008). Nonetheless, the present chapter is the first to assess mitochondrial function in CFS/ME muscle samples *in vitro* via XF analysis.

The primary findings were firstly, basal respiration was lower in CFS/ME myoblast samples compared to controls when incubated in media supplemented with 2.5mM glucose media, which was in agreement with the experimental hypotheses. However, no difference was observed in basal OCR across all glucose media concentrations for CFS/ME compared to control myotube samples. Therefore, contrasting the experimental hypotheses.

Secondly, ATP-linked respiration was reduced in CFS/ME myoblasts compared to controls following treatment with 10mM glucose, in agreement with the experimental hypothesis. However, this effect was not observed in myotube samples.

Finally, contrary to the experimental hypotheses no difference in maximal respiratory capacity or spare respiratory capacity was exhibited between CFS/ME and control myoblast and myotube samples with any of the glucose media concentrations tested, therefore rejecting the experimental hypotheses.

6.4.1 Mitochondrial parameters

In the present chapter skeletal muscle samples were exposed to varying glucose substrate concentrations (2.5-10mM). It is important to note that the 2.5mM glucose concentration was representative of hypoglycaemia as typically normal serum glucose levels are maintained within 4mM-6mM (approximately 72-108mg/dL). However, in the presence of low nutrient availability levels can drop to around 2.5mM (45mg/dL) with tissue levels reportedly lower [Zhuang et al. 2014]. The utilisation of low glucose media to assess mitochondrial function was justified by previous studies that have reported muscle cells to be highly glycolytic in the presence of excess glucose availability, thus impairing mitochondrial function. A glycolytic phenotype with hyperglycaemia was first noted in cancer cell lines and is referred to as the 'Crabtree effect'. However, this effect has since been reported in a variety of other cell lines including skeletal muscle cells [Elkalaf et al. 2013; Marroquin et al. 2007; Shulga et al. 2010; Rossignol et al. 2004].

The first mitochondrial parameter obtained from XF testing was basal respiration. This measure has been described as an OCR, which reflects coupled mitochondrial respiration and the uncoupled consumption of O₂ to form reactive oxygen species at mitochondrial and non-mitochondrial enzymatic sites [Hartman et al. 2014]. In terms of XF analysis basal respiration was measured prior to the injection of any mitochondrial inhibitors. In this study basal OCR was reduced in CFS/ME myoblasts compared to control samples following incubation with the lowest glucose media concentration only, which is displayed in Figure 6.6 , however CFS/ME myotube basal OCR was comparable to controls at all glucose media concentrations, displayed in Figure 6.7.

It is important to note that when cells are exposed to low glucose medium ATP is exclusively produced by oxidative phosphorylation [Marroquin et al. 2007]. Therefore, in the present study by reducing substrate availability the muscle cells were experimentally forced to utilise oxidative phosphorylation as the primary energy-producing pathway. At first glance, a lowered basal respiration in CFS/ME myoblasts would appear to be suggestive of underlying mitochondrial dysfunction when the cells are experimentally manipulated to produce ATP solely via oxidative phosphorylation. However, this interpretation is questionable, as low substrate availability did not impact upon basal OCR in CFS/ME myotube samples.

This discrepancy could be related to the shift in the dominant energy-producing pathway during myogenic differentiation, initially with naïve muscle cells primarily utilising glycolysis before steadily moving towards predominantly oxidative phosphorylation [Wagatsuma et al. 2013]. For example, it has been reported that in proliferating myoblasts approximately only 30% of ATP is produced via oxidative phosphorylation, compared to 60% in differentiated myotubes [Leary et al. 1998]. Additionally, from a molecular perspective myoblasts have been reported to exhibit a reduction in mitochondrial enzyme activity and a lowered respiratory chain complex content when compared to myotubes [Barberi et al. 2011; Moyes et al. 1997]. While it is evident that myoblasts and myotubes exhibit distinct differences in mitochondrial capacity it is difficult to ascertain why control myoblasts did not exhibit a comparable OCR when incubated in low glucose media.

The additional mitochondrial parameter ATP-linked respiration was also measured in the present study. Effectively, the difference between cellular basal OCR and the oligomycin insensitive OCR yields the amount of O₂ that is linked to ATP-production [Jekabsons. 2004]. XF analysis revealed CFS/ME myoblasts to exhibit a lower OCR, translating to a reduced cellular oxidative ATP production but only under hyperglycaemic conditions (Figure 6.8). However, no differences in OCR were observed in myotube samples (Figure 6.9). Possible reasons for this finding may relate to the previously described glycolytic phenotype acquired when cells are cultured in high glucose medium [Elkalaf et al. 2013]. For example, as previously described studies have demonstrated myoblasts during early stage differentiation to rely predominantly on lactate production from glucose so meet their cellular demands [Elkalaf et al. 2013; Leary et al. 1998]. Again, it is difficult to ascertain why control myoblasts did not exhibit a comparable OCR with hyperglycaemia but suggests CFS/ME myoblasts to exhibit a

more glycolytic phenotype prior to differentiation; however, this effect appears to be lost once terminally differentiated.

Maximal respiration was also determined in the present study. No differences were observed between CFS/ME and control muscle samples (Figure 7.0 and 7.1). Maximal respiration OCR was determined following the injection of FCCP. This inhibitor functions to allow the uninhibited movement of protons across the mitochondrial inner membrane, acting to collapse the mitochondrial membrane capacity. Oxygen consumption is then dramatically increased enabling the determination of maximal OCR [Dranka et al. 2011]. Interestingly, a decrease in maximal respiration has been reported to be a pivotal indicator in determining potential cellular mitochondrial dysfunction. For example, Elkalaf et al. [2013] reported uncoupling rates to provide a measurement of the maximum capability of the ETC and substrate oxidation that the cells are capable of when under assay conditions. Therefore, comparable OCR of CFS/ME and control samples would suggest CFS/ME skeletal muscle cells do not exhibit mitochondrial dysfunction.

Similarly, spare respiratory capacity has been suggested to be an important diagnostic measure of mitochondrial dysfunction. It was calculated by dividing the OCR response following FCCP injection by the basal OCR. Effectively, the measure provides an indication of cellular stress and provides information regarding the capability of the ETC and substrate supply to respond to increased energy demand, with cells with a higher capacity better able to respond to stress [Brand and Nicholls. 2011]. In the present study, spare respiratory capacity was comparable in CFS/ME and control myoblast samples (Figure 7.2).

Taken together the findings suggest CFS/ME myoblasts do exhibit a reduced oxidative phosphorylation capacity when compared to controls. However, once terminally differentiated into myotubes this effect appears to be lost and suggests that CFS/ME patients exhibit normal mitochondrial function. It is important to remember that muscle is formed by the fusion of many muscle pre-cursor cells (myoblasts) to form multinucleated myotubes which then mature into myofibres [Berendse et al, 2003]. Unlike myoblasts, myotubes have been suggested to exhibit morphological, metabolic and biochemical properties akin to intact skeletal muscle fibres [Olsson et al. 2015] and in terms of experimentation represent the best alternative to intact human skeletal muscle [Nikolic et al.2012] .

It is difficult to directly compare the results of the present investigation with previous research, as this is the first study to utilise an *in vitro* testing platform to experimentally induce mitochondrial stress in CFS/ME muscle samples. Presently, the majority of studies have investigated skeletal muscle mitochondrial function *in vivo* typically via MRS approaches. Lane et al. [1998] utilised the aforementioned technique and in contrast to the present study reported a reduction in ATP-production and re-synthesis in CFS/ME patients. Nevertheless, in agreement with the present study others have reported limited evidence of mitochondrial dysfunction in the CFS/ME patient cohort. For example, Vermeulen et al. [2010] reported normal oxidative phosphorylation capacity in muscle following a repeat exercise protocol to exhaustion. Alternatively, Barnes et al. [1993] reported mitochondrial dysfunction in some but not the entire patient cohort, suggestive of a sub-group of CFS/ME patients that exhibited mitochondrial dysfunction. Possible reasons for the discrepancies between the present study and others that have alternatively reported mitochondrial dysfunction in CFS/ME may relate to the use of skeletal muscle cells. Although myotubes have purported to exhibit morphological, metabolic and biochemical properties similar to intact adult skeletal muscle fibres [Olsson et al. 2015], it is important to note that they also exhibit key differences, including the expression of immature muscle proteins [Larkin et al. 2006], alterations in the abundance and distribution of glucose transporters and a slightly more glycolytic phenotype [Baker et al. 2003; Sarabia et al. 1992].

6.4.2 Limitations

CFS/ME patients frequently report a changeable pattern to their symptoms and physical capabilities, often with severe exacerbation following physical exercise [Whiteside et al. 2004; Fukuda et al. 1994]. Therefore, in terms of experimentation the ability to assess mitochondrial parameters post-exercise is warranted and has been conducted in previous *in vitro* studies [Lane et al. 2003; Vermeulen et al. 2010; Hollingsworth et al. 2010]. To overcome this obstacle EPS was applied in previous chapters to simulate physical activity *in vitro*. However, in this study it was not possible to perform EPS as the process required cells to be seeded and differentiated in 35mm dishes which were compatible with the c-pace EP cell culture pacer (Ion Optix, Dublin). Whereas for the XF analysis it was necessary to seed cells into XF-96 culture plates. It would be advantageous to develop an EPS device, which would be compatible with the XF-96 plate to enable mitochondrial bioenergetics to be interpreted following exercise simulation.

6.4.3 Conclusion

This chapter investigated CFS/ME skeletal muscle mitochondrial function via XF analysis and is presently the first study to use this methodology to provide a direct measurement of cellular mitochondrial bioenergetics in the muscle of CFS/ME patients. Ultimately, CFS/ME skeletal muscle cells exhibited normal mitochondrial function, which was evidenced by OCR values comparable to controls for all myotube mitochondrial parameters. This finding is in agreement with some studies that have reported normal oxidative phosphorylation capacity in the muscle of CFS/ME patients [Vermeulen et al. 2010] and contrasts others who have alternatively reported impaired ATP production and resynthesis in a CFS/ME patient cohort [Lane et al, 1998].

6.5 References

- Aguer, C. Gambarotta, D. Mailloux, R, J. Moffat, C. Dent, R. (2011) Galactose Enhances Oxidative Metabolism and Reveals Mitochondrial Dysfunction in Human Primary Muscle Cells. *PLoS ONE* 6(12)
- Baker, E, L. Dennis, R, G. Larkin, L, M. (2003) Glucose transporter content and glucose uptake in skeletal muscle constructs engineered in vitro. *In vitro Cell Dev Biol Animal*. 39 (10),434–9.
- Barbieri, E. Battistelli, M. Casadei, L. Vallorani, L. Piccoli, G. Guescini, M. Falcieri, E. (2011). Morphofunctional and Biochemical Approaches for Studying Mitochondrial Changes during Myoblasts Differentiation. *Journal of Aging Research*.
- Barnes, P, R. Taylor, D, J. Kemp, G, J. Radda, G, K. (1993). Skeletal muscle bioenergetics in chronic fatigue syndrome. *J Neurol Neurosurg Psychiatry*. 56, 679-683
- Behan WMH, More IAR, Behan PO. (1991) Mitochondrial abnormalities in the postviral fatigue syndrome. *Acta Neuropathol (Berl)* 83:61–65
- Berendse, M. Grounds, M, D. Lloyd, C, M. (2003) Myoblast structure affects subsequent skeletal myotube morphology and sarcomere assembly. *Exp Cell Res* 291, 435–450
- Booth, N, E. Myhill, S. McLaren-Howard, J. (2012). Mitochondrial dysfunction and the pathophysiology of Myalgic Encephalomyelitis/Chronic Fatigue Syndrome (ME/CFS). *International Journal of Clinical and Experimental Medicine*, 5 (3), 208–220.
- Brand, M. D. Nicholls, D. G. (2011). Assessing mitochondrial dysfunction in cells. *Biochemical Journal*, 435(Pt 2), 297–312.
- Dott, W. Mistry, P. Wright, J. Cain, K. (2014) Modulation of mitochondrial bioenergetics in a skeletal muscle cell line. *Redox Biology*. 2, 224-233
- Diepart, C. Verrax, J. Calderon, P, B. Feron, O. Jordan, B, F. Gallez, B.(2010) Comparison of methods for measuring oxygen consumption in tumor cells in vitro. *Anal Biochem*. 396 (2) 250–256.

Dranka, B, P. Benavides, G, A. Diers, A, R. Glordano, S. Zelickson, D, K. Reily, C. Darley-Usmar, V, M. (2011) Assessing bioenergetics function in response to oxidative stress by metabolic profiling. *Free radical biology and medicine*. 51 (9) 1621-1635

Dranka, B, P. Hill, B, G. Darley-Usmar, V, M. (2010) Mitochondrial reserve capacity in endothelial cells: The impact of nitric oxide and reactive oxygen species. *Free radical biology*. 48, 905-9

Elkalaf, M. Andeřl, M. Trnka, J. (2013) Low Glucose but Not Galactose Enhances Oxidative Mitochondrial Metabolism in C2C12 Myoblasts and Myotubes. *PLoS ONE* 8(8):

Ferrick, D, A. Neilson, A. Beeson, C. (2008) Advances in measuring cellular bioenergetics using extracellular flux. *Drug discovery today*. 13: 268–274.

Filler, K. Lyon, D. Bennet, J. McCain, N. Elswick, R. Lukkahatai, N. Saligan, L, N. (2014) Association of mitochondrial dysfunction and fatigue: A review of the literature. *BBA Clinical*. 1, 12-23

Fukuda, K. Straus, S, E. Hickie, I. Sharpe, M, C. Dobbins, J, G. Komaroff, A. (1994) The chronic fatigue syndrome: a comprehensive approach to its definition and study. *Annals of Internal Medicine*. 121, 953–9.

Fulle, S, Pietrangelo, T, Mancinelli, R, Saggini, R, Fano, G. (2007) Specific correlations between muscle oxidative stress and chronic fatigue syndrome: a working hypothesis. *Journal of Muscle Research Cell Motility*. 28: 355-362

Gnaiger, E. Steiniechnermaran, R. Mendez, G. Eberl, T. Margreiter, R. (1995) Control of mitochondrial and cellular respiration by oxygen. *Journal of bioenergetic biomembr*. 27, 583-596

Gnaiger, E. (2009) Capacity of oxidative phosphorylation in human skeletal muscle: new perspectives in mitochondrial physiology. *International journal of biochemical cell biology*. 41. 1837-1845

Hartman, M.-L. Shirihai, O. S. Holbrook, M. Xu, G. Kocherla, M. Shah, A. Vita, J, A. (2014). Relation of Mitochondrial Oxygen Consumption in Peripheral Blood Mononuclear Cells to Vascular Function in Type 2 Diabetes Mellitus. *Vascular Medicine (London, England)*, 19(1), 67–74.

- Hollingsworth, K, G. Jones, D, E. Taylor, R. Blamire, A, M. Newton, J, L. (2010) Impaired cardiovascular response to standing in chronic fatigue syndrome. *European Journal of Clinical Investigation*. 40 (7) 608-615
- Horan, M, P. Pichaud, N. Ballard, W, J, O. (2012) Review: Quantifying mitochondrial dysfunction in complex diseases of ageing. *Journal of Gerontology, Biological sciences*. 1-14
- Hutteman, M. Lee, I. Samavati, L. Hong, Y. Doan, J,W. (2007) Regulation of mitochondrial oxidative phosphorylation through cell signalling. *Molecular cell research*. 1773, 12, 1701-1720
- Ibsen, K, H. (1961) The Crabtree effect: a review. *Cancer Res*. 21, 829–841. 17
- Jekabsons, M, B. Nicholls, D, G. (2004) in situ respiration status in primary cerebellar granule neuronal cultures exposed to glutamate. *Journal of biological chemistry*. 279, 32989-33000
- Jones, D ,E. Hollingsworth, K, G. Jakovljevic, D, G. Faltakhova, G. Pairman, J. Blamire, A, M. Trennel, M, I. Newton, J, L.(2012) Loss of capacity to recover from acidosis on repeat exercise in chronic fatigue syndrome: A case control study. *European Journal of Clinical Investigation*. 42 (2) 184-194
- Jones, D, E, J. Hollingsworth, K. Blamire, A, M. Taylor, R. Newton, J, L.(2010) Abnormalities in pH handling by peripheral muscle and potential regulation by the autonomic nervous system in chronic fatigue syndrome. *Journal of Internal Medicine*. 26, 394–401
- Lane, RJ; Barrett, MC; Taylor, DJ; Kemp, GJ; Lodi, R. (1998). Heterogeneity in chronic fatigue syndrome: evidence from magnetic resonance spectroscopy of muscle. *Neuromuscul Disord*. 8, 204-209
- Lane, R, J. Soteriou, B, A. Zhang, H. Archard, J. (2003) Enterovirus related metabolic myopathy: a postviral fatigue syndrome. *J Neurol Neurosurg Psychiatry*. 74, 1382–1386
- Larkin, L, M. Van der Meulen, J, H. Dennis, R, G. Kennedy, J, B. (2006) Functional evaluation of nerve-skeletal muscle constructs engineered in vitro. *In vitro Cell Dev Biol Animal*. 42(3–4) 75–82
- Leary, S, C. Battersby, B, J. Hansford, R, G. Moyes, C, D. (1998) Interactions between bioenergetics and mitochondrial biogenesis. *Biochim Biophys Acta* 1365: 522–530

- Nicholls, D, G. Ferguson, S, J. (2002) *Bioenergetics*. Academic press. New York.
- Marroquin, L, D. Hynes, J. Dykens, J, A. Jamieson, J, D. Will, Y. (2007) Circumventing the crabtree effect: replacing media glucose with galactose increases susceptibility of HepG2 cells to mitochondrial toxicants. *Toxicol. Sci.* 97, 539–547
- McCully, K, K. Smith, S. Rajaei, S. Leigh, J, S. Natelson, B, H. (2003) Blood flow and muscle metabolism in chronic fatigue syndrome. *Clin Sci.* 104(6) 641–647
- Morris, G. Maes, M. (2014) Mitochondrial dysfunction in myalgic encephalomyelitis/Chronic fatigue syndrome, explained by activated immune-inflammatory, oxidative and nitrosative stress pathways. *Metabolic Brain Disease.* (1) 19-36
- Moyes, C, D. Mathieu-Costello, O, A. Tsuchiya, N. Filburn, C. Hansford, R, G.(1997) Mitochondrial biogenesis during cellular differentiation. *American Journal of Physiology.* 272(4)1345–1351
- Myhill, S. Booth, N,E. McLaren-Howard, J. (2009) Chronic Fatigue Syndrome and mitochondrial dysfunction. *International Journal Clinical Experimental Medicine.* 2, 1-16
- Nikolic, N. Bakke, S, S. Kase, E, T. Rudberg, I. Flo Halle, I. Rustan, A, C. (2012) Electrical pulse stimulation of cultured human skeletal muscle cells as an in vitro model of exercise. *PLoS One.* 7 (3)
- Olsson, K. Cheng, A, J. Alam, S. Al-Ameri, M. Rullman, E. Westerblad, H. Gustafsson, T. (2015). Intracellular Ca²⁺-handling differs markedly between intact human muscle fibers and myotubes. *Skeletal Muscle,* 5, 26.
- Perry, G, R. Kane, D, A. Lanza, I, R. Neuffer, D. (2013) Methods for assessing mitochondrial function in diabetes. *Diabetes.* 62, 1041-1053
- Rossignol, R. Gilkerson, R. Aggeler, R. Yamagata, K. Remington, S, J. (2004) Energy substrate modulates mitochondrial structure and oxidative capacity in cancer cells. *Cancer Res* 64: 985–993
- Salebei, J, K. Gibb, A, A. Hill, B, G. (2014) Comprehensive measurement of respiratory activity in permeabilised cells using XF analysis. *Nature protocols.* 9 (2) 421-438

Sarabia, V. Lam, L. Burdett, E. Leiter, L, A. Klip, A. (1992) Glucose transport in human skeletal muscle cells in culture. Stimulation by insulin and metformin. *J Clin Invest.* 90 (4) 1386–95.

Sauerbeck, A. Pandya, J. Singh, I. (2011) Analysis of regional brain bioenergetics and susceptibility to mitochondrial inhibition utilising a microplate based system. *Journal of neuroscience methods.* 198, 36-43

Shulga, N. Wilson-Smith, R. Pastorino, J, G. (2010) Sirtuin-3 deacetylation of cyclophilin D induces dissociation of hexokinase II from the mitochondria. *J Cell Sci.* 123, 894–902.

Vermeulen, R, C. Kurk, R, M. Visser, F, C. Sluiter, W. Scholte, H, R. (2010) Patients with chronic fatigue syndrome performed worse than controls in a controlled repeated exercise study despite a normal oxidative phosphorylation capacity. *J Transl Med.* 8, 93

Wagatsuma, A. Sakuma, K. (2013) Mitochondria as a potential regulator of myogenesis. *The Scientific World Journal.* 593267

Wang, D. Green, M. F. McDonnell, E. Hirschey, M, D. (2013) Oxygen Flux Analysis to Understand the Biological Function of Sirtuins. *Methods in Molecular Biology (Clifton, N.J.)*1077

Whiteside, A. Hansen, S. Chaudhuri, A. (2004) Exercise lowers pain threshold in chronic fatigue syndrome. *Pain* 109, 497–9

Yong-Ling, P. Green, D, R. Hao, Z. Tak, W. (2008) Cytochrome C functions beyond respiration. *Nature reviews: Molecular cell biology.* 9, 532-542

Zhuang, Y. Chan, D, K. Haugrud, A, B. Miskimins, W, K. (2014) Mechanisms by Which Low Glucose Enhances the Cytotoxicity of Metformin to Cancer Cells Both In Vitro and In Vivo. *PLoS ONE* 9(9):

Chapter 7

General Conclusions and Future Directions

7.1 Conclusions

The overriding aim of this PhD thesis was to provide a new insight into the biochemical basis of muscle cell dysfunction in patients with CFS/ME through the use of novel *in vitro* technologies.

One of the primary symptoms of CFS/ME is generalised abnormal muscle fatigue that occurs following relatively mild physical activity. Additionally, patients frequently report an inability to maintain muscle activity due to a perceived ‘lack of energy’ and ‘muscle pain’, which can be severe enough to lead the patient to avoid physical activity completely. Previous *in vivo* studies have revealed CFS/ME patients to exhibit profound and sustained intramuscular acidosis following a standardised exercise protocol [Jones et al. 2012; 2010]. Whereas others have reported either no evidence of enhanced acidosis in CFS/ME patients post-exercise [Wong et al. 1992] or in only some of the CFS/ME patient cohort [Barnes et al. 1993], demonstrating the heterogeneity of the CFS/ME patient population.

An *in vitro* pilot study reported aberrantly low intracellular pH in CFS/ME patient myoblasts, which was normalised following treatment with PDK inhibitor DCA [Boulton. 2012]. In this study intracellular pH was measured via a novel fluorescent pH responsive nanosensor system. This study provided preliminary evidence to suggest a role of bio-energetic dysfunction in CFS/ME because of an over utilisation of the lactate dehydrogenase pathway. Therefore, a key aim of this PhD thesis was to build upon pilot work to further develop and validate the pH responsive nanosensor system to confirm the presence of acidosis in CFS/ME patient muscle cells and also the capacity to modulate bio-energetic function and inform the treatment of peripheral muscle fatigue.

Chapter 2 aimed to develop and further develop the fluorescent pH responsive nanosensors system, however the work carried out in this chapter was unable to reliably detect intracellular acidosis in CFS/ME patient myoblast cells. Additionally, DCA did not modulate intracellular pH in either CFS/ME or control cells.

In chapter 4 the fluorophore BCECF-AM was used as an alternative strategy to measure intracellular pH, to confirm the presence of acidosis in CFS/ME patient muscle and investigate the ability of DCA to modulate normalise pH. Additionally, EPS was used to simulate exercise *in vitro*. In contrast to chapter 2, BCECF enabled the reliable determination of intracellular pH. However, contrary to pilot data, no evidence of elevated intracellular acidosis at rest or following EPS was found in CFS/ME patient muscle samples. Rather intracellular pH measurements were comparable to control cells. Additionally, DCA did not modulate intracellular pH in either CFS/ME patient or control cells. This work highlighted the importance of adequate patient numbers when investigating a heterogeneous patient population. Furthermore, it also illustrated the difficulty in directly comparing *in vitro* and *in vivo* data.

Chapter 5 further developed upon chapter 4 by using alternative techniques to measure cellular glycolytic function, these were XF analysis and the measurement of L-lactate. In agreement with chapter 4, no evidence of increased glycolytic function was found in CFS/ME patient muscle cells when compared to controls. This was demonstrated by comparable measurements in the basal state, post-EPS and following glycolytic stress testing. Similarly, DCA did not alter glycolysis in either patient or control cells.

In chapter 6 muscle mitochondrial function was assessed via XF analysis. In this chapter, glucose substrate availability was manipulated to induce mitochondrial stress. CFS/ME patient muscle cells exhibited normal mitochondrial function, which was evidenced by OCR values comparable to control cells for all mitochondrial parameters.

The possible role of enhanced oxidative stress in CFS/ME was investigated in chapter 3. A direct real-time electrochemical technique was used to measure $O_2^{\cdot-}$ generation in CFS/ME patient myoblast cells. To stimulate $O_2^{\cdot-}$ generation cells were treated with ethanol or experienced lactic acidification. The data revealed there to be no evidence of enhanced oxidative stress in CFS/ME patient muscle samples, rather levels of $O_2^{\cdot-}$ generated were comparable to control cells.

Taken together the *in vitro* muscle culture approaches reported in this thesis have enabled the investigation of the biochemical basis of muscle cell dysfunction in patients with CFS/ME. It is possible to conclude there to be no evidence of impaired muscle function in CFS/ME patients. Additionally, there was no impairment found in PDK enzyme function. Therefore, it

is possible to determine that bioenergetic function is normal in CFS/ME patients and does not explain the excessive peripheral muscle fatigue phenotype exhibited in patients with CFS.

7.2 Future Work

In this thesis, there was no evidence of biochemical abnormality at the skeletal muscle level of patients with CFS/ME. However, investigating the muscle in isolation failed to take into account systemic biochemical factors that may influence muscle function *in vivo*. It would be advantageous for future studies to investigate bioenergetic function in isolated peripheral blood mononuclear cells. Specifically, this could be achieved with XF analysis to enable glycolytic and mitochondrial stress testing. Also in line with previous *in vivo* investigations, blood sampling could be obtained from CFS/ME patients in the resting state and also following a standardised exercise protocol. Such strategies would help to bridge the gap between *in vivo* and *in vitro* investigations and promote improved understanding of the impact of systemic factors on muscle function.

7.3 References

Barnes, P, R. Taylor, D, J. Kemp, G, J. Radda, G, K. (1993). Skeletal muscle bioenergetics in chronic fatigue syndrome. *J Neurol Neurosurg Psychiatry*. 56, 679-683

Boulton, S, J. (2012) Integrated free radical sensor systems for investigation of cellular models of disease. PhD thesis, Newcastle University. Identifier:
<http://hdl.handle.net/10443/1427>

Wong, R. Lopaschuk, G. Zhu, G. Walker, D. Catellier, D. Burton, D. Teo, K. Collins-Nakai, R. Montague, T. (1992). Skeletal muscle metabolism in the chronic fatigue syndrome. In vivo assessment by ³¹P nuclear magnetic resonance spectroscopy. *Chest* . 102, 1716-1722

